DOKTORSAVHANDLINGAR
VID
CHALMERS TEKNISKA HÖGSKOLA
Nr 28

ON THE THEORY OF MONOPULSE RADAR

BY

GÖSTA HELLGREN

GÖTEBORG 1960

DOKTORSAVHANDLINGAR
VID
CHALMERS TEKNISKA HÖGSKOLA

ON THE THEORY OF MONOPULSE RADAR

by

GÖSTA HELLGREN

GÖTEBORG
ELANDERS BOKTRYCKERI AKTIEBOLAG
1960

This thesis includes the following two papers:

1. G. Hellgren: On the principles and angular accuracy of monopulse radar. SAAB Technical Notes, TN 42, March 1959.

2. G. Hellgren: Some characteristics of two simple linear and stochastically time-varying control systems of interest in angle and range measurement and tracking by monopulse radar. SAAB Technical Notes, TN 47, May 1960.

Introduction and summary

Monopulse radar is the result of intensive post-war research and development work in the field of military radar, especially in USA [1], [2]. A monopulse radar and a conventional radar for angle and range measurement and tracking differ in the way in which information on angular position of the target is obtained. In conventional beam-scanning radar, information on target angle is obtained from a comparison in the video part of the receiver, as the receiving beam scans in space, of amplitudes of consecutive echos. In radar of monopulse type, on the other hand, each individual echo from the target gives full information on its angular position. This is attained by a simultaneous comparison, in the high frequency (hf) or intermediate frequency (if) part of the receiver, of the amplitude and phase of echo signals picked up by four stationary antennas. Because of this, monopulse radar offers great possibilities in obtaining high angular accuracy. Low frequency amplitude-scintillations of the echos do not for instance result in angle-measuring errors in monopulse radar, as they do in conventional beam-scanning radar, in which echo amplitude-fluctuations with a frequency in the vicinity of the frequency of beam rotation are interpreted as target angle changes. In military applications monopulse radar has further advantages compared to conventional radar, but is technically more complex.

The present thesis is of purely theoretical nature. It deals with the principles of monopulse radar and discusses how angular measuring accuracy is influenced by electrical imperfections of the receiver circuits, receiver internal noise, target glint, and target echo fading. The thesis does not claim to cover all aspects of monopulse radar techniques but only to increase our knowledge in this wide field.

Many of the formulas employed in the thesis are rather complicated, and numerical evaluation of the results has therefore required the utilization of a digital computing machine (SARA).

Paper no. 1

On the principles and angular accuracy of monopulse radar

In paper no. 1 of this thesis the general principles of one-dimensional angle-measuring monopulse radar are first discussed. Expressions for angle-detector output signal for one or several targets are derived in section 2.1. In 2.2 the two limiting cases of monopulse radar, the amplitude-comparison and the phase-comparison types, are defined, studied, and compared with respect to angle-detector characteristic and sum-beam antenna pattern. It is shown that for a fixed antenna spacing a more linear detector characteristic can be obtained in an amplitude-comparison than in a phase-comparison monopulse radar at the price of a somewhat lower maximum antenna gain of the sum-signal channel. In addition the relative side lobes are lower in the amplitude-comparison than in the phase-comparison case.

In section 2.3 special interest is paid to the behaviour of angle-detector output for small target angle deviations from the reference direction given by the monopulse antenna system. For an ideal system the output signal is then directly proportional to the target angle deviation. The case is of current interest in connection with an automatic target-tracking servo system, in which the radar is the error sensing device. The angular gain of the monopulse radar, defined as the ratio between detector output and target angle deviation, is studied under rather general assumptions. In the case of a phase-comparison monopulse radar the angular gain is entirely determined by the distance between the phase-centres of the individual antennas while in the case of an amplitude-comparison system it is strongly dependent upon the tilting of the individual antenna lobes.

The angle-discrimination property of monopulse radar is discussed in some detail in section 2.4. The effects of the presence of an interfering target upon the detector output signal from a legitimate target close to the reference direction are a lower angular gain and an additive angular error depending upon the angular position and the relative echo-signal strength of the interfering target. The magnitudes of these effects are given in two cases of phase-comparison and amplitude-comparison monopulse radars of current interest.

The influence of electrical imperfections in the hf parts of the receiver upon the angle-measuring capability of the monopulse radar is studied in chapter 3, neglecting the pulse character of the signals. Analytical expressions for the angle-detector output signal are given

for different types of circuit anomalies. First order effects of some typical circuit imperfections for small target angle deviations are discussed in more detail in the two cases of phase-comparison and amplitude-comparison monopulse radar. It is shown that attenuation and phase difference between the two signal channels of a monopulse radar before the forming of the sum- and difference-signals in the hybrid junction will cause an error in determination of the angle in the first approximation only. In a phase-comparison radar only a phase difference and in an amplitude-comparison radar only an attenuation difference will give this result. The same effect is also caused by attenuation and phase unbalances of the hybrid junction itself. Attenuation and phase differences introduced after the hybrid junction, on the contrary, result only in a change of angular gain.

In chapter 4 the effect of imperfections in if-circuits upon detector output signal is discussed, taking into account the pulse character of the echo signals and the frequency band restrictions of the if-circuits. It is shown quite generally that such anomalies only cause a change of the detector output-target angle curve but do not introduce any shift of its zero cross-over point, i. e. the angle reference direction of the antenna system. Therefore, for small target angle deviations a decrease of angular gain is obtained but without additive angular error. The behaviour of angular gain is especially investigated if one or the other of the two if-amplifiers is detuned a certain amount. This detuning may be caused, for example by an unequal variation of tube input capacitances of the amplifiers due to the action of the automatic gain control (AGC). It is found that the detector output signal is more sensitive to detuning of the difference-signal amplifier than to detuning of the sum-signal amplifier, the underlying reason being the tendency of the AGC to neutralize changes in the if sum-channel output.

The decrease of angular gain due to frequency detuning mentioned above is studied numerically in section 4.3 in the two cases that the if-amplifiers are of the maximally-flat delay type and the maximally-flat amplitude type. These can be said to represent the two extremes of amplifier design. Generally, large detuning, for an amplifier bandwidth that is small compared with the spectral width of the echo pulses, and a large number of amplifier stages, causes a large decrease of angular gain. A comparison between the results obtained for the two types of amplifiers shows that the angular gain decreases more rapidly with increasing detuning for a given echo signal pulse-length, a given amplifier bandwidth, and a given number of stages in the maximally-

flat amplitude case than in the maximally-flat delay case. Unfortunately, a good deal of the advantage in non-criticalness of maximally-flat delay amplifiers over maximally-flat amplitude amplifiers is lost in practice because of the fact that for a given overall amplification and bandwidth an amplifier of the maximally-flat delay type requires more stages.

In the last chapter of paper no. 1, chapter 5, there is discussed the ultimate limit of the attainable angular measuring accuracy of a monopulse radar which is set by receiver internal noise together with target glint (or angular scintillation) and echo fading for ordinary types of targets such as airplanes and ships. The limited accuracy of monopulse radar due to receiver internal noise has earlier been discussed schematically by BUDENBOM [3], and a theory of target glint in radar tracking (especially with regard to a conical scanning radar) has been given by DELANO [4]. In [4] DELANO also points out the influence of echo signal fading upon the angle measurement through the action of the AGC. This effect has later been studied experimentally by DELANO and PFEFFER [5] and recently by DUNN and HOWARD [6] in the case of monopulse radar.

Starting from the given theory of monopulse radar and taking echo fading into account, an expression is deduced in section 5.1 for the angle-detector output in the presence of receiver internal noise. The expression holds in the practically important case in which the signal-to-noise ratio in the sum-signal channel is greater than one. The effect of internal noise is in this case an additive random angular error. Expressions for angle-detector output are deduced in section 5.2 in the case of a glinting and fading target. As done by DELANO [4], the target is supposed to consist of a large number of elementary reflectors inside the linear angle-measuring region of the radar, which, statistically independently of each other, reflect a part of the incident signal in a random manner. The effect of the interference between the echo signals from the elementary reflectors is an additive random contribution to detector output and a fading resultant target echo amplitude. Through the action of the AGC this influences the output signal. An AGC slow compared to the fading results in large variations of the legitimate angle-detector output from a target (large multiplicative angular error). A fast AGC, on the other hand, eliminates these variations, but enlarges the additive contribution to the output due to internal noise and target glint (additive angular error). In section 5.1 and 5.2 formulas are given for computing the root mean

square values of the additive angular errors due to receiver noise and target glint with and without post-detector smoothing. The AGC is supposed to be slow and only the case of an angle-measuring radar (open loop system) is considered. The problem regarding the influence of an arbitrarily fast AGC upon the angle-measuring accuracy of monopulse radar is treated theoretically in paper no. 2 of this thesis. There is also discussed the effect of the feedback of the angle-measuring error in case of an automatic target tracking radar (closed loop system).

The detection system of the radar may be either of a square-law or of a linear type. A square-law detection system is composed of a phase sensitive detector of product type (mixer) for the extraction of information on the angular position of the target and a square-law AGC-detector. A linear system contains as a phase detector, for instance, a diode phase detector according to [7] and a linear envelope AGC-detector. In order to facilitate the theoretical treatment in paper no. 1, especially in chapter 4, a monopulse radar with a square-law detection system has been assumed. If the detection system is linear the expressions for the angle-detector output deduced in paper no. 1 will be the same as long as the pulse character of the signals and the presence of internal noise and target glint are not taken into consideration. However, the choice of detection system should not significantly affect the results in these two cases.

Concerning investigations in the published literature on the principles and angular accuracy of monopulse radar at about the same time as and after paper no. 1 the following can be said. In his book [2] RHODES gives a unified theory of all types of monopulse radars starting from three very general postulates. The book contains, however, very little specific design information on practical monopulse radar systems, and the effect of noise on monopulse angle accuracy is not discussed. RHODES defines three different classes of monopulse radar. Class I, without question the most important one, is identical with the type of monopulse radar treated here. BARTON's work [8] is an experimental verification of the fact that the limit of the attainable angular accuracy of monopulse radar is today set by receiver internal noise, target glint, and propagation errors. In [9] COHEN and STEINMETZ analyze the influence of attenuation and phase unbalances introduced before and after the hybrid junction upon the angle-measurement in case of phase-comparison and amplitude-comparison monopulse radar. In doing this they start

from a given specific form of the individual monopulse antenna patterns. They do not take into consideration the pulse character of the signals and the frequency band restrictions of the if-circuits.

Paper no. 2

Some characteristics of two simple linear and stochastically time-varying control systems of interest in angle and range measurement and tracking by monopulse radar

In paper no. 2 a theoretical study is made of the effect of echo signal fading upon target angle-measurement and tracking by monopulse radar in the presence of internal receiver noise and target glint. As mentioned above this effect has been examined experimentally by DELANO and PFEFFER [5] and by DUNN and HOWARD [6]. The purpose of the present treatment is to give a somewhat wider aspect to the problem and thereby a better understanding of how the results are influenced by different factors, for instance the statistical distribution of the fading echo amplitude, the power spectra of the echo signal and the random additive angular errors, and the bandwidth of the AGC.

An analytical treatment of the whole question of the effect of echo signal fading upon the angular accuracy of monopulse radar at an arbitrarily fast AGC is not possible in practice. Great simplification of the problem is necessary and results obtained can therefore only serve as a guide in the design of such a radar. The final design must be determined by means of field tests and simulation experiments in the laboratory.

The first simplification of the problem made in paper no. 2 is a linearization of the function of the AGC and an assumption that all circuits are linear and constant. An equivalent circuit of an amplifier with a linearized AGC is deduced in appendix I, in which the justification of such a simplification is also discussed. On the basis of the monopulse radar theory given in paper no. 1 and the linearization of the AGC a completely linear equivalent circuit for a one-dimensional monopulse radar is given in appendix II. Here are assumed a fading target echo and the presence of additive random angular error due to internal noise and target glint. In this connection we distinguish between the cases that the radar detection system is linear or square-law. For simplicity we treat in paper no. 2 only the first case, but the results should not differ significantly from those obtained for a radar with a square-law detection system.

The linearized equivalent circuit of a target tracking monopulse radar consists of two coupled linear servo systems, the so called tracking servo and the AGC-servo. Each of these contains a randomly time-varying amplification factor directly proportional to the echo signal amplitude. In order to simplify the problem further, it is supposed that the antenna controller of the tracking servo is a single integrator and that the smoothing filter of the AGC-circuit is a simple low-pass filter of RC-type. The result of these assumptions is that each of the two coupled servo systems can be described by a first order linear differential equation with one stochastically time-varying parameter (the echo amplitude). Moreover, in paper no. 2 we restrict ourselves to studying the accuracy of an angular target tracking monopulse radar with a slowly acting AGC and the influence of an arbitrarily fast AGC upon the angle-measurement of a non-tracking radar. In these cases the coupling between the tracking servo and the AGC-servo disappears. The problem has then been reduced to a study of the characteristics of two separate first order linear servo systems with one randomly time-varying parameter. As a matter of fact paper no. 2 has the character of a general study under rather general conditions of the characteristics of the stochastically time-varying tracking servo and AGC-servo. The results of this investigation have then been applied to the monopulse radar cases mentioned above.

In the general theoretical analysis of the servo systems two cases of randomly time-varying parameter are treated. In the one case the parameter is supposed to be generated by a stationary random Gaussian process with arbitrary power spectrum. In the other case, which appears not to have been treated previously in the literature, the system parameter is assumed to be generated by a quasi-stationary arbitrarily distributed random process with a low-pass spectrum of the type $\sin^2 \frac{\pi\omega}{2\,\omega_0} \Big/ \left(\frac{\pi\omega}{2\,\omega_0}\right)^2$, where the cut-off angular frequency ω_0 can be chosen at will. The Rayleigh-distributed quasi-stationary process is supposed to generate the echo signal amplitude in the monopulse radar applications. The echo amplitude of a fading airplane or ship target can often be assumed to be Rayleigh-distributed and to have a low-pass power spectrum.

After deduction in chapter 2 of some fundamental relations holding for the linear randomly time-varying tracking servo, its characteristics are investigated in somewhat more detail in the following. In chapter 3 the case of a Gaussian-distributed parameter with arbitrary spectrum

is treated and in chapter 4 the case of an arbitrarily distributed parameter with the given type of low-pass spectrum. The stability of the tracking servo is discussed and it is found that with a Gaussian-distributed parameter the tracking servo as well as the AGC-servo can become instable, which is not the case if the parameter is Rayleigh-distributed for instance. The average value of the output signal of the tracking servo and the dynamic error are studied for both deterministic and stationary stochastic inputs. By dynamic error is meant the average square deviation of the output from a desired value equal to the input. The contribution to the output of additive stationary random noise is also discussed. The random input, noise, and parameter processes are assumed to be statistically independent of each other. For a stationary Gaussian parameter with a rectangular low-pass spectrum and for a quasi-stationary Rayleigh-distributed parameter the following two cases are analyzed numerically. In the one case the input is a unit step at time $t = 0$ and in the other case the input as well as the additive input noise is generated by a stationary stochastic process with an autocorrelation function of simple exponential form.

It is observed that the form of the distribution of the randomly time-varying parameter has a great effect upon the numerical results obtained. This is also the case for the AGC-servo. The dynamic error for random inputs as well as the additive output noise becomes larger than that for a corresponding time-invariant tracking servo, as it ought to be. The numerical results are applied to an angular target tracking monopulse radar with a slow AGC, an assumed Rayleigh-distributed echo amplitude, and random inputs. It is found that the increase of the dynamic error due to the echo fading is relatively small even for a large ratio between the servo and the fading bandwidths and a slowly varying input signal compared to the fading. On the other hand, the additive output noise caused by receiver internal noise and target glint is increased by the amplitude fluctuations more than the dynamic error. This is especially the case for a large ratio between the servo and fading bandwidths and a small input noise bandwidth compared with the fading bandwidth.

In chapter 5 some fundamental relations holding for the simple randomly time-varying AGC-servo are deduced. In the following two chapters the stability of the system, the average value and the average square deviation from the desired value of the output, and the average square value of the so called resultant signal amplification

of the AGC are then studied in the two cases of random parameters. The following conclusion can be drawn from the numerical results obtained, regarding the influence of the speed of the AGC upon the simple one-dimensional angle-measuring monopulse radar in the case of a Rayleigh-distributed echo amplitude with a low-pass spectrum of the assumed form:

1. The multiplicative angular error, i. e. the variations of the legitimate angle-detector output from a target caused by echo fading, decreases with increasing bandwidth of the AGC-servo. This decrease occurs very slowly, which is intimately related to the fact that for a Rayleigh-distributed echo signal amplitude the fading is heavy or the "signal-to-noise ratio" is small. For an AGC-bandwidth equal to 10 times the bandwidth of the fading, for instance, the variance of the multiplicative noise has only decreased to about 20 per cent of its maximum value, occurring at an extremely small AGC-bandwidth.
2. The additive angular error caused by receiver internal noise and target glint increases with increasing speed of the AGC, although rather slowly. When the ratio between the AGC- and fading bandwidths is 10, the variance of the additive angular error has increased to about 4 times its minimum value, occurring for an extremely slow AGC.
3. There exists an optimal AGC-speed at which the sum of the multiplicative and additive angular noise components becomes a minimum.

The theoretical results obtained in the present paper for the two simple monopulse radar cases agree satisfactorily with those obtained experimentally by DUNN and HOWARD [6] and by DELANO and PFEFFER [5].

Summing up it can be said that paper no. 2 shows the conditions under which a target angular tracking monopulse radar with slow AGC can function satisfactorily in the case of a fading target. It also gives information on how the AGC-speed shall be chosen with regard to the fading-speed of the echo in order that the resultant multiplicative and additive angular errors for an angle-measuring monopulse radar shall be as small as possible. Paper no. 2 is futhermore a contribution to the theory of linear, randomly time-varying control systems.

Acknowledgements

To the Saab Aircraft Company, Linköping, I should like to express my sincere thanks for the permission to publish the material presented here. I am also very much obliged to Professor Henry Wallman of the Chalmers University of Technology, without whom this thesis would never have come about, for his encouragement on many occasions. In this connection I should also like to thank Dr. Gunnar Lindström, head of the Electronics Department of the Saab Company, and Mr. Olof Perers. For many stimulating discussions on monopulse radar and valuable criticism I am greatly indebted to my colleagues Mr. Gunnar Cervin-Ellqvist and Mr. Ingemar Olsson. The numerical computations were carried out with the valuable assistance of Mr. Tore Andersson and Mr. Magnus Tideman, to whom I desire to express my gratitude, as well as to Mrs. Elsa Johansson and Miss Kerstin Franzén who helped me with the manuscript.

Linköping, 1 August 1960.

Gösta Hellgren

References

1. Page, R. M. Monopulse radar. IRE Convention Record. Part 8, 1955, pp 132—134.
2. Rhodes, Donald R. Introduction to monopulse. McGraw-Hill, New York 1959.
3. Budenbom, H. T. Monopulse automatic tracking and the thermal bound. IRE—PGMIL National Convention Record, June 19, 1957, pp 287—392.
4. Delano, R. H. A theory of target glint or angular scintillation in radar tracking. Proceedings of the IRE. Vol. 41, 1953, pp 1778—1784.
5. Delano, R. H. and Pfeffer, Irwin. The effect of AGC on radar tracking noise. Proceedings of the IRE, Vol. 47, June 1956, pp 801—810.
6. Dunn, J. H. and Howard, D. D. Phenomena of scintillation noise in radar-tracking systems. Proceedings of the IRE, Vol. 47, No. 5, May 1959, pp 855—863.
7. Krishnan, S. Diode phase detectors. Electronic & Radio Engineer, February 1959, pp. 45—60.
8. Barton, David K. Accuracy of a monopulse radar. Conference Proceedings 3rd National Convention on Military Electronics, June 29, 30, July 1, 1959, pp 179—186.
9. Cohen, William and Steinmetz, C. Martin. Amplitude- and phase-sensing monopulse system parameters. Microwave Journal, October 1959, pp 27—33 November 1959, pp. 33—38.
10. Manasse, Roger. Maximum angular accuracy of tracking a radio star by lobe comparison. IRE Transactions, Vol. AP-8, January 1960, pp 50—56.
11. Muchmore, Robert B. Aircraft scintillation spectra. IRE Transactions, Vol. AP-8, March 1960, pp 201—212.
12. Thunqvist, D. Circle diagram applied to monopulse. Foa 3 Rapport A 428, Mars 1960.

SAAB TECHNICAL NOTES
TN 42

ON THE PRINCIPLES AND ANGULAR ACCURACY OF MONOPULSE RADAR

by

GÖSTA HELLGREN

Summary

In this article the general principles of one-dimensional angle-measuring monopulse radar are first discussed. An expression for detector output signal for one or several targets is derived, and the two limiting cases of monopulse radar, the amplitude-comparison and phase-comparison types, are defined and studied in some detail. Detector output signal for small target angle deviations and the property of angle-discrimination are then discussed as well as the effects of imperfections in the high frequency and intermediate frequency parts of the receiver upon detector output signal and the angle-measuring capabilities of monopulse radar. The last part of the article deals with the contribution of internal receiver noise and target glint, or angular scintillation, to measuring error.

Saab Aircraft Company

Linköping, 18 March, 1959.

The work reported in this article is based on internal Saab-reports of the author dated 27 March 1958, 11 November 1958, and 2 December 1958.

Contents

1. Introduction

In recent years a new type of radar, called monopulse radar, has come into use, especially for automatic tracking of a target in angle and range. The principles of monopulse radar were first described by Page [1], and the method developed by Bell Telephone Laboratories, Naval Research Laboratory, and the General Electric Company in USA. Monopulse radar and conventional conical scanning radar used for automatic tracking differ mainly in the way in which information on angular position of the target is obtained.

In conical scanning radar a radar beam is rotated in space around the angular reference direction in such a way that the direction of maximum radiation describes a cone. The frequency of rotation is considerably lower than the pulse repetition frequency, and the received echo signals from a target having a direction differing from the angular reference are amplitude modulated at the rotation frequency. The two-dimensional angular position of the target is uniquely determined by the amount and phase of the amplitude modulation of the train of echo pulses. The underlying basic principle in this type of radar in obtaining angle information from a target is thus the comparison of amplitudes of consecutive echos in the video part of the receiver, as the receiving beam scans in space.

In radar of monopulse type, on the other hand, each individual echo from the target gives full information on its angular position. This is attained by a simultaneous comparison, in the high frequency (or intermediate frequency) part of the receiver, of the amplitude and phase of echo signals picked up by four stationary antennas, with beams suitably displaced in space relative to the angular reference direction. Monopulse radar has certain important advantages over conventional radar but is more complex and the electrical and mechanical requirements on a monopulse system are difficult to satisfy in practice. Low frequency amplitude-scintillations of the echos do not for instance result in angle-measuring errors in monopulse radar, as they do in conventional beam-scanning radar, in which echo amplitude-fluctuations with a frequency in the vicinity of the frequency of beam rotation are interpreted as target angle changes. In military applications monopulse radar has the further advantage of being more difficult to jam than conventional radar.

2. General principles of monopulse radar

2.1 General expression for detector output signal for one or several targets

Let us sketch the principles of monopulse radar and first restrict ourselves to the one-dimensional case, in which the purpose of the radar is to determine the direction angle in a plane of a target. Such a radar, with block-diagram given in fig. 1, generally consists of two identical antennas at distance $2\,d$ from each other and with beams inclined at an angle $\pm\,\Theta_0$ from a certain reference direction. After the antennas there follows a hybrid junction ("magic T") yielding the sum S' and the difference D' of the high frequency echo signals S_1 and S_2 picked up by the two antennas. As will become more evident below, the amplitude of the difference signal contains the information on the absolute value of the angular position Θ of the target and the phase relationship between the difference and sum signals determines the sign of Θ. After mixing the sum S' and the difference D' with the same local oscillator signal, the corresponding intermediate frequency signals are amplified in separate if-amplifiers. If the amplifications and phase shifts of the amplifiers are identical, the same relation holds between the if-output signals S_{if} and D_{if} as between S' and D', and a signal proportional to the angular position Θ can be obtained by feeding the signals S_{if} and D_{if} to a phase sensitive detector. The dependence of the constant of proportionality on the strength of the echo signal is eliminated by means of an automatic gain control that keeps the output sum-signal amplitude constant and the amplification of the two if-channels equal.

In monopulse radars using the same antennas for transmission and reception, the pulse transmitter is connected via an ordinary TR-switch to the sum-signal output of the hybrid junction. During transmission, therefore, each antenna will deliver half of the total transmitted power.

In the two-dimensional case another pair of antennas is needed, situated in a plane perpendicular to that of the preceding antennas.

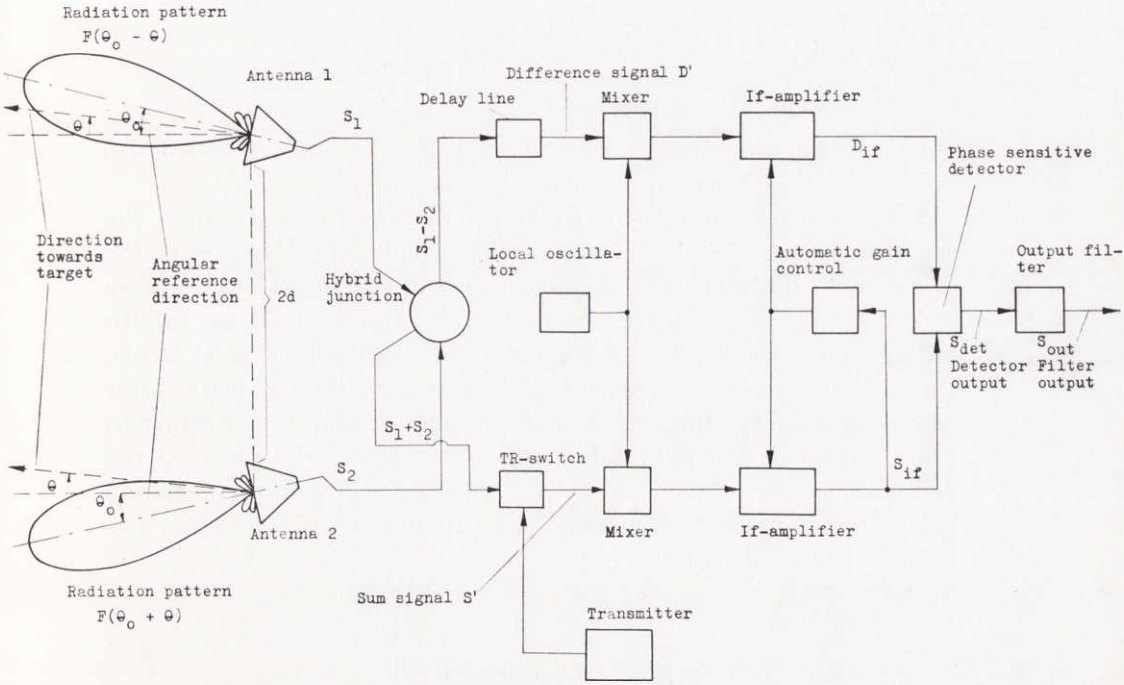

Fig. 1. Block diagram of one-dimensional angle-measuring monopulse radar.

The new angular component is obtained in the same manner as the first by forming a suitable high frequency difference signal, which requires its special if-amplifier and a second phase sensitive detector. A complete monopulse radar is consequently considerably more complicated than a radar of ordinary type.

The determination of target range is identical in monopulse and conventional radar and is therefore not described. For range determination the sum signal in monopulse radar is the suitable datum.

We now return to the one-dimensional monopulse radar shown in fig. 1 and study its angle-measuring properties in more detail. Let us suppose that the beam patterns of the individual antennas 1 and 2 are $F(\Theta_0 - \Theta)$ and $F(\Theta_0 + \Theta)$ respectively. The echo signals picked up by these antennas from a point target in the direction Θ can therefore be written as

$$\left.\begin{aligned} S_1 &= E(t)\, F(\Theta_0 - \Theta) \exp[j(\omega_c t + kd \sin \Theta)], \\ S_2 &= E(t)\, F(\Theta_0 + \Theta) \exp[j(\omega_c t - kd \sin \Theta)], \end{aligned}\right\} \qquad (2\text{-}1)$$

where

t = time,

ω_c = angular carrier frequency,

k = propagation constant ($k = 2\pi/\lambda_c$ with λ_c = carrier wavelength).

The amplitude function $E(t)$ in (2-1), which depends upon the shape and energy level of the transmitted pulses, the distance to the target, and the reflection characteristics of the target, varies very slowly from pulse to pulse. Neglecting for the moment bandwidth restrictions in the hf, if, and video parts of the receiver, $E(t)$ can be regarded as a constant independent of time, as in the CW-case. After adding and subtracting the antenna signals S_1 and S_2 according to (2-1) by means of a hybrid junction and delaying the phase of the difference signal a certain amount ψ_0, the resulting signals immediately before the mixers of the sum-signal and difference-signal channels have the following form:

$$\left.\begin{aligned} S' &= ES\, e^{j\omega_c t}, \\ D' &= ED\, e^{j(\omega_c t - \varphi_0)}, \end{aligned}\right\} \tag{2-2}$$

where

$$\left.\begin{aligned} S &= F(\Theta_0 - \Theta)\exp(jkd\sin\Theta) + F(\Theta_0 + \Theta)\exp(-jkd\sin\Theta), \\ D &= F(\Theta_0 - \Theta)\exp(jkd\sin\Theta) - F(\Theta_0 + \Theta)\exp(-jkd\sin\Theta). \end{aligned}\right\} \tag{2-3}$$

Assuming that the amplifications of the if-amplifiers of the sum and difference signals are K_S and K_D, and the corresponding phase shifts φ_S and φ_D, then the if-output signals are

$$\left.\begin{aligned} S_{\mathrm{if}} &= EK_S S e^{j(\omega_{\mathrm{if}} t - \varphi_S)}, \\ D_{\mathrm{if}} &= EK_D D e^{j(\omega_{\mathrm{if}} t - \varphi_0 - \varphi_D)}, \end{aligned}\right\} \tag{2-4}$$

where ω_{if} is the angular intermediate frequency. If the phase sensitive detector is of product type, it generates the product $s_{\mathrm{if}}\, d_{\mathrm{if}}$ of the components $s_{\mathrm{if}} = \mathrm{Re}(S_{\mathrm{if}})$ and $d_{\mathrm{if}} = \mathrm{Re}(D_{\mathrm{if}})$ of the signal vectors S_{if} and D_{if} according to (2-4), where "Re" stands for "real part of".

Of this product signal only the low (video) frequency part is used. It is easily seen that this can be written as

$$S_{\text{det}} = \tfrac{1}{2} \operatorname{Re} (S_{\text{if}} \overline{D_{\text{if}}})$$

or

$$S_{\text{det}} = \tfrac{1}{2} E^2 K_S K_D \operatorname{Re} \{e^{j(\varphi_0 + \varphi_D - \varphi_S)} S \bar{D}\}, \tag{2-5}$$

where $\bar{D}$ signifies the complex conjugate of the vector D. The purpose of the automatic gain control is to change the amplification K_S so that the sum-signal amplitude is a constant A independent of E, i. e.

$$S_{\text{if}} \overline{S_{\text{if}}} = E^2 K_S^2 S \bar{S} = A^2, \tag{2-6}$$

and at the same time maintain $K_D = K_S$. Equations (2-5) and (2-6) therefore result in the following detector output signal in the general case that the gain control does not exactly give $K_D = K_S$:

$$S_{\text{det}} = \tfrac{1}{2} A^2 K_D/K_S \frac{\operatorname{Re} \{e^{j(\varphi_0 + \varphi_D - \varphi_S)} S \bar{D}\}}{S \bar{S}}. \tag{2-7}$$

As can be seen from (2-5) and (2-7) a difference in phase shift of the if-amplifiers $\varphi_D - \varphi_S$ has the same influence on detector signal as a phase delay of the same amount in the hf-part of the difference channel, and for that reason we put

$$\psi_0' = \psi_0 + \varphi_D - \varphi_S. \tag{2-8}$$

If we finally normalize detector output by dividing by $\frac{1}{2} A^2 K_D/K_S$ we get

$$s_{\text{det}} = S_{\text{det}}/(\tfrac{1}{2} A^2 K_D/K_S) = \frac{\operatorname{Re} \{e^{j\psi_0'} S \bar{D}\}}{S \bar{S}}. \tag{2-9}$$

For N targets present at about the same range, i. e. inside the same range gate, the above derivation of detector signal can easily be generalized. Let us suppose that the n:th target has angular position Θ_n and that the corresponding echo signal is characterized by amplitude E_n and carrier phase $-\varphi_n$. Then equations (2-5), (2-6), and (2-7) are modified to read

$$S_{\text{det}} = \tfrac{1}{2}\, K_S\, K_D\, \text{Re}\, \{e^{j\varphi_0'} \sum_{n,\,m}^{N} E_n\, E_m\, S_n\, \overline{D_m}\, e^{j(\varphi_m - \varphi_n)}\}, \tag{2-10 a}$$

$$S_{\text{if}}\, \overline{S_{\text{if}}} = K_S^2 \sum_{n,\,m}^{N} E_n\, E_m\, S_n\, \overline{S_m}\, e^{j(\varphi_m - \varphi_n)} = A^2, \tag{2-10 b}$$

$$S_{\text{det}} = \tfrac{1}{2}\, A^2\, K_D/K_S\, \frac{\text{Re}\, \{e^{j\varphi_0'} \sum_{n,\,m}^{N} E_n\, E_m\, S_n\, \overline{D_m}\, e^{j(\varphi_m - \varphi_n)}\}}{\sum_{n,\,m}^{N} E_n\, E_m\, S_n\, \overline{S_m}\, e^{j(\varphi_m - \varphi_n)}}, \tag{2-10 c}$$

where

$$\left.\begin{matrix} S_n \\ D_n \end{matrix}\right\} = F\,(\Theta_0 - \Theta_n)\, \exp\,(jkd \sin\,\Theta_n) \pm$$

$$\pm\, F\,(\Theta_0 + \Theta_n)\, \exp\,(-\,jkd \sin\,\Theta_n). \tag{2-11}$$

The cross terms in equations (2-10) are harmonic functions of the phase differences $\varphi_m - \varphi_n$. In many applications these vary comparatively rapidly with time even if the relative movements between the various targets are small. Under such restrictions, which we shall assume to be satisfied in section 2.4 below, low-pass filters after the phase detector and in the AGC-circuit with a cut-off frequency less than $\left[\frac{1}{2\pi}\frac{d}{dt}\,(\varphi_m - \varphi_n)\right]_{\text{min}}$ eliminate the cross terms of the numerator and denominator in equation (2-10 c), and the normalized detector output signal can be written as

$$s_{\text{det}} = \frac{\text{Re}\, \{e^{j\varphi_0'} \sum_{n=1}^{N} E_n^2\, S_n\, \overline{D_n}\}}{\sum_{n=1}^{N} E_n^2\, S_n\, \overline{S_n}}. \tag{2-12}$$

2.2 Monopulse radar of amplitude-comparison and phase-comparison type

We now return to the case of one target and the expression for detector signal according to equation (2-9) above. With the help of (2-3) this becomes

$$s_{\text{det}} = \frac{R\,(\Theta, \Theta_0, d, \psi_0')}{[F_S\,(\Theta, \Theta_0, d)]^2}, \tag{2-13}$$

where

$$R(\Theta, \Theta_0, d, \psi_0') = \{[F(\Theta_0 - \Theta)]^2 - [F(\Theta_0 + \Theta)]^2\} \cos \psi_0' + \\ + 2 F(\Theta_0 - \Theta) F(\Theta_0 + \Theta) \sin(2 kd \sin \Theta) \sin \psi_0' \qquad (2\text{-}14)$$

and

$$[F_S(\Theta, \Theta_0, d)]^2 = [F(\Theta_0 - \Theta)]^2 + [F(\Theta_0 + \Theta)]^2 + \\ + 2 F(\Theta_0 - \Theta) F(\Theta_0 + \Theta) \cos(2 kd \sin \Theta). \qquad (2\text{-}15)$$

F_S in equation (2-15) represents the sum-beam radiation pattern of the antenna system. The first term of (2-14) is caused by a difference in sensitivity of the individual antennas in the direction of the target, while the second term is caused by difference in phase due to the different path lengths of the echo signals picked up by the antennas.

A monopulse radar is of amplitude-comparison type when the distance $2d$ between the two antennas is zero or can be neglected ($d \ll 1/(2k)$). This type of antenna system can for example be realized in the form of a parabolic reflector, in the present one-dimensional case illuminated by two feed horns that have been suitably defocused perpendicularly to the focal axis of the reflector. For a pure amplitude-comparison monopulse radar, (2-13) and (2-15) become

$$\left.\begin{aligned} s_{\text{det}} &= \frac{F(\Theta_0 - \Theta) - F(\Theta_0 + \Theta)}{F(\Theta_0 - \Theta) + F(\Theta_0 + \Theta)} \cos \psi_0', \\ F_S &= F(\Theta_0 - \Theta) + F(\Theta_0 + \Theta). \end{aligned}\right\} \qquad (2\text{-}16)$$

A certain amount of antenna beam tilting Θ_0 is necessary and maximum detector signal is obtained when $\psi_0' = 0$. If ψ_0' can not be chosen zero because of undesirable phase shifts of the sum or difference signals in the hf- or if-parts of the receiver the scale factor of the output detector signal is changed by $\cos \psi_0'$. In order to illustrate the general behaviour of the detector signal s_{det} and the sum pattern $F_S(\psi_0' = 0)$ as functions of target angle Θ when the monopulse radar is of amplitude-comparison type figs 2, 3, and 4 have been prepared, assuming an individual antenna pattern

$$F(\Theta) = \frac{1}{2} \frac{\sin(k \frac{1}{2} D\Theta)}{k \frac{1}{2} D\Theta} \qquad (2\text{-}17\text{ a})$$

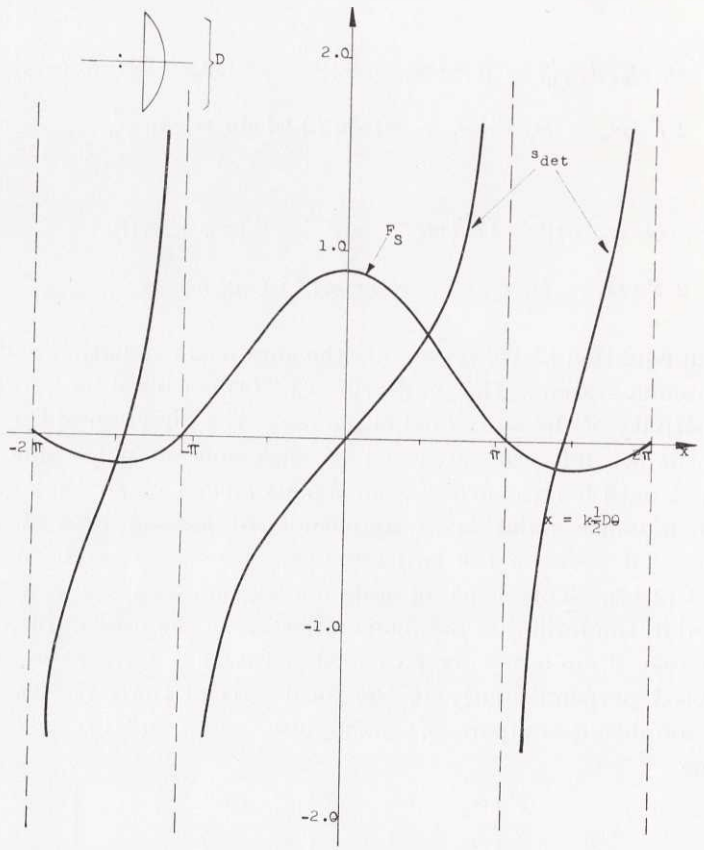

Fig. 2. Detector signal s_{det} and sum-beam pattern F_S of an amplitude-comparison monopulse radar ($d=0$), for $\psi_0'=0$, $F(\Theta)=\frac{1}{2}\,\frac{\sin(k\frac{1}{2}D\Theta)}{k\frac{1}{2}D\Theta}$, and $x_0 = k\frac{1}{2}D\Theta_0 = \pi/4$.

and the tilt angles Θ_0 given by

$$x_0 = k\,\tfrac{1}{2}\,D\Theta_0, \tag{2-17 b}$$

where x_0 is $\pi/4$, $\pi/2$, and $3\pi/4$ respectively. D in equations (2-17 a) and (2-17 b) is an antenna diameter, for example the diameter of a parabolic reflector with two defocused feeds. $F(\Theta)$ in (2-17 a) is a good approximation when Θ is small of the beam pattern of form $\sin(k\frac{1}{2}D\sin\Theta)/(k\frac{1}{2}D\sin\Theta)$ that is obtained for a uniformly illuminated rectangular aperture. In the "optimal case" $x_0=\pi/2$,

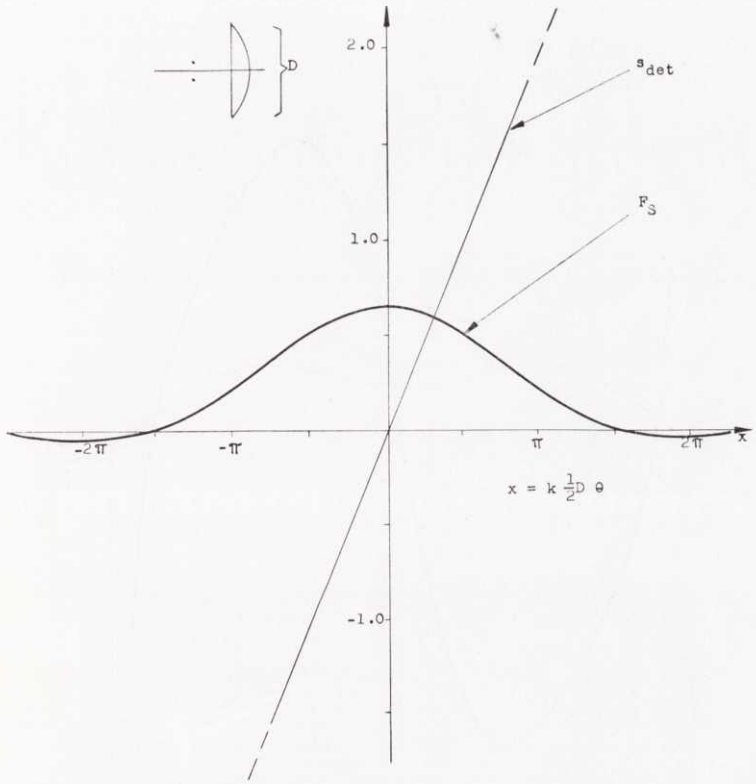

Fig. 3. Detector signal s_{det} and sum-beam pattern F_S of an amplitude-comparison monopulse radar ($d = 0$), for $\psi_0' = 0$, $F(\Theta) = \frac{1}{2} \frac{\sin (k \frac{1}{2} D\Theta)}{k \frac{1}{2} D\Theta}$, and $x_0 = k \frac{1}{2} D\Theta_0 = \frac{1}{2}\pi$.

which shows a linear relationship between s_{det} and Θ, the analytical expressions for s_{det} and F_S are

$$\left.\begin{aligned} s_{\mathrm{det}} &= (2/\pi)\, k \tfrac{1}{2} D\Theta, \\ F_S &= \frac{\frac{1}{2}\pi}{(\frac{1}{2}\pi)^2 - (k \frac{1}{2} D\Theta)^2} \cos (k \tfrac{1}{2} D\Theta). \end{aligned}\right\} \qquad (2\text{-}18)$$

When the tilt angle Θ_0 is zero or small the second term in (2-14) dominates and the monopulse radar is of phase-comparison type.

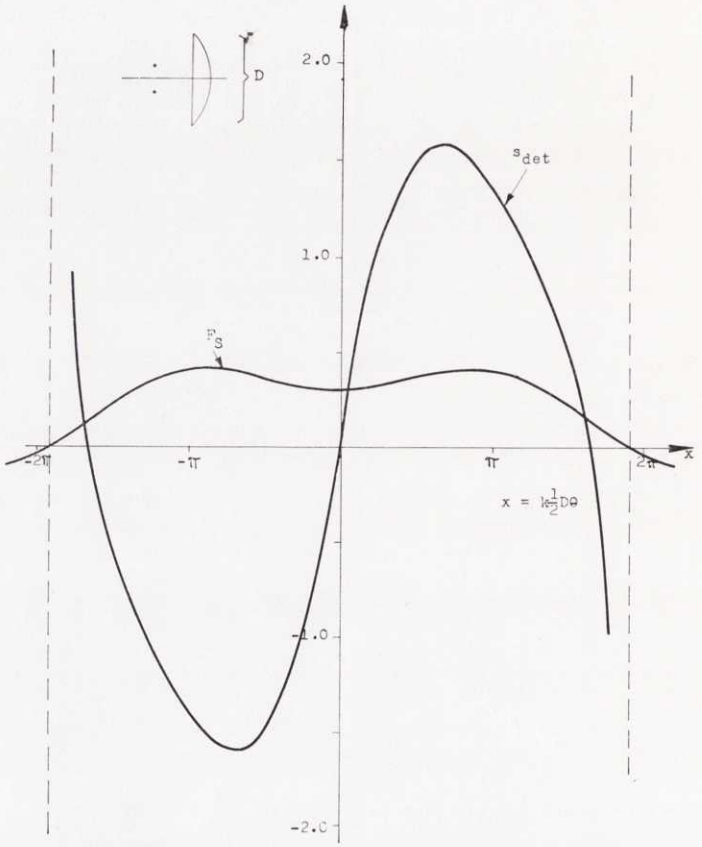

Fig. 4. Detector signal s_{det} and sum-beam pattern F_S of an amplitude-comparison monopulse radar ($d = 0$), for $\psi_0' = 0$, $F(\Theta) = \frac{1}{2} \frac{\sin (k \frac{1}{2} D\Theta)}{k \frac{1}{2} D\Theta}$, and $x_0 = k \frac{1}{2} D\Theta_0 = \frac{3\pi}{4}$.

If $\Theta_0 = 0$ the detector signal and the sum-beam pattern are as follows ($F(\Theta)$ is supposed to be an even function of Θ):

$$\left.\begin{aligned} s_{\mathrm{det}} &= \tan (kd \sin \Theta) \sin \psi_0', \\ F_S &= 2 F(\Theta) \cos (kd \sin \Theta). \end{aligned}\right\} \tag{2-19}$$

Maximum detector signal amplitude is obtained for $\psi_0' = 90°$, i. e. a phase shift $\psi_0 = 90°$ should be introduced into the difference signal

channel. Undesirable phase shifts φ_D and φ_S reduce the amplitude by the factor $\cos(\varphi_D - \varphi_S)$ in this case. It is to be observed that the detector signal is independent of the individual antenna pattern $F(\Theta)$. The ambiguity in determining target angle from detector signal, which is also present in amplitude-comparison monoupulse systems (compare figs 2 and 4), is evident from equation (2-19) and the appearance of "false" detector signal zeros when $\Theta = \arcsin[n\pi/(kd)]$, $n = 1, 2, \ldots$. However, the ambiguity is not very serious if these false zeros appear outside the main beam of the sum signal; this requires, for example, that the distance $2d$ between individual antennas in the form of electromagnetic horns should not be chosen large compared with the antenna diameter. Fig. 5 shows the detector signal s_{det} and the sum-beam pattern F_S as a function of target angle Θ in the case of a phase-comparison monopulse radar ($\Theta_0 = 0$) when $\psi_0' = 90°$ and $F(\Theta) = \frac{1}{2}\sin(kd\Theta)/(kd\Theta)$. With these assumptions equation (2-19) becomes (for Θ not too large)

$$\left.\begin{aligned} s_{\text{det}} &\cong \tan(kd\,\Theta), \\ F_S &\cong \frac{\sin(k\,2\,d\Theta)}{k\,2\,d\Theta}. \end{aligned}\right\} \tag{2-20}$$

This system can be practically realized, at least approximately, in the form of two antennas placed side by side and each with diameter $2d$. If we put $4d = D$ in the examples considered above of amplitude-comparison and phase-comparison monopulse systems, these systems can be compared on an equal footing. From fig. 3, which represents the amplitude-comparison case of greatest interest, and fig. 5, we conclude that the linearity between s_{det} and Θ is better in amplitude-comparison than in phase-comparison monopulse radar. However, the maximum antenna gain corresponding to the sum-signal is greater in the phase-comparison case, which is also characterized by greater relative side lobes.

2.3 Detector output signal for small target angle deviations

When the target angle Θ is small, as is always true when a monopulse radar receiver is the error-sensing device of an automatic target-tracking servo system, the relation between the target angle deviation

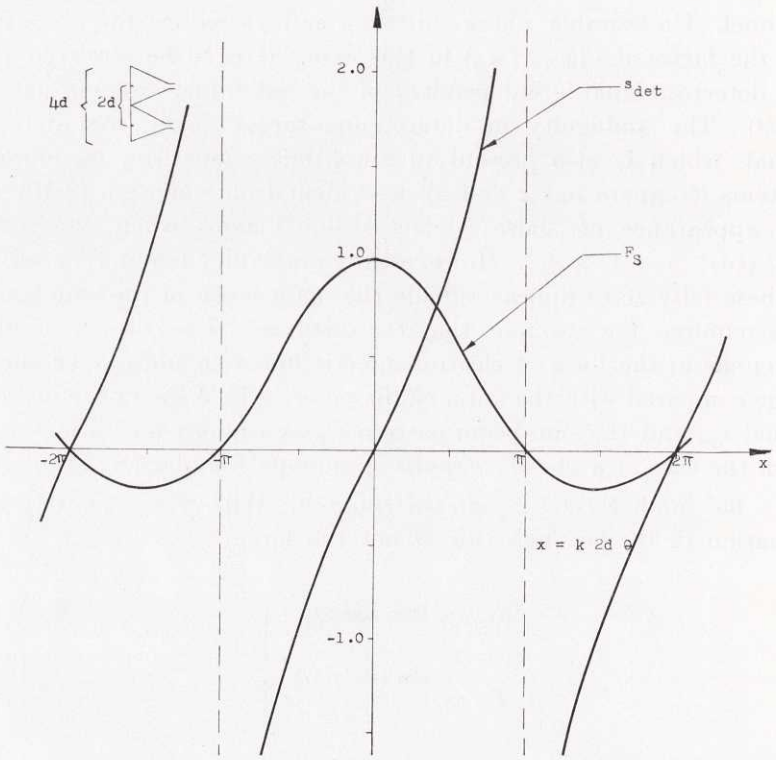

Fig. 5. Detector signal s_{det} and sum-beam pattern F_S of a phase-comparison monopulse radar ($\Theta_0 = 0$), for $\psi_0' = 90°$ and $F(\Theta) = \frac{1}{2} \frac{\sin kd\Theta}{kd\Theta}$.

Θ and the detector output signal is readily obtained from equations (2-13), (2-14), and (2-15) as

$$s_{\mathrm{det}} \cong [\cos \psi_0' \, G_A(\Theta_0) + \sin \psi_0' \, G_P(d)] \, \Theta \tag{2-21 a}$$

or

$$s_{\mathrm{det}} \cong G(\Theta_0, d, \psi_0') \, \Theta, \tag{2-21 b}$$

where

$$G(\Theta_0, d, \psi_0') = G_m(\Theta_0, d) \cos(\psi - \psi_0'), \tag{2-22}$$

$$G_m(\Theta_0, d) = \left\{ [G_A(\Theta_0)]^2 + [G_P(d)]^2 \right\}^{\frac{1}{2}}, \tag{2-23}$$

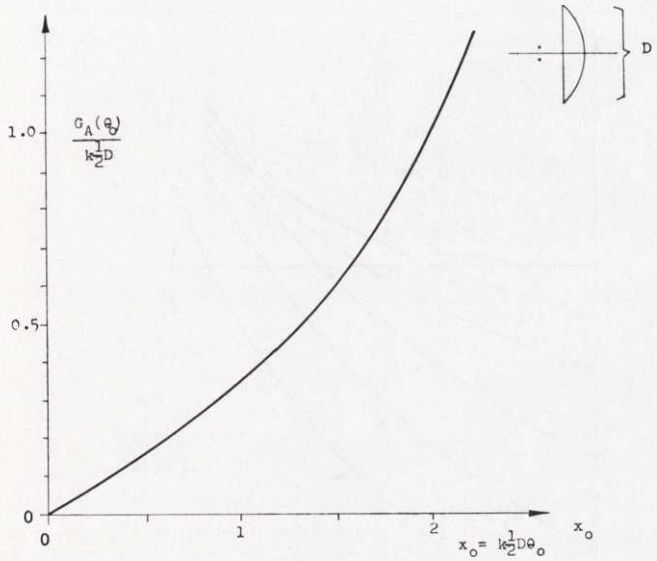

Fig. 6. Maximum angular gain G_A of an amplitude-comparison monopuse radar ($d = 0$, $\psi_0' = 0$) as a function of tilt angle for $F(\Theta) = \frac{1}{2} \sin (k \frac{1}{2} D\Theta)/(k \frac{1}{2} D\Theta)$.

$$\psi = \arctan [G_P (d)/G_A (\Theta_0)], \tag{2-24}$$

and

$$G_A (\Theta_0) = \left[- \frac{1}{F (\xi)} \frac{dF (\xi)}{d\xi} \right]_{\xi = \theta_0}, \tag{2-25}$$

$$G_P (d) = kd. \tag{2-26}$$

In the equations above the quantities G, G_m, G_A, and G_P have the character of angular gains. Maximum angular gain, $G = G_m$, is obtained when $\psi_0' = \psi$.

Fig. 6 shows as a function of the tilt angle Θ_0 the angular gain G_A of an amplitude-comparison monopulse radar ($d = 0$, $\psi_0' = 0$) according to (2-25) if the radiation pattern of the individual antennas is $F (\Theta) = \frac{1}{2} \sin (k \frac{1}{2} D\Theta)/(k \frac{1}{2} D\Theta)$. As is evident from equation (2-26) the angular gain G_P of a phase-comparison monopulse radar depends only on the distance between the antennas. In order to illustrate the behaviour in the general case of the angular gain G as a function

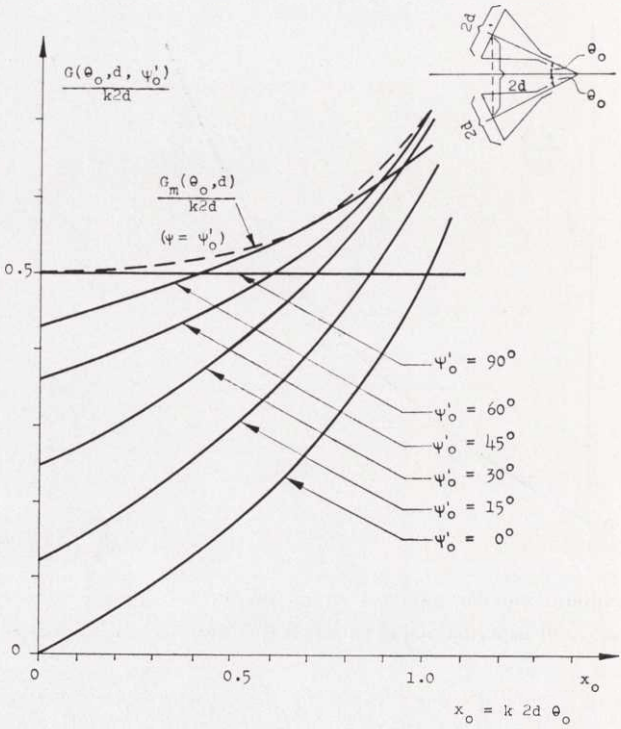

Fig. 7. Angular gain G as a function of tilt angle Θ_0 and ψ_0' for the antenna pattern $F(\Theta) = \frac{1}{2} \sin(kd\Theta)/(kd\Theta)$ and the antenna configuration shown above.

of Θ_0, d, and ψ_0' the collection of graphs of fig. 7 has been prepared. These show the angular gain obtained if, starting from the previous example of a pure phase-comparison monopulse radar, the beams of the individual antennas are tilted. For the sake of simplicity it has been assumed that the distance between the two antennas is equal to their widths, independent of the tilt angle. By tilting the individual antennas it is consequently possible to increase the maximum angular gain. This increase, however, is rather small, unless the tilt angle is chosen large. A large tilt angle has, however, a detrimental effect on the shape of the detector output curve and the sum-signal radiation pattern, as can be seen from figs 8 and 9.

2.4 The angle-discrimination property of monopulse radar

When more than one target is present in the antenna beams at about the same range the radar can not discriminate one target from

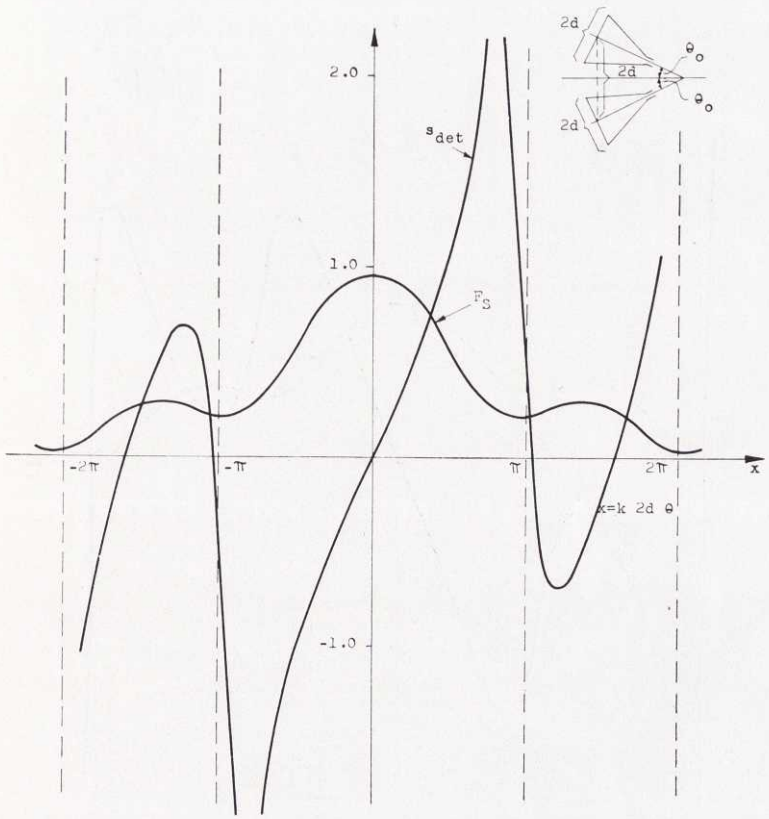

Fig. 8. Detector signal s_{det} and sum pattern F_S for $F(\Theta) = \frac{1}{2} \sin(kd\Theta)/(kd\Theta)$, $\psi_0' = \psi$, $x_0 = k2d\Theta_0 = 0.25$, and the antenna configuration shown above.

the other. In the presence of an interfering echo signal of amplitude E_2 from a target in direction Θ_2, the detector output from a legitimate target, characterized by amplitude E_1 and direction Θ_1, will be disturbed. With the help of equation (2-12) we see that the detector signal s_{det} becomes in this case

$$s_{\mathrm{det}} = \frac{E_1^2 R(\Theta_1, \Theta_0, d, \psi_0') + E_2^2 R(\Theta_2, \Theta_0, d, \psi_0')}{E_1^2 [F_S(\Theta_1, \Theta_0, d)]^2 + E_2^2 [F_S(\Theta_2, \Theta_0, d)]^2}, \qquad (2\text{-}27)$$

where as before the functions R and F_S are defined by (2-14) and (2-15). It is of special interest to study the case in which the legitimate target angle Θ_1 is small, i. e. $kd \sin \Theta_1 \ll 1$. With this assumption relation (2—27) turns out to be

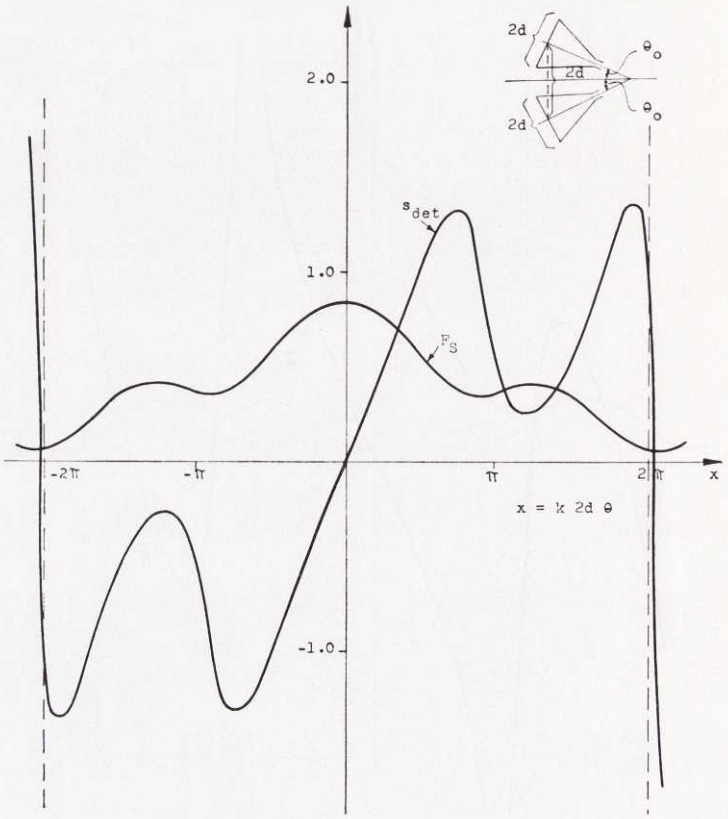

Fig. 9. Detector signal s_{det} and sum pattern F_S for $F(\Theta) = \frac{1}{2}\sin(kd\Theta)/(kd\Theta)$, $\psi_0' = \psi$, $x_0 = k2d\Theta_0 = 0.5$, and the antenna configuration shown above.

$$s_{\mathrm{det}} = \frac{G(\Theta_0, d, \psi_0')}{1 + \left[\frac{F_S(\Theta_2, \Theta_0, d)}{2F(\Theta_0)}\frac{E_2}{E_1}\right]^2} \cdot$$

$$\cdot \left\{\Theta_1 + \left[\frac{F_S(\Theta_2, \Theta_0, d)}{2F(\Theta_0)}\frac{E_2}{E_1}\right]^2 \frac{1}{G(\Theta_0, d, \psi_0')} \frac{R(\Theta_2, \Theta_0, d, \psi_0')}{[F_S(\Theta_2, \Theta_0, d)]^2}\right\}. \quad (2\text{-}28)$$

The effect of a disturbing echo signal is consequently a change of angular gain from G to G', where

$$G' = \frac{G}{1 + \left[\frac{F_S(\Theta_2)}{2F(\Theta_0)}\frac{E_2}{E_1}\right]^2}, \quad (2\text{-}29)$$

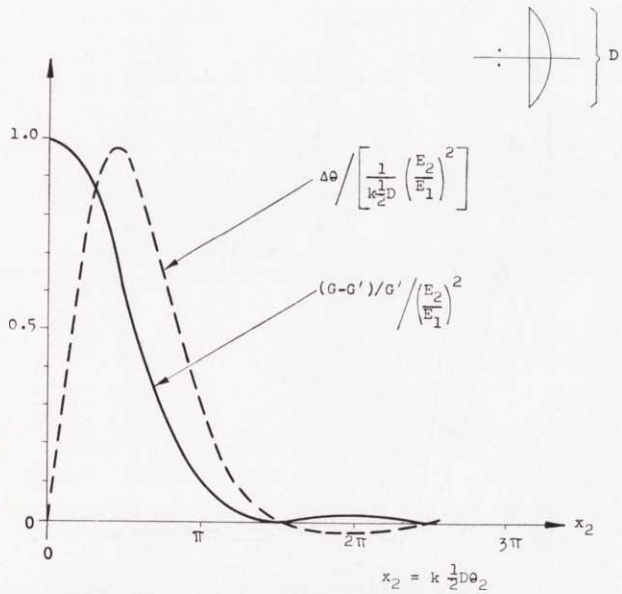

Fig. 10. The change of angular gain $(G - G') / G'$ and the angular error $\Delta\Theta$ due to an interfering target in an amplitude-comparison monopulse radar with $\psi_0' = 0°$, $F(\Theta) = \frac{1}{2} \sin(k \frac{1}{2} D \Theta) / (k \frac{1}{2} D \Theta)$, and $k \frac{1}{2} D \Theta_0 = \frac{1}{2} \pi$.

and an angular measuring error

$$\Delta\Theta = \left[\frac{F_S(\Theta_2)}{2 F(\Theta_0)} \frac{E_2}{E_1}\right]^2 \frac{1}{G} \frac{R(\Theta_2)}{[F(\Theta_2)]^2}. \tag{2-30}$$

For monopulse radar of amplitude-comparison or phase-comparison type expressions (2-29) and (2-30) can be written

a) Amplitude-comparison; $d = 0$, $\psi_0' = 0$:

$$\frac{G - G'}{G'} = \left(\frac{E_2}{E_1}\right)^2 \left[\frac{F(\Theta_0 - \Theta_2) + F(\Theta_0 + \Theta_2)}{2 F(\Theta_0)}\right]^2, \tag{2-31}$$

$$\Delta\Theta = \left(\frac{E_2}{E_1}\right)^2 \frac{1}{G_A(\Theta_0)} \frac{[F(\Theta_0 - \Theta_2)]^2 - [F(\Theta_0 + \Theta_2)]^2}{[2 F(\Theta_0)]^2}. \tag{2-32}$$

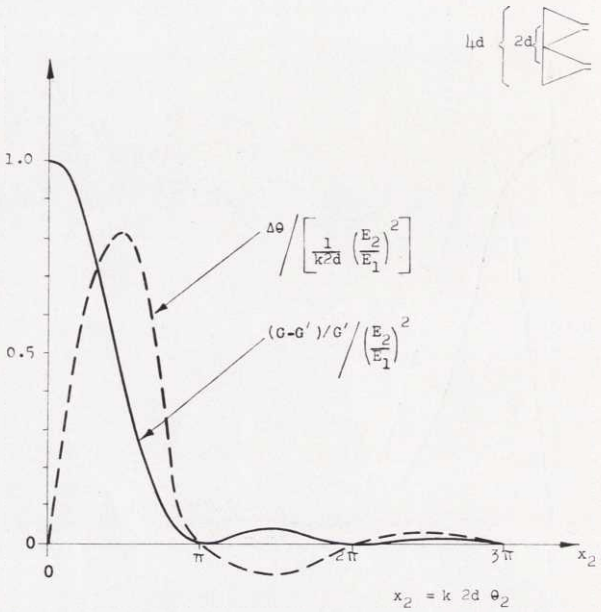

Fig. 11. The change of angular gain $(G - G') / G'$ and the angular error $\Delta\Theta$ due to an interfering target in a phase-comparison monopulse radar with $\psi_0' = 90°$ and $F(\Theta) = \frac{1}{2} \sin(kd\Theta) / (kd\Theta)$.

b) Phase-comparison; $\Theta_0 = 0$, $\psi_0' = 90°$:

$$\frac{G - G'}{G'} = \left(\frac{E_2}{E_1}\right)^2 \left[\frac{F(\Theta_2)}{F(0)}\right]^2 \cos^2(kd \sin \Theta_2), \tag{2-33}$$

$$\Delta\Theta = \left(\frac{E_2}{E_1}\right)^2 \left[\frac{F(\Theta_2)}{F(0)}\right] \frac{\sin(2\,kd \sin \Theta_2)}{2\,G_P(d)}. \tag{2-34}$$

Fig. 10 illustrates graphically the dependence of $(G - G') / G'$ and $\Delta\Theta$ upon Θ_2 according to (2-31) and (2-32), when the antenna pattern and the tilt angle have been chosen as $F(\Theta) = \frac{1}{2} \sin(k \frac{1}{2} D\Theta) / / (k \frac{1}{2} D\Theta)$ and $k \frac{1}{2} D\Theta_0 = \frac{1}{2}\pi$. Fig. 11, finally, shows $(G - G') / G'$ and $\Delta\Theta$ as functions of Θ_2 in the phase-comparison case, equations (2-33) and (2-34), with $F(\Theta) = \frac{1}{2} \sin(kd\,\Theta) / (kd\,\Theta)$. A comparison between the two examples of monopulse radar for the same total antenna area $D = 4\,d$ reveals that the amplitude type is somewhat

more sensitive to a disturbing target inside the sum-signal beam. Outside the beam the situation is reversed.

As for the effect of an interfering echo signal on the change of angular gain and the angular error in the general case of arbitrary d, Θ_0, and ψ_0', equations (2-29) and (2-30), we restrict ourselves to giving the results of a conservative estimate of these effects:

$$\frac{G - G'}{G'} \leq \left(\frac{E_2}{E_1}\right)^2 \left[\frac{F(\Theta_0 - \Theta_2) + F(\Theta_0 + \Theta_2)}{2F(\Theta_0)}\right]^2, \quad (2\text{-}35)$$

$$|\Delta\Theta| \leq \left(\frac{E_2}{E_1}\right)^2 \frac{1}{G} \frac{[F(\Theta_0 - \Theta_2)]^2 + [F(\Theta_0 + \Theta_2)]^2}{2[F(\Theta_0)]^2}. \quad (2\text{-}36)$$

In this connection it should be pointed out that what we have discussed above is the discrimination property of the monopulse receiver itself. If the monopulse radar is active and the transmitter connected to the sum-signal channel via the TR-switch the echo amplitudes E_1 and E_2 become proportional to $F_S(\Theta_1, \Theta_0, d)$ and $F_S(\Theta_2, \Theta_0, d)$, which must be taken into consideration when studying the resultant detector signal s_{det}, G' and $\Delta\Theta$.

3. The influence of imperfections in hf-circuits upon detector output signal

3.1 General expression for detector signal for nonideal hf-circuits

A question of great practical importance in connection with monopulse radar is the influence of imperfections in the hf and if parts of the receiver upon detector output signal and angle-measuring capability of the radar. The imperfections may be due to difficulties in realizing the necessary electrical and mechanical tolerances, unavoidable misalignment of the circuits when used in a certain band of frequencies etc. In this chapter we shall study the effect of hf-imperfections. This has recently been done by L. THOUREL for a certain monopulse radar of amplitude-comparison type [2]. Our treatment here is somewhat more general and results in analytical expressions for various effects of imperfections upon angular gain and accuracy of angular measurement.

In studying the influence of hf-imperfections we may neglect the pulse character of the signals because the hf-bandwidth is almost always considerably greater than the width of the pulse spectrum (this simplification is not permissible in a study of if-imperfections, which case is treated in the next chapter). Under these circumstances, the primary formal effect of imperfections in the hf-circuits is a change of the expressions for the sum S and the difference signal vectors D of equations (2-3). The ideal forms of these expressions are, in matrix notation,

$$\begin{bmatrix} S \\ D \end{bmatrix} = \begin{bmatrix} 1 & 1 \\ 1 & -1 \end{bmatrix} \times \begin{bmatrix} s_1 \\ s_2 \end{bmatrix}, \tag{3-1}$$

where

$$\left.\begin{aligned} s_1 &= F(\Theta_0 - \Theta) \exp(jkd \sin \Theta), \\ s_2 &= F(\Theta_0 + \Theta) \exp(-jkd \sin \Theta). \end{aligned}\right\} \tag{3-2}$$

The matrix in (3-1) can for convenience be denoted by A_0, i. e.

$$A_0 = \begin{bmatrix} 1 & 1 \\ 1 & -1 \end{bmatrix}. \tag{3-3}$$

In the general case of non-ideal hf-circuits the matrix A_0 is changed to A, i. e.

$$\begin{bmatrix} S \\ D \end{bmatrix} = A \times \begin{bmatrix} s_1 \\ s_2 \end{bmatrix}, \tag{3-4}$$

where A may be supposed to have the form

$$A = \begin{bmatrix} \varrho_{11}\, e^{j\varphi_{11}} & \varrho_{12}\, e^{j\varphi_{12}} \\ \varrho_{21}\, e^{j\varphi_{21}} & -\varrho_{22}\, e^{j\varphi_{22}} \end{bmatrix}. \tag{3-5}$$

The quantities $\varrho_{\mu\nu}$ of (3-5) are all assumed to be positive and real and all $\varphi_{\mu\nu}$ real.

To start with, we readily deduce the complete expression for the detector output signal s_{det} from equation (2-9) subject to (3-4) and (3-5), which is

$$s_{\text{det}} = \frac{R'(\Theta, \Theta_0, d, \psi_0')}{[F_S'(\Theta, \Theta_0, d)]^2}, \tag{3-6}$$

where

$$\begin{aligned} R'(\Theta, \Theta_0, d, \psi_0') = {} & \varrho_{11}\varrho_{21}[F(\Theta_0 - \Theta)]^2 \cos(\psi_0' + \varphi_{11} - \varphi_{21}) - \\ & - \varrho_{12}\varrho_{22}[F(\Theta_0 + \Theta)]^2 \cos(\psi_0' + \varphi_{12} - \varphi_{22}) - \\ & - F(\Theta_0 - \Theta)\, F(\Theta_0 + \Theta) \cdot \\ & \cdot [\varrho_{11}\varrho_{22} \cos(2\,kd \sin\Theta + \psi_0' + \varphi_{11} - \varphi_{22}) - \\ & - \varrho_{12}\varrho_{21} \cos(2\,kd \sin\Theta - \psi_0' - \varphi_{12} + \varphi_{21})], \end{aligned} \tag{3-7}$$

and

$$\begin{aligned} [F_S'(\Theta, \Theta_0, d)]^2 = {} & \varrho_{11}^2 [F(\Theta_0 - \Theta)]^2 + \varrho_{12}^2 [F(\Theta_0 + \Theta)]^2 + \\ & + 2\,\varrho_{11}\varrho_{12}\, F(\Theta_0 - \Theta)\, F(\Theta_0 + \Theta) \cos(2\,kd \sin\Theta + \varphi_{11} - \varphi_{12}). \end{aligned} \tag{3-8}$$

In practice the quantities $\varrho_{\mu\nu}$ are almost always very close to unity and the phase angles $\varphi_{\mu\nu}$ can be considered small, which helps in dealing with the general expressions above. We therefore suppose that

$$\left.\begin{aligned} &\varrho_{\mu\nu} = 1 + \Delta\varrho_{\mu\nu}, \\ &|\Delta\varrho_{\mu\nu}| \ll 1, \\ &|\varphi_{\mu\nu}| \ll 1, \\ &\mu \text{ and } \nu = 1, 2. \end{aligned}\right\} \tag{3-9}$$

After some tedious but straightforward algebraic manipulations we arrive at the following first order approximation of the detector output signal, which holds for small target angle deviations Θ (compare equation (2-21 a)):

$$s_{\text{det}} \cong \left[\frac{\cos\psi_0' \left(1 + \frac{1}{2}\left[\Delta\varrho_{11} + \Delta\varrho_{12} + \Delta\varrho_{21} + \Delta\varrho_{22}\right]\right) - \frac{1}{2}\sin\psi_0' \left(\varphi_{11} + \varphi_{12} - \varphi_{21} - \varphi_{22}\right)}{1 + \Delta\varrho_{11} + \Delta\varrho_{12}} G_A(\Theta_0) + \right.$$

$$\left. + \frac{\sin\psi_0' \left(1 + \frac{1}{2}\left[\Delta\varrho_{11} + \Delta\varrho_{12} + \Delta\varrho_{21} + \Delta\varrho_{22}\right]\right) + \frac{1}{2}\cos\psi_0' \left(\varphi_{11} + \varphi_{12} - \varphi_{21} - \varphi_{22}\right)}{1 + \Delta\varrho_{11} + \Delta\varrho_{12}} G_P(d) \right] \cdot$$

$$\cdot \left\{ \Theta + \frac{1}{2} \frac{\left(\Delta\varrho_{21} - \Delta\varrho_{22}\right)\cos\psi_0' + \left(\varphi_{21} - \varphi_{22}\right)\sin\psi_0'}{\cos\psi_0' G_A(\Theta_0) + \sin\psi_0' G_P(d)} \right\}. \tag{3-10}$$

As is seen from (3-10) the effects of imperfections in the hf-part of the monopulse receiver are a change of angular gain and a shift of the angular reference direction of the system, which is converted into a degradation of the angle-measuring functions of the radar in the case that the effects can not be predicted or compensated for.

When the monopulse radar is of amplitude-comparison or phase-comparison type, (3-10) takes the forms

a) Amplitude-comparison; $d = 0$:

$$s_{\text{det},\,A} \cong \left[1 + \frac{1}{2}\left(-\Delta\varrho_{11} - \Delta\varrho_{12} + \Delta\varrho_{21} + \Delta\varrho_{22}\right) - \right.$$

$$\left. - \frac{1}{2}\left(\varphi_{11} + \varphi_{12} - \varphi_{21} - \varphi_{22}\right)\tan\psi_0' \right] \cos\psi_0' G_A(\Theta_0) \cdot$$

$$\cdot \left\{ \Theta + \frac{1}{2} \frac{\left(\Delta\varrho_{21} - \Delta\varrho_{22}\right) + \left(\varphi_{21} - \varphi_{22}\right)\tan\psi_0'}{G_A(\Theta_0)} \right\}. \tag{3-11}$$

b) Phase-comparison; $\Theta_0 = 0$:

$$s_{\text{det},P} \cong \left[1 + \tfrac{1}{2}(-\Delta\varrho_{11} - \Delta\varrho_{12} + \Delta\varrho_{21} + \Delta\varrho_{22}) + \right.$$
$$\left. + \tfrac{1}{2}(\varphi_{11} + \varphi_{12} - \varphi_{21} - \varphi_{22}) \cot \psi_0'\right] \sin \psi_0' \, G_P(d) \cdot$$
$$\cdot \left\{\Theta + \frac{1}{2} \frac{(\Delta\varrho_{21} - \Delta\varrho_{22}) \cot \psi_0' + (\varphi_{21} - \varphi_{22})}{G_P(d)}\right\}. \quad (3\text{-}12)$$

According to the last two expressions the shift of the angular reference (the angular error) of a monopulse radar of amplitude type ($\psi_0' \cong 0$) is more sensitive to amplitude than to phase imperfections, but in the case of a radar of phase type ($\psi_0' \cong 90°$) the situation is the reverse, as might be expected. The angular gain is mainly influenced by amplitude anomalies in the two cases.

3.2 Angular gain and angular error for typical hf-circuit imperfections

We shall now give some examples of hf-circuit anomalies and numerically estimate their influence upon angular error in the two fundamental types of monopulse radars as given by (3-11) and (3-12) above.

Case I. If there is somewhat more attenuation and/or phase shift before the hybrid junction in one channel, say in the one transmitting the signal S_2, than in the other, the matrix A becomes

$$A = \begin{bmatrix} 1 & \mu e^{-j\varphi} \\ 1 & -\mu e^{-j\varphi} \end{bmatrix}, \quad (3\text{-}13)$$

where $|1 - \mu| \ll 1$ and $|\varphi| \ll 1$. Putting $\Delta\varrho_{11} = \Delta\varrho_{21} = 0$, $\Delta\varrho_{12} = \Delta\varrho_{22} = -(1 - \mu)$, $\varphi_{11} = \varphi_{21} = 0$, and $\varphi_{12} = \varphi_{22} = -\varphi$ into (3-11) and (3-12) respectively gives

$$\left.\begin{aligned} s_{\text{det},A} &\cong \cos \psi_0' \, G_A(\Theta_0) \left[\Theta + \frac{1}{2}\frac{1-\mu}{G_A} + \frac{1}{2}\frac{\varphi}{G_A} \tan \psi_0'\right], \\ s_{\text{det},P} &\cong \sin \psi_0' \, G_P(d) \left[\Theta + \frac{1}{2}\frac{1-\mu}{G_P} \cot \psi_0' + \frac{1}{2}\frac{\varphi}{G_P}\right]. \end{aligned}\right\} \quad (3\text{-}14)$$

In this connection it should be mentioned that the reciprocal of G_A is always about half the sum-pattern beamwidth Θ_b and the

same is usually true with G_P, as in the example given in chapter 2 and shown in fig. 5. Assuming $1/G_A \cong 1/G_P \cong \frac{1}{2}\,\Theta_b$ and requiring for example that the individual contributions to the angular shift given by (3-14) in the two cases with optimal choice of ψ_0' should not exceed $0.01\,\Theta_b$, then $1 - \mu$ should be less than $4 \cdot 10^{-2}$, which corresponds to a maximum attenuation of 0.3 dB, and φ not larger than 2°.

Case II. Suppose that there is more attenuation and/or more phase shift than necessary after the hybrid junction in one channel, say in the one transmitting the difference signal D' according to fig. 1. The matrix A is now

$$A = \begin{bmatrix} 1 & 1 \\ \mu e^{-j\varphi} & -\mu e^{-j\varphi} \end{bmatrix} \tag{3-15}$$

and the output signals become

$$\left.\begin{aligned} s_{\mathrm{det},\,A} &\cong \left[1 - (1-\mu) - \varphi \tan \psi_0'\right] \cos \psi_0'\, G_A\,(\Theta_0)\; \Theta, \\ s_{\mathrm{det},\,P} &\cong \left[1 - (1-\mu) + \varphi \cot \psi_0'\right] \sin \psi_0'\, G_P\,(d)\; \Theta, \end{aligned}\right\} \tag{3-16 a}$$

with $|1 - \mu| \ll 1$ and $|\varphi| \ll 1$.

In fact, all the analytical expressions for detector signal derived in the preceding chapter, e. g. (2-13), (2-16), (2-19), and (2-21), cover the case treated for arbitrarily large μ and φ. It is only necessary to replace ψ_0' by $\psi_0' + \varphi$ and introduce the factor μ, as is evident from relation (2-9) on replacing D by $\mu e^{-j\varphi} D$. According to (2-21 a), therefore, for small angles Θ the detector signal should read

$$\left.\begin{aligned} s_{\mathrm{det},\,A} &\cong \mu \cos\,(\psi_0' + \varphi)\, G_A\,(\Theta_0)\; \Theta, \\ s_{\mathrm{det},\,P} &\cong \mu \sin\,(\psi_0' + \varphi)\, G_P\,(\Theta_0)\; \Theta, \end{aligned}\right\} \tag{3-16 b}$$

to which (3-16 a) is a good approximation for $|1 - \mu| \ll 1$ and $|\varphi| \ll 1$.

Consequently, there is only a change of angular gain due to attenuation and phase shift in this case. For $\mu = 0.9$, which corresponds to an attenuation of 0.9 dB, the angular gain is decreased by 10 percent. A phase shift of 25° will also give the same decrease, if ψ_0' is optimally chosen in the two types of monopulse radar.

Case III. If the hybrid junction is not completely balanced the matrix A may happen to take the form

$$A = \begin{bmatrix} 1 & \mu e^{-j\varphi} \\ \mu e^{-j\varphi} & -1 \end{bmatrix}, \tag{3-17}$$

where μ is assumed to be close to 1 and φ small. Putting $\Delta\varrho_{11} = \Delta\varrho_{22} = 0$, $\Delta\varrho_{12} = \Delta\varrho_{21} = \mu - 1$, $\varphi_{11} = \varphi_{22} = 0$, and $\varphi_{12} = \varphi_{21} = -\varphi$ into (3-11) and (3-12) gives

$$\left.\begin{aligned} s_{\text{det},A} &\cong \cos\psi_0' \, G_A(\Theta_0) \left[\Theta - \frac{1}{2}\frac{1-\mu}{G_A} - \frac{1}{2}\frac{\varphi}{G_A}\tan\psi_0'\right], \\ s_{\text{det},P} &\cong \sin\psi_0' \, G_P(d) \left[\Theta - \frac{1}{2}\frac{1-\mu}{G_P}\cot\psi_0' - \frac{1}{2}\frac{\varphi}{G_P}\right]. \end{aligned}\right\} \tag{3-18}$$

Because (3-18) and (3-14) are almost identical, the same comments as given under "Case I" apply here and need therefore not be repeated.

Case IV. If the input and output arms of the hybrid junction are not perfectly matched, the matrix A is easily shown to be of the following form (see for example [2], pp 138—139):

$$A = c \begin{bmatrix} 1 + \Gamma_2\Gamma_3 & 1 + \Gamma_1\Gamma_3 \\ 1 + \Gamma_2\Gamma_4 & -(1 + \Gamma_1\Gamma_4) \end{bmatrix}, \tag{3-19}$$

where the Γ_ν are the reflection coefficients in the different arms, and c is a constant depending upon the Γ_ν which can be neglected in this connection because both S and D are to be multiplied by c. If the absolute values of the individual Γ_ν are small, A can be written (neglecting c) as

$$A \cong \begin{bmatrix} [1+|\Gamma_2\Gamma_3|\cos(\varphi_2+\varphi_3)]\, e^{j|\Gamma_2\Gamma_3|\sin(\varphi_2+\varphi_3)} & [1+|\Gamma_1\Gamma_3|\cos(\varphi_1+\varphi_3)]\, e^{j|\Gamma_1\Gamma_3|\sin(\varphi_1+\varphi_3)} \\ [1+|\Gamma_2\Gamma_4|\cos(\varphi_2+\varphi_4)]\, e^{j|\Gamma_2\Gamma_4|\sin(\varphi_2+\varphi_4)} & -[1+|\Gamma_1\Gamma_4|\cos(\varphi_1+\varphi_4)]\, e^{j|\Gamma_1\Gamma_4|\sin(\varphi_1+\varphi_4)} \end{bmatrix}, \tag{3-20}$$

where φ_ν is the phase angle of Γ_ν.

If in order to make a conservative estimate of these effects of mismatch upon detector signal we put $|\Delta\varrho_{11}| = |\Delta\varrho_{12}| = |\Delta\varrho_{21}| = |\Delta\varrho_{22}| = |\Gamma^2|$ and $|\varphi_{11}| = |\varphi_{12}| = |\varphi_{21}| = |\varphi_{22}| = |\Gamma^2|$, which is a

reasonable choice according to (3-20), then by means of (3-11) and (3-12) we arrive at the following detector signals:

$$\left.\begin{aligned} s_{\mathrm{det},\,A} &\cong \left[1 \pm 2\,|\Gamma|^2\,(1+\tan\psi_0')\right]\cos\psi_0'\,G_A(\Theta_0)\left[\Theta \pm \frac{|\Gamma|^2}{G_A}\,(1+\tan\psi_0')\right], \\ s_{\mathrm{det},\,P} &\cong \left[1 \pm 2\,|\Gamma|^2\,(1+\cot\psi_0')\right]\sin\psi_0'\,G_P(d)\quad\left[\Theta \pm \frac{|\Gamma|^2}{G_P}\,(1+\cot\psi_0')\right]. \end{aligned}\right\} \tag{3-21}$$

Assuming, as under "Case I" above, that $1/G_A \cong 1/G_P \cong \frac{1}{2}\,\Theta_b$, where Θ_b is the sum-pattern beamwidth, and requiring for instance that the angular error given by (3-21) in the two cases should not exceed $0.01\,\Theta_b$ with $\psi_0' = 0$ and $90°$ respectively, then $|\Gamma|$ must be less than 15 percent or the standing wave ratio less than 1.3.

From the cases treated above it is seen that attenuation and phase difference between the two signal channels of a monopulse receiver before the hybrid junction will in the first approximation only cause error in determination of angle, as is also the case for phase and attenuation unbalances of the hybrid junction itself. The examples show that even small differences of this type give rise to significant angular errors. Attenuation and phase differences introduced after the hybrid junction result on the contrary only in a change of angular gain. This is generally less important than angular error, especially in the case of an automatic tracking monopulse radar, and larger attenuations and phase shifts can therefore be tolerated.

4. The influence of imperfections in if-circuits upon detector output signal

4.1 General expression for detector output signal for pulsed signals and band-limited if-circuits

Neglecting (as is permissible when CW or comparatively long pulses are used) the difficulties imposed by the fact that the frequency transmission band of the if-amplifiers is limited, it has already been shown in chapter 2 that a difference in phase shift, or amplification, of the if-amplifiers influences the value of ψ_0' and the normalizing constant $\frac{1}{2} A^2 K_D/K_S$ of the detector output. This type of if-circuit imperfection is therefore equivalent to the hf-type treated in the preceding chapter under 3.2 "Case II", and does not require further study. In many practical cases, however, the frequency-band limitations of the if-circuits must be taken into account, and one very important question in this connection is the effect upon detector output signal of changes in the phase and amplitude characteristics of the two if-channels for different types of if-amplifiers and amplifier bandwidths. Such changes may for instance be due to the fact that the input capacitances of the tubes of the amplifiers vary with AGC-voltage. In order to be able to study this question we shall first derive a general expression for detector output signal when the pulse character of the echos and the frequency band restrictions of the if-circuits are taken into account.

We assume, as before, that there are no bandwidth limitations in the hf-circuits of the monopulse receiver, i. e. in the antennas, transmission lines (wave guides), hybrid junction, and mixers. Let us also suppose that the echo signal S_0 is a train of rectangular radar pulses of amplitude E_0, pulse length τ, pulse repetition frequency f_r, and carrier frequency $f_c = 2\pi\omega_c$, which has the following Fourier representation

$$S_0 = E_0 f_r \tau \sum_{n=-\infty}^{+\infty}{}' \frac{\sin(n\pi f_r \tau)}{n\pi f_r \tau} \exp[j\, 2\pi (f_c - n f_r)\, t]. \qquad (4\text{-}1)$$

The echo signals picked up by the two antennas can now be written as

$$\left.\begin{aligned} S_1 &= E_0 f_r \tau F(\Theta_0 - \Theta) \exp(jkd \sin\Theta) \sum_{n=-\infty}^{+\infty} \frac{\sin(n\pi f_r \tau)}{n\pi f_r \tau} \exp[j 2\pi (f_c - n f_r) t], \\ S_2 &= E_0 f_r \tau F(\Theta_0 + \Theta) \exp(-jkd \sin\Theta) \sum_{n=-\infty}^{+\infty} \frac{\sin(n\pi f_r \tau)}{n\pi f_r \tau} \exp[j 2\pi (f_c - n f_r) t]. \end{aligned}\right\} \quad (4\text{-}2)$$

Immediately before the mixers the signals of the sum and difference channels therefore become

$$\left.\begin{aligned} S' &= E_0 f_r \tau S \sum_{n=-\infty}^{+\infty} \frac{\sin(n\pi f_r \tau)}{n\pi f_r \tau} \exp[j 2\pi (f_c - n f_r) t], \\ D' &= E_0 f_r \tau D \sum_{n=-\infty}^{+\infty} \frac{\sin(n\pi f_r \tau)}{n\pi f_r \tau} \exp[j 2\pi (f_c - n f_r) t - j\psi_0], \end{aligned}\right\} \quad (4\text{-}3)$$

where S and D are defined as before by (2-3).

Before proceeding we define the if-amplifier frequency functions G_S and G_D of the sum and difference signals as

$$\left.\begin{aligned} G_S(f) &= K_S a_S(f - f_{if} - \Delta_S) \exp[-j\varphi_S(f - f_{if} - \Delta_S)], \\ G_D(f) &= K_D a_D(f - f_{if} - \Delta_D) \exp[-j\varphi_D(f - f_{if} - \Delta_D)]. \end{aligned}\right\} \quad (4\text{-}4)$$

In (4-4) a_S and a_D are amplitude functions, which have been normalized so that $a_S(0) = a_D(0) = 1$. The corresponding phase functions are φ_S and φ_D, and K_S and K_D are as before the amplifications of the two channels and f_{if} the intermediate frequency ($= 2\pi\omega_{if}$). The symbol Δ_S and Δ_D represent the detuning of the sum and difference signal if-amplifier relative to the intermediate frequency. After mixing and amplification of the resulting if-signals the following output signals are obtained in the sum and difference signal channels, as follows from (4-3) and the definitions in (4-4):

$$\left.\begin{aligned} S_{if} &= E_0 f_r \tau K_S S \sum_{n=-\infty}^{+\infty} a_S(n f_r - \Delta_S) \frac{\sin(n\pi f_r \tau)}{n\pi f_r \tau} \exp[j 2\pi (f_{if} + \\ &\quad + n f_r) t - j\varphi_S(n f_r - \Delta_S)], \\ D_{if} &= E_0 f_r \tau K_D D \sum_{n=-\infty}^{+\infty} a_D(n f_r - \Delta_D) \frac{\sin(n\pi f_r \tau)}{n\pi f_r \tau} \exp[j 2\pi (f_{if} + \\ &\quad + n f_r) t - j\varphi_D(n f_r - \Delta_D) - j\psi_0]. \end{aligned}\right\} \quad (4\text{-}5)$$

The phase sensitive detector is supposed to generate the product of the components of the signal vectors S_{if} and D_{if}, of which only the low (video) frequency component is used:

$$S'_{\text{det}} = \frac{1}{2}(E_0 f_r \tau)^2 K_S K_D \operatorname{Re}\left\{e^{j\varphi_0} S \bar{D} \sum_{m,n} a_S(nf_r - \Delta_S)\, a_D(mf_r - \Delta_D) \cdot \right.$$

$$\cdot \frac{\sin(n\pi f_r \tau)}{n\pi f_r \tau} \frac{\sin(m\pi f_r \tau)}{m\pi f_r \tau} \exp[j\,2\pi(n-m) f_r t +$$

$$\left. + j\varphi_D(mf_r - \Delta_D) - j\varphi_S(nf_r - \Delta_D)]\right\}. \qquad (4\text{-}6)$$

As is seen from relation (4-6), the low frequency output signal from the phase detector consists of a dc-signal ($m = n$) and harmonic signals ($m \neq n$), with frequencies that are multiples of the pulse repetition frequency f_r, usually about 1000 c/s. In the following we assume that the harmonic components are filtered out and that we are only interested in the dc-signal, i. e.

$$S_{\text{det}} = \frac{1}{2}(E_0 f_r \tau)^2 K_S K_D \operatorname{Re}\left\{e^{j\varphi_0} S \bar{D} \sum_{n=-\infty}^{+\infty} a_S(nf_r - \Delta_S) \cdot \right.$$

$$\left. \cdot a_D(nf_r - \Delta_D) \left[\frac{\sin(n\pi f_r \tau)}{n\pi f_r \tau}\right]^2 \exp[j\varphi_D(nf_r - \Delta_D) - j\varphi_S(nf_r - \Delta_S)]\right\}. \qquad (4\text{-}7)$$

The automatic gain control, the input of which is the output S_{if} of the sum-signal channel, is assumed to control the amplification K_S so that

$$(E_0 f_r \tau)^2 K_S S\bar{S} \sum_{n=-\infty}^{+\infty} [a_S(nf_r - \Delta_S)]^2 \left[\frac{\sin(n\pi f_r \tau)}{n\pi f_r \tau}\right]^2 = A^2, \qquad (4\text{-}8)$$

where as before A is constant. Such a control requires a square-law detector in the AGC-circuit and the filtering out of signal components after the detector with frequencies including and exceeding the pulse repetition frequency f_r. The assumption of a square-law AGC-detector is consistent with the assumption of a phase sensitive detector of product type. If a linear envelope detector is used in the AGC-circuit the phase detector should also be of a "linear" type. In this case the mathematical treatment of the present problem is much

more difficult, but it does not, as may be expected, radically alter the results. For a phase sensitive detector of product type and a square-law AGC-detector equation (4-7) and (4-8) give the desired output signal

$$s_{\text{det}} = \frac{\operatorname{Re}\left\{e^{j\varphi_0} S \bar{D} \sum_{n=-\infty}^{+\infty} a_S(nf_r - \Delta_S)\, a_D(nf_r - \Delta_D) \left[\frac{\sin(n\pi f_r \tau)}{n\pi f_r \tau}\right]^2 \exp\left[j\varphi_D(nf_r - \Delta_D) - j\varphi_S(nf_r - \Delta\right.\right.}{S \bar{S} \sum_{n=-\infty}^{+\infty} [a_S(nf_r - \Delta_S)]^2 \left[\frac{\sin(n\pi f_r \tau)}{n\pi f_r \tau}\right]^2} \tag{4}$$

where $s_{\text{det}} = S_{\text{det}}/(\frac{1}{2} A^2 K_D/K_S)$. Expression (4-9) for the detector output passes over, as it should, into that given by equation (2-9) when the pulse character of the echo signals disappears, i. e. when $f_r \tau = 1$, and $\Delta_S = \Delta_D = 0$.

If we introduce the vector ϱ of absolute value $|\varrho|$ and phase angle φ_ρ defined by

$$\varrho = |\varrho| e^{j\varphi_\rho} = \frac{\sum_{n=-\infty}^{+\infty} a_S(nf_r - \Delta_S)\, a_D(nf_r - \Delta_D) \left[\frac{\sin(n\pi f_r \tau)}{n\pi f_r \tau}\right]^2 \exp\left[j\varphi_D(nf_r - \Delta_D) - j\varphi_S(nf_r - \Delta_S)\right]}{\sum_{n=-\infty}^{+\infty} [a_S(nf_r - \Delta_S)]^2 \left[\frac{\sin(n\pi f_r \tau)}{n\pi f_r \tau}\right]^2}, \tag{4-10}$$

expression (4-9) can be written as

$$s_{\text{det}} = |\varrho| \frac{\operatorname{Re}\{e^{j\varphi_0'} S \bar{D}\}}{S \bar{S}}, \tag{4-11}$$

where ψ_0' is here defined as

$$\psi_0' = \psi_0 + \varphi_\rho. \tag{4-12}$$

As in the case of CW-echo signals, the effect of if-circuit or amplifier imperfections is a change of the detector signal normalizing factor determined by $|\varrho|$ and an increase of ψ_0 in the amount φ_ρ; the increase in ψ_0 causes a change of the detector output — target angle curve but does not introduce any shift of the angle reference direction or any additive angular measuring error.

4.2 The influence of if-circuit characteristics upon detector output for small target-angle deviations

In order not to complicate the discussion unduly we shall now study the influence of if-circuit or amplifier characteristics upon detector signal in the important automatic tracking case of small target-angle deviations Θ. For this case we have from (2-3)

$$\frac{S\,\bar{D}}{S\,\bar{S}} \cong G_m(\Theta_0, d)\, e^{-j\psi}\, \Theta, \tag{4-13}$$

where G_m and ψ are defined by (2-23) and (2-24).

Equations (4-11), (4-12), and (4-13) show the detector signal to become

$$s_{\text{det}} \cong |\varrho| \cos(\psi_0 - \psi + \varphi_\varrho)\, G_m(\Theta_0, d)\, \Theta. \tag{4-14}$$

In practice ψ_0 is chosen equal to ψ and (4-14) can be written

$$s_{\text{det}} \cong \chi\, G_m(\Theta_0, d)\, \Theta, \tag{4-15}$$

where

$$\chi = \operatorname{Re}\{\varrho\} = \frac{\sum_{n=-\infty}^{+\infty} a_S(nf_r - \Delta_S)\, a_D(nf_r - \Delta_D) \left[\frac{\sin(n\pi f_r \tau)}{n\pi f_r \tau}\right]^2 \cos[\varphi_D(nf_r - \Delta_D) - \varphi_S(nf_r - \Delta_S)]}{\sum_{n=-\infty}^{+\infty} [a_S(nf_r - \Delta_S)]^2 \left[\frac{\sin(n\pi f_r \tau)}{n\pi f_r \tau}\right]^2}. \tag{4-16}$$

In most applications $f_r \ll 1/\tau$, and therefore the sums in (4-16) can be replaced by the corresponding integrals, or

$$\chi = \frac{\int_{-\infty}^{+\infty} a_S(f - \Delta_S)\, a_D(f - \Delta_D) \left[\frac{\sin(\pi f \tau)}{\pi f \tau}\right]^2 \cos[\varphi_D(f - \Delta_D) - \varphi_S(f - \Delta_S)]\, df}{\int_{-\infty}^{+\infty} [a_S(f - \Delta_S)]^2 \left[\frac{\sin(\pi f \tau)}{\pi f \tau}\right]^2 df}. \tag{4-17}$$

From equation (4-17) the effect upon χ and detector output signal of any change of the if-amplifier frequency functions can be determined. However, this is usually a very laborious investigation because of the complicated expression for χ and the fact that the amplitude and phase functions, i. e. a_S and φ_S, are not independent of each other. In the following, therefore, we study only one practically

important type of if-amplifier imperfection, namely the effect upon detector output of equal or unequal detuning of the individual amplifiers, caused either by local oscillator frequency drift and/or variation of tube input capacitances due to AGC-action. We shall further assume that the two if-amplifiers are of the same kind, i. e.

$$\left.\begin{aligned} a_S(f) &= a_D(f) = a(f), \\ \varphi_S(f) &= \varphi_D(f) = \varphi(f). \end{aligned}\right\} \tag{4-18}$$

If the detuning of the two if-amplifiers is the same, $\Delta_S = \Delta_D = \Delta$, which is equivalent to a drift Δ of the local oscillator signal frequency, then $\chi = 1$ according to (4-17) and (4-18), and there is consequently no effect upon detector output. Too large a detuning, however, is not permissible because the signal-to-noise ratio then becomes too low and the internal noise of the monopulse receiver, which has been neglected here, will destroy angular measurement accuracy (see chapter 5). If the detuning of the sum-signal channel amplifier is zero but the detuning of the other amplifier is not zero (or vice versa), χ becomes according to (4-17) and (4-18):

a) For detuning of difference-signal amplifier only ($\Delta_S = 0$):

$$\chi = \chi_1 = \frac{\int_{-\infty}^{+\infty} a(f)\, a(f-\Delta_D) \left[\frac{\sin(\pi f \tau)}{\pi f \tau}\right]^2 \cos[\varphi(f-\Delta_D) - \varphi(f)]\, df}{\int_{-\infty}^{+\infty} [a(f)]^2 \left[\frac{\sin(\pi f \tau)}{\pi f \tau}\right]^2 df}. \tag{4-19}$$

b) For detuning of sum-signal amplifier only ($\Delta_D = 0$):

$$\chi = \chi_2 = \frac{\int_{-\infty}^{+\infty} a(f-\Delta_S)\, a(f) \left[\frac{\sin(\pi f \tau)}{\pi f \tau}\right]^2 \cos[\varphi(f) - \varphi(f-\Delta_S)]\, df}{\int_{-\infty}^{+\infty} [a(f-\Delta_S)]^2 \left[\frac{\sin(\pi f \tau)}{\pi f \tau}\right]^2 df}. \tag{4-20}$$

If the frequency shifts are equal in the two cases above, $\Delta_S = \Delta_D = \Delta$, the ratio χ_1/χ_2 becomes

$$\chi_1/\chi_2 = \frac{\int_{-\infty}^{+\infty} [a(f-\Delta)]^2 \left[\frac{\sin(\pi f \tau)}{\pi f \tau}\right]^2 df}{\int_{-\infty}^{+\infty} [a(f)]^2 \left[\frac{\sin(\pi f \tau)}{\pi f \tau}\right]^2 df}. \tag{4-21}$$

If the amplitude function $a\,(f)$ is an even function of f, and if it has its maximum at $f = 0$ and is monotonically decreasing for $|f| > 0$, an often desirable case in practice, the ratio χ_1/χ_2 is always less than one. This means that the detector output signal is more sensitive to detuning of the difference-signal amplifier than to detuning of the sum-signal amplifier, the underlying reason being the tendency of the AGC to neutralize changes in the if sum-channel output.

4.3 Comparison between the effects upon detector output of detuning of if-amplifiers of maximally-flat delay type and maximally-flat amplitude type

In this section we shall compare and numerically study the effects upon detector output of frequency detuning for two types of if-amplifiers, the maximally-flat delay amplifier and the maximally-flat amplitude amplifier. These can be said to represent the two extremes of amplifier design.

Let us first define the amplitude and the phase functions of an ideal bandpass amplifier of the maximally-flat delay type as

$$a\,(f) = \exp\,[-\tfrac{1}{2}\ln 2\,(f/B)^2], \tag{4-22}$$

$$\varphi\,(f) = \sqrt{(2\,N-1)\ln 2}\,f/B, \tag{4-23}$$

where f is as before the difference between the frequency of the input if-signal and the centre frequency of the amplifier, $2\,B$ the $3\,dB$-bandwidth, and N the number of amplifier stages. This type of amplifier has a constant group delay $t_0 = \dfrac{1}{2\pi}\dfrac{d\varphi}{df} = \sqrt{(2\,N-1)\ln 2}\cdot$ $\cdot\dfrac{1}{2\pi B}$, as is evident from equation (4-23). It is possible to realize physically the ideal maximally-flat delay amplifier defined above with very good approximation [3], [4], [5] (see also [6] p. 724). The agreement between the physically realizable amplifier and the ideal one is better the greater the number of stages N. This can be seen from the expressions for the amplitude and group delay functions of the physical amplifier, taken from [3]:

$$a'(f) = \exp\left[-\frac{1}{2}\,\frac{1}{2N-1}\,(f/B_0)^2\right]\cdot$$

$$\cdot\left\{1+\frac{1}{2(2N-3)}\,\frac{(f/B_0)^4}{(2N-1)^2}+\frac{2}{3(2N-3)(2N-5)}\,\frac{(f/B_0)^6}{(2N-3)^3}+\ldots\right\}, \tag{4-24}$$

$$\frac{1}{2\pi}\,\frac{d\varphi'}{df}=\frac{1}{2\pi B_0}\left[1-\frac{(f/B_0)^{2N}}{1\cdot3\cdot5\cdot7\cdot\ldots\cdot(2N-1)}\,[a'(f)]^2\right], \tag{4-25}$$

where

$$B_0 = B/\sqrt{(2N-1)\ln 2}. \tag{4-26}$$

In the numerical computations of the detuning effect upon detector output in the case of maximally-flat delay amplifiers, which are carried out for $N \geq 4$ and presented below, it has been assumed that (4-22) and (4-23) can be used in describing this type of amplifier.

If the sum and difference if-amplifiers of the monopulse receiver are of the maximally-flat delay type, the quantity χ_1 and the ratio χ_1/χ_2 become, according to (4-19), (4-21), (4-22), and (4-23)

$$\chi_1 = \frac{I_1'(x_0, B\tau, N)}{I_1'(0, B\tau, N)}\,, \tag{4-27}$$

where

$$I_1'(x_0, B\tau, N) = \exp\left[-(1/4)\ln 2\left(\frac{x_0}{B\tau}\right)^2\right]\cos\left[\sqrt{(2N-1)\ln 2}\,\frac{x_0}{B\tau}\right]\cdot$$

$$\cdot\int_{-\infty}^{+\infty}\exp\left[-\ln 2\left(\frac{x-\frac{1}{2}x_0}{B\tau}\right)^2\right]\left(\frac{\sin\pi x}{\pi x}\right)^2 dx \tag{4-28}$$

with

$$x_0 = \Delta_D\tau,$$

and

$$\chi_1/\chi_2 = \frac{I_1''(x_0, B\tau)}{I_1''(0, B\tau)}, \tag{4-29}$$

where

$$\left.\begin{aligned} I_1''(x_0, B\tau) &= \int_{-\infty}^{+\infty}\exp\left[-\ln 2\left(\frac{x-x_0}{B\tau}\right)^2\right]\left(\frac{\sin\pi x}{\pi x}\right)^2 dx \\ &\text{with } x_0 = \Delta\tau \qquad (\text{and } \Delta_S = \Delta_D = \Delta). \end{aligned}\right\} \tag{4-30}$$

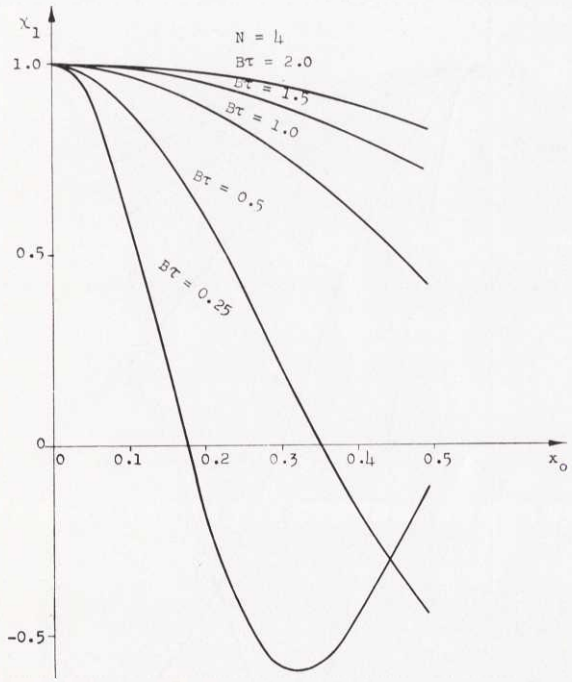

Fig. 12. The factor χ_1 as a function of the detuning $x_0 = \Delta_D \tau$ with $B\tau$ as parameter in the case of if-amplifiers of maximally-flat delay type having 4 stages.

Both χ_1 and χ_1/χ_2 are even functions of the detuning x_0. Further, in this case χ_1/χ_2 is independent of the number of stages N. The results of numerical calculations of χ_1 and the ratio χ_1/χ_2 carried out on SARA, the electronic digital computer of the Saab Company (see Saab Sonics, No. 27, 1959, p. 11), for $N = 4$, 6, and 8, $B\tau = 0.25$, 0.5, 1.0, 1.5, 2.0, and x_0 in the interval $0 \leq x_0 \leq 0.5$ are shown in figs 12—15, to which we shall return later.

An if-amplifier of the maximally-flat amplitude type, which can be realized physically, is the "flat-staggered n-uple" described in [6] pp 166—200. According to [6] this amplifier has the following amplitude and phase functions:

$$a(f) = \frac{1}{[1 + (f/B)^{2N}]^{\frac{1}{2}}}, \qquad (4\text{-}31)$$

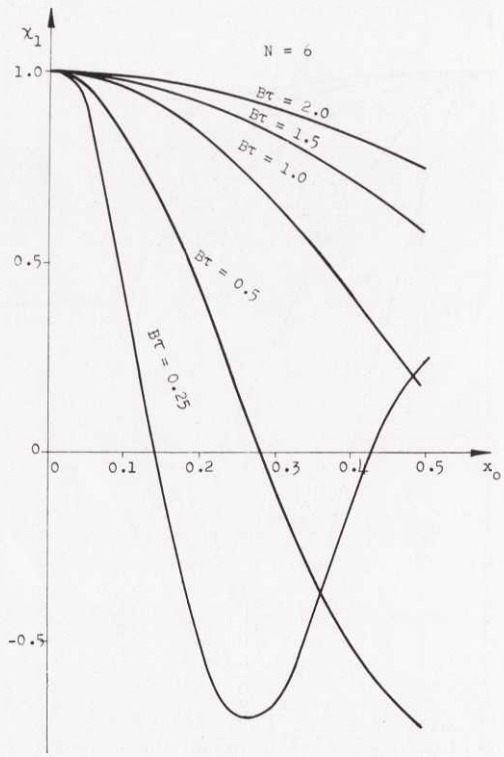

Fig. 13. The factor χ_1 as a function of the detuning $x_0 = \Delta_D \tau$ with $B\tau$ as parameter for if-amplifiers of maximally-flat delay type having 6 stages.

$$\left.\begin{aligned} \varphi(f) &= \sum_{n=1}^{N/2} \arctan \frac{2\,(f/B) \sin \dfrac{\pi\,(2\,n-1)}{2\,N}}{1-(f/B)^2}, \\ &(N \text{ even}) \\ \varphi(f) &= \sum_{n=1}^{\frac{N-1}{2}} \arctan \frac{2\,(f/B) \sin \dfrac{\pi\,(2\,n-1)}{2\,N}}{1-(f/B)^2} + \arctan\,(f/B), \\ &(N \text{ odd}). \end{aligned}\right\} \quad (4\text{-}32)$$

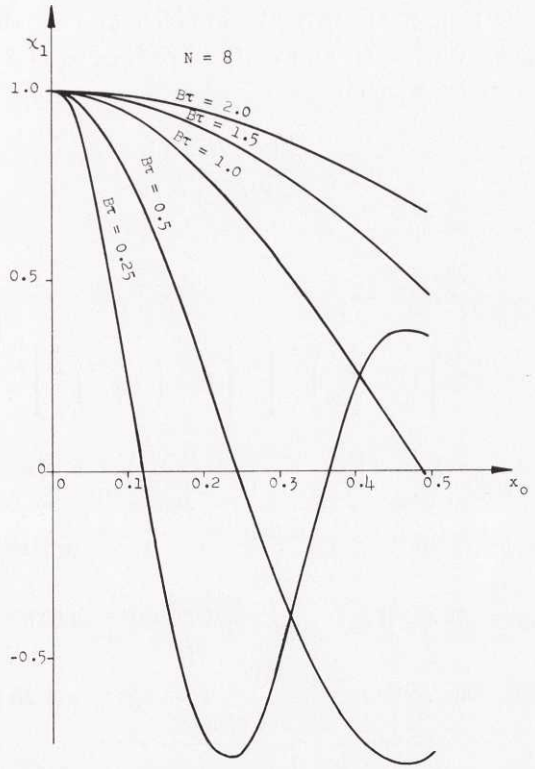

Fig. 14. The factor χ_1 as a function of the detuning $x_0 = \Delta_D \tau$ with $B\tau$ as parameter for if-amplifiers of maximally-flat delay type having 8 stages.

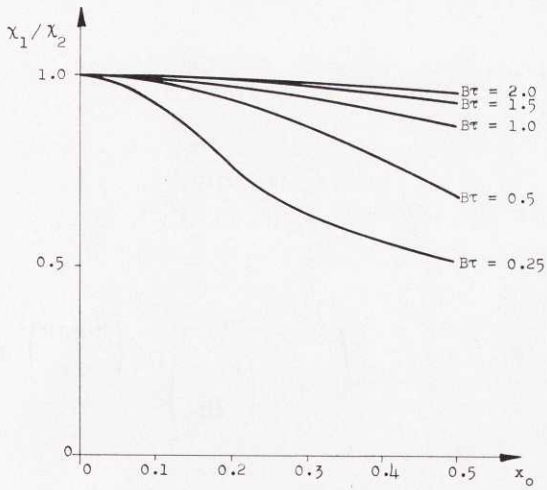

Fig. 15. The ratio χ_1/χ_2 as a function of the detuning $x_0 = \Delta\tau$ with $B\tau$ as parameter for if-amplifiers of maximally-flat delay type.

As before, B is half the 3 dB-bandwidth and N the number of amplifier stages. With $a(f)$ and $\varphi(f)$ according to (4-31) and (4-32), χ_1 and χ_1/χ_2 can be written

$$\chi_1 = \frac{I_2'(x_0, B\tau, N)}{I_2'(0, B\tau, N)}, \tag{4-33}$$

where

$$I_2'(x_0, B\tau, N) = \int_{-\infty}^{+\infty} \frac{1}{\left[1 + \left(\frac{x}{B\tau}\right)^{2N}\right]^{\frac{1}{2}}} \frac{1}{\left[1 + \left(\frac{x-x_0}{B\tau}\right)^{2N}\right]^{\frac{1}{2}}} \left(\frac{\sin \pi x}{\pi x}\right)^2 \cdot$$

$$\cdot \left\{ \begin{array}{l} \cos\left[\sum_{n=1}^{N/2} \arctan \frac{\frac{2x}{B\tau} \sin \frac{\pi(2n-1)}{2N}}{1-(x/B\tau)^2} - \arctan \frac{\frac{2(x-x_0)}{B\tau} \sin \frac{\pi(2n-1)}{2N}}{1-[(x-x_0)/B\tau]^2}\right]_{N \text{ even}} \\ \cos\left[\sum_{n=1}^{\frac{N-1}{2}} \arctan \frac{\frac{2x}{B\tau} \sin \frac{(2n-1)}{2N}}{1-(x/B\tau)^2} - \arctan \frac{\frac{2(x-x_0)}{B\tau} \sin \frac{\pi(2n-1)}{2N}}{1-[(x-x_0)/B\tau]^2} + \right. \\ \left. + \arctan(x/B\tau) - \arctan \frac{x-x_0}{B\tau}\right]_{N \text{ odd}} \end{array} \right\} dx \tag{4-34}$$

with

$$x_0 = \Delta_D \tau,$$

and

$$\chi_1/\chi_2 = \frac{I_2''(x_0, B\tau, N)}{I_2''(0, B\tau, N)}, \tag{4-35}$$

where

$$I_2''(x_0, B\tau, N) = \int_{-\infty}^{+\infty} \frac{1}{1 + \left(\frac{x-x_0}{B\tau}\right)^{2N}} \left(\frac{\sin \pi x}{\pi x}\right)^2 dx \tag{4-36}$$

with

$$x_0 = \Delta\tau \text{ (and } \Delta_S = \Delta_D = \Delta).$$

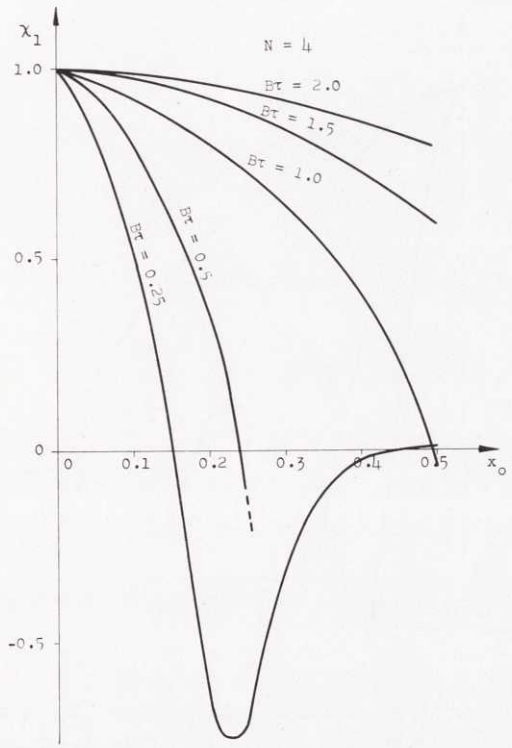

Fig. 16. The factor χ_1 as a function of the detuning $x_0 = \Delta_D \tau$ with $B\tau$ as parameter for if-amplifiers of maximally-flat amplitude type having 4 stages.

As is easily seen, both χ_1 and the ratio χ_1/χ_2 are even functions of the detuning x_0. The results of numerical computations of χ_1 and the ratio χ_1/χ_2 carried out on SARA for $N = 4$, 6, and 8, $B\tau = 0.25$, 0.50, 1.0, 1.5, 2.0, and x_0 in the interval $0 \leq x_0 \leq 0.5$ are shown in figs 16—21.

From figs 12—21 we see that the factor χ_1 decreases as the detuning x_0 increases. This decrease is greater the smaller the product $B\tau$, i. e. the smaller the bandwidth $2\,B$ of the amplifier compared with the spectral width ($\simeq 1/\tau$) of the echo pulses.

For small $B\tau$-values χ_1 relatively soon passes through zero and becomes negative, a fatal case for automatic tracking monopulse systems. As is also to be expected, the decrease of χ_1 with increasing x_0 is greater the greater the number of stages N. The ratio χ_1/χ_2 behaves in about the same way as χ_1 with respect to increasing x_0

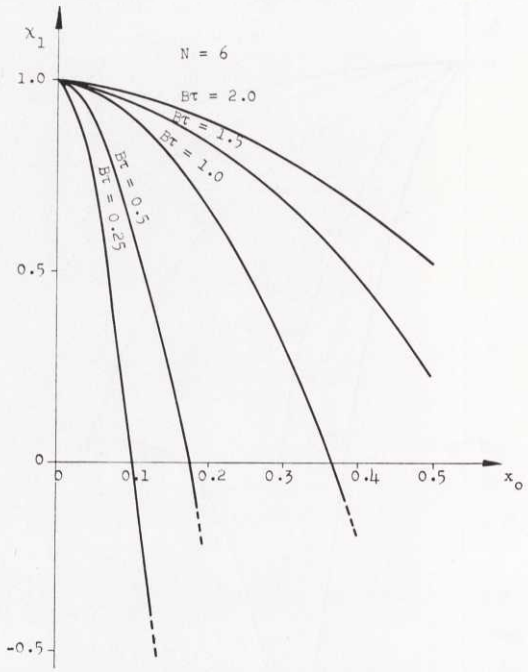

Fig. 17. The factor χ_1 as a function of the detuning $x_0 = \Delta_D \tau$ with $B\tau$ as parameter for if-amplifiers of maximally-flat amplitude type having 6 stages.

and decreasing $B\tau$. In the case of amplifiers of maximally-flat delay type χ_1/χ_2 is independent of N, and in the maximally-flat amplitude case the dependence upon N is relatively small for reasonable values of the detuning x_0.

A comparison between the results obtained for amplifiers of maximally-flat delay and amplifiers of maximally-flat amplitude shows that χ_1 decreases more rapidly with increasing detuning for a given number of stages and a given product $B\tau$ in the maximally-flat amplitude case than in the maximally-flat delay case. This difference in behaviour is more pronounced the greater the number of stages. For the ratio χ_1/χ_2 the situation is reversed provided $B\tau$ is not extremely small.

Which of the two types of if-amplifier displays the smallest influence upon detector output signal due to detuning depends upon the values of $B\tau$ and N used. The product $B\tau$ is often determined by the desire to maximize the ratio between the echo pulse amplitude and the root

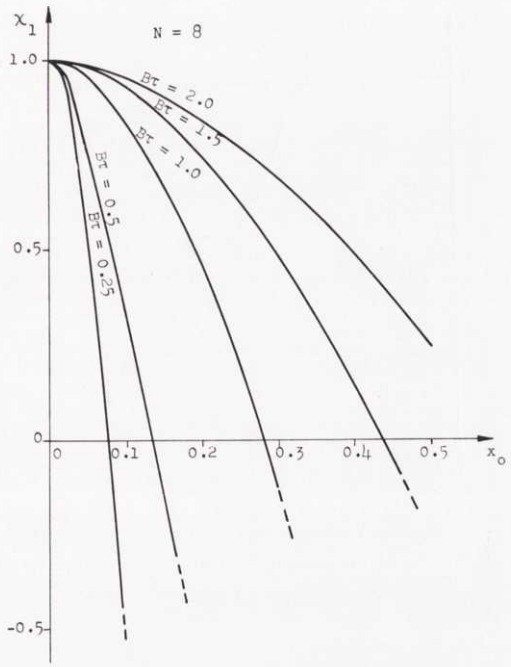

Fig. 18. The factor χ_1 as a function of the detuning $x_0 = \Delta_D \tau$ with $B\tau$ as parameter for if-amplifiers of maximally-flat amplitude type having 8 stages.

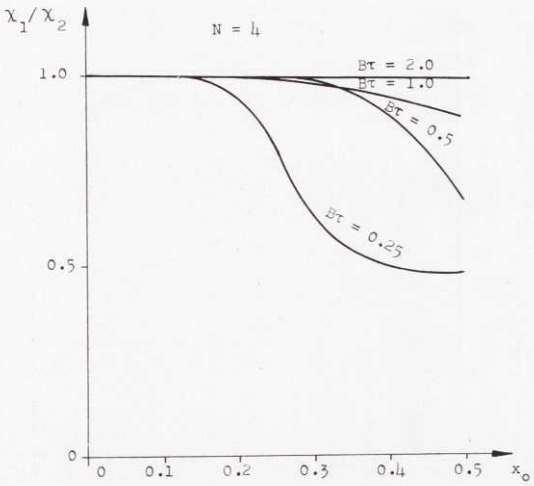

Fig. 19. The ratio χ_1/χ_2 as a function of the detuning $x_0 = \Delta\tau$ with $B\tau$ as parameter for if-amplifiers of maximally-flat amplitude type having 4 stages.

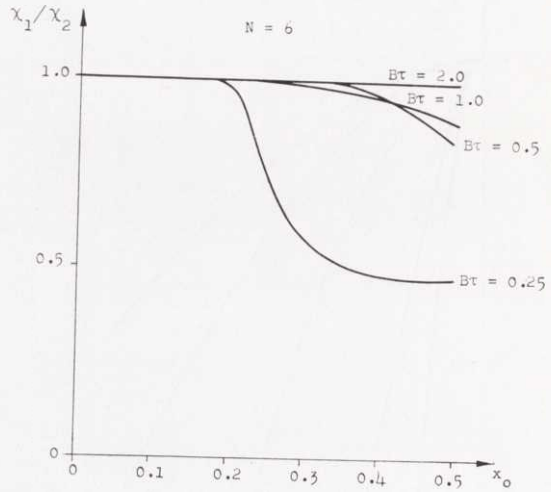

Fig. 20. The ratio χ_1/χ_2 as a function of the detuning $x_0 = \Delta\tau$ with $B\tau$ as parameter for if-amplifiers of maximally-flat amplitude type having 6 stages.

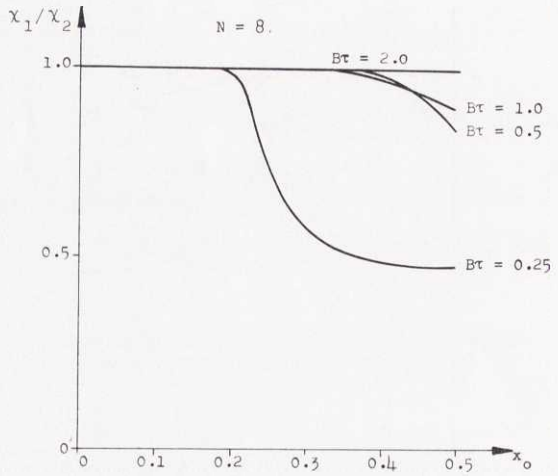

Fig. 21. The ratio χ_1/χ_2 as a function of the detuning $x_0 = \Delta\tau$ with $B\tau$ as parameter for if-amplifiers of maximally-flat amplitude type having 8 stages.

mean square-value of the internal receiver noise, because this maximizes the probability of discovering a target signal in noise. The optimal theoretical value of $B\tau$ in this respect is about 0.4 for the maximally-flat delay type of amplifier (rectangular pulse and Gaussian if-passband) and 0.7 for the maximally-flat amplitude type (rectangular pulse and rectangular if-passband) ([7] pp 204—210). However, experimental results do not show significant differences in optimal $B\tau$-value for different types of amplifiers. The optimum has been demonstrated ([7] pp 204—210), both theoretically and experimentally, to be rather broad, and therefore $B\tau$ is in practice usually chosen equal to 0.5, independently of amplifier type, or even $B\tau = 1$ in order to ease the tuning problem.

Unfortunately, a good deal of the advantage shown above of maximally-flat delay amplifiers over maximally-flat amplitude amplifiers is lost in practice because of the fact that for a given overall amplification and bandwidth an amplifier of the maximally-flat delay type requires more stages. This is due to the circumstance that such amplifiers have lower "gain-bandwidth factor" ("GB-factor") than maximally-flat amplitude amplifiers, the GB-factor of which is always one ([6] p. 176). The GB-factor of the maximally-flat delay amplifier decreases with increasing number of stages N from a maximum value of unity, as is shown by table 4 in [3]. The number of stages necessary for an if-amplifier of maximally-flat delay type, N_D, and maximally-flat amplitude type, N_A, for the same overall amplification G_t and overall bandwidth B_t ($B_t = 2\,B$) is easily shown to be given by

$$N_D \left\{ 1 + \frac{\log F_D\,(N_D)}{\log \dfrac{C}{B_t}} \right\} = \frac{\log G_t}{\log \dfrac{C}{B_t}} \tag{4-37}$$

and

$$N_A = \frac{\log G_t}{\log \dfrac{C}{B_t}}, \tag{4-38}$$

where $F_D\,(N_D)$ is the GB-factor of a maximally-flat delay amplifier with N_D stages, given by table 4 in [3] and C is the "gain-bandwidth product" ("GB-product") of the tube type used. Figs 22 and 23

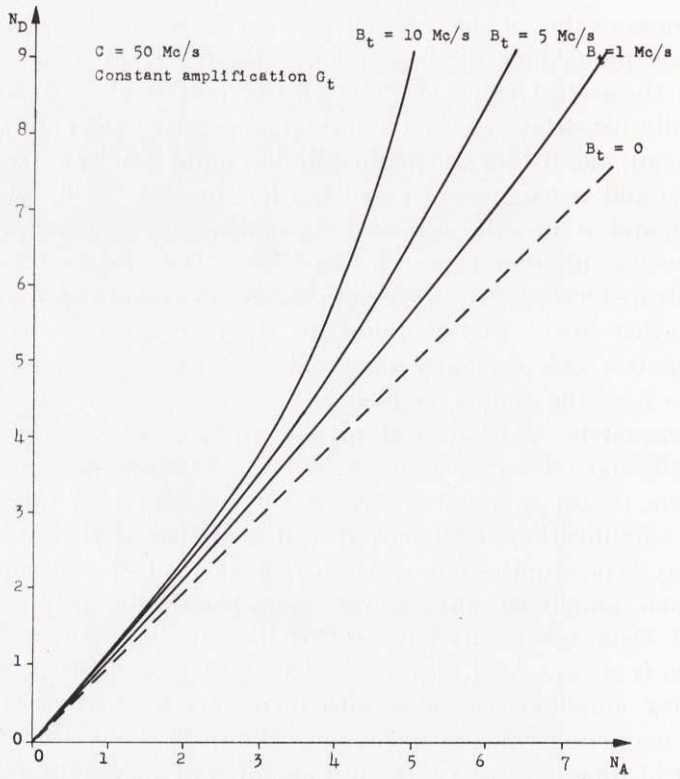

Fig. 22. The relation between the required number of stages N_D and N_A (N_D for the maximally-flat delay case, N_A for the maximally-flat amplitude case) for given overall amplification G_t and overall bandwidth B_t, assuming a tube type with gain-bandwidth product $C = 50$ Mc/s.

show the relations between N_D and N_A and between N_A and G_t for certain values of B_t and for $C = 50$ Mc/s, a usual but conservative value.

We shall consider the following examples of the difference in effect upon detector output of detuning of the if-amplifiers: Suppose that the pulse length τ is taken as 0.5 μs and that the required overall amplification is $G_t = 10^6$ or 120 dB. If we choose $B\tau = 0.5$ for both types of amplifiers, an overall bandwidth $B_t = 2$ Mc/s is needed in both cases, which according to (4-37) and (4-38) with $G_t = 120$ dB and $C = 50$ Mc/s requires $N_D = 6$ stages of amplification in the case of maximally-flat delay amplifiers and $N_A = 5$ stages in the case of maximally-flat amplitude amplifiers. From figs 13, 16, and 17 it is

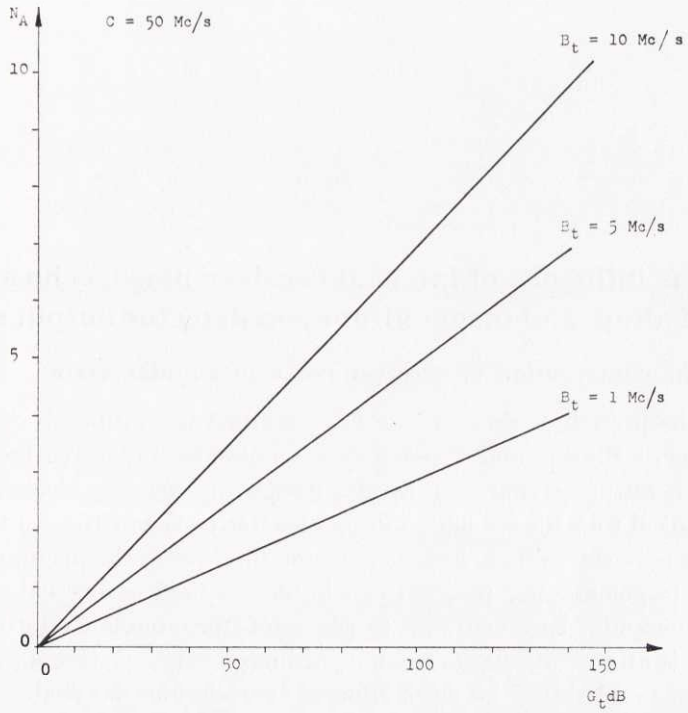

Fig. 23. The required number of stages N_A in an if-amplifier of maximally-flat amplitude type as a function of overall amplification G_t with overall bandwidth B_t as parameter assuming a tube type with gain-bandwidth product $C = 50$ Mc/s.

seen that the flat-delay amplifier is somewhat less sensitive to frequency detuning than the flat-amplitude amplifier. With $x_0 = 0.1$ or $\Delta = 100$ kc/s, χ_1 is about 0.85 and 0.75 in the two cases, which corresponds to a decrease of the angular gain of 15 and 25 percent respectively. If, on the other hand, the amplifiers are so dimensioned that $B\tau = 0.4$ in the case of maximally-flat delay and $B\tau = 0.7$ in the case of maximally-flat amplitude amplifiers, the bandwidths are $B_t = 1.6$ Mc/s and $B_t = 2.8$ Mc/s respectively, and according to (4-37) and (4-38) the same number of stages $N_D = N_A = 5$ is needed. Interpolation of the results given in figs 12, 13, 16, and 17 for $N = 4$ and 6 shows that now the amplifier of maximally-flat amplitude type is less sensitive than the amplifier of maximally-flat delay type. If we put $x_0 = 0.1$ or $\Delta = 100$ kc/s, χ_1 becomes about 0.85 and 0.75 respectively, corresponding to a decrease in angular gain of 15 and 25 percent.

5. The influence of internal receiver noise, echo amplitude fading, and target glint upon detector output signal

5.1 The contribution of receiver noise to angular error

In the preceding chapters we have studied the influence of imperfections of the hf- and if-parts of a monopulse radar receiver upon detector output signal. By careful design, by keeping electrical and mechanical tolerances small, and by exact adjustment these influences can be reduced. What, however, ultimately limits the accuracy with which target angular position can be determined is internal noise in the monopulse receiver and target glint (or angular scintillation), which is almost always present in ordinary types of targets such as airplanes and ships. In the following two sections we shall study in some detail the influence of receiver noise and target glint upon detector output.

In discussing the contribution of receiver noise to angular error we restrict ourselves as before to the one-dimensional angular measurement case. In the two-dimensional case the two angular errors may with good approximation be assumed to be independent of each other and equal to the corresponding one-dimensional error.

We shall first derive an expression for detector output signal in the presence of internal noise for the practically important case in which the signal-to-noise ratio in the sum-signal channel is substantially greater than one. We shall then specialize the discussion to the automatic angular tracking case with small target angle deviation.

To start with we neglect the influence of the hf-circuits and if-amplifiers upon the shape of the echo pulses, supposed to be rectangular. Because the signal-to-noise ratio is much greater than one in the sum channel we may neglect the presence of noise in that channel. We also assume that by means of a range gate the difference-signal if-amplifier delivers a signal only during the intervals of echo pulse arrival. Under these assumptions the output signals S_{if} and

D_{if} of the if-amplifiers of the sum and difference channels can be written

$$\left.\begin{aligned} S_{\mathrm{if}} &= E_a(t)\, K_S(t)\, S\, e^{j(\omega_{\mathrm{if}} t - \Phi_a(t) - \varphi_S)}\, U_{T,\tau}(t), \\ D_{\mathrm{if}} &= [E_a(t)\, K_D(t)\, D\, e^{j(\omega_{\mathrm{if}} t - \varphi_0 - \Phi_a(t) - \varphi_D)} + \\ &\quad + K_D(t)\, N_D(t)\, e^{j(\omega_{\mathrm{if}} t - \varphi_{nD}(t))}]\, U_{T,\tau}(t). \end{aligned}\right\} \qquad (5\text{-}1)$$

In (5-1) $U_{T,\tau}(t)$ is the infinite train of rectangular pulses with unit amplitude, width τ, and period $T = 1/f_r$, and $E_a(t)$ is the envelope and $\Phi_a(t)$ the phase of the target echos. The echo envelope $E_a(t)$ and phase $\Phi_a(t)$ are here supposed to be independent of each other and assumed to vary stochastically with time. The variation of E_a and Φ_a with time which is typical for ordinary kinds of targets such as airplanes and ships is to be regarded as small from echo pulse to pulse. In many practical cases the stochastic variables E_a and Φ_a may be supposed to be Rayleigh-distributed and uniformly distributed in the interval 0 to 2π respectively and generated by more or less stationary processes, if the distance to target does not change too rapidly with time. The power spectrum of the processes usually has cut-off frequencies of about 5 to 10 c/s in the case of airplane targets (see further section 5.2 below). Echo fading is taken into account in the present case in view of the action of the automatic gain control upon the additive noise component of the detector output, as will be evident in the following.

The amplifications $K_S(t)$ and $K_D(t)$ of (5-1) are supposed to vary slowly from pulse to pulse, as do also S and D, which depend upon the target angle deviation Θ. $N_D(t) \exp\{j(\omega_{if} t - \varphi_{nD}(t))\}$ is the equivalent internal noise signal at the input of the difference channel if-amplifier. The stochastic noise signal may be assumed to be stationary and originating from a band centered around the intermediate frequency of white Gaussian noise having width B_t and power density $F_n kT$, where F_n is the receiver noise figure, k Boltzmann's constant, and T absolute temperature. In this case the amplitude N_D and phase φ_{nD} are independent, N_D is Rayleigh-distributed and φ_{nD} uniformly distributed in the interval 0 to 2π. N_D and φ_{nD} change from pulse to pulse, because their correlation time is approximately $1/B_t$ according to the above assumptions, and B_t is usually about $1/\tau$.

With S_{if} and D_{if} given by (5-1) the useful video signal immediately after the phase sensitive detector, S_{det}, is readily obtained as

$$S_{\mathrm{det}} = \tfrac{1}{2} K_S(t) K_D(t) \left[[E_a(t)]^2 \operatorname{Re}\{e^{j\varphi_0'} S\bar{D}\} + E_a(t) N_D(t) \operatorname{Re}\{S e^{j\Phi_{nD}(t)}\} \right] U_{T,\tau}(t), \quad (5\text{-}2)$$

where

$$\Phi_{nD}(t) = \varphi_{nD}(t) - \Phi_a(t) - \varphi_s. \quad (5\text{-}3)$$

In the following we also need an expression for the video output immediately after the AGC-detector, the input of which is the sum channel if-output S_{if}. As in chapter 4 we assume that the AGC-detector is of the square-law type. The output signal is therefore proportional to $S_{if}\ \bar{S}_{if}$, or according to (5-1),

$$S_{AGC} = [K_S(t)]^2 [E_a(t)]^2 S\bar{S}\ U_{T,\tau}(t). \quad (5\text{-}4)$$

According to (5-2) and (5-4) the envelopes of the signals S_{det} and S_{AGC} are

$$S^a_{\mathrm{det}} = \tfrac{1}{2} K_S(t) K_D(t) \left[[E_a(t)]^2 \operatorname{Re}\{e^{j\varphi_0'} S\bar{D}\} + E_a(t) N_D(t) \operatorname{Re}\{S e^{j\Phi_{nD}(t)}\} \right], \quad (5\text{-}5)$$

$$S^a_{AGC} = [K_S(t)]^2 [E_a(t)]^2 S\bar{S}, \quad (5\text{-}6)$$

and the signals S_{det} and S_{AGC} can be looked upon as obtained by sampling the primary signals S^a_{det} and S^a_{AGC} with the period T.

Let us now study the two limiting cases of a slow and a fast automatic gain control. By a slow AGC we mean an AGC that does not respond to the rapid variations of the echo envelope $E_a(t)$ but controls the amplification K_S so that the time average of S^a_{AGC} is constant, or

$$[S^a_{AGC}]_{\mathrm{Av}} = [K_S(t)]^2 \left[[E_a(t)]^2 \right]_{\mathrm{Av}} S\bar{S} = A^2. \quad (5\text{-}7)$$

(Negligible variation of target angle Θ with time assumed.)

In the case of a fast AGC, i. e. an AGC responding to all variations of $E_a(t)$, on the other hand, the amplification K_S satisfies the relation

$$S^a_{AGC} = [K_S(t)]^2 [E_a(t)]^2 S\bar{S} = A^2. \quad (5\text{-}8)$$

Equations (5-2), (5-7), and (5-8), therefore, give the following detector outputs in the two limiting cases:

a) Slow AGC:

$$S_{\mathrm{det}} = \frac{1}{2}\frac{K_D}{K_S} A^2 \left[\frac{[E_a(t)]^2}{[E_a^2]_{\mathrm{Av}}} \frac{\mathrm{Re}\,\{e^{j\psi_0'} S\bar{D}\}}{S\bar{S}} + \frac{E_a(t)\, N_D(t)}{[E_a^2]_{\mathrm{Av}}} \frac{\mathrm{Re}\,\{e^{j\Phi_{nD}(t)} S\}}{S\bar{S}} \right] U_{T,\tau}(t). \quad (5\text{-}9)$$

b) Fast AGC:

$$S_{\mathrm{det}} = \frac{1}{2}\frac{K_D}{K_S} A^2 \left[\frac{\mathrm{Re}\,\{e^{j\psi_0'} S\,\bar{D}\}}{S\bar{S}} + \frac{N_D(t)}{E_a(t)} \frac{\mathrm{Re}\,\{e^{j\Phi_{nD}(t)} S\}}{S\bar{S}} \right] U_{T,\tau}(t). \quad (5\text{-}10)$$

When the target-angle deviation Θ is small, $K_D(t) = K_S(t)$, and with $s_{\mathrm{det}} = S_{\mathrm{det}}/(\frac{1}{2} A^2 K_D/K_S) = S_{\mathrm{det}}/(\frac{1}{2} A^2)$, relations (5-9) and (5-10) reduce to:

a) Slow AGC:

$$s_{\mathrm{det}} \cong G(\Theta_0, d, \psi_0') \left[\frac{[E_a(t)]^2}{[E_a^2]_{\mathrm{Av}}} \Theta + \frac{1}{G} \frac{E_a(t)\, N_D(t) \cos \Phi_{nD}(t)}{2F(\Theta_0)\,[E_a^2]_{\mathrm{Av}}} \right] U_{T,\tau}(t). \quad (5\text{-}11)$$

b) Fast AGC:

$$s_{\mathrm{det}} \cong G(\Theta_0, d, \psi_0') \left[\Theta + \frac{1}{G} \frac{N_D(t) \cos \Phi_{nD}(t)}{2F(\Theta_0)\, E_a(t)} \right] U_{T,\tau}(t). \quad (5\text{-}12)$$

The effect of receiver internal noise is consequently a random angular error. Amplitude fading of the echo amplitude E_a causes a random change of angular gain in the case of slow AGC. In the case of fast AGC amplitude fading has a detrimental effect upon the angular error, because the noise term contains in its denominator the time-varying amplitude $E_a(t)$, which can sometimes become very small.

According to (5-11) for slow AGC the instantaneous additive angular error $\Delta\Theta(t)$ immediately after the phase sensitive detector but before a possible smoothing filter following the detector, can be defined as

$$\Delta\Theta(t) = \frac{1}{G} \frac{E_a(t)\, N_D(t) \cos \Phi_{nD}(t)}{2F(\Theta_0)\,[E_a^2]_{\mathrm{Av}}}. \quad (5\text{-}13)$$

If $E_a(t)$, $N_D(t)$, and $\Phi_{nD}(t)$ are independent of each other and $\Phi_{nD}(t)$ uniformly distributed in the interval 0 to 2π the corresponding time average square-value, $[(\Delta\Theta)^2]_{\mathrm{Av}}$, becomes

$$[(\Delta\Theta)^2]_{\mathrm{Av}} = \frac{1}{G^2} \frac{\frac{1}{2}[N_D{}^2]_{\mathrm{Av}}}{4[F(\Theta_0)]^2[E_a{}^2]_{\mathrm{Av}}}, \tag{5-14}$$

where according to the previous assumptions on internal noise

$$\tfrac{1}{2}[N_D{}^2]_{\mathrm{Av}} = F_n kTB_t. \tag{5-15}$$

If we define the following signal-to-noise power ratio

$$(P/N)_{\mathrm{in}} = \frac{2[F(\Theta_0)]^2[E_a{}^2]_{\mathrm{Av}}}{\frac{1}{2}[N_D{}^2]_{\mathrm{Av}}}, \tag{5-16}$$

which in the case of equal noise figure F_n and bandwidth B_t in the sum and difference channels is the signal-to-noise power ratio that can be observed in the if part of the sum-signal channel, relation (5-14) can be written

$$[(\Delta\Theta)^2]_{\mathrm{Av}} = \frac{1}{2}\frac{1}{G^2}\frac{1}{(P/N)_{\mathrm{in}}}. \tag{5-17}$$

The variations of angular gain for slow AGC can be considerably reduced if the detector signal s_{det} according to (5-11) is passed through some sort of smoothing low-pass filter with a cut-off frequency f_f considerably below the cut-off frequency f_g of $E_a(t)$. This case assumes that the variations of the legitimate target angle Θ are slow; the angular error $\Delta\Theta(t)$ is then also smoothed, and after the filter the time average of the square of the output angular error $\Delta\Theta(t)_{\mathrm{out}}$ is approximately

$$[(\Delta\Theta_{\mathrm{out}})^2]_{\mathrm{Av}} \cong \frac{1}{2}\frac{1}{G^2}\frac{1}{(P/N)_{\mathrm{in}}}\frac{1}{f_r\tau_f}, \tag{5-18}$$

where, if τ_f denotes the "effective integration time" of the filter, $f_r\tau_f$ is the average number of pulses or independent $\Delta\Theta$-values smoothed in getting a single output signal value.

For fast AGC the instantaneous angular error immediately after the phase sensitive detector is according to (5-12)

$$\Delta\Theta(t) = \frac{1}{G} \frac{N_D(t) \cos \Phi_{nD}(t)}{2 F(\Theta_0) E_a(t)}. \tag{5-19}$$

Because of the appearance of $E_a(t)$ in the denominator of (5-19), as already mentioned, the angular error $\Delta\Theta(t)$ will be very large. Theoretically, it is easy to show for example that the variance $[\Delta\Theta^2]_{Av}$ is infinite if the stochastic variables $E_a(t)$ and $N_D(t) \cos \Phi_{nD}(t)$ are independent and if $E_a(t)$ is Rayleigh-distributed and $N_D(t) \cdot \cos \Phi_{nD}(t)$ Gaussian-distributed. How large the angular variance will be in practice after a smoothing filter is difficult to determine. It depends on various factors, among them the specific type of AGC employed. Under certain circumstances the combination of fast AGC and smoothing of detector output can give an angular error variance that is 2 to 3 times larger than the error variance obtained in the case of slow AGC and the same smoothing of the phase sensitive detector output [8]. In practical applications one can neither accept too large variations of the angular gain nor too large angular errors. A compromise reached by suitable choice of AGC and output smoothing filter is therefore necessary.

5.2 Echo amplitude fading and the contribution of target glint to angular error

The fading of the echo pulses and the glint or angular scintillation of a complex target such as an airplane can be explained if one supposes the target to consist of a large number N of surface elements which independently of each other reflect a part of the incident energy in a random manner [9]. In the present section we shall apply this hypothesis to the case of a one-dimensional monopulse radar and assume that the radar signal is reflected from a one-dimensional target consisting of a large number of independent elements arranged on a line. With the geometry defined by fig. 24 and supposing $d \ll R$ and $\delta_n \ll R$ the distances R_1 and R_2 from a certain target element to antenna 1 and 2 of the monopulse radar become

$$\left.\begin{aligned} R_1 &\cong R + \frac{1}{2}\frac{d^2}{R} + \delta_n \cos \Phi + \frac{1}{2}\frac{\delta_n^2}{R} - d\frac{\delta_n \sin \Phi}{R}, \\ R^2 &\cong R + \frac{1}{2}\frac{d^2}{R} + \delta_n \cos \Phi + \frac{1}{2}\frac{\delta_n^2}{R} + d\frac{\delta_n \sin \Phi}{R}, \end{aligned}\right\} \tag{5-20}$$

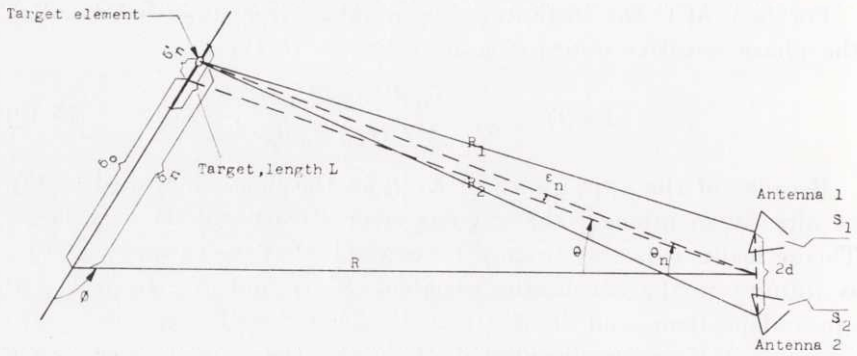

Fig. 24. The geometry for a one-dimensional target consisting of a number of elementary reflectors.

and the angular deviation of the element Θ_n is

$$\Theta_n \cong \frac{\delta_n \sin \Phi}{R}. \tag{5-21}$$

We assume that the echo signal reflected from the n:th elementary target in the case of an active radar has the random amplitude $E_n(t) = a_n(t)\, U_{T,\tau}(t)$ measured at the antenna and that its phase changes by a random amount $-\psi_n(t)$ during the reflection. The amplitude envelope $a_n(t)$ and phase $\psi_n(t)$ are also supposed to be generated by stationary stochastic processes. According to (5-20) and (5-21) the echo signals from the target element picked up by the two antennas can now be written

$$\left.\begin{aligned} S_{1n} &= E_n(t)\, F(\Theta_0 - \Theta_n) \exp[j(\omega_c t + kd\,\Theta_n - \varphi_n(t))], \\ S_{2n} &= E_n(t)\, F(\Theta_0 + \Theta_n) \exp[j(\omega_c t - kd\,\Theta_n - \varphi_n(t))], \end{aligned}\right\} \tag{5-22}$$

where

$$\varphi_n(t) = 2kR + \tfrac{1}{2}k\frac{d^2}{R} + 2k\delta_n \cos\Phi + k\frac{\delta_n^2}{R} + \psi_n(t). \tag{5-23}$$

Assuming further that the amplitude envelope $a_n(t)$ and the phase $\varphi_n(t)$ vary very slowly with time and neglecting the influence of the hf and if-circuits upon the pulse shape, then according to equations

(2-10 a) and (2-10 b) the resultant phase sensitive and AGC detector outputs are

$$S_{\text{det}} = \tfrac{1}{2} K_S(t)\, K_D(t)\, \text{Re}\left\{ e^{j\varphi_s'} \sum_{n,m}^{N} a_n a_m S_n \bar{D}_m\, e^{j(\varphi_m - \varphi_n)} \right\} U_{T,\tau}(t), \quad (5\text{-}24)$$

and

$$S_{AGC} = [K_S(t)]^2 \sum_{n,m}^{N} a_n a_m S_n \bar{S}_m\, e^{j(\varphi_m - \varphi_n)}\, U_{T,\tau}(t), \quad (5\text{-}25)$$

where S_n and D_n are defined by (2-11).

We now specialize our investigation to the case in which the complete target is inside the linear angular measuring region of the monopulse radar. After some algebraic manipulations we get

$$S_{\text{det}} \cong 2\,[F(\Theta_0)]^2 K_S(t)\, K_D(t)\, G(\Theta_0, d, \psi_0')\, [(\alpha_1^2 + \alpha_2^2)\,\Theta + \\ + (\alpha_1\beta_1 + \alpha_2\beta_2) + (\alpha_2\beta_1 - \alpha_1\beta_2)\tan(\psi_0' - \psi)]\, U_{T,\tau}(t), \quad (5\text{-}26)$$

$$S_{AGC} \cong 4\,[F(\Theta_0)]^2\,[K_S(t)]^2\,(\alpha_1^2 + \alpha_2^2)\, U_{T,\tau}(t), \quad (5\text{-}27)$$

where Θ is the mean target-angle deviation, defined below, and the random time-variable quantities α_1, α_2, β_1, and β_2 are given by

$$\left.\begin{aligned} \alpha_1 &= \sum_{n=1}^{N} a_n \cos\varphi_n, \\ \alpha_2 &= \sum_{n=1}^{N} a_n \sin\varphi_n, \end{aligned}\right\} \quad (5\text{-}28)$$

$$\left.\begin{aligned} \beta_1 &= \sum_{n=1}^{N} \varepsilon_n a_n \cos\varphi_n, \\ \beta_2 &= \sum_{n=1}^{N} \varepsilon_n a_n \sin\varphi_n. \end{aligned}\right\} \quad (5\text{-}29)$$

ε_n in (5-29) is the angular deviation of the n:th target element from the mean angular position of the target or

$$\varepsilon_n = \Theta_n - \Theta = \frac{\delta_n' \sin\Phi}{R} \quad (5\text{-}30)$$

(see fig. 24). Expression (5-26) for detector output has the same form as the one given in [9] (p. 1780, equation 11) for a conical-scanning radar; this expression should also hold for any linear type of angle-measuring radar. If we introduce the echo envelope $E_a(t)$ and the glint function $V(t)$ defined by

$$E_a(t) = \sqrt{\alpha_1^2 + \alpha_2^2}\,, \tag{5-31}$$

$$V(t) = \frac{\alpha_1\beta_1 + \alpha_2\beta_2 + (\alpha_2\beta_1 - \alpha_1\beta_2)\tan(\psi_0' - \psi)}{\sqrt{\alpha_1^2 + \alpha_2^2}}, \tag{5-32}$$

expressions (5-26) and (5-27) can be written

$$S_{\text{det}} \cong 2\,[F(\Theta_0)]^2\,K_S(t)\,K_D(t)\,G(\Theta_0, d, \psi_0')\,\big[[E_a(t)]^2\,\Theta + \\ + E_a(t)\,V(t)\big]\,U_{T,\tau}(t), \tag{5-33}$$

$$S_{AGC} \cong 4\,[F(\Theta_0)]^2\,[K_S(t)]^2\,[E_a(t)]^2\,U_{T,\tau}(t). \tag{5-34}$$

Les us now, as in [9], make the assumptions that the random envelope and phase $a_n(t)$ and $\varphi_n(t)$ of the n:th target element are independent of each other and of the corresponding quantities of another target element, i. e.

$$\left.\begin{aligned}[a_n\,a_m]_{\text{Av}} &= [a_n]_{\text{Av}}\,[a_m]_{\text{Av}},\ m \neq n,\\ [\varphi_n\,\varphi_m]_{\text{Av}} &= [\varphi_n]_{\text{Av}}\,[\varphi_m]_{\text{Av}},\ m \neq n,\end{aligned}\right\} \tag{5-35}$$

where $[\,]_{\text{Av}}$ stands as before for the average with respect to time. Let us also assume that φ_n is rectangularly distributed in the interval $-\pi$ to π, which means that $[\varphi_n]_{\text{Av}} = [\cos\varphi_n]_{\text{Av}} = [\sin\varphi_n]_{\text{Av}} = 0$. When the number of elements N is large, as is supposed to be the case, α_1 and α_2 become Gaussian-distributed with average value zero and equal variances, or

$$\left.\begin{aligned}[\alpha_1]_{\text{Av}} &= [\alpha_2]_{\text{Av}} = 0,\\ [\alpha_1^2]_{\text{Av}} &= [\alpha_2^2]_{\text{Av}} = \tfrac{1}{2}\sum_{n=1}^{N}[a_n^2]_{\text{Av}}.\end{aligned}\right\} \tag{5-36}$$

α_1 and α_2 are also independent because the covariance $[\alpha_1 \alpha_2]_{\mathrm{Av}}$ is zero. The same holds for β_1 and β_2, the variances of which are given by

$$[\beta_1^2]_{\mathrm{Av}} = [\beta_2^2]_{\mathrm{Av}} = \tfrac{1}{2} \sum_{n=1}^{N} \varepsilon_n^2 \, [a_n^2]_{\mathrm{Av}}. \tag{5-37}$$

The covariances $[\alpha_\mu \beta_\nu]_{\mathrm{Av}}$ with $\mu, \nu = 1, 2$ are easily shown to be equal and

$$[\alpha_\mu \beta_\nu]_{\mathrm{Av}} = \tfrac{1}{2} \sum_{n=1}^{N} \varepsilon_n \, [a_n^2]_{\mathrm{Av}}. \tag{5-38}$$

The various α and β therefore become independent if, as we also assume, the target centre is defined so that

$$\sum_{n=1}^{N} \varepsilon_n \, [a_n^2]_{\mathrm{Av}} = 0. \tag{5-39}$$

This centre and the geometrical centre of the target coincide if $[a_n^2]_{\mathrm{Av}}$ is a constant for all n.

Under the above conditions $E_a(t)$ and $V(t)$ also become independent of each other with $E_a(t)$ Rayleigh-distributed and $V(t)$ Gaussian-distributed. The variances $[E_a^2]_{\mathrm{Av}}$ and $[V^2]_{\mathrm{Av}}$ are

$$\left.\begin{aligned} [E_a^2]_{\mathrm{Av}} &= [\alpha_1^2]_{\mathrm{Av}} + [\alpha_2^2]_{\mathrm{Av}} = \sum_{n=1}^{N} [a_n^2]_{\mathrm{Av}}, \\ [V^2]_{\mathrm{Av}} &= \tfrac{1}{2} \{1 + \tan^2 (\psi_0' - \psi)\} \sum_{n=1}^{N} \varepsilon_n^2 \, [a_n^2]_{\mathrm{Av}}. \end{aligned}\right\} \tag{5-40}$$

If the elements are uniformly distributed along the target of length L and all $[a_n^2]_{\mathrm{Av}}$ are equal, from (5-30) and (5-40) the ratio $[V^2]_{\mathrm{Av}}/[E_a^2]$ is

$$\frac{[V^2]_{\mathrm{Av}}}{[E_a^2]_{\mathrm{Av}}} = \frac{1 + \tan^2 (\psi_0' - \psi)}{24} \left(\frac{L \sin \Phi}{R} \right)^2. \tag{5-41}$$

The cut-off frequency of the power spectrum of $E_a(t)$ is usually less than 10 c/s for ordinary targets and the cut-off frequencies of $V(t)$ and $E_a(t)\, V(t)$ usually do not differ very much from that of $E_a(t)$. A very rough estimate of this frequency f_g can be obtained if one assumes that the amplitude fading and the target glint are

caused by variations of the phases φ_n alone due to a slow random change of the aspect angle Φ of the target. For constant R and $\Theta = 0$, differentiation of (5-23) gives in this case

$$\left|\frac{d\varphi_n}{dt}\right| = 2k\,|\delta_n' \sin \Phi|\left|\frac{d\Phi}{dt}\right| \leq 2\pi\,\frac{(L \sin \Phi)}{\lambda}\left|\frac{d\Phi}{dt}\right| \cong 2\pi f_g$$

or

$$f_g \cong \frac{(L \sin \Phi)}{\lambda}\left|\frac{d\Phi}{dt}\right|. \tag{5-42}$$

With $L = 10$ m, $\Phi = 90°$, $\lambda = 3$ cm, and $|d\Phi/dt| = 0.03$ rad/s, $f_g \cong 10$ c/s.

Let us return to equations (5-33) and (5-34) and as in the preceding section discuss the two limit cases of slow and fast automatic gain control. Immediately after the phase sensitive detector the useful output signal becomes:

a) Slow AGC:

$$s_{\text{det}} \cong G(\Theta_0, d, \psi_0')\left[\frac{[E_a(t)]^2}{[E_a^2]_{\text{Av}}}\,\Theta + \frac{E_a(t)\,V(t)}{[E_a^2]_{\text{Av}}}\right] U_{T,\tau}(t). \tag{5-43}$$

b) Fast AGC:

$$s_{\text{det}} \cong G(\Theta_0, d, \psi_0')\left[\Theta + \frac{V(t)}{E_a(t)}\right] U_{T,\tau}(t). \tag{5-44}$$

Relations (5-43) and (5-44) have the same forms as (5-11) and (5-12) of the preceding section, and the conclusions drawn there are equally applicable in the present case and need not be repeated. Let us, however, compute the time average of the square of the additive angular error

$$\Delta\Theta(t) = \frac{E_a(t)\,V(t)}{[E_a^2]_{\text{Av}}} \tag{5-45}$$

in the case of slow AGC. Because of the independence of $E_a(t)$ and $V(t)$ this becomes

$$[(\Delta\Theta)^2]_{\text{Av}} = \frac{[E_a^2]_{\text{Av}}\,[V^2]_{\text{Av}}}{\{[E_a^2]_{\text{Av}}\}^2} = \frac{[V^2]_{\text{Av}}}{[E_a^2]_{\text{Av}}}. \tag{5-46}$$

When the target elements are uniformly distributed and all $[a_n^2]_{\mathrm{Av}}$ equal, (5-41) and (5-46) give

$$[(\Delta\Theta)^2]_{\mathrm{Av}} = \frac{1 + \tan^2(\psi_0' - \psi)}{24} \left(\frac{L \sin \Phi}{R}\right)^2. \tag{5-47}$$

If, finally, in the case of slow AGC the detector output is passed through a smoothing low-pass filter with cut-off frequency considerably below the cut-off frequency of $\Delta\Theta(t)$, supposed to be f_g, the variance of the smoothed output angular error can be written approximately as

$$[(\Delta\Theta_{\mathrm{out}})^2]_{\mathrm{Av}} \cong \frac{[V^2]_{\mathrm{Av}}}{[E_a^2]_{\mathrm{Av}}} \frac{1}{f_g \tau_f}, \tag{5-48}$$

or, when relation (5-41) is applicable,

$$[(\Delta\Theta_{\mathrm{out}})^2]_{\mathrm{Av}} \cong \frac{1 + \tan^2(\psi_0' - \psi)}{24} \left(\frac{L \sin \Phi}{R}\right)^2 \frac{1}{f_g \tau_f}. \tag{5-49}$$

In the last two expressions τ_f is a suitably defined "effective integration time" of the filter, and the quantity $f_g \tau_f$ is the average number of independent $\Delta\Theta(t)$ values smoothed in getting one output signal value. (The pulse repetition frequency f_r is always very much higher than f_g). The quantity $\tan^2(\psi_0' - \psi)$ appearing in the expressions for the angular error is generally very small and is zero in the case of an ideal monopulse radar.

The angular error of the monopulse radar obtained above varies inversely with distance to target and is entirely due to the glint, that is the angular scintillation of the apparent reflection centre of the target. In the case of a conventional conical-scanning radar there is an additional angular-error component independent of range, caused by the presence of amplitude fading with frequencies close to the beam-scanning frequency. The disappearance of this additional angular-error component explains why monopulse radar has better angular accuracy than conventional radar.

6. Acknowledgement

The author wishes to express his sincere thanks to Professor Henry Wallman of the Chalmers University of Technology, Gothenburg, Sweden, for very valuable help and encouragement in connection with this work.

7. References

1. Page, R. M. Monopulse radar. IRE Convention Record. Part 8, 1955, pp 132—134.
2. Thourel, L. Théorie des circuits hyperfréquence à comparaison de phase ou d'amplitude. Annales de Radioélectricité. No. 52, 1958, pp 130—139.
3. Thomson, W. E. Networks with maximally-flat delay. Wireless Engineer. October 1952, pp 256—263.
4. Storch, Leo. An application of modern network synthesis to the design of constant-time-delay networks with low-Q elements. IRE Convention Record. Part 2, 1954, pp 105—117.
5. Guillemin, E. A. Synthesis of passive networks. John Wiley & Sons, New York 1957.
6. Valley, George E. and Wallman, Henry. Vacuum tube amplifiers. MIT Radiation Laboratory Series No. 18, McGraw-Hill, New York 1958.
7. Lawson, James L. and Uhlenbeck, George E. Threshold signals. MIT Radiation Laboratory Series No. 24, McGraw-Hill, New York 1948.
8. Delano, R. H. and Pfeffer, Irwin. The effect of AGC on radar tracking noise. Proceedings of the IRE. Vol. 44, 1956, pp 801—810.
9. Delano, R. H. A theory of target glint or angular scintillation in radar tracking. Proceedings of the IRE. Vol. 41, 1953, pp 1778—1784.

SAAB TECHNICAL NOTES
TN 47

SOME CHARACTERISTICS OF TWO SIMPLE LINEAR AND STOCHASTICALLY TIME-VARYING CONTROL SYSTEMS OF INTEREST IN ANGLE AND RANGE MEASUREMENT AND TRACKING BY MONOPULSE RADAR

by

GÖSTA HELLGREN

Summary

In the present paper are studied some characteristics of two simple linear but stochastically time-varying control systems, a so called tracking servo and an AGC-servo, the functions of which can be described by linear differential equations of the first order with one stochastically time-varying parameter. Two cases of randomly time-varying system parameters are discussed. In the one case the parameter is supposed to be generated by a stationary random Gaussian process with arbitrary spectrum, which is specialized in the numerical treatment to a rectangular low-pass spectrum. In the other case the system parameter is assumed to be generated by a quasi-stationary arbitrarily distributed random process with a low-pass spectrum of the type $\sin^2 \frac{\pi\omega}{2\omega_0} \Big/ \left(\frac{\pi\omega}{2\omega_0}\right)^2$, where the cut-off angular frequency ω_0 can be chosen at will. The case of a Rayleigh-distributed quasi-stationary process is treated numerically.

The stability of the tracking servo is discussed and some characteristics of the output, in the form of its average value, average square value, and average square deviation from a certain desired output are studied for both deterministic and stationary stochastic inputs as well as in the presence of additive stationary random noise. Regarding stochastic inputs and additive noise it is assumed in the numerical treatment that the autocorrelation functions of the processes are of the simple exponential forms $\exp\{-K_s|\tau|\}$ and $\exp\{-K_n|\tau|\}$, where K_s and K_n are the cut-off angular frequencies of the input and additive noise processes. As for the AGC-servo its stability is studied, and the average value of the output and the average square deviation of the output from a desired value are analyzed as well as the average square value of the so called resultant signal amplification of the system.

The numerical results obtained from the study of the tracking servo and AGC-servo according to the above in the case of a quasi-stationary Rayleigh-distributed random system parameter are applied

to a simple angular target tracking monopulse radar with a slowly acting AGC and an angle-measuring monopulse radar (open-loop system) with an arbitrarily fast AGC. The agreement between these theoretical results and experimental results of measurements made on practical and more complicated monopulse radar systems is satisfactory.

Saab Aircraft Company

Linköping, May, 1960.

Contents

1. Introduction

In the case of linear and constant (time-invariant) control systems, i. e. such systems that can be described by linear differential equations with constant coefficients, it is comparatively easy to calculate the effect on the output signal of stationary random noise introduced somewhere into the system, as well as the resulting dynamic errors for different types of deterministic or stochastic inputs [1], [2]. The analytical treatment of similar problems is considerably more difficult if the characteristics of the control systems vary randomly with time, in which case the system is described by a linear differential equation with stochastic coefficients. In practice this can be done only for some simple special systems.

The literature includes the results of some investigations of linear systems with randomly varying parameters, among which the following should be mentioned. ROSENBLOM, HEILFRON, and TRAUTMAN [3] have studied the statistical characteristics of the output signal of a system described by a linear differential equation of the first order with randomly varying coefficients for which the coefficients are generated by a stationary random Gaussian (normal) process with arbitrary power spectrum, or are certain simple regular functions of such Gaussian processes, for instance χ^2-processes. The same authors have also theoretically treated systems governed by a linear differential equation of arbitrary order with one stochastically varying coefficient having the character of white Gaussian noise. TIKHONOV [4] discusses, like ROSENBLOM, HEILFRON, and TRAUTMAN, the first order randomly time-varying linear system and also assumes stationary stochastic Gaussian processes. In a recent paper SAMUELS and ERINGEN [5] study the solutions of linear differential equations of arbitrary order with small randomly varying coefficients which vary slowly, and equations containing only one random coefficient. In all these cases stationary stochastic Gaussian processes are assumed.

The present paper discusses some characteristics of the output signals of two simple linear stochastically time-varying control systems described by linear differential equations of the first order

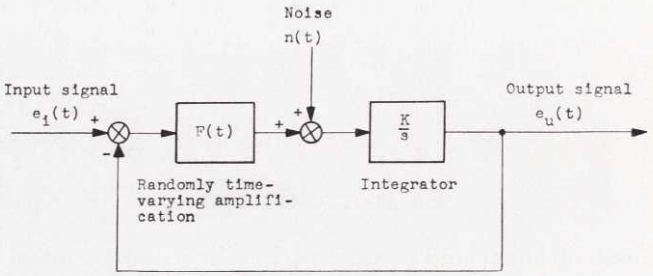

Fig. 1. Simple linear stochastically time-varying control system ("tracking servo").

with one randomly varying parameter. These systems are of great technical interest in various connections, among them angle and range measurement and tracking by monopulse radar. Two cases of stochastically varying parameter of the systems are discussed. In one case we suppose, as in [3] and [4], that the random parameter is generated by a stationary Gaussian process with arbitrary power spectrum, while in the other — and this is the most interesting case in radar applications — the stochastically varying parameter is assumed to be arbitrarily distributed, for instance Rayleigh-distributed, and generated by a quasi-stationary process with a certain power spectrum of low-pass character. This latter case of a first order linear system with a randomly time-varying, not necessarily Gaussian-distributed parameter, appears not to have been treated previously in the literature.

The first simple linear but stochastically time-varying control system treated is shown in block-diagram form in fig. 1. In order to simplify the description in the following we shall introduce the term "tracking servo" for this system. In fig. 1 the input signal of the tracking servo is denoted by $e_i(t)$ and the output by $e_u(t)$. The symbol $n(t)$ stands for an undesirable noise signal and $F(t)$ represents an amplification factor that varies stochastically with time. The servo loop also contains an integrator K/s, where K is an arbitrary positive constant. If $F(t)$ is a positive constant independent of time t, say $F(t) = \varkappa$, the tracking servo becomes time-invariant and is evidently equivalent to a simple linear constant low-pass filter of RC-type with cut-off angular frequency $K_0 = \varkappa K$.

An example of a stochastically time-varying control system of the above type is provided by a one-dimensional automatic target tracking monopulse radar with a simple tracking servo and a slowly acting

automatic gain control (AGC). In this case the input signal $e_i(t)$ in fig. 1 represents the actual position of the target in angle or range and the output signal $e_u(t)$ stands for the angular position of the antenna platform or the output voltage of the range servo. The stochastically time-varying amplification $F(t)$ of the system is due to the inability of the slow AGC to compensate for the rapid variations of the amplitude of the received target echos. The quantity $F(t)$ can be supposed to be Rayleigh-distributed and generated by a more or less stationary random process with a power spectrum of low-pass character. The noise signal $n(t)$ is caused by both the internal noise of the radar receiver and the target glint or scintillations in angle and range of ordinary targets such as airplanes and ships (see appendix II).

In this article are studied the characteristics of the output signal of the tracking servo for both deterministic and stationary stochastic noise. The random amplification $F(t)$ can be generated either by a stationary Gaussian process with arbitrary power spectrum or by an arbitrary — not necessarily Gaussian — quasi-stationary process with a power density function of the type $\sin^2\left(\frac{\omega t_0}{2}\right)\Big/\left(\frac{\omega t_0}{2}\right)^2$, where ω denotes angular frequency and the "time-constant" t_0 and consequently the bandwidth of the spectrum can be chosen at will. All the random processes mentioned above are assumed to be independent. The results obtained in the analysis of the tracking servo of fig. 1 are applied to an angular tracking monopulse radar with a slow AGC.

In this connection it should be mentioned that by means of a pertubation procedure BUCHAN and RAVEN have studied in some detail a tracking servo of the above type in the case that the stochastic variations of amplifications is small [6]. Our study does not imply such a restriction.

The other simple linear stochastically time-varying control system, which is intimately related to the one mentioned above, and which will also be studied in the present paper, is shown in block-diagram in fig. 2. Many automatic gain control systems are of this type, at least approximately (see appendix I). For simplicity we shall call the control system of fig. 2 the "AGC servo". The quantity α in fig. 2 denotes the cut-off angular frequency of the linear constant low-pass filter in the feed-back branch of the AGC servo, K is a positive constant, and g_0 represents the signal amplification without AGC. What

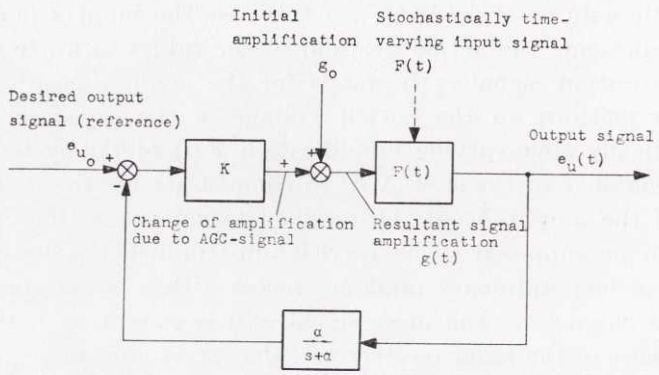

Fig. 2. Simple linear stochastically time-varying control system ("AGC-servo").

one particularly wishes to investigate is the magnitude of the undesirable variations of the output signal $e_u(t)$ due to the random variations with time of the input signal $F(t)$ when the rapidity of the AGC system (determined among other things by the parameters α and K) is related in some way to the speed of variation of $F(t)$. Further, one desires to study what we call the resultant signal amplification $g(t)$ defined in fig. 2.

As in the case of the tracking servo of fig. 1, the behaviour of the AGC servo is analyzed for two cases: $F(t)$ generated either by a stationary random Gaussian process with arbitrary power spectrum, or by a quasi-stationary random process with a power spectrum of type $\sin^2\left(\frac{\omega t_0}{2}\right)\Big/\left(\frac{\omega t_0}{2}\right)^2$ and an arbitrary distribution. The results of these investigations are used to examine the influence of the AGC upon the angular accuracy of a non-tracking angle-measuring monopulse radar.

The theoretical results obtained from a study of the two simple randomly time-varying control systems, the tracking servo and the AGC servo reported above, agree satisfactorily, when applied to angular monopulse radars, with the results obtained experimentally with actual radar systems of this type, even though these are more complicated [7], [8], [9].

2. Fundamental relations in the case of a linear randomly time-varying tracking servo

Let us first study the characteristics of the linear randomly time-varying control system or tracking servo of fig. 1, the purpose of which is to give an output signal $e_u(t)$ that differs as little as possible from the given input $e_i(t)$. As is immediately evident from the block-diagram of fig. 1, the function of the tracking servo is described by the following linear differential equation of the first order

$$\frac{de_u}{dt} + K F(t) e_u = K F(t) e_i(t) + K n(t). \tag{2-1}$$

This differential equation can be integrated directly for arbitrary functions $F(t)$. If the control system starts from rest at time $t = 0$ the solution has the simple analytical form

$$e_u(t) = \int_0^t W_{e_i}(t, \tau)\, e_i(\tau)\, d\tau + \int_0^t W_n(t, \tau)\, n(\tau)\, d\tau, \tag{2-2}$$

where the weighting functions or the unit-impulse responses $W_{e_i}(t, \tau)$ and $W_n(t, \tau)$ of the system corresponding to the input or noise signals are

$$W_{e_i}(t, \tau) = KF(\tau) \exp\left\{-K \int_\tau^t F(\varrho)\, d\varrho\right\} = \frac{\partial}{\partial \tau}\left[\exp\left\{-K \int_\tau^t F(\varrho)\, d\varrho\right\}\right] \tag{2-3}$$

and

$$W_n(t, \tau) = K \exp\left\{-K \int_\tau^t F(\varrho)\, d\varrho\right\}. \tag{2-4}$$

If the amplification $F(t)$ of the servo is a positive constant independent of time, $F(t) = \varkappa$, the tracking servo becomes time-invariant and the two weighting functions depend only upon the interval

$t - \tau$ between the observation of the output and the application of the impulse. In this case

$$\left.\begin{aligned} & W_{e_i}(t, \tau) = \varkappa W_n(t, \tau) = K_0 \exp\{- K_0 (t - \tau)\} \\ & \text{with} \\ & K_0 = \varkappa K. \end{aligned}\right\} \qquad (2\text{-}5)$$

A simple low-pass filter of RC-type with cut-off angular frequency K_0 has a weighting function or an impulse response of the form above.

Of considerable more interest is the case for which the amplification $F(t)$ varies stochastically with time. As was mentioned in the introduction we shall study two such cases in this article. In the first case we shall make the assumption that $F(t)$ can be written as the sum of a positive constant $\varkappa$ and stationary normal (Gaussian) band-limited random noise with zero mean but arbitrary spectrum. Under these assumptions we write, following RICE [10], the amplification $F(t)$ as

$$F(t) = {}^kF(t) = \varkappa + \sum_{n=1}^{N} {}^ka_n \cos n\Delta\omega t + {}^kb_n \sin n\Delta\omega t, \qquad (2\text{-}6)$$

where ${}^ka_n$ and ${}^kb_n$ are members of ensembles $\{{}^ka_n\}$ and $\{{}^kb_n\}$ of independent normally distributed random variables with zero mean value (index k indicates a certain member of the ensemble). The coefficients ${}^ka_n$ and ${}^kb_n$ are supposed to have the following statistical characteristics:

$$\left.\begin{aligned} & \langle {}^ka_n \rangle = \langle {}^kb_n \rangle = 0, \\ & \langle {}^ka_n^2 \rangle = \langle {}^kb_n^2 \rangle = G(n\Delta\omega)\,\Delta\omega, \\ & \langle {}^ka_n\, {}^ka_m \rangle = \langle {}^kb_n\, {}^kb_m \rangle = 0 \quad \text{if } m \neq n, \text{ and} \\ & \langle {}^ka_n\, {}^kb_n \rangle = 0 \quad \text{for all } m \text{ and } n, \end{aligned}\right\} \qquad (2\text{-}7)$$

where $\langle\ \rangle$ denotes an average value taken over all members k of the ensemble. The quantity $G(n\Delta\omega)$, called the power spectral density at the angular frequency $n\Delta\omega$, is the ensemble average of the power of the components of ${}^kF(t)$ lying in the frequency interval $n\Delta\omega \leqq \omega < (n + 1)\Delta\omega$. The purpose of the representation (2-6) of $F(t)$ is to let $N \to \infty$ and $\Delta\omega \to 0$ at a suitable phase of the analysis of the

tracking servo and thereby change from a discrete to a continuous spectrum for the process $\{{}^kF(t)\}$.

In the second case we shall suppose that the amplification $F(t)$ is generated by a quasi-stationary random process $\{{}^kF(t)\}$ and thereby assume that $F(t)$ takes on different constant values in consecutive intervals of time with length t_0. We put $F(t)$ in the form

$$\left.\begin{aligned} &F(t) = {}^kF(t) = {}^kF_n, \quad nt_0 < t \leqq (n+1)\,t_0, \\ &n = \ldots -1, 0, +1, \ldots, \end{aligned}\right\} \tag{2-8}$$

where ${}^kF_n$ is a member k of an ensemble $\{{}^kF_n\}$ of independent arbitrarily but equally distributed random variables, with average value $\varkappa$ and dispersion σ_0, i. e.

$$\left.\begin{aligned} &\langle {}^kF_n \rangle = \varkappa \qquad \text{for all } n, \\ &\langle ({}^kF_n - \varkappa)^2 \rangle = \sigma_0^2 \qquad \text{for all } n, \\ &\langle ({}^kF_n - \varkappa)\,({}^kF_m - \varkappa) \rangle = \langle {}^kF_n - \varkappa \rangle \langle {}^kF_m - \varkappa \rangle = 0 \\ &\text{for all } m \text{ and } n \text{ except } m = n. \end{aligned}\right\} \tag{2-9}$$

From the above it follows that the amplification $F(t)$ has the same distribution as the random variables F_n. The average value at time t and the autocorrelation function corresponding to the times t and $t + \tau$ of the process $\{{}^kF(t)\}$ are

$$\left.\begin{aligned} &\varkappa = \langle {}^kF(t) \rangle, \\ &\gamma(t, t+\tau) = \langle {}^kF(t)\ {}^kF(t+\tau) \rangle. \end{aligned}\right\} \tag{2-10}$$

The random process $\{{}^kF(t)\}$ is not stationary, i. e. its statistical properties in general change with the time of observation t. From (2-8) and (2-10) we see that the autocorrelation function γ is a function of both t and τ, but periodic in t with the period t_0, which means that

$$\left.\begin{aligned} &\gamma(t, t+\tau) = \gamma(t + nt_0, t + nt_0 + \tau), \\ &n = \ldots -1, 0, +1, \ldots. \end{aligned}\right\} \tag{2-11}$$

This is the reason why we denote the process $\{{}^kF(t)\}$ as quasi-stationary.

Let us define the time average $\bar{\gamma}(\tau)$ of the autocorrelation function $\gamma(t, t+\tau)$ as

$$\bar{\gamma}(\tau) = \lim_{T \to \infty} \frac{1}{2T} \int_{-T}^{+T} \gamma(t, t+\tau)\, dt, \tag{2-12}$$

which in the present case of a periodic correlation function γ becomes

$$\bar{\gamma}(\tau) = \frac{1}{t_0} \int_0^{t_0} \langle {}^kF(t)\, {}^kF(t+\tau) \rangle\, dt. \tag{2-13}$$

Under the assumptions given in (2-9) we readily obtain

$$\bar{\gamma}(\tau) = \left\{ \begin{array}{ll} \varkappa^2 + \sigma_0^2 (1 - |\tau|/t_0), & 0 \leqq |\tau|/t_0 \leqq 1; \\ \varkappa^2 \qquad\qquad\qquad\quad , & 1 \leqq |\tau|/t_0. \end{array} \right\} \tag{2-14}$$

If we disregard the "d. c. component" $\varkappa$ of the process $\{{}^kF(t)\}$ we can, starting from the correlation function $\bar{\gamma}(\tau)$, define the power spectral density function of the process as the Fourier transform of $\bar{\gamma}_0(\tau) = \bar{\gamma}(\tau) - \varkappa^2$, or

$$G(\omega) = \frac{2}{\pi} \int_0^{\infty} \bar{\gamma}_0(\tau) \cos \omega\tau\, d\tau, \tag{2-15}$$

where ω is the angular frequency ($\geqq 0$). From (2-15) there also follows the inverse relation

$$\bar{\gamma}_0(\tau) = \int_0^{\infty} G(\omega) \cos \omega\tau\, d\omega. \tag{2-16}$$

The definition above of the power density (power spectrum) of a random process agrees with the one given in [2], pp 65—70. By means of (2-15) och (2-14) we obtain the following power density $G(\omega)$ in the present case

$$\left. \begin{array}{l} G(\omega) = \dfrac{{\sigma_0}^2 t_0}{\pi} \dfrac{\sin^2 \dfrac{\omega t_0}{2}}{\left(\dfrac{\omega t_0}{2}\right)^2}, \\ \omega \geqq 0. \end{array} \right\} \tag{2-17}$$

The power density $G(\omega)$ has consequently a low-pass character with value $G(0) = \sigma_0^2 t_0/\pi$ at $\omega = 0$. We define the bandwidth ω_0 of the spectrum as

$$\omega_0 = \int_0^\infty G(\omega)\, d\omega \Big/ G(0) = \pi/t_0. \tag{2-18}$$

If the amplification $F(t)$ of the tracking servo is stochastic the output signal $e_u(t)$ and the weighting functions also become stochastic. Let us denote the random output and the weighting functions corresponding to the ensemble member ${}^kF(t)$ by ${}^ke_u(t)$, ${}^kW_{e_i}(t, \tau)$, and ${}^kW_n(t, \tau)$. For these, according to (2-2)—(2-4) we have

$${}^ke_u(t) = \int_0^t {}^kW_{e_i}(t, \tau)\, e_i(\tau)\, d\tau + \int_0^t {}^kW_n(t, \tau)\, n(\tau)\, d\tau, \tag{2-19}$$

$${}^kW_{e_i}(t, \tau) = -\frac{\partial}{\partial \tau}\left[\exp\left\{- K \int_\tau^t {}^kF(\varrho)\, d\varrho\right\}\right], \tag{2-20}$$

and

$${}^kW_n(t, \tau) = K \exp\left\{- K \int_\tau^t {}^kF(\varrho)\, d\varrho\right\}. \tag{2-21}$$

The undesirable noise signal $n(t)$ is supposed to be a stationary random time function, statistically independent of $F(t)$, with zero ensemble average value and the autocorrelation function $\Phi_{nn}(\tau) = \langle {}^kn(t)\, {}^kn(t+\tau)\rangle$. The input signal $e_i(t)$ can be either deterministic or stochastic. In the latter case we assume that $n(t)$, $F(t)$, and $e_i(t)$ are statistically independent of each other and that $e_i(t)$ is stationary with zero average value and the autocorrelation function $\Phi_{e_ie_i}(\tau) = \langle {}^ke_i(t)\, {}^ke_i(t+\tau)\rangle$.

Let us first consider the simple deterministic case that the input $e_i(t)$ is a unit step signal occurring at time $t = 0$ and that the noise $n(t)$ is zero. From (2-19) and (2-20) we immediately get

$${}^ke_u(t) = 1 - \exp\left\{- K \int_0^t {}^kF(\varrho)\, d\varrho\right\}. \tag{2-22}$$

The ensemble average $m(t)$ of the output signal at time t can therefore be written

$$m(t) = \langle {}^ke_u(t)\rangle = 1 - \left\langle \exp\left\{- K \int_0^t {}^kF(\varrho)\, d\varrho\right\}\right\rangle, \tag{2-23}$$

and the square mean deviation of the output from this average value at time t becomes

$$[\sigma(t)]^2 = \langle[{}^k e_u(t) - m(t)]^2\rangle =$$

$$= \langle \exp\{-2K \int_0^t {}^k F(\varrho)\, d\varrho\}\rangle - [\langle \exp\{-K \int_0^t {}^k F(\varrho)\, d\varrho\}\rangle]^2. \quad (2\text{-}24)$$

The expressions (2-23) and (2-24), to which we return in chapter 3 and 4 below, reduce to $1 - \exp\{-K_0 t\}$ and zero, if $F(t)$ is time-invariant: $F(t) = \varkappa$. A further investigation of expressions (2-23) and (2-24) will disclose the magnitude of the disturbances in the output signal caused by the fact that the amplification of the tracking servo contains a random component.

If the input signal is stochastic, $e_i(t) = {}^k e_i(t)$, and the noise $n(t)$ still zero, the output and its ensemble average at time t are

$${}^k e_u(t) = \int_0^t {}^k W_{e_i}(t, \tau)\, {}^k e_i(\tau)\, d\tau \quad (2\text{-}25)$$

and

$$\langle {}^k e_u(t)\rangle = \int_0^t \langle {}^k W_{e_i}(t, \tau)\rangle \langle {}^k e_i(\tau)\rangle\, d\tau, \quad (2\text{-}26)$$

assuming that the averaging process can be carried out under the integral sign. Because the processes $\{{}^k F(t)\}$ and $\{{}^k e_i(t)\}$ were supposed to be independent the average of the product ${}^k W_{e_i}(t, \tau)\, {}^k e_i(\tau)$ becomes the product of the corresponding average values, or $\langle {}^k W_{e_i}(t, \tau)\, {}^k e_i(\tau)\rangle = \langle {}^k W_{e_i}(t, \tau)\rangle \langle {}^k e_i(\tau)\rangle$. From (2-26) it is seen that the average output is zero, as according to the assumptions the input signal average is zero.

The dynamic error of the tracking servo, by which we mean the difference between a desired output equal to the system input and the actual output signal, becomes

$${}^k e_i(t) - {}^k e_u(t) = {}^k e_i(t) - \int_0^t {}^k W_{e_i}(t, \tau)\, {}^k e_i(\tau)\, d\tau. \quad (2\text{-}27)$$

The ensemble average value of this error is zero. The average square value $[\sigma_d(t)]^2$ of the dynamic error at time t is readily obtained as

$$[\sigma_d(t)]^2 = \langle[{}^k e_i(t)]^2\rangle - 2 \int_0^t \langle {}^k W_{e_i}(t, \tau)\rangle \langle {}^k e_i(\tau)\, {}^k e_i(t)\rangle\, d\tau +$$

$$+ \int_0^t \int_0^t \langle {}^k W_{e_i}(t, \tau)\, {}^k W_{e_i}(t, \nu)\rangle \langle {}^k e_i(\tau)\, {}^k e_i(\nu)\rangle\, d\tau\, d\nu.$$

After introducing the autocorrelation function of the input signal $\Phi_{e_i e_i}(\tau) = \langle {}^k e_i(t)\, {}^k e_i(t+\tau)\rangle$ and a simple change of variables of integration, $[\sigma_d(t)]^2$ becomes

$$[\sigma_d(t)]^2 = \Phi_{e_i e_i}(0) - 2\int_0^t \langle {}^k W_{e_i}(t, t-\tau)\rangle\, \Phi_{e_i e_i}(\tau)\, d\tau + \\ + \int_0^t\int_0^t \langle {}^k W_{e_i}(t, t-\tau)\, {}^k W_{e_i}(t, t-\nu)\rangle\, \Phi_{e_i e_i}(\tau-\nu)\, d\tau d\nu. \quad (2\text{-}28)$$

If we neglect all transient phenomena and confine our interest to the value of $\sigma_d{}^2$ holding for large t (stationary case) we can write

$$[\sigma(t)]^2 \cong \Phi_{e_i e_i}(0) - 2\int_0^\infty \langle {}^k W_{e_i}(t, t-\tau)\rangle\, \Phi_{e_i e_i}(\tau)\, d\tau + \\ + \int_0^\infty\int_0^\infty \langle {}^k W_{e_i}(t, t-\tau)\, {}^k W_{e_i}(t, t-\nu)\rangle\, \Phi_{e_i e_i}(\tau-\nu)\, d\tau\, d\nu. \quad (2\text{-}29)$$

If the random amplification $F(t)$ is normal and stationary, the dynamic error according to (2-29) is independent of the time of observation t, whereas in the other case of a quasi-stationary arbitrarily distributed amplification the dynamic error varies periodically with time with a period t_0. In the latter case we compute the time-average $\overline{\sigma_d{}^2}$ of $[\sigma_d(t)]^2$, which is the quantity of interest. Putting $t = nt_0 + \Delta t$ this time-average $\overline{\sigma_d{}^2}$ becomes

$$\overline{\sigma_d{}^2} = \frac{1}{t_0}\int_0^{t_0} [\sigma_d(\Delta t)]^2\, d(\Delta t). \quad (2\text{-}30)$$

[Compare the earlier definition of the autocorrelation function $\bar{\gamma}(\tau)$ and the power density function $G(\omega)$ of a quasi-stationary random process.] In the following we shall investigate in somewhat more detail the dynamic errors according to (2-29) and (2-30) in some cases of considerable practical interest.

Let us finally study the part of the output signal of the tracking servo that originates from an undesirable, additive, stationary random noise signal ${}^k n(t)$, i. e. according to (2-19),

$${}^k e_u(t) = \int_0^t {}^k W_n(t, \tau)\, {}^k n(\tau)\, d\tau. \quad (2\text{-}31)$$

We see immediately that the ensemble average $\langle {}^k e_u(t) \rangle$ is equal to zero in this case because of the assumptions made that the processes $\{{}^k F(t)\}$ and $\{{}^k n(t)\}$ are independent and that the average $\langle {}^k n(t) \rangle$ is equal to zero. The ensemble average value at time t of the square of the noise output, $[\sigma_n(t)]^2$, we easily find as

$$[\sigma_n(t)]^2 = \int_0^t \int_0^t \langle {}^k W_n(t, t-\tau)\, {}^k W_n(t, t-\nu) \rangle\, \Phi_{nn}(\tau - \nu)\, d\tau\, d\nu, \quad (2\text{-}32)$$

where $\Phi_{nn}(\tau)$ is the autocorrelation function of the stationary noise process, i. e. $\Phi_{nn}(\tau) = \langle {}^k n(t)\, {}^k n(t+\tau) \rangle$. We shall only be interested in the stationary value of the noise output contribution holding for large t and we therefore write

$$[\sigma_n(t)]^2 \cong \int_0^\infty \int_0^\infty \langle {}^k W_n(t, t-\tau)\, {}^k W_n(t, t-\nu) \rangle\, \Phi_{nn}(\tau - \nu)\, d\tau\, d\nu. \quad (2\text{-}33)$$

If the random amplification of the tracking servo is stationary the noise output $[\sigma_n(t)]^2$ is independent of time for large t, but in the case of a quasi-stationary amplification the noise output varies periodically with time with the period t_0. In this latter case we therefore regard the time-average value

$$\overline{\sigma_n^2} = \frac{1}{t_0} \int_0^{t_0} [\sigma_n(\Delta t)]^2\, d(\Delta t) \quad (2\text{-}34)$$

for $t = nt_0 + \Delta t$ and n large. It is to be expected that the contribution of the additive noise to the output, as well as the dynamic error of the tracking servo, will be increased by the presence of a random component in the amplification $F(t)$ of the system compared with the case that $F(t)$ is constant. As for the additive noise output this phenomenon will be studied below in more detail on the basis of relations (2-33) and (2-34).

3. The characteristics of the tracking servo for Gaussian-distributed, stationary random amplification with arbitrary spectrum

3.1 Deduction of the expressions for certain ensemble average values

In order to be able to investigate the influence of a stochastically time-varying amplification $F(t)$ of the tracking servo upon the output in the presence of different types of inputs $e_i(t)$ and noise signals $n(t)$ according to the above, we need analytical expressions for the ensemble averages $\langle \exp\{-K\int_0^t {}^kF(\varrho)\,d\varrho\}\rangle$, $\langle \exp\{-2K\int_0^t {}^kF(\varrho)\,d\varrho\}\rangle$, $\langle {}^kW_{e_i}(t, t-\tau)\rangle$, $\langle {}^kW_{e_i}(t, t-\tau)\,{}^kW_{e_i}(t, t-\nu)\rangle$, and $\langle {}^kW_n(t, t-\tau)\,{}^kW_n(t, t-\nu)\rangle$. It turns out to be comparatively easy to derive these expressions in the case of Gaussian-distributed, stationary random amplification with arbitrary spectrum.

Let us introduce the following function-notations:

$$P(t,\tau) = \langle \exp\{-K\int_\tau^t {}^kF(\varrho)\,d\varrho\}\rangle, \tag{3.1-1}$$

and

$$Q(t,\tau,\nu) = \langle \exp\{-K\int_\tau^t {}^kF(\varrho)\,d\varrho - K\int_\nu^t {}^kF(\varrho)\,d\varrho\}\rangle. \tag{3.1-2}$$

Starting from equation (2-20) of the preceding chapter, therefore, the ensemble average $\langle {}^kW_{e_i}(t,\tau)\rangle$ ought to be obtained as

$$\langle {}^kW_{e_i}(t,\tau)\rangle = \langle \frac{\partial}{\partial\tau}[\exp\{-K\int_\tau^t {}^kF(\varrho)\,d\varrho\}]\rangle = \frac{\partial}{\partial\tau}P(t,\tau), \tag{3.1-3}$$

because the average value of the difference of two functions is equal to the difference of the corresponding function averages and, as a matter of principle, a differentiation is the same as the forming of a

difference. In a similar way the average $\langle {}^kW_{e_i}(t,\tau)\,{}^kW_{e_i}(t,\nu)\rangle$ ought to be obtained as

$$\langle {}^kW_{e_i}(t,\tau)\,{}^kW_{e_i}(t,\nu)\rangle = \frac{\partial^2}{\partial\tau\,\partial\nu}\,Q\,(t,\tau,\nu). \tag{3.1-4}$$

Equation (2-21) and the definition (3.1-2) above immediately give

$$\langle {}^kW_n(t,\tau)\,{}^kW_n(t,\nu)\rangle = K^2\,Q\,(t,\tau,\nu). \tag{3.1-5}$$

We start by computing the integral $K\int_\tau^t {}^kF(\varrho)\,d\varrho$. With ${}^kF(\varrho)$ given by relation (2-6) we readily get

$$K\int_\tau^t {}^kF(\varrho)\,d\varrho = K_0\,[t-\tau+\sum_{n=1}^{N} A'_n\,{}^ka_n - B'_n\,{}^kb_n], \tag{3.1-6}$$

where

$$\left.\begin{aligned} A'_n &= \frac{1}{\varkappa}\,\frac{\sin n\Delta\omega t - \sin n\Delta\omega\tau}{n\Delta\omega}, \\ B'_n &= \frac{1}{\varkappa}\,\frac{\cos n\Delta\omega t - \cos n\Delta\omega\tau}{n\Delta\omega}, \end{aligned}\right\} \tag{3.1-7}$$

and as before

$$K_0 = \varkappa K. \tag{3.1-8}$$

In the following we also need expressions for the sum of two such integrals $K\int_\tau^t {}^kF(\varrho)\,d\varrho + K\int_\nu^t {}^kF(\varrho)\,d\varrho$, which for convenience we write in a similar way:

$$K\int_\tau^t {}^kF(\varrho)\,d\varrho + K\int_\nu^t {}^kF(\varrho)\,d\varrho = K_0\,[t-\tau+$$

$$+\,t-\nu+\sum_{n=1}^{N} A_n\,{}^ka_n - B_n\,{}^kb_n], \tag{3.1-9}$$

where consequently

$$\left.\begin{aligned} A_n &= \frac{1}{\varkappa}\,\frac{2\sin n\Delta\omega t - \sin n\Delta\omega\tau - \sin n\Delta\omega\nu}{n\Delta\omega}, \\ B_n &= \frac{1}{\varkappa}\,\frac{2\cos n\Delta\omega t - \cos n\Delta\omega\tau - \cos n\Delta\omega\nu}{n\Delta\omega}. \end{aligned}\right\} \tag{3.1-10}$$

From the relations (3.1-1), (3.1-2), (3.1-6), and (3.1-9) the functions P and Q are given as

$$P(t,\tau) = \exp\{-K_0(t-\tau)\}\,\langle\exp\{-K_0\sum_{n=1}^{N} A_n'\,{}^k a_n - B_n'\,{}^k b_n\}\rangle \tag{3.1-11}$$

and

$$Q(t,\tau,\nu) = \exp\{-K_0(t-\tau+t-\nu)\}\,\langle\exp\{-K_0\sum_{n=1}^{N} A_n\,{}^k a_n - B_n\,{}^k b_n\}\rangle, \tag{3.1-12}$$

where the coefficients A_n', A_n, B_n', and B_n are independent of the normally distributed random variables a_n and b_n.

We now examine the ensemble average in (3.1-11). As, according to the assumptions, the random variables a_n, a_m, b_n, b_m $(n \neq m)$, and a_n and b_m (all n) are independent of each other, and because the average of the product of functions of independent random variables is equal to the product of the averages of each individual function, we can write

$$\langle\exp\{-K_0\sum_{n=1}^{N} A_n'\,{}^k a_n - B_n'\,{}^k b_n\}\rangle =$$

$$= \prod_{n=1}^{N}\langle\exp\{-K_0 A_n'\,{}^k a_n\}\rangle \prod_{n=1}^{N}\langle\exp\{K_0 B_n'\,{}^k b_n\}\rangle. \tag{3.1-13}$$

The probability density function of the normally distributed random variable a_n is

$$\left.\begin{aligned} f(a_n) &= \frac{1}{\sqrt{2\pi}\,\sigma_n}\exp\left\{-\frac{1}{2}\,\frac{a_n^2}{\sigma_n^2}\right\} \\ &\text{with, according to (2-7),} \\ \sigma_n^2 &= \langle {}^k a_n^2\rangle = G(n\Delta\omega)\,\Delta\omega, \end{aligned}\right\} \tag{3.1-14}$$

and the average $\langle \exp \{- K_0 A'_n \, {}^k a_n\} \rangle$ becomes

$$\langle \exp \{- K_0 A'_n \, {}^k a_n\} \rangle = \frac{1}{\sqrt{2\pi}\, \sigma_n} \int_{-\infty}^{+\infty} \exp \left\{ - K_0 A'_n x - \frac{1}{2} \frac{x^2}{\sigma_n^2} \right\} dx =$$

$$= \exp \{\tfrac{1}{2} K_0^2 (A'_n)^2 \sigma_n^2\}. \tag{3.1-15}$$

In the same way one gets

$$\langle \exp \{K_0 B'_n \, {}^k b_n\} \rangle = \exp \{\tfrac{1}{2} K_0^2 (B'_n)^2 \sigma_n^2\}, \tag{3.1-16}$$

and therefore

$$\langle \exp \{- K_0 \sum_{n=1}^{N} A'_n \, {}^k a_n - B'_n \, {}^k b_n\} \rangle = \exp \{\tfrac{1}{2} K_0^2 \sum_{n=1}^{N} [(A'_n)^2 + (B'_n)^2] \sigma_n^2\}. \tag{3.1-17}$$

By means of the result (3.1-17) and the definitions of A'_n, B'_n, A_n, B_n, and σ_n^2 given in (3.1-7), (3.1-10), and (3.1-14) we can determine the two functions P and Q according to (3.1-11) and (3.1-12). After some computation we get

$$P(t, \tau) = \exp \left\{ - K_0 (t - \tau) + \frac{1}{2} \frac{K_0^2}{\varkappa^2} \sum_{n=1}^{N} \frac{4 \sin^2 \dfrac{n \Delta\omega \, (t - \tau)}{2}}{(n \Delta\omega)^2} G(n \Delta\omega) \Delta\omega \right\} \tag{3.1-18}$$

and

$$Q(t, \tau, \nu) = \exp \left\{ - K_0 (t - \tau + t - \nu) + \frac{1}{2} \frac{K_0^2}{\varkappa^2} \cdot \right.$$

$$\cdot \sum_{n=1}^{N} \frac{8 \sin^2 \dfrac{n \Delta\omega \, (t - \tau)}{2} + 8 \sin^2 \dfrac{n \Delta\omega \, (t - \nu)}{2} - 4 \sin^2 \dfrac{n \Delta\omega \, (\tau - \nu)}{2}}{(n \Delta\omega)^2} \cdot$$

$$\left. \cdot \, G(n \Delta\omega) \, \Delta\omega \right\}. \tag{3.1-19}$$

We observe that P is a function only of the time difference $t - \tau$ and Q of the differences $t - \tau$ and $t - \nu$. This is a consequence of the assumption that the process $\{{}^kF(t)\}$ is stationary. The averages $\langle {}^kW_{e_i}(t, \tau)\rangle$, equation (3.1-3), and $\langle {}^kW_{e_i}(t, \tau)\, {}^kW_{e_i}(t, \nu)\rangle$, equation (3.1-4) can now be computed from (3.1-18) and (3.1-19). The result becomes

$$\langle {}^kW_{e_i}(t, \tau)\rangle = K_0 \left\{1 - \frac{K_0}{\varkappa^2} \sum_{n=1}^{N} \frac{\sin n\Delta\omega\,(t-\tau)}{n\Delta\omega}\, G(n\Delta\omega)\,\Delta\omega\right\} \cdot$$

$$\cdot \exp\left\{- K_0(t-\tau) + \frac{1}{2}\frac{K_0^2}{\varkappa^2} \sum_{n=1}^{N} \frac{4\sin^2 \frac{n\Delta\omega\,(t-\tau)}{2}}{(n\Delta\omega)^2}\, G(n\Delta\omega)\,\Delta\omega\right\}, \quad (3.1\text{-}20)$$

$$\langle {}^kW_{e_i}(t, \tau)\, {}^kW_{e_i}(t, \nu)\rangle = K_0^2 \left[1 - 2\frac{K_0}{\varkappa^2} \cdot\right.$$

$$\cdot \sum_{n=1}^{N} \frac{\sin n\Delta\omega\,(t-\tau) + \sin n\Delta\omega\,(t-\nu)}{n\Delta\omega} G(n\Delta\omega)\,\Delta\omega + \frac{K_0^2}{\varkappa^4} \cdot$$

$$\cdot \sum_{m,n=1}^{N} \frac{1}{m\,n\,(\Delta\omega)^2} \left[4\sin m\Delta\omega\,(t-\tau)\sin n\Delta\omega\,(t-\nu) + 2\sin m\Delta\omega\,(t-\tau)\right.\cdot$$

$$\cdot \sin n\Delta\omega\,(\nu-\tau) - 2\sin m\Delta\omega\,(\nu-\tau)\sin n\Delta\omega\,(t-\nu) - \sin m\Delta\omega\,(\nu-\tau)\cdot$$

$$\left.\cdot \sin n\Delta\omega\,(\nu-\tau)\right] G(m\Delta\omega)\, G(n\Delta\omega)\,(\Delta\omega)^2 + \frac{1}{\varkappa^2} \sum_{n=1}^{N} \cos n\Delta\omega\,(\tau-\nu)\cdot$$

$$\left.\cdot\, G(n\Delta\omega)\,\Delta\omega\right] \exp\left\{- K_0(t-\tau+t-\nu) + \frac{1}{2}\frac{K_0^2}{\varkappa^2} \cdot\right.$$

$$\cdot \sum_{n=1}^{N} \frac{8\sin^2 \frac{n\Delta\omega\,(t-\tau)}{2} + 8\sin^2 \frac{n\Delta\omega\,(t-\nu)}{2} - 4\sin^2 \frac{n\Delta\omega\,(\tau-\nu)}{2}}{(n\Delta\omega)^2} \cdot$$

$$\left.\cdot\, G(n\Delta\omega)\,\Delta\omega\right\}. \quad (3.1\text{-}21)$$

In the ensemble averages deduced above it is now appropriate to let $N \to \infty$, $\Delta\omega \to 0$, and $n\Delta\omega \to \omega$, whereupon the assumed discrete spectrum of the amplification $F(t)$ changes into a continuous spectrum. Let us first introduce some notations. We denote the autocorrelation function corresponding to the spectral density function $G(\omega)$ by $\varrho_{FF}(\tau)$, i. e.

$$\left.\begin{aligned} &\varrho_{FF}(\tau) = \int_0^\infty \cos \omega\tau \, G(\omega) \, d\omega \\ &\text{and inversely} \\ &G(\omega) = \frac{2}{\pi} \int_0^\infty \cos \omega\tau \, \varrho_{FF}(\tau) \, d\tau. \end{aligned}\right\} \tag{3.1-22}$$

Further, we introduce the functions $g_1(\tau)$ and $g_2(\tau)$ determined by the spectral density $G(\omega)$ according to

$$\left.\begin{aligned} g_1(\tau) &= \int_0^\infty \frac{4 \sin^2 \frac{\omega\tau}{2}}{\omega^2 \tau^2} \, G(\omega) \, d\omega, \\ g_2(\tau) &= \int_0^\infty \frac{\sin \omega\tau}{\omega\tau} \, G(\omega) \, d\omega. \end{aligned}\right\} \tag{3.1-23}$$

For small and large values of τ compared to $1/\omega_g$, where ω_g [the cut-off angular frequency of the spectral density $G(\omega)$] is a measure of the magnitude of the highest frequencies appearing in the randomly time-varying amplification $F(t)$, we have approximately

$$\left.\begin{aligned} &g_1(\tau) \cong \varrho_{FF}(0), \quad g_2(\tau) \cong \varrho_{FF}(0); \quad \tau \ll \omega_g^{-1}, \\ &g_1(\tau) \cong \frac{1}{\tau} \pi \, G(0), \quad g_2(\tau) \cong \frac{1}{\tau} \frac{\pi}{2} \, G(0); \quad \tau \gg \omega_g^{-1}. \end{aligned}\right\} \tag{3.1-24}$$

It is easy to carry through the limiting process $N \to \infty$, $\Delta\omega \to 0$, and $n\Delta\omega \to \omega$. By means of relations (3.1-18) — (3.1-23) and (3.1-5) we obtain

$$
\left.
\begin{aligned}
&\langle \exp\{-K\int_0^t {}^kF(\varrho)\,d\varrho\}\rangle = P(t,0),\\
&\langle \exp\{-2K\int_0^t {}^kF(\varrho)\,d\varrho\}\rangle = Q(t,0,0),\\
&\langle {}^kW_{e_i}(t,t-\tau)\rangle = K_0\left[1-\frac{K_0}{\varkappa^2}\tau\, g_2(\tau)\right]P(t,t-\tau),\\
&\langle {}^kW_{e_i}(t,t-\tau)\,{}^kW_{e_i}(t,t-\nu)\rangle = K_0^2\left[\left\{1-\frac{K_0}{\varkappa^2}[\tau\, g_2(\tau)+\nu\, g_2(\nu)]\right\}^2-\right.\\
&-\frac{K_0^2}{\varkappa^4}\{\tau\, g_2(\tau)-\nu\, g_2(\nu)-(\tau-\nu)\, g_2(\tau-\nu)\}^2+\\
&\left.+\frac{1}{\varkappa^2}\varrho_{FF}(\tau-\nu)\right]Q(t,t-\tau,t-\nu),\\
&\langle {}^kW_n(t,t-\tau)\,{}^kW_n(t,t-\nu)\rangle = \frac{K_0^2}{\varkappa^2}\,Q(t,t-\tau,t-\nu),
\end{aligned}
\right\} \quad (3.1\text{-}25)
$$

where

$$
P(t,t-\tau) = \exp\left\{-K_0\tau+\frac{1}{2}\frac{K_0^2}{\varkappa^2}\tau^2 g_1(\tau)\right\}
$$

and

$$
Q(t,t-\tau,t-\nu) = \exp\left\{-K_0(\tau+\nu)+\frac{K_0^2}{\varkappa^2}\left[\tau^2 g_1(\tau)+\nu^2 g_1(\nu)-\right.\right.
$$

$$
\left.\left.-\frac{1}{2}(\tau-\nu)^2 g_1(\tau-\nu)\right]\right\}.
$$

3.2 The output of the tracking servo when the input is a unit step signal

In chapter 2 general expressions for the output signal of the tracking servo, its ensemble average value $m(t)$, and its average square deviation $\sigma(t)$ from $m(t)$, relations (2-22), (2-23), and (2-24), were deduced for the case that the input is a unit step signal occurring at time $t = 0$. If the randomly time-varying amplification $F(t)$ of the system

has the character of stationary band-limited Gaussian noise, the function averages $\langle \exp \{ - K \int_0^t {}^k F(\varrho)\, d\varrho \} \rangle$ and $\langle \exp \{ - 2K \int_0^t {}^k F(\varrho)\, d\varrho \} \rangle$ appearing in (2-23) and (2-24) are given by relation (3.1-25) of the preceding section, and the averages $m(t)$ and $\sigma(t)$ can be written

$$m(t) = 1 - P(t, 0) = 1 - \exp \left\{ - \left[1 - \frac{1}{2} \frac{K_0}{\varkappa^2} t\, g_1(t) \right] K_0 t \right\} \qquad (3.2\text{-}1)$$

and

$$\sigma(t) = \{ Q(t, 0, 0) - [P(t, 0)]^2 \}^{1/2} =$$

$$= \left[1 - \exp \left\{ - \frac{K_0}{\varkappa^2} t\, g_1(t)\, K_0 t \right\} \right]^{1/2} \exp \left\{ - \left[1 - \frac{K_0}{\varkappa^2} t\, g_1(t) \right] K_0 t \right\}. \qquad (3.2\text{-}2)$$

From the expression (3.2-1) we see that the output average $m(t)$ gradually reaches the desired value 1 if for large values of time t

$$1 - \frac{1}{2} \frac{K_0}{\varkappa^2} t\, g_1(t) > 0$$

or, with the help of (3.1-23), if

$$1 - \frac{\pi}{2} \frac{K_0}{\varkappa^2} G(0) > 0. \qquad (3.2\text{-}3)$$

On the other hand, equation (3.2-2) shows that the dispersion $\sigma(t) \to 0$ for large values of t if

$$1 - \frac{K_0}{\varkappa^2} t\, g_1(t) > 0,$$

i. e. if

$$1 - \pi \frac{K_0}{\varkappa^2} G(0) > 0. \qquad (3.2\text{-}4)$$

The tracking servo can consequently become instable in the sense that $\sigma(t)$ increases without limit. Relation (3.2-4) can be said to represent the condition that the randomly time-varying control system is stable. The underlying reason why the tracking servo can become instable is that for a supposed Gaussian-distributed ampli-

fication there is always a certain probability that the amplification is negative, which means positive feedback.

The specific problem of the stability of randomly time-varying linear systems has recently been discussed in [11] by Samuels and in [12] by Bertram and Sarachik.

In the rest of this section we shall specialize our study of the output average $m(t)$ and the root mean square (rms) deviation $\sigma(t)$ to the case that the power density function $G(\omega)$ of the random amplification $F(t)$ of the tracking servo is a constant up to a certain angular frequency ω_0, the cut-off frequency of the stochastic variations of amplification, and zero above this frequency (rectangular spectrum). Let us put

$$G(\omega) = \begin{cases} \sigma_0^2/\omega_0, & 0 \leqq \omega \leqq \omega_0, \\ 0, & \omega > \omega_0, \end{cases} \tag{3.2-5}$$

where the total power or variance σ_0^2 is given by [see relation (3.1-22)]

$$\sigma_0^2 = \varrho_{FF}(0) = \int_0^\infty G(\omega)\, d\omega. \tag{3.2-6}$$

With these assumptions the functions $g_1(\tau)$ and $g_2(\tau)$ defined in (3.1-23) become

$$\left.\begin{aligned} g_1(\tau) &= \frac{\pi}{\tau}\,\frac{\sigma_0^2}{\omega_0}\, I_1(\omega_0\,\tau/2), \\ g_2(\tau) &= \frac{\pi}{2\,\tau}\,\frac{\sigma_0^2}{\omega_0}\, I_2(\omega_0\,\tau), \end{aligned}\right\} \tag{3.2-7}$$

where I_1 and I_2 are given by

$$I_1(\xi) = \frac{2}{\pi}\int_0^\xi \frac{\sin^2 y}{y^2}\, dy \tag{3.2-8}$$

and

$$I_2(\xi) = \frac{2}{\pi}\int_0^\xi \frac{\sin y}{y}\, dy. \tag{3.2-9}$$

For infinitely large values of the argument ξ the functions I_1 and I_2 have the value 1. In the chosen case of a rectangular spectrum it

is also convenient to introduce the notation x for the ratio between K_0, which we can call the cut-off angular frequency of the undisturbed (time-invariant) tracking servo, and ω_0. We further denote by η (the "noise-signal power ratio") the ratio between the powers σ_0^2 and $\varkappa^2$ of the randomly time-varying and the d. c. components of the amplification $F(t)$, i. e.

$$\left.\begin{aligned} x &= K_0/\omega_0, \\ \eta &= \sigma_0^2/\varkappa^2. \end{aligned}\right\} \tag{3.2-10}$$

With the help of (3.2-7) and (3.2-10) the quantities $m(t)$ and $\sigma(t)$ according to (3.2-1) and (3.2-2) become

$$m(t) = 1 - \exp\left\{-\left[1 - \frac{\pi}{2}\,\eta x\, I_1\left(\frac{K_0 t}{2x}\right)\right] K_0 t\right\} \tag{3.2-11}$$

and

$$\sigma(t) = \left[1 - \exp\left\{-\pi\eta x\, I_1\left(\frac{K_0 t}{2x}\right) K_0 t\right\}\right]^{1/2} \exp\left\{-\left[1 - \pi\eta x\, I_1\left(\frac{K_0 t}{2x}\right)\right] K_0 t\right\}. \tag{3.2-12}$$

The condition for stability, equation (3.2-4), is satisfied if the product $\pi \dfrac{\sigma_0^2}{\varkappa^2} \dfrac{K_0}{\omega_0}$ or $\pi\eta x$ is less than 1. In order to obtain good stability it is consequently necessary that either η or x is small, i. e. that either the relative variation of the amplification of the tracking servo is small or that the control system has a pronounced smoothing effect upon these variations. For small values of x the quantity $\pi \dfrac{\sigma_0^2}{\varkappa^2} \dfrac{K_0}{\omega_0}$ represents the noise power received after filtering of a noise signal with the power density (3.2-5) by a simple linear constant low-pass filter of RC-type with cut-off angular frequency K_0.

The asymptotic expressions for the average $m(t)$ and the deviation $\sigma(t)$ which hold for large t such that $t \gg 1/(2xK_0)$ are

$$m(t) \sim 1 - \exp\left\{-\left[1 - \frac{\pi}{2}\,\eta x\right] K_0 t\right\} \tag{3.2-13}$$

and

$$\sigma(t) \sim \left[1 - \exp\left\{-\pi\eta x\, K_0 t\right\}\right]^{1/2} \exp\left\{-\left[1 - \pi\eta x\right] K_0 t\right\}. \tag{3.2-14}$$

From the expressions above we see that for not too small values of t the output average $m(t)$ behaves in the same way as the output signal from a simple linear constant low-pass filter of RC-type with cut-off angular frequency $\left[1 - \frac{\pi}{2}\eta x\right] K_0$, when in both cases the input is a unit step signal at $t = 0$. Summing up we can say that the stochastic variations with time of the amplification of the tracking servo partly cause a decrease of the cut-off frequency of the system compared with the time-invariant case with regard to the average m of the output, partly an extra undesired random noise component in the output of the control system.

In order to illustrate in somewhat more detail the general behaviour of the average value $m(t)$ and the deviation $\sigma(t)$ in the case of a unit step input signal to the tracking servo and a rectangular spectrum of random amplification variations the collection of graphs given in figs 3—5 has been prepared. Fig. 3 shows m as a function of t for $\eta = 1/\pi$ and $x = 1/4$ and fig. 4 the same quantity for $\eta = 1/\pi$ and $x = 1/2$. In the figures there have also been drawn the output for constant amplification $F(t) = \varkappa$, i. e. $1 - \exp\{-K_0 t\}$, the asymptote of m, relation (3.2-13), and the curves $m \pm \sigma$ that give an idea of the dispersion of the output signal curves. Fig. 5, finally, shows the behaviour of $\sigma(t)$ for constant $\eta = 1/\pi$ and $x = 1/8$, $1/4$, $1/2$, and 1.

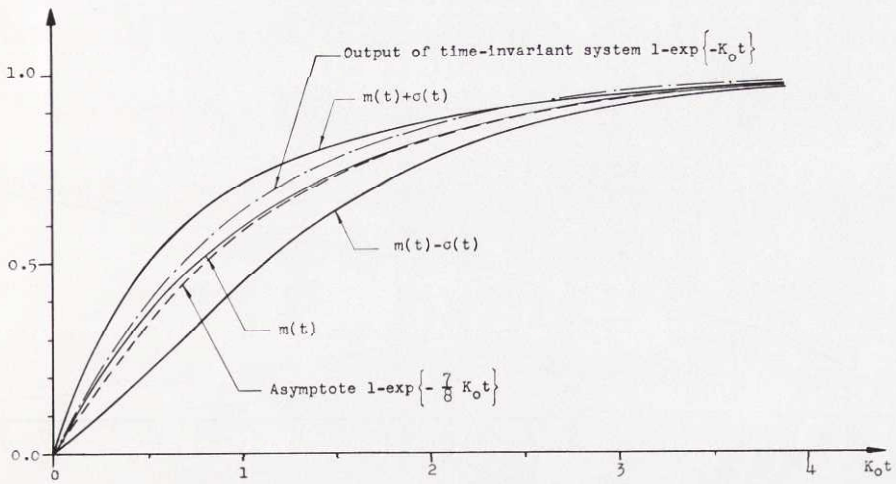

Fig. 3. The average value $m(t)$ of the output of the tracking servo when the input signal is a unit step at $t = 0$. The randomly time-varying amplification is supposed to be stationary and Gaussian with $\eta = 1/\pi$ and $x = 1/4$.

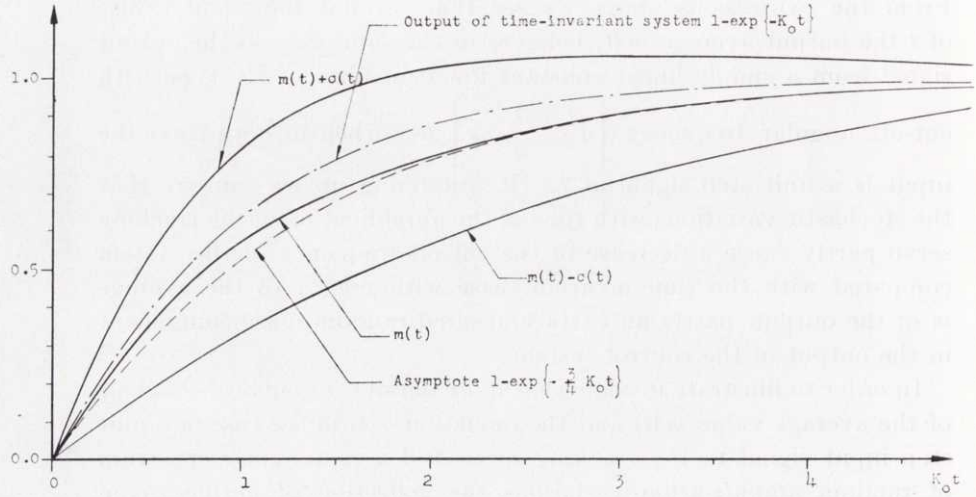

Fig. 4. The average value $m(t)$ of the output of the tracking servo when the input signal is a unit step at $t = 0$. The randomly time-varying amplification is supposed to be stationary and Gaussian with $\eta = 1/\pi$ and $x = 1/2$.

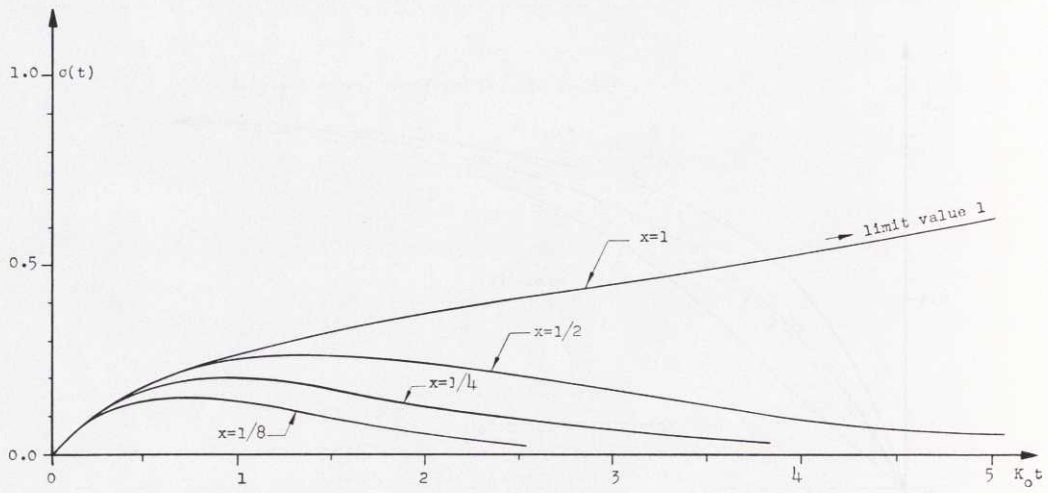

Fig. 5. The deviation $\sigma(t)$ of the output of the tracking servo from its average value $m(t)$ when the input is a unit step at $t = 0$. The randomly time-varying amplification is supposed to be stationary and Gaussian with $\eta = 1/\pi$ and $x = 1/8$, $1/4$, $1/2$, and 1.

3.3 The dynamic error of the tracking servo when the input is a stationary stochastic signal

In chapter 2 we derived a general expression, relation (2-29), for the ensemble average value at time t of the square of the deviation of the tracking servo output from a desired output signal equal to the input, $[\sigma_d(t)]^2$, when the input signal is generated by a stationary random process and the amplification $F(t)$ of the servo is also random. The expression given for $\sigma_d(t)$, the dynamic error, is valid on the assumption that the time of observation t is so large that all transient phenomena can be neglected. Starting from the expression (2-29) for $[\sigma_d(t)]^2$ and the weighting function averages deduced in section 3.1 above and appearing in (2-29), we shall now in somewhat more detail investigate the dynamic error of the tracking servo in the case that its amplification $F(t)$ is stationary stochastic and Gaussian.

If the expressions of the average values $\langle {}^kW_{e_i}(t, t-\tau)\rangle$ and $\langle {}^kW_{e_i}(t, t-\tau)\, {}^kW_{e_i}(t, t-\nu)\rangle$ given in (3.1-25) are put into relation (2-29) we get the following stationary value σ_d^2 for the dynamic error of the tracking servo

$$\sigma_d^2 = \Phi_{e_i e_i}(0) - 2K_0 \int_0^\infty \left[1 - \frac{K_0}{\varkappa^2}\,\tau\, g_2(\tau)\right] \exp\left\{-K_0\tau + \right.$$

$$\left. + \frac{1}{2}\,\frac{K_0^2}{\varkappa^2}\,\tau^2\, g_1(\tau)\right\} \Phi_{e_i e_i}(\tau)\, d\tau + K_0^2 \int_0^\infty \int_0^\infty \left[\left\{1 - \frac{K_0}{\varkappa^2}\,[\tau\, g_2(\tau) + \right.\right.$$

$$\left.\left. + \nu\, g_2(\nu)]\right\}^2 - \frac{K_0^2}{\varkappa^4}\,\{\tau\, g_2(\tau) - \nu\, g_2(\nu) - (\tau-\nu)\, g_2(\tau-\nu)\}^2 + \right.$$

$$\left. + \frac{1}{\varkappa^2}\,\varrho_{FF}(\tau-\nu)\right] \exp\left\{-K_0(\tau+\nu) + \frac{K_0^2}{\varkappa^2}\left[\tau^2 g_1(\tau) + \right.\right.$$

$$\left.\left. + \nu^2 g_1(\nu) - \frac{1}{2}\,(\tau-\nu)^2\, g_1(\tau-\nu)\right]\right\} \Phi_{e_i e_i}(\tau-\nu)\, d\tau\, d\nu. \quad (3.3\text{-}1)$$

In (3.3-1) the functions $\Phi_{e_i e_i}$ and ϱ_{FF} are the autocorrelation functions of the input signal and the random amplification of the tracking servo. The functions $g_1(\tau)$ and $g_2(\tau)$ are determined by the correlation function ϱ_{FF} or its corresponding spectral density $G(\omega)$, relations (3.1-23) and (3.1-22).

By using the final expression (3.3-1) above, applicable to the simple tracking servo with the chosen type of random amplification

variations, the dynamic error can be computed for arbitrary stationary stochastic input signals with the given autocorrelation function $\Phi_{e_i e_i}(\tau)$. We shall specialize our study to treat numerically the case that the spectral density $G(\omega)$ is rectangular in accordance with (3.2-5) and the correlation function $\Phi_{e_i e_i}(\tau)$, normalized so that $\Phi_{e_i e_i}(0) = 1$, has the form

$$\Phi_{e_i e_i}(\tau) = \exp\{- K_s |\tau|\}, \tag{3.3-2}$$

where K_s is the cut-off angular frequency of the input signal process. [An autocorrelation function according to the above is equivalent to a power density function $G_{e_i e_i}(\omega) = \dfrac{2 K_s}{\pi(\omega^2 + K_s^2)}$ given by the inverse Fourier transform $G_{e_i e_i}(\omega) = \dfrac{2}{\pi} \int_0^\infty \Phi_{e_i e_i}(\tau) \cos \omega\tau \, d\tau$, equation (3.1-22).] In this case the functions $g_1(\tau)$ and $g_2(\tau)$ are defined by the relations (3.2-7), (3.2-8), and (3.2-9). The correlation function $\varrho_{FF}(\tau)$ becomes

$$\varrho_{FF}(\tau) = \int_0^\infty \cos \omega\tau \, G(\omega) \, d\omega = \sigma_0^2 \frac{\sin \omega_0 \tau}{\omega_0 \tau}. \tag{3.3-3}$$

After all functions appearing in (3.3-1) have been determined we readily get the dynamic error σ_d^2 as

$$\sigma_d^2 = 1 - 2 \int_0^\infty \left[1 - \frac{\pi}{2} \eta x I_2\left(\frac{\tau}{x}\right)\right] \exp\left\{- \tau - \frac{\tau}{y_s} + \frac{\pi}{2} \eta x \tau I_1\left(\frac{\tau}{2x}\right)\right\} d\tau +$$

$$+ \int_0^\infty \int_0^\infty \left[\left\{1 - \frac{\pi}{2} \eta x \left[I_2\left(\frac{\tau}{x}\right) + I_2\left(\frac{\nu}{x}\right)\right]\right\}^2 - \frac{\pi^2}{4} \eta^2 x^2 \cdot \right.$$

$$\left. \cdot \left\{I_2\left(\frac{\tau}{x}\right) - I_2\left(\frac{\nu}{x}\right) - I_2\left(\frac{\tau - \nu}{x}\right)\right\}^2 + \eta \frac{\sin \dfrac{\tau - \nu}{x}}{\dfrac{\tau - \nu}{x}}\right] \exp\left\{- (\tau + \nu) - \right.$$

$$\left. - \frac{|\tau - \nu|}{y_s} + \pi \eta x \left[\tau I_1\left(\frac{\tau}{2x}\right) + \nu I_1\left(\frac{\nu}{2x}\right) - \frac{1}{2}(\tau - \nu) I_1\left(\frac{\tau - \nu}{2x}\right)\right]\right\} d\tau \, d\nu, \tag{3.3-4}$$

where

$$y_s = K_0/K_s \tag{3.3-5}$$

and as before

$$\left.\begin{aligned} &x = K_0/\omega_0, \quad \eta = \sigma_0^2/\varkappa^2, \\ &I_1(\xi) = \frac{2}{\pi}\int_0^{\xi} \frac{\sin^2 y}{y^2}\,dy, \quad I_2(\xi) = \frac{2}{\pi}\int_0^{\xi} \frac{\sin y}{y}\,dy. \end{aligned}\right\} \tag{3.3-6}$$

If we put $\eta = 0$ in (3.3-4) we obtain the dynamic error $\sigma_{d_0}^2$ in the time-invariant case that $F(t) = \varkappa$ as

$$\sigma_{d_0}^2 = (\sigma_d^2)_{\eta=0} = \frac{1}{1 + y_s}. \tag{3.3-7}$$

From the expression (3.3-4) for σ_d^2 we see that the dynamic error increases without limit if the product $\pi\eta x \to 1$. This is in agreement with the condition for stability formulated in (3.2-4). As pointed out earlier, the reason the system becomes instable is the fact that the Gaussian-distributed amplification $F(t)$ can be negative (positive feedback). This tendency increases with increasing noise-signal power ratio η of $F(t)$ and it is greater the slower the variations of amplification are, i. e. the greater x is. A certain amount of care is therefore always advisable if in a practical tracking servo where the random amplification can never become negative, one approximates the actual distribution of $F(t)$ with a Gaussian distribution and makes use of the results obtained for this case. Such a procedure is permissible only for small values of the product $\pi\eta x$.

The results of some numerical calculations of the dynamic error σ_d^2 according to (3.3-4) above were carried out on SARA, the electronic digital computer of the SAAB Company, and are presented in figs 6—11. As expected, the dynamic error of a randomly time-varying tracking servo is always larger than that of a corresponding time-invariant system, i. e. $\sigma_d^2 \geqq \sigma_{d_0}^2$. Figures 6 and 7 show the ratio $\sigma_d^2/\sigma_{d_0}^2$ as a function of the variable $\varrho = \eta x$ with y_s as a parameter in the two cases that $x = 0.1$ and 1.0. From the figures we conclude that for given ω_0, K_0, and K_s, i. e. given x and y_s values, the ratio $\sigma_d^2/\sigma_{d_0}^2$ increases with increasing ϱ or η, as it ought to. This increase of the ratio $\sigma_d^2/\sigma_{d_0}^2$ with η is larger for larger y_s, while the resultant absolute value of the dynamic error σ_d^2 is smaller for larger y_s, because of a more pronounced decrease of $\sigma_{d_0}^2$ with increasing y_s.

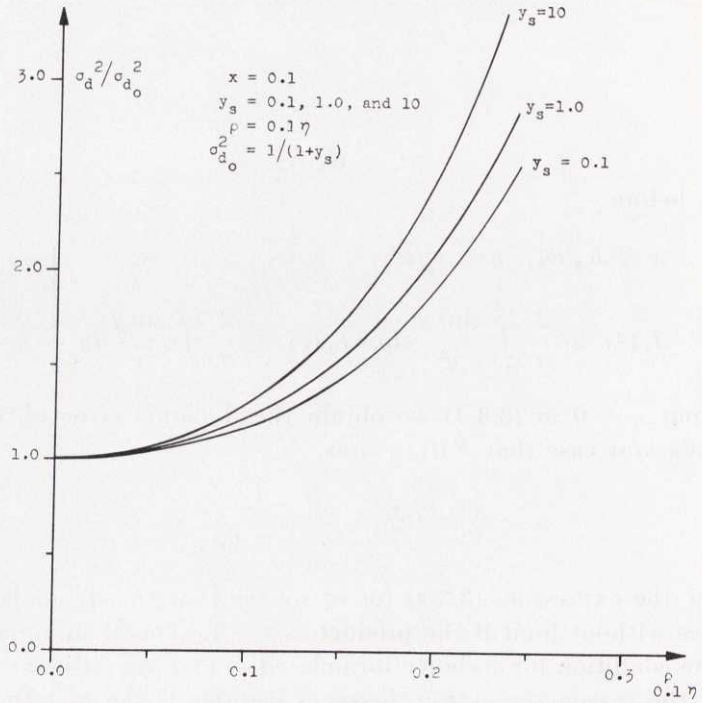

Fig. 6. The dynamic error σ_d^2 of the tracking servo for Gaussian-distributed stationary random amplification as a function of $\varrho = \eta\, x$ with $x = 0.1$ and various values of y_s.

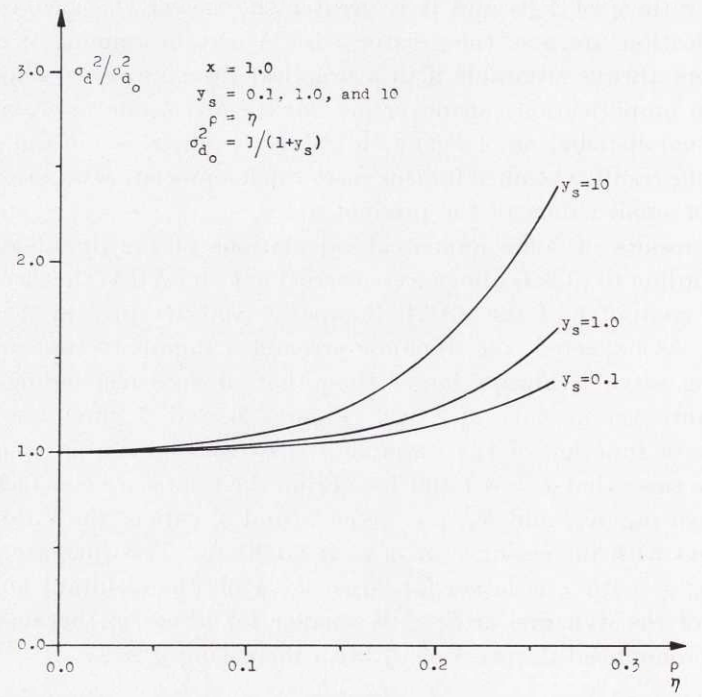

Fig. 7. The dynamic error σ_d^2 of the tracking servo for Gaussian-distributed stationary random amplification as a function of $\varrho = \eta\, x$ with $x = 1.0$ and various values of y_s.

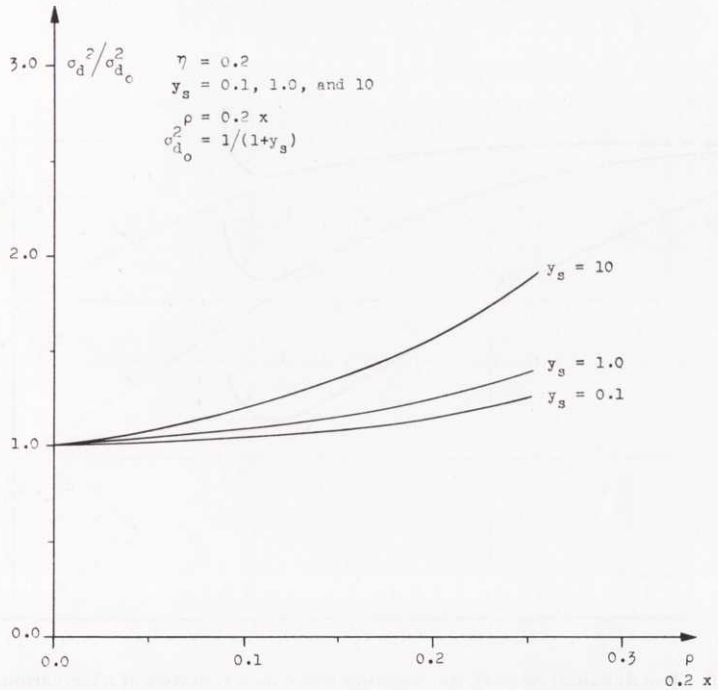

Fig. 8. The dynamic error σ_d^2 of the tracking servo for Gaussian-distributed stationary random amplification as a function of $\varrho = \eta\, x$ with $\eta = 0.2$ and various values of y_s.

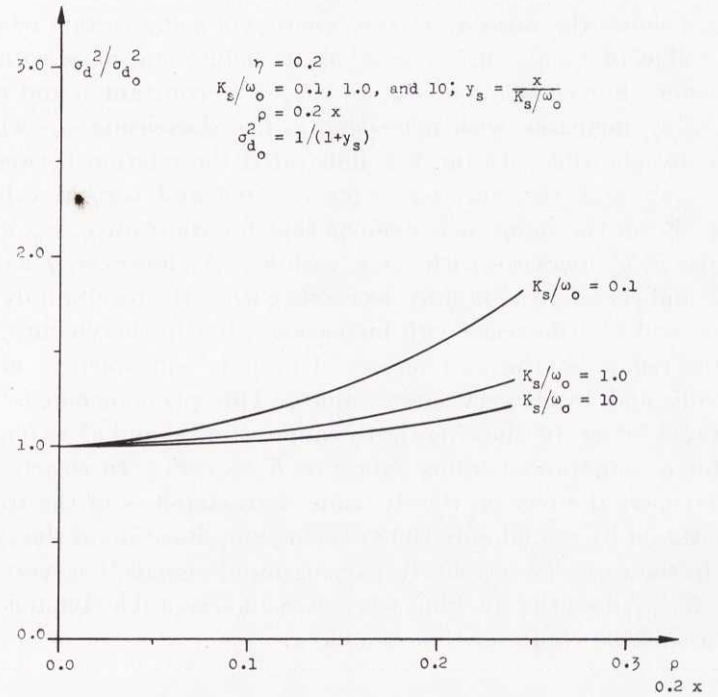

Fig. 9. The dynamic error σ_d^2 of the tracking servo for Gaussian-distributed stationary random amplification as a function of $\varrho = \eta\, x$ with $\eta = 0.2$ and various values of K_s/ω_0.

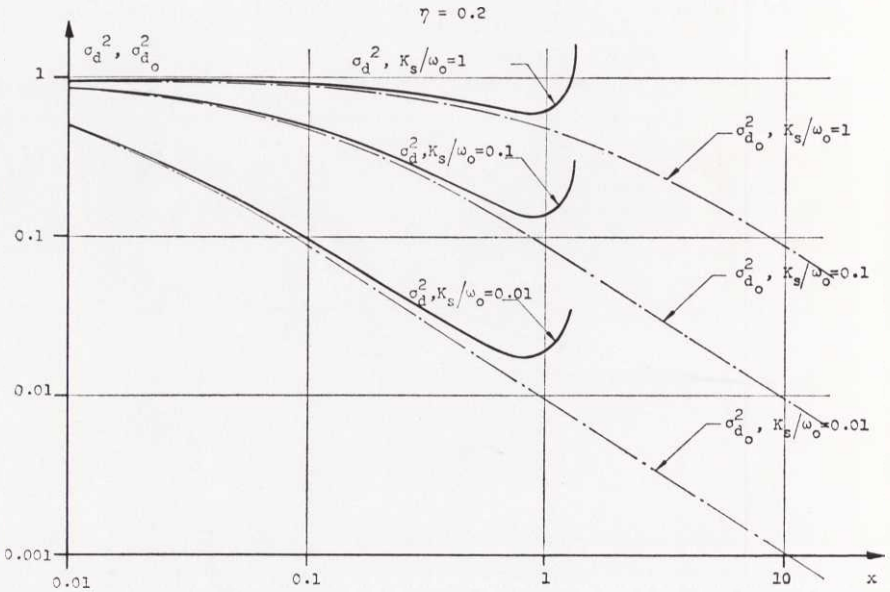

Fig. 10. The dynamic error of the tracking servo as a function of x for various values of K_s/ω_0 for constant $(\sigma_{d_0}^2)$ and stationary random Gaussian amplification with $\eta = 0.2$ (σ_d^2).

Fig. 8 shows the ratio $\sigma_d^2/\sigma_{d_0}^2$ as a function of ϱ at a certain relatively large value of η, $\eta = 0.2$, i. e. $\sigma_d^2/\sigma_{d_0}^2$ as a function of x, with y_s as parameter. For constant η, K_0, and K_s, i. e. constant η and y_s, the ratio $\sigma_d^2/\sigma_{d_0}^2$ increases with increasing x, i. e. decreasing ω_0, which is physically plausible. In fig. 9 is illustrated the relation between the ratio $\sigma_d^2/\sigma_{d_0}^2$ and the variable x for $\eta = 0.2$ and certain values of K_s/ω_0. From the figure it is evident that for constant η, ω_0, and K_s the ratio $\sigma_d^2/\sigma_{d_0}^2$ increases with x, i. e. with K_0. As, however, y_s increases with x and therefore $\sigma_{d_0}^2$ rapidly decreases with x, the resultant dynamic error σ_d^2 will first decrease with increasing x but in the vicinity of the instable region of the system, $x = 1/(\pi\eta)$, it will start to increase markedly and reach very large values. This phenomenon is better illustrated by fig. 10, showing the dynamic errors σ_d^2 and $\sigma_{d_0}^2$ as functions of x for $\eta = 0.2$ and various values of K_s/ω_0. Fig. 10 clearly shows the detrimental effect on the dynamic characteristics of the tracking servo caused by a randomly time-varying amplification of the system. Only in the case of very slowly varying input signals, i. e. very small ratios K_s/ω_0, does the tracking servo give an acceptable dynamic error after a suitable choice of the variable x.

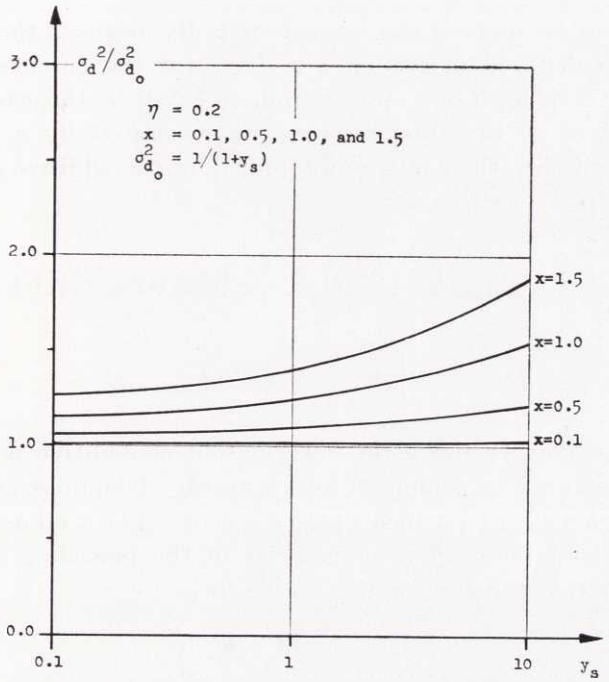

Fig. 11. The dynamic error σ_d^2 of the tracking servo for Gaussian-distributed stationary random amplification with $\eta = 0.2$ as a function of y_s for various values of x.

Fig. 11, finally, shows the ratio $\sigma_d^2/\sigma_{d_o}^2$ as a function of y_s with x as a parameter for $\eta = 0.2$. For constant η, ω_0, and K_0, i. e. constant η and x, the ratio $\sigma_d^2/\sigma_{d_o}^2$ increases with increasing y_s, i. e. decreasing K_s, more rapidly the larger the value of x. As, however, $\sigma_{d_o}^2$ decreases more rapidly with y_s than the ratio $\sigma_d^2/\sigma_{d_o}^2$ increases, the resultant dynamic error σ_d^2 will decrease with increasing y_s if the value of x is not too large.

3.4 The contribution of additive noise to the output of the tracking servo

The ensemble average square value $[\sigma_n(t)]^2$ of the part of the output of the randomly time-varying tracking servo that originates from an undesirable stationary stochastic noise signal $n(t)$ (see fig. 1) with zero mean value and the autocorrelation function $\Phi_{nn}(\tau)$ was derived in chapter 2 and given in relation (2-33). This expression of the output noise holds for values of the time of observation t large enough that

all transient phenomena can be neglected. By means of the analytical expression deduced in section 3.1 above for the ensemble average $\langle {}^{k}W_n(t, t-\tau)\, {}^{k}W_n(t, t-\nu)\rangle$, relation (3.1-25), in the case that the amplification of the tracking servo is generated by a stationary Gaussian process, the contribution $[\sigma_n(t)]^2$ of the additive output can immediately be written as

$$\sigma_n^2 = \frac{K_0^2}{\varkappa^2} \int_0^\infty \int_0^\infty \exp\left\{ - K_0(\tau+\nu) + \frac{K_0^2}{\varkappa^2}\left[\tau^2 g_1(\tau) + \nu^2 g_1(\nu) - \right.\right.$$

$$\left.\left. - \tfrac{1}{2}(\tau-\nu)^2 g_1(\tau-\nu)\right]\right\} \Phi_{nn}(\tau-\nu)\, d\tau\, d\nu. \tag{3.4-1}$$

By using (3.4-1) above the contribution of additive noise to the output signal can be computed for arbitrarily given noise autocorrelation functions $\Phi_{nn}(\tau)$ or noise power spectra. For a numerical study of the output noise σ_n^2 we choose, as in the preceding section, an autocorrelation function of the simple form

$$\Phi_{nn}(\tau) = \exp\{- K_n |\tau|\}, \tag{3.4-2}$$

where K_n is the cut-off angular frequency of the random noise process. Further we suppose as before that the power density function $G(\omega)$ of the random amplification of the tracking servo is rectangular according to (3.2-5). Under these assumptions and by means of (3.4-1), (3.4-2), (3.2-7), (3.2-8), and (3.2-9), the additive output noise σ_n^2 becomes

$$\sigma_n^2 = \frac{1}{\varkappa^2} \int_0^\infty \int_0^\infty \exp\left\{ - (\tau+\nu) - \frac{|\tau-\nu|}{y_n} + \pi\eta x \left[\tau I_1\left(\frac{\tau}{2x}\right) + \nu I_1\left(\frac{\nu}{2x}\right) - \right.\right.$$

$$\left.\left. - \frac{1}{2}(\tau-\nu) I_1\left(\frac{\tau-\nu}{2x}\right)\right]\right\} d\tau\, d\nu, \tag{3.4-3}$$

where

$$y_n = K_0/K_n \tag{3.4-4}$$

and as before

$$\left.\begin{aligned} & x = K_0/\omega_0, \quad \eta = \sigma_0^2/\varkappa^2, \\ & I_1(\xi) = \frac{2}{\pi}\int_0^\xi \frac{\sin^2 y}{y^2}\, dy, \quad I_2(\xi) = \frac{2}{\pi}\int_0^\xi \frac{\sin y}{y}\, dy. \end{aligned}\right\} \tag{3.4-5}$$

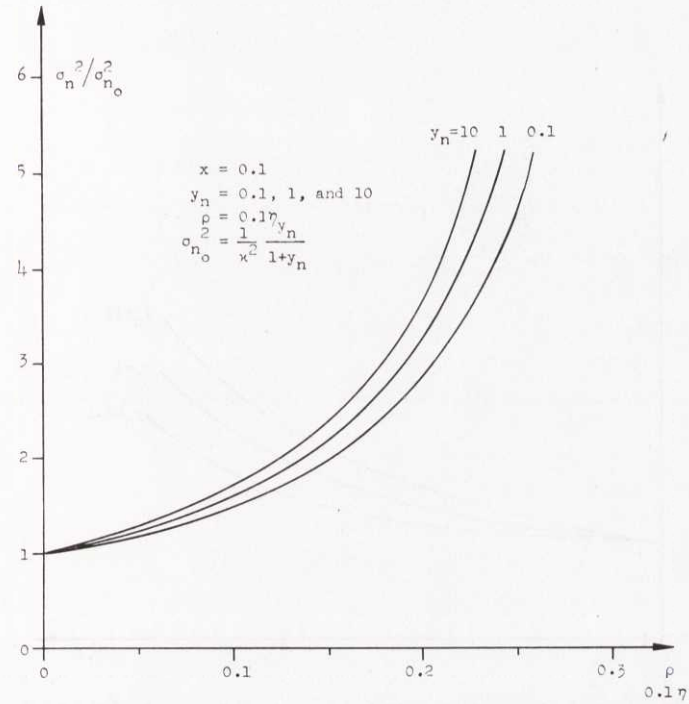

Fig. 12. The contribution σ_n^2 of additive noise to the output of the tracking servo for Gaussian-distributed stationary random amplification as a function of $\varrho = \eta x$ with $x = 0.1$ and various values of y_n.

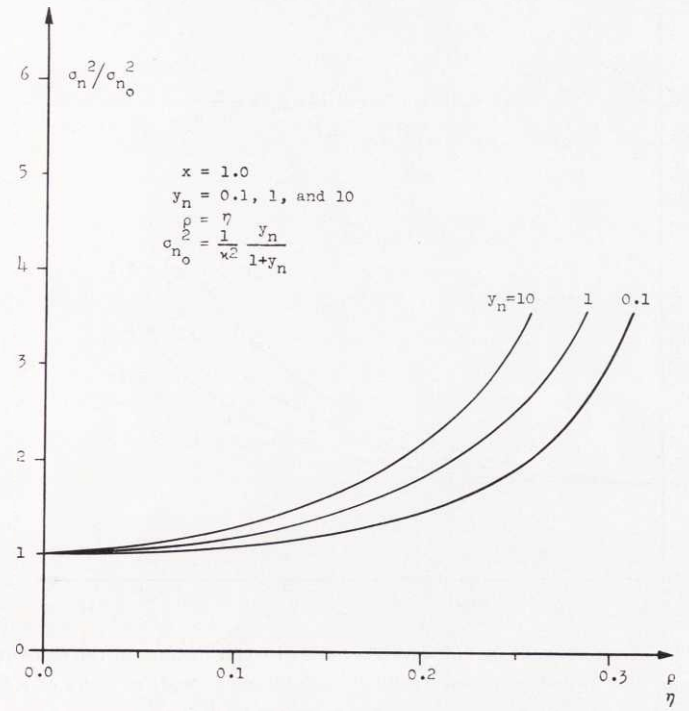

Fig. 13. The contribution σ_n^2 of additive noise to the output of the tracking servo for Gaussian-distributed stationary random amplification as a function of $\varrho = \eta x$ with $x = 1.0$ and various values of y_n.

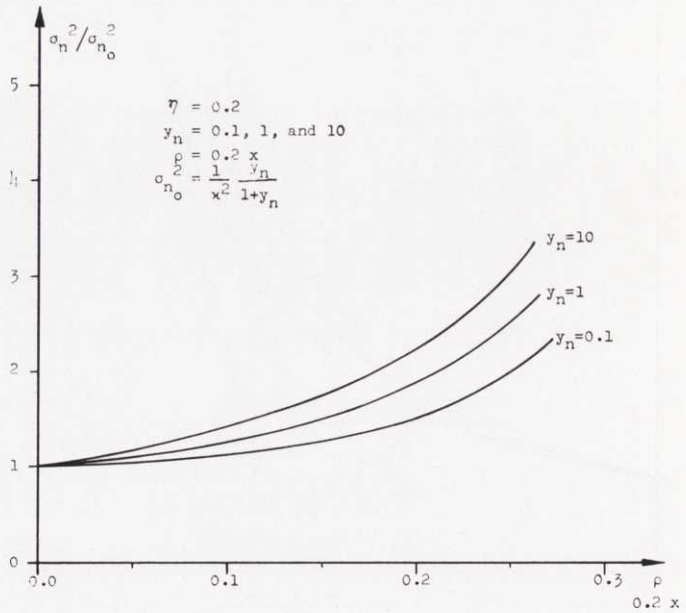

Fig. 14. The contribution σ_n^2 of additive noise to the output of the tracking servo for Gaussian-distributed stationary random amplification with $\eta = 0.2$ as a function of $\varrho = \eta\, x$ for various values of y_n.

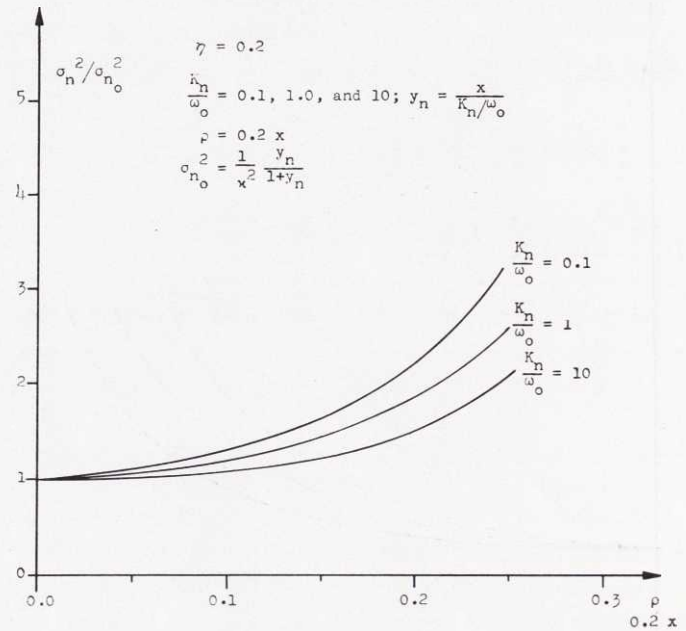

Fig. 15. The contribution σ_n^2 of additive noise to the output of the tracking servo for Gaussian-distributed stationary random amplification with $\eta = 0.2$ as a function of $\varrho = \eta\, x$ for various values of K_n/ω_0.

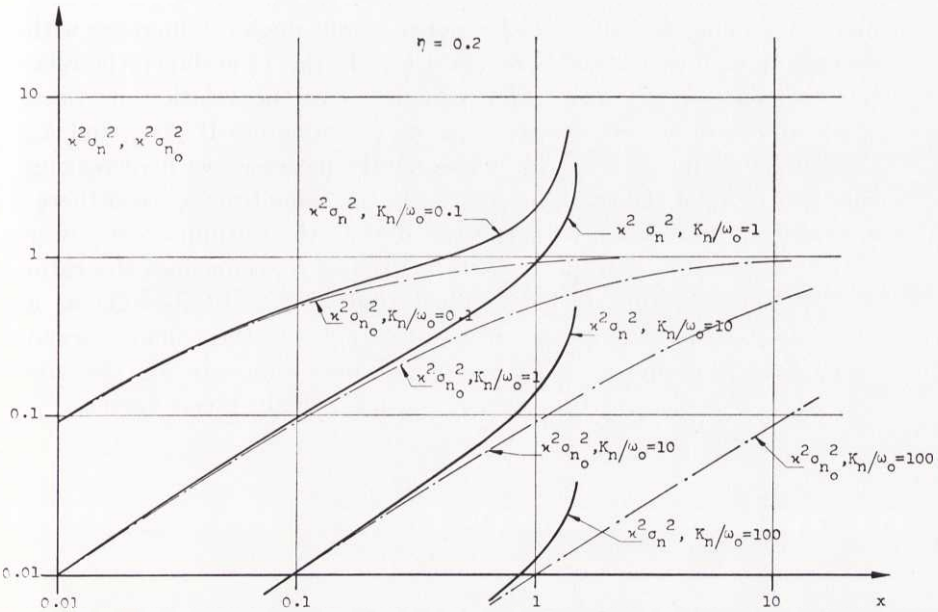

Fig. 16. The contribution of additive noise to the output of the tracking servo as a function of x for various values of K_n/ω_0 for constant $(\sigma_{n_o}^2)$ and stationary random Gaussian amplification with $\eta = 0.2$ (σ_n^2).

If we put $\eta = 0$ in relation (3.4-3) we easily obtain the additive noise output $\sigma_{n_o}^2$ in the time-invariant case that $F(t) = \varkappa$ as

$$\sigma_{n_o}^2 = (\sigma_n^2)_{\eta=0} = \frac{1}{\varkappa^2} \frac{y_n}{1 + y_n}. \tag{3.4-6}$$

From the expression (3.4-3) we also infer that σ_n^2 increases without limit as the product $\pi\eta x$ approaches the value 1 in accordance with the stability condition (3.2-4).

In figs 12—16 are shown the results of some numerical calculations of the noise output σ_n^2 according to (3.4-3) which have been carried out on SARA. The figures 12 and 13 illustrate the ratio $\sigma_n^2/\sigma_{n_o}^2$ as a function of the variable $\varrho = \eta x$ with y_n as a parameter in the two cases that $x = 0.1$ and 1.0. From these figures it follows that $\sigma_n^2/\sigma_{n_o}^2$ increases with increasing η for given constant values of ω_0, K_0, and K_n, the increase being larger the smaller K_n is. Fig 14, which gives the ratio $\sigma_n^2/\sigma_{n_o}^2$ as a function of ϱ for $\eta = 0.2$, i. e. $\sigma_n^2/\sigma_{n_o}^2$ as a function of x, and some given values of y_n, confirms the correctness of the

physical feeling that the additive noise output ought to increase with decreasing ω_0 for constant η, K_n, and K_0. In fig. 15 is shown the relation between $\sigma_n^2/\sigma_{n_0}^2$ and ϱ for $\eta = 0.2$, i. e. the relation between $\sigma_n^2/\sigma_{n_0}^2$ and x for $\eta = 0.2$, with K_n/ω_0 as a parameter. If η, ω_0, and K_n are constant the ratio $\sigma_n^2/\sigma_{n_0}^2$ consequently increases with increasing bandwidth K_0 of the tracking servo. At the same time y_n, and therefore also $\sigma_{n_0}^2$, increases, with the result that the output noise power σ_n^2 will increase more rapidly with increasing K_0 than does the ratio $\sigma_n^2/\sigma_{n_0}^2$. The situation is better illustrated by fig. 16 showing as a function of x the contribution of additive noise to the tracking servo output for time-invariant ($\sigma_{n_0}^2$) and randomly time-varying systems (σ_n^2) when $\eta = 0.2$ and the ratio K_n/ω_0 has certain given values.

4. The characteristics of the tracking servo for arbitrarily distributed quasi-stationary random amplification with a power spectrum of low-pass character

4.1 Deduction of the expressions for certain ensemble average values

In the present chapter we shall investigate for different types of inputs $e_i(t)$ and noise signals $n(t)$ the effect upon the output signal of the quasi-stationary stochastically time-varying amplification $F(t)$ with a certain power spectrum of low-pass character that we previously assumed in chapter 2, relations (2-8) and (2-9). To do this we need analytical expressions for the ensemble averages $\langle \exp\{-K\int_0^t {}^kF(\varrho)\,d\varrho\}\rangle$, $\langle \exp\{-2K\int_0^t {}^kF(\varrho)\,d\varrho\}\rangle$, $\langle {}^kW_{e_i}(t,t-\tau)\rangle$, $\langle {}^kW_{e_i}(t,t-\tau)\,{}^kW_{e_i}(t,t-\nu)\rangle$, and $\langle {}^kW_n(t,t-\tau)\,{}^kW_n(t,t-\nu)\rangle$ which we now derive.

For the fixed time of observation t and the two time variables τ and ν let us suppose that

$$\left.\begin{aligned} &nt_0 < t \leqq (n+1)\,t_0,\\ &t = nt_0 + \Delta t,\\ &n = 0, 1, 2, \ldots,\\ &0 \leqq \nu \leqq \tau \leqq t, \end{aligned}\right\} \tag{4.1-1}$$

and let us denote the constant random value of the amplification ${}^kF(t)$ in the interval $\mu t_0 < t \leqq (\mu+1)\,t_0$, $\mu = \ldots, -1, 0, +1, \ldots$ by ${}^kF_{n-\mu}$ instead of ${}^kF_\mu$ as used before (see fig. 17). It may also be convenient to introduce the following notations

$$\left.\begin{aligned} I_1(t,\tau) &= K\int_{t-\tau}^{t} {}^kF(\varrho)\,d\varrho,\\ I_2(t,\tau,\nu) &= K\int_{t-\tau} {}^kF(\varrho)\,d\varrho + K\int_{t-\nu} {}^kF(\varrho)\,d\varrho. \end{aligned}\right\} \tag{4.1-2}$$

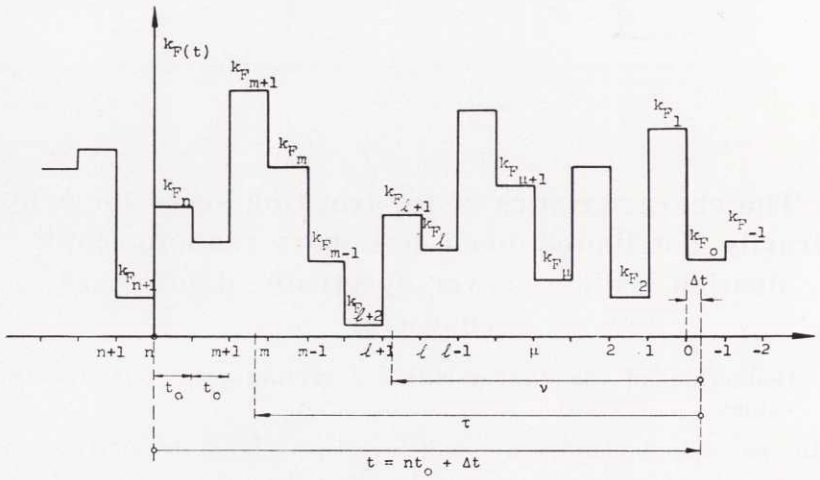

Fig. 17. Quasi-stationary randomly time-varying function ${}^kF(t)$.

Under the assumption (4.1-1) these integrals I_1 and I_2 can be written ($K_0 = \varkappa K$):

$$
\left.
\begin{aligned}
&1)\ 0 \leqq \tau < \Delta t, \\
&\quad I_1(t, \tau) = \frac{K_0}{\varkappa}\, {}^kF_0, \\
&2)\ \Delta t + mt_0 \leqq \tau < \Delta t + (m+1)\, t_0, \quad m = 0, 1, 2, \ldots (n-1), \\
&\quad I_1(t, \tau) = \frac{K_0}{\varkappa}\left[{}^kF_0\, \Delta t + \sum_{\mu+1}^{m} {}^kF_\mu t_0 + {}^kF_{m+1}(\tau - mt_0 - \Delta t)\right],
\end{aligned}
\right\} \quad (4.1\text{-}3)
$$

and ($n > 1$)

$$
\left.
\begin{aligned}
&1)\ 0 \leqq \tau < \Delta t, \\
&\quad 0 \leqq \nu \leqq \tau, \\
&\quad I_2(t, \tau, \nu) = \frac{K_0}{\varkappa}\, {}^kF_0(\tau + \nu), \\
&2)\ \Delta t + mt_0 \leqq \tau < \Delta t + (m+1)\, t_0, \quad m = 0, 1, 2, \ldots (n-1), \\
&\quad 0 \leqq \nu < \Delta t, \\
&\quad I_2(t, \tau, \nu) = \frac{K_0}{\varkappa}\left[{}^kF_0(\Delta t + \nu) + \sum_{\mu=1}^{m} {}^kF_\mu t_0 + {}^kF_{m+1}(\tau - mt_0 - \Delta t)\right],
\end{aligned}
\right.
$$

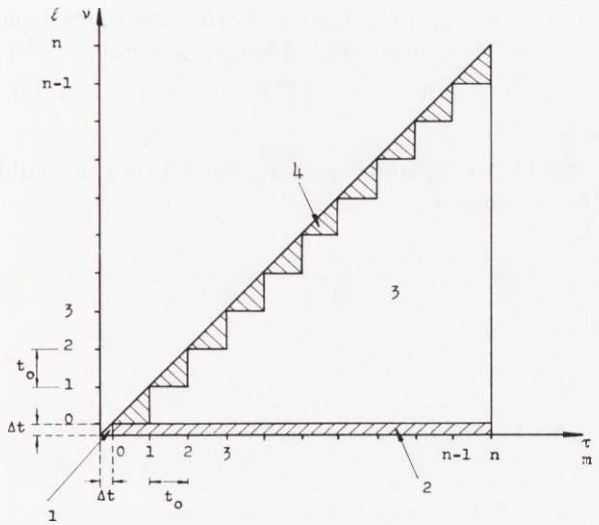

Fig. 18. The regions of definition for the functions $I_2(t, \tau, \nu)$, $\langle {}^kW_{e_i}(t, t-\tau) \cdot {}^kW_{e_i}(t, t-\nu)\rangle$, and $\langle {}^kW_n(t, t-\tau)\, {}^kW_n(t, t-\nu)\rangle$ in the τ, ν-plane ($\nu \leq \tau$).

$$
\left.
\begin{aligned}
&3)\ \Delta t + m t_0 \leqq \tau < \Delta t + (m+1)\, t_0, \quad m = 1, 2, \ldots (n-1),\\
&\Delta t + l\, t_0 \leqq \nu < \Delta t + (l+1)\, t_0, \quad l = 0, 1, \ldots (m-1),\\
&I_2(t,\tau,\nu) = \frac{K_0}{\varkappa}\left[2\, {}^kF_0\, \Delta t + 2 \sum_{\mu=1}^{l} {}^kF_\mu\, t_0 + {}^kF_{l+1}\,(t_0 + \nu - l\, t_0 - \Delta t) + \right.\\
&\qquad \left. + \sum_{\mu=l+2}^{m} {}^kF_\mu\, t_0 + {}^kF_{m+1}\,(\tau - m\, t_0 - \Delta t)\right],\\
&4)\ \Delta t + m t_0 \leqq \tau < \Delta t + (m+1)\, t_0, \quad m = 0, 1, 2, \ldots (n-1),\\
&\Delta t + m t_0 \leqq \nu \leqq \tau,\\
&I_2(t,\tau,\nu) = \frac{K_0}{\varkappa}\left[2\, {}^kF_0\, \Delta t + 2 \sum_{\mu=1}^{m} {}^kF_\mu\, t_0 + \right.\\
&\qquad \left. + {}^kF_{m+1}\ (\tau - m t_0 - \Delta t + \nu - m t_0 - \Delta t)\right].
\end{aligned}
\right\} \quad (4.1\text{-}4)
$$

The different regions of definition in the τ, ν-plane for the integral I_2 above are shown in fig. 18. From relation (4.1-2) we conclude that the function $I_2(t, \tau, \nu)$ is symmetric around the straight line $\tau = \nu$ in

the τ, ν-plane, i. e. $I_2(t, \tau, \nu) = I_2(t, \nu, \tau)$, which is the reason why only the case $\nu \leqq \tau$ need be considered. The average values $\langle {}^kW_{e_i}(t, t-\tau) \cdot {}^kW_{e_i}(t, t-\nu)\rangle$ and $\langle {}^kW_n(t, t-\tau)\, {}^kW_n(t, t-\nu)\rangle$ exhibit the same kind of symmetry.

By means of the integrals I_1 and I_2 the wanted ensemble average values can be expressed as

$$\left.\begin{aligned}
&\langle \exp\ \{-K \int_0^t {}^kF(\varrho)\, d\varrho\}\rangle = \langle \exp\{-I_1(t,t)\}\rangle,\\
&\langle {}^kW_{e_i}(t, t-\tau)\rangle = K_0 \left\langle \frac{{}^kF(t-\tau)}{\varkappa} \exp\{-I_1(t,\tau)\}\right\rangle,\\
&\langle {}^kW_{e_i}(t, t-\tau)\, {}^kW_{e_i}(t, t-\nu)\rangle = K_0^2 \left\langle \frac{{}^kF(t-\tau)}{\varkappa} \frac{{}^kF(t-\nu)}{\varkappa} \cdot \right.\\
&\left. \exp\ \{-I_2(t, \tau, \nu)\}\right\rangle,\\
&\text{and}\\
&\langle {}^kW_n(t, t-\tau)\, {}^kW_n(t, t-\nu)\rangle = \frac{K_0^2}{\varkappa^2} \langle \exp\{-I_2(t, \tau, \nu)\}\rangle.
\end{aligned}\right\} \quad (4.1\text{-}5)$$

In order to be able to compute the averages appearing in (4.1-5) analytical expressions are needed for ensemble average values of the type $\langle ({}^kF_\mu/\varkappa)^n \exp\{-\xi\, {}^kF_\mu/\varkappa\}\rangle$, where $n = 0$, 1, and 2 and ξ is a constant independent of the random variable F_μ. According to the assumptions, the different random variables F_μ are independent of each other but otherwise equally distributed with the same average value $\varkappa$ and dispersion σ_0. We suppose that the common probability density function of the random variables is $f(F)$, and we consequently have

$$\left.\begin{aligned}
1 &= \int_{-\infty}^{+\infty} f(F)\, dF,\\
\varkappa &= \int_{-\infty}^{+\infty} F\, f(F)\, dF,\\
\sigma_0^2 &= \int_{-\infty}^{+\infty} (F-\varkappa)^2 f(F)\, dF.
\end{aligned}\right\} \quad (4.1\text{-}6)$$

With this assumption we get

$$\left.\begin{aligned} \langle \exp\{-\xi\,{}^{k}F_{\mu}/\varkappa\}\rangle &= \int_{-\infty}^{+\infty} \exp\{-\xi\,F/\varkappa\}\,f(F)\,dF = \\ &= \exp\{-\chi(\xi)\,\xi\}, \end{aligned}\right\} \tag{4.1-7}$$

where

$$\chi(\xi) = -\frac{1}{\xi}\ln\left[\int_{-\infty}^{+\infty}\exp\{-\xi\,F/\varkappa\}\,f(F)\,dF\right],$$

and, generally, for positive real numbers n

$$\langle({}^{k}F_{\mu}/\varkappa)^{n}\exp\{-\xi\,{}^{k}F_{\mu}/\varkappa\}\rangle = (-1)^{n}\frac{d^{n}}{d\xi^{n}}\exp\{-\chi(\xi)\,\xi\}. \tag{4.1-8}$$

In particular we write for $n = 1$ and 2

$$\left.\begin{aligned} &\langle({}^{k}F_{\mu}/\varkappa)\exp\{-\xi\,{}^{k}F_{\mu}/\varkappa\}\rangle = \Lambda(\xi)\exp\{-\chi(\xi)\,\xi\} \\ &\text{and} \\ &\langle({}^{k}F_{\mu}/\varkappa)^{2}\exp\{-\xi\,{}^{k}F_{\mu}/\varkappa\}\rangle = [\{\Lambda(\xi)\}^{2} - \Lambda'(\xi)]\exp\{-\chi(\xi)\,\xi\}, \\ &\text{where} \\ &\Lambda(\xi) = \frac{d}{d\xi}[\chi(\xi)\,\xi] \text{ and} \\ &\Lambda'(\xi) = \frac{d}{d\xi}\Lambda(\xi). \end{aligned}\right\} \tag{4.1-9}$$

The relations (4.1-5), (4.1-3), (4.1-4), (4.1-7), and (4.1-9), together with the condition that the random variables F_{μ} are independent of each other, now make it possible to compute the desired ensemble average values. One readily gets

$$\left.\begin{aligned} \langle \exp\{-K\int_{0}^{t}{}^{k}F(\varrho)\,d\varrho\}\rangle &= \exp\{-K_{0}\chi(K_{0}t_{0})\,nt_{0} - \\ &- K_{0}\chi(K_{0}\Delta t)\,\Delta t\}, \\ \langle \exp\{-2K\int_{0}^{t}{}^{k}F(\varrho)\,d\varrho\}\rangle &= \exp\{-2K_{0}\chi(2K_{0}t_{0})\,nt_{0} - \\ &- 2K_{0}\chi(2K_{0}\Delta t)\,\Delta t\}, \end{aligned}\right\} \tag{4.1-10}$$

$$
\left.\begin{aligned}
&1)\ 0 \leqq \tau < \Delta t,\\
&\langle {}^{k}W_{e_i}(t, t-\tau)\rangle = K_0 \Lambda (K_0 \tau) \exp\{- K_0 \chi (K_0 \tau)\, \tau\},\\
&2)\ \Delta t + m t_0 \leqq \tau < \Delta t + (m+1)\, t_0,\ m = 0, 1, 2, \ldots (n-1),\\
&\langle {}^{k}W_{e_i}(t, t-\tau)\rangle = K_0 \Lambda (K_0 [\tau - m t_0 - \Delta t]) \exp\{- K_0 \chi (K_0 \Delta t)\, \Delta t -\\
&- K_0 \chi (K_0 t_0)\, m t_0 - K_0 \chi (K_0 [\tau - m t_0 - \Delta t])\, (\tau - m t_0 - \Delta t)\},
\end{aligned}\right\} \quad (4.1\text{-}11)
$$

$$
\left.\begin{aligned}
&1)\ 0 \leqq \tau < \Delta t,\\
&0 \leqq \nu \leqq \tau,\\
&\langle {}^{k}W_{e_i}(t, t-\tau)\, {}^{k}W_{e_i}(t, t-\nu)\rangle = K_0^2 \left[\{\Lambda (K_0 [\tau + \nu])\}^2 -\right.\\
&\left. - \Lambda' (K_0 [\tau + \nu])\right] \psi (\tau, \nu),\\
&\langle {}^{k}W_n (t, t-\tau)\, {}^{k}W_n (t, t-\nu)\rangle = \frac{K_0^2}{\varkappa^2}\, \psi (\tau, \nu),\\
&\psi (\tau, \nu) = \exp\{- K_0 \chi (K_0 [\tau + \nu])\, (\tau + \nu)\},\\
&2)\ \Delta t + m t_0 \leqq \tau < \Delta t + (m+1)\, t_0,\ m = 0, 1, 2, \ldots (n-1),\\
&0 \leqq \nu < \Delta t,\\
&\langle {}^{k}W_{e_i}(t, t-\tau)\, {}^{k}W_{e_i}(t, t-\nu)\rangle = K_0^2 \Lambda (K_0 [\Delta t + \nu])\, \Lambda (K_0 [\tau -\\
&- m t_0 - \Delta t])\, \psi (\tau, \nu),\\
&\langle {}^{k}W_n (t, t-\tau)\, {}^{k}W_n (t, t-\nu)\rangle = \frac{K_0^2}{\varkappa^2}\, \psi (\tau, \nu),\\
&\psi (\tau, \nu) = \exp\{- K_0 \chi (K_0 t_0)\, m t_0 - K_0 \chi (K_0 [\tau - m t_0 -\\
&- \Delta t])\, (\tau - m t_0 - \Delta t) - K_0 \chi (K_0 [\Delta t + \nu])\, (\Delta t + \nu)\},\\
&3)\ \Delta t + m t_0 \leqq \tau < \Delta t + (m+1)\, t_0,\ m = 1, 2, \ldots (n-1),\\
&\Delta t + l t_0 \leqq \nu < \Delta t + (l+1)\, t_0,\ l = 0, 1, \ldots (m-1),\\
&\langle {}^{k}W_{e_i}(t, t-\tau)\, {}^{k}W_{e_i}(t, t-\nu)\rangle = K_0^2 \Lambda (K_0 [t_0 + \nu - l t_0 - \Delta t]) \cdot\\
&\cdot \Lambda (K_0 [\tau - m t_0 - \Delta t])\, \psi (\tau, \nu),
\end{aligned}\right\} \quad (4.1\text{-}12)
$$

$$\langle {}^{k}W_n(t, t-\tau)\, {}^{k}W_n(t, t-\nu)\rangle = \frac{K_0^2}{\varkappa^2}\,\psi(\tau, \nu),$$

$$\psi(\tau, \nu) = \exp\{-2K_0\chi(2K_0 t_0)\, l t_0 - K_0\chi(K_0 t_0)(m-l-$$

$$-1)\, t_0 - 2K_0\chi(2K_0\Delta t)\,\Delta t - K_0\chi(K_0[\tau - mt_0 - \Delta t])(\tau -$$

$$-mt_0 - \Delta t) - K_0\chi(K_0[t_0 + \nu - lt_0 - \Delta t])(t_0 +$$

$$+\nu - lt_0 - \Delta t)\},$$

and

4) $\Delta t + mt_0 \leqq \tau < \Delta t + (m+1)\, t_0,\ m = 0, 1, 2, \ldots (n-1),$

$$\Delta t + mt_0 \leqq \nu \leqq \tau,$$

$$\langle {}^{k}W_{e_i}(t, t-\tau)\, {}^{k}W_{e_i}(t, t-\nu)\rangle = K_0^2\,[\{\Lambda(K_0[\tau - mt_0 - \Delta t +$$

$$+\nu - mt_0 - \Delta t])\}^2 - \Lambda'(K_0[\tau - mt_0 - \Delta t + \nu - mt_0 -$$

$$-\Delta t])]\,\psi(\tau, \nu),$$

$$\langle {}^{k}W_n(t, t-\tau)\, {}^{k}W_n(t, t-\nu)\rangle = \frac{K_0^2}{\varkappa^2}\,\psi(\tau, \nu),$$

$$\psi(\tau, \nu) = \exp\{-2K_0\chi(2K_0 t_0)\, mt_0 - 2K_0\chi(2K_0\Delta t)\,\Delta t -$$

$$-K_0\chi(K_0[\tau - mt_0 - \Delta t + \nu - mt_0 - \Delta t])(\tau - mt_0 - \Delta t +$$

$$+\nu - mt_0 - \Delta t)\}.$$

As for the different regions of definition in the τ, ν-plane for the average values $\langle {}^{k}W_{e_i}(t, t-\tau)\, {}^{k}W_{e_i}(t, t-\nu)\rangle$ and $\langle {}^{k}W_n(t, t-\tau) \cdot {}^{k}W_n(t, t-\nu)\rangle$ we refer to fig. 18.

4.2 The output of the tracking servo when the input is a unit step signal

In the case investigated of quasi-stationary random variations of amplification of the tracking servo it is now possible to study in somewhat more detail the output signal when the input of the servo is a unit step signal occurring at time $t = 0$. Relations (2-23), (2-24), and (4.1-10) directly give the following expressions for the average value $m(t)$ and the average square deviation $[\sigma(t)]^2$ from its average

value of the output signal at time $t = nt_0 + \Delta t$ with $nt_0 < t \leqq \leqq (n+1)\,t_0$:

$$m(t) = 1 - \exp\{-K_0\,[\chi(K_0\,t_0)\,nt_0 + \chi(K_0\,\Delta t)\,\Delta t]\} \tag{4.2-1}$$

and

$$[\sigma(t)]^2 = \exp\{-2\,K_0\,[\chi(2\,K_0\,t_0)\,nt_0 + \chi(2\,K_0\,\Delta t)\,\Delta t]\} - \\ - \exp\{-2\,K_0\,[\chi(K_0\,t_0)\,nt_0 + \chi(K_0\,\Delta t)\,\Delta t]\}, \tag{4.2-2}$$

where as earlier $K_0 = \varkappa K$ and the function χ is given by relation (4.1-7).

In the case of Gaussian-distributed amplification $F(t)$ of the tracking servo with the average value $\varkappa$ and the dispersion σ_0, the probability density function.

$$f(F) = \frac{1}{\sqrt{2\,\pi}\,\sigma_0} \exp\left\{-\frac{(F-\varkappa)^2}{2\,\sigma_0^2}\right\},$$

and according to (4.1-7) the function χ therefore becomes

$$\chi(\xi) = 1 - \frac{1}{2}\,\frac{\sigma_0^2}{\varkappa^2}\,\xi. \tag{4.2-3}$$

If, for instance, the amplification is Rayleigh-distributed, a case that has the greatest interest in radar applications, the probability density function f is given by

$$\left.\begin{aligned} f(F) &= \frac{F}{\sigma_1} \exp\left\{-\frac{F^2}{2\,\sigma_1^2}\right\},\ F \geqq 0;\ f(F) = 0,\ F < 0, \\ \varkappa &= \sqrt{\frac{\pi}{2}}\,\sigma_1,\ \sigma_0 = \sqrt{\frac{4-\pi}{\pi}}\,\sigma_1, \\ \sigma_0^2/\varkappa^2 &= (4-\pi)/\pi \cong 0.27. \end{aligned}\right\} \tag{4.2-4}$$

The corresponding χ-function is easily obtained from (4.1-7) as

$$\left.\begin{aligned} \chi(\xi) &= -\frac{\ln\left(1 - \xi \exp\{\xi^2/\pi\}\left[1 - \Phi\left(\xi/\sqrt{\pi}\right)\right]\right)}{\xi}, \\ &\text{where} \\ \Phi(\xi) &= \frac{2}{\sqrt{\pi}} \int_0^{\xi} \exp\{-t^2\}\,dt. \end{aligned}\right\} \tag{4.2-5}$$

(As for the "error integral" $\Phi(\xi)$ see for example [13].)

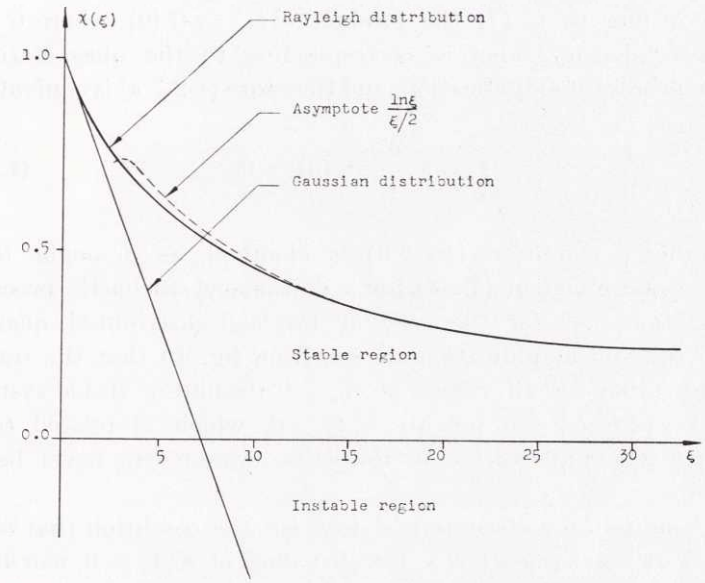

Fig. 19. The function $\chi(\xi)$ for Rayleigh-distributed and Gaussian-distributed amplification $F(t)$.

For small and large values of the argument ξ the following power-series and asymptotic expansions of $\chi(\xi)$ hold in the present case:

$$\left.\begin{aligned} \chi(\xi) &\cong 1 - \frac{4-\pi}{2\pi}\,\xi, \quad \xi \ll 1, \\ \chi(\xi) &\sim 2\,\frac{\ln \xi}{\xi}, \qquad \xi \gg 1. \end{aligned}\right\} \tag{4.2-6}$$

Fig. 19 shows $\chi(\xi)$ as a function of ξ for Rayleigh-distributed and Gaussian-distributed amplification with the same average value $\varkappa$ and dispersion σ_0 in the two cases, i. e. with $\sigma_0^2/\varkappa^2 = \dfrac{4-\pi}{\pi}$. As is evident from (4.2-3) and (4.2-6), the two functions χ coincide for small ξ under these assumptions.

The tracking servo is stable for Gaussian-distributed amplification, i. e. $m(t) \to 1$ and $\sigma(t) \to 0$ for large values of t, if, as is evident from (4.2-1) — (4.2-3),

$$\chi(2\,K_0 t_0) = 1 - \frac{\sigma_0^2}{\varkappa^2}\,K_0 t_0 > 0. \tag{4.2-7 a}$$

But according to (2-17) the product $\sigma_0^2 t_0 = \pi G(0)$, where $G(\omega)$ is the power density function corresponding to the quasi-stationary random process of amplification, and therefore (4.2-7 a) is equivalent to

$$1 - \pi \frac{K_0}{\varkappa^2} G(0) > 0. \tag{4.2-7 b}$$

The stability condition (4.2-7 b) is identical, as it ought to be, with the one given in (3.2-4) for a stationary stochastic process of amplification. As for the case of Rayleigh-distributed quasi-stationary random amplification we see from fig. 19 that the tracking servo is stable for all values of $K_0 t_0$ ("absolutely stable system"), because $\chi(2 K_0 t_0) > 0$ for all $K_0 t_0 > 0$, which is related to the fact that the amplification of the servo system can never become negative.

The condition for absolute stability, i. e. the condition that $m(t) \to$ $\to 1$ and $\sigma(t) \to 0$ when $t \to \infty$ for all values of $K_0 t_0 > 0$, can also be formulated in the following way

$$\left.\begin{aligned} &\exp\{-\chi(\xi)\,\xi\} = \int_{-\infty}^{+\infty} \exp\{-\xi F/\varkappa\} f(F)\, dF < 1 \\ &\text{for all } \xi > 0. \end{aligned}\right\} \tag{4.2-8}$$

With ξ and $\varkappa > 0$ we have for an arbitrary number A

$$\int_{-\infty}^{+\infty} \exp\{-\xi F/\varkappa\} f(F)\, dF \geqq \int_{-\infty}^{A} \exp\{-\xi F/\varkappa\} f(F)\, dF \geqq$$

$$\geqq \exp\{-\xi A/\varkappa\} \int_{-\infty}^{A} f(F)\, dF. \tag{4.2-9}$$

A necessary condition for the relation (4.2-8) to be satisfied is consequently that the integral $\int_{-\infty}^{A} f(F)\, dF = 0$ for all $A < 0$, i. e. the probability that the quantity F takes on negative values must be equal to zero. It is very easy to see that this condition is also a sufficient condition for absolute stability according to (4.2-8).

If we only consider such values of the time of observation that $t = nt_0$, we get from (4.2-1) the output average $m(t)$:

$$m(nt_0) = 1 - \exp\{-K_0 \chi(K_0 t_0)\, nt_0\}. \tag{4.2-10}$$

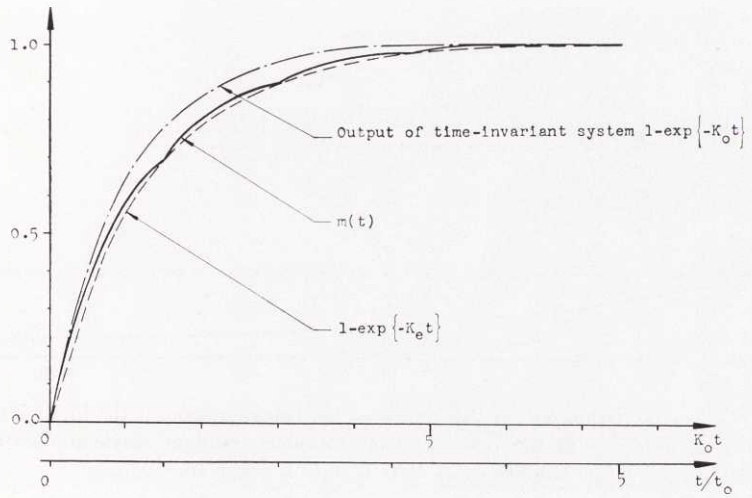

Fig. 20. The average value $m(t)$ of the output of the tracking servo if the input signal is a unit step at $t = 0$. The randomly time-varying amplification is supposed to be quasi-stationary and Rayleigh-distributed with $K_0 t_0 = 1.5$.

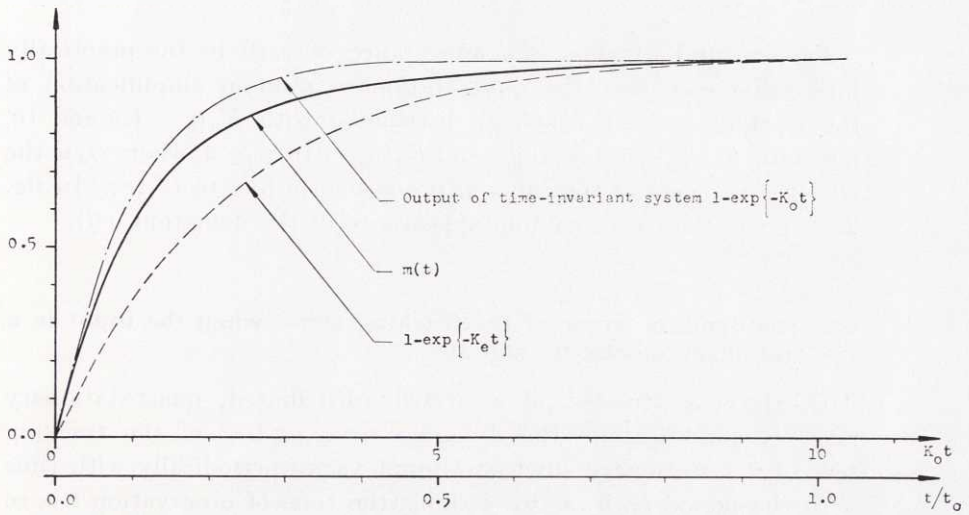

Fig. 21. The average value $m(t)$ of the output of the tracking servo if the input signal is a unit step at $t = 0$. The randomly time-varying amplification is supposed to be quasi-stationary and Rayleigh-distributed with $K_0 t_0 = 10$.

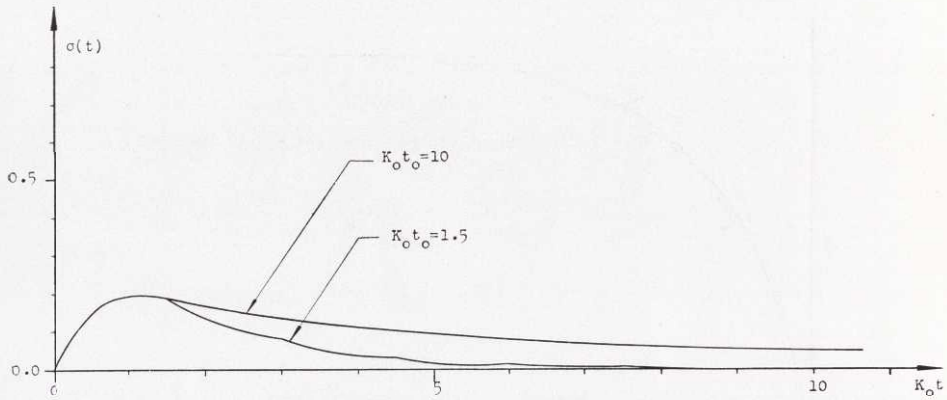

Fig. 22. The deviation $\sigma(t)$ of the output of the tracking servo if the input is a unit step signal at $t = 0$ in the case of quasi-stationary random Rayleigh-distributed amplification with $K_0 t_0 = 1.5$ and 10.

Under this assumption, as far as the output average value $m(t)$ is concerned, we can consequently speak of an "effective cut-off angular frequency" K_e of the tracking servo, given by

$$K_e/K_0 = \chi(K_0 t_0). \tag{4.2-11}$$

Figs 20 and 21 show the appearance of $m(t)$ in the practically interesting case that the quasi-stationary random amplification of the tracking servo is Rayleigh-distributed with $K_0 t_0 = 1.5$ and 10, i. e. with $K_0/\omega_0 = 1.5/\pi \simeq 1/2$ and $K_0/\omega_0 = 10/\pi \simeq 3$, where ω_0 is the cut-off frequency of the random process according to (2-18). In fig. 22 is given the corresponding appearance of the deviation $\sigma(t)$.

4.3 The dynamic error of the tracking servo when the input is a stationary stochastic signal

In the case treated of arbitrarily distributed, quasi-stationary random amplification, the dynamic error $[\sigma_d(t)]^2$ of the tracking servo for a stationary stochastic input varies periodically with time with the period t_0, if, as we assume, the time of observation t is so large that all transient phenomena can be neglected. As an alternative to the expression (2-29) and with $t = nt_0 + \Delta t$, the dynamic error $[\sigma_d(t)]^2$ can be written as

$$[\sigma_d(\Delta t)]^2 = \Phi_{e_i e_i}(0) - 2\int_0^\infty \langle {}^kW_{e_i}(t, t-\tau)\rangle \Phi_{e_i e_i}(\tau)\, d\tau +$$

$$+ 2\int_0^\infty \int_0^\tau \langle {}^kW_{e_i}(t, t-\tau)\, {}^kW_{e_i}(t, t-\nu)\rangle \Phi_{e_i e_i}(\tau-\nu)\, d\tau\, d\nu, \quad (4.3\text{-}1)$$

because both $\langle {}^kW_{e_i}(t, t-\tau)\, {}^kW_{e_i}(t, t-\nu)\rangle$ and $\Phi_{e_i e_i}(\tau-\nu)$ are symmetric functions around the straight line $\tau = \nu$ in the τ, ν-plane. With a knowledge of the autocorrelation function $\Phi_{e_i e_i}(\tau)$ of the input signal and by means of the expressions given in (4.1-11) and (4.1-12) for the weighting function averages $\langle {}^kW_{e_i}(t, t-\tau)\rangle$ and $\langle {}^kW_{e_i}(t, t-\tau)\cdot {}^kW_{e_i}(t, t-\nu)\rangle$ the dynamic error $[\sigma_d(t)]^2$ can be computed and the desired time-average $\overline{\sigma_d^2}$ obtained from [relation (2-30)]

$$\overline{\sigma_d^2} = \frac{1}{t_0}\int_0^{t_0} [\sigma_d(\Delta t)]^2\, d(\Delta t). \quad (4.3\text{-}2)$$

As in the case of Gaussian-distributed stationary random amplification, treated in section 3.3 above, we shall specialize in the following the input correlation function to the form

$$\Phi_{e_i e_i}(\tau) = \exp\{-K_s|\tau|\}. \quad (4.3\text{-}3)$$

Under this assumption it turns out to be possible to deduce comparatively simple expressions for both $[\sigma_d(\Delta t)]^2$ and $\overline{\sigma_d^2}$. Making use of (4.3-3) we write (4.3-1)

$$\left.\begin{aligned} &[\sigma_d(\Delta t)]^2 = 1 - 2M_1 + 2M_2, \\ &\text{where} \\ &M_1 = \int_0^\infty \langle {}^kW_{e_i}(t, t-\tau)\rangle \exp\{-K_s\tau\}\, d\tau \\ &\text{and} \\ &M_2 = \int_0^\infty \int_0^\tau \langle {}^kW_{e_i}(t, t-\tau)\, {}^kW_{e_i}(t, t-\nu)\rangle \exp\{-K_s(\tau-\nu)\}\, d\tau\, d\nu. \end{aligned}\right\} \quad (4.3\text{-}4)$$

Starting from (4.3-4), (4.1-11), and (4.1-12), the integrals M_1 and M_2 can be obtained after some time-consuming but in principle elementary computations (summation of various geometric series) as

$$M_1 = \int_0^{\Delta} \Lambda(\xi) \exp\left\{-\left[\chi(\xi) + \frac{x_s}{x_0}\right]\xi\right\} d\xi +$$

$$+ \frac{\exp\left\{-\left[\chi(\Delta) + \frac{x_s}{x_0}\right]\Delta\right\}}{1 - \exp\left\{-\left[\chi(x_0) + \frac{x_s}{x_0}\right]x_0\right\}} \int_0^{x_0} \Lambda(\xi) \exp\left\{-\left[\chi(\xi) + \frac{x_s}{x_0}\right]\xi\right\} d\xi \quad (4.3\text{-}5)$$

and

$$M_2 = \int_0^{\Delta} d\xi \int_0^{\xi} \left[\{\Lambda(\xi+\eta)\}^2 - \Lambda'(\xi+\eta)\right] \exp\left\{-\left[\chi(\xi+\eta)(\xi+\eta) +\right.\right.$$

$$\left.\left. + \frac{x_s}{x_0}(\xi-\eta)\right]\right\} d\eta + \frac{1}{1 - \exp\left\{-\left[\chi(x_0) + \frac{x_s}{x_0}\right]x_0\right\}} \int_0^{x_0} \Lambda(\xi) \exp\left\{-\left[\chi(\xi) +\right.\right.$$

$$\left.\left. + \frac{x_s}{x_0}\right]\xi\right\} d\xi \int_0^{\Delta} \Lambda(\Delta+\xi) \exp\left\{-\left[\chi(\Delta+\xi)(\Delta+\xi) + \frac{x_s}{x_0}(\Delta-\xi)\right]\right\} d\xi +$$

$$+ \frac{1}{1 - \exp\left\{-\left[\chi(x_0) + \frac{x_s}{x_0}\right]x_0\right\}} \frac{\exp\{-2\chi(2\Delta)\Delta\}}{1 - \exp\{-2\chi(2x_0)x_0\}} \cdot$$

$$\cdot \int_0^{x_0} \Lambda(\xi) \exp\left\{-\left[\chi(\xi) + \frac{x_s}{x_0}\right]\xi\right\} d\xi \int_0^{x_0} \Lambda(x_0+\xi) \exp\left\{-\left[\chi(x_0+\xi)(x_0+\xi) +\right.\right.$$

$$\left.\left. + \frac{x_s}{x_0}(x_0-\xi)\right]\right\} d\xi + \frac{\exp\{-2\chi(2\Delta)\Delta\}}{1 - \exp\{-2\chi(2x_0)x_0\}} \int_0^{x_0} d\xi \int_0^{\xi} \left[\{\Lambda(\xi+\eta)\}^2 -\right.$$

$$\left. - \Lambda'(\xi+\eta)\right] \exp\left\{-\left[\chi(\xi+\eta)(\xi+\eta) + \frac{x_s}{x_0}(\xi-\eta)\right]\right\} d\eta, \quad (4.3\text{-}6)$$

where

$$\left.\begin{aligned} x_s &= K_s\, t_0, \\ x_0 &= K_0\, t_0, \\ \Delta &= K_0\, \Delta t. \end{aligned}\right\} \tag{4.3-7}$$

The expressions above for M_1 and M_2 exist for all $K_s > 0$ if $\chi\,(x_0)$ and $\chi\,(2\,x_0) > 0$, i. e. if the tracking servo is stable [compare (4.2-7 a)].

The two double integrals in (4.3-6) can be reduced to single integrals: One can easily show by means of a pair of simple substitutions of variables that

$$\int_0^a d\xi \int_0^\xi f_1\,(\xi - \eta)\, f_2\,(\xi + \eta)\, d\eta = \tfrac{1}{2} \int_0^a f_2\,(\varrho)\, d\varrho \int_0^\rho f_1\,(\nu)\, d\nu +$$

$$+ \tfrac{1}{2} \int_0^a f_2\,(a + \varrho)\, d\varrho \int_0^{a-\rho} f_1\,(\nu)\, d\nu, \tag{4.3-8}$$

which expression changes into the sum of two single integrals if — as in our case — the function f_1 can be integrated directly. The result of such operations is that $[\sigma_d\,(\Delta t)]^2$ or $[\sigma_d\,(\Delta)]^2$ can be written as

$$\left.\begin{aligned} [\sigma_d\,(\Delta)]^2 = 1 - 2\, \frac{\exp\left\{-\left[\chi\,(\Delta) + \dfrac{x_s}{x_0}\right]\Delta\right\}}{1 - \exp\left\{-\left[\chi\,(x_0) + \dfrac{x_s}{x_0}\right] x_0\right\}}\, g_d\,(x_0) - 2\, g_d\,(\Delta) + \\ + \frac{\exp\{-\,2\,\chi\,(2\,\Delta)\,\Delta\}}{1 - \exp\{-\,2\,\chi\,(2\,x_0)\,x_0\}}\, h_d\,(x_0) + h_d\,(\Delta), \end{aligned}\right\}$$

where

$$g_d\,(\Delta) = \int_0^\Delta \Lambda\,(\xi) \exp\left\{-\left[\chi\,(\xi) + \frac{x_s}{x_0}\right]\xi\right\} d\xi$$

and

$$h(\Delta) = \int_0^{\Delta} \xi \frac{1 - \exp\left\{-\frac{x_s}{x_0}\xi\right\}}{\frac{x_s}{x_0}\xi} \left[\{\Lambda(\xi)\}^2 - \Lambda'(\xi)\right] \exp\{-\chi(\xi)\,\xi\}\,d\xi + \tag{4.3-9}$$

$$+ \int_0^{\Delta} (\Delta - \xi) \frac{1 - \exp\left\{-\frac{x_s}{x_0}(\Delta - \xi)\right\}}{\frac{x_s}{x_0}(\Delta - \xi)} \left[\{\Lambda(\Delta + \xi)\}^2 - \Lambda'(\Delta + \xi)\right] \cdot$$

$$\cdot \exp\{-\chi(\Delta + \xi)(\Delta + \xi)\}\,d\xi + \frac{2}{1 - \exp\left\{-\left[\chi(x_0) + \frac{x_s}{x_0}\right]x_0\right\}} \int_0^{x_0} \Lambda(\xi) \cdot$$

$$\cdot \exp\left\{-\left[\chi(\xi) + \frac{x_s}{x_0}\right]\xi\right\} d\xi \int_0^{\Delta} \Lambda(\Delta + \xi) \exp\left\{-\left[\chi(\Delta + \xi)(\Delta + \xi) + \right.\right.$$

$$\left.\left. + \frac{x_s}{x_0}(\Delta - \xi)\right]\right\} d\xi.$$

The time-average $\overline{\sigma_d^2}$ of the dynamic error, relation (4.3-2), can now be obtained from (4.3-9) above. After in principle elementary but time-consuming computations, in which relation (4.3-8) among others is employed, and, in connection with partial integrations, the fact is used that the function $\Lambda(\xi)$ is the derivative $\frac{d}{d\xi}[\chi(\xi)\,\xi]$, relation (4.1-9), one arrives at the following final expression for $\overline{\sigma_d^2}$ that is suitable for a numerical treatment:

$$\overline{\sigma_d^2} = \frac{1}{x_0}\frac{x_s}{x_0} \int_0^{x_0} (x_0 - \xi) \exp\left\{-\left[\chi(\xi) + \frac{x_s}{x_0}\right]\xi\right\} d\xi - \frac{1}{2\,x_0} \cdot$$

$$\cdot \left(1 - 2\,\frac{x_s}{x_0} \frac{\int_0^{x_0} \exp\left\{-\left[\chi(\xi) + \frac{x_s}{x_0}\right]\xi\right\} d\xi}{1 \quad \exp\left\{-\left[\chi(x_0) + \frac{x_s}{x_0}\right]x_0\right\}} + \frac{x_s}{x_0} \frac{\int_0^{2x_0} \exp\{-\chi(\xi)\,\xi\}\,d\xi}{1 - \exp\{-2\,\chi(2x_0)\,x_0\}} \right) \cdot$$

$$\cdot \left(\int_0^{x_0} \exp\left\{ -\left[\chi(\xi) + \frac{x_s}{x_0} \right] \xi \right\} d\xi + \int_0^{x_0} \exp\left\{ -\left[\chi(x_0+\xi)(x_0+\xi) + \right.\right.\right.$$

$$\left.\left.\left. + \frac{x_s}{x_0}(x_0-\xi) \right] \right\} d\xi \right) + \frac{1}{2x_0} \frac{\int_0^{2x_0} \exp\{-\chi(\xi)\,\xi\}\, d\xi}{1 - \exp\{-2\,\chi(2x_0)\,x_0\}} \cdot$$

$$\cdot \left[1 - 2\exp\left\{ -\left[\chi(x_0) + \frac{x_s}{x_0} \right] x_0 \right\} + \exp\{-2\,\chi(2x_0)\,x_0\} + \right.$$

$$+ 2\left(1 - \frac{x_s}{x_0} \frac{\int_0^{x_0} \exp\left\{ -\left[\chi(\xi) + \frac{x_s}{x_0} \right] \xi \right\} d\xi}{1 - \exp\left\{ -\left[\chi(x_0) + \frac{x_s}{x_0} \right] x_0 \right\}} \right) \left(\exp\left\{ -\left[\chi(x_0) + \frac{x_s}{x_0} \right] x_0 \right\} - \right.$$

$$- \exp\{-2\,\chi(2x_0)\,x_0\} + \frac{x_s}{x_0} \int_0^{x_0} \exp\left\{ -\left[\chi(x_0+\xi)(x_0+\xi) + \right.\right.$$

$$\left.\left.\left.\left. + \frac{x_s}{x_0}(x_0-\xi) \right] \right\} d\xi \right) \right] . \qquad (4.3\text{-}10)$$

If the stochastically time-varying tracking servo changes into a time-invariant control system $[F(t) = \varkappa]$, the function $\chi(\xi)$ approaches the value 1, as is evident from its definition (4.1-7). If in the expression (4.3-10) above for $\overline{\sigma_d^2}$ we let the function $\chi(\xi)$ approach the value 1 the quantity $\overline{\sigma_d^2}$ also approaches the dynamic error $\sigma_{d_0}^2$ of the time-invariant system, relation (3.3-7), or

$$(\overline{\sigma_d^2})_{\chi(\xi)\to 1} = \frac{x_s}{x_0 + x_s} = \frac{1}{1 + K_0/K_s} = \frac{1}{1 + y_s} = \sigma_{d_0}^2 . \qquad (4.3\text{-}11)$$

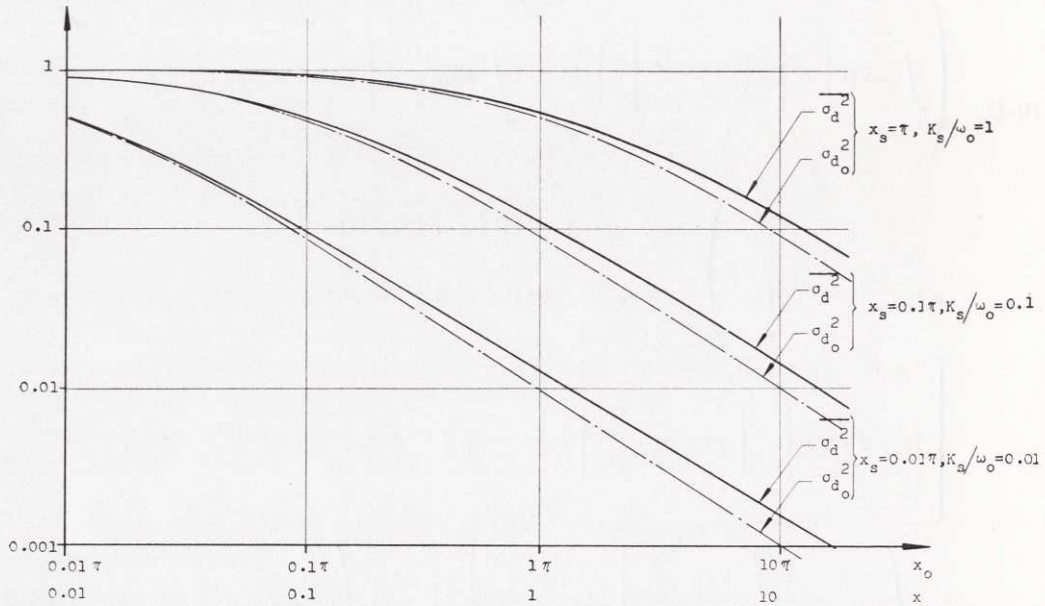

Fig. 23. The dynamic error of the tracking servo as a function of x_0 or x for various values of x_s or K_s/ω_0 for constant $(\sigma_{d_0}^2)$ and quasi-stationary random Rayleigh-distributed amplification $(\overline{\sigma_d^2})$.

Numerical calculations carried out on SARA for the case of Rayleigh-distributed amplification [$\chi(\xi)$ given by (4.2-5)] show the dynamic error $\overline{\sigma_d^2}$ in fig. 23 as a function of x_0 or the previously used variable $x = K_0/\omega_0 = x_0/\pi$ with x_s or $K_s/\omega_0 = x_s/\pi$ as a parameter. As distinguished from the analogous case of Gaussian-distributed stationary random amplification discussed in chapter 3.3 and presented in fig. 10, the dynamic error is bounded for all values of x_0 and approaches the value zero for large values of x_0, although more slowly than the corresponding error $\sigma_{d_0}^2$ of the time-invariant system.

Under the assumptions made, the results presented in fig. 23 for the dynamic error are applicable to the case of an angle-tracking monopulse radar with a linear detection system, a slowly acting AGC, and a simple tracking servo. Such a radar is treated in more detail in appendix II. Fig. 37 of this appendix shows the equivalent circuit of the radar. If the quantity $K_s(t)$ of fig. 37 representing the amplification of the radar angular error measuring device is supposed to be constant and independent of time, which is approximately the case when the AGC is slow, the transfer function of the antenna

controller is of the type $1/s$, and if our $F(t)$ is identified as the radar echo signal amplitude $E_a(t)$ the block-diagram of figure 37 of appendix II becomes the tracking servo treated in fig. 1. For ordinary types of targets, such as airplanes and ships, the echo signal envelope $E_a(t)$ is more or less Rayleigh-distributed and, the cut-off angular frequency can amount to about 50 radians per second.

As is clear from fig. 23 the dynamic error of such a radar for randomly varying input signal can be kept at a suitably low level by a suitable choice of x_0 (the larger the x_0 value, the larger K_s/ω_0). However, large x_0 values (fast tracking servos) will cause a large increase of the contribution of additive noise to the output, as will be evident in the following section, and it is therefore desirable to keep the value of x_0 small. This is possible for slowly varying inputs, i. e. for small values of K_s/ω_0.

4.4 The contribution of additive noise to the output of the tracking servo

It now remains in the present case of a tracking servo with quasi-stationary stochastically time-varying amplification to study the contribution of stationary random additive noise to the output of the control system. Starting from relation (2-33) for large values of the time of observation, $t = nt_0 + \Delta t$, the ensemble average value of the noise output $[\sigma_n(t)]^2$ can be written as

$$[\sigma_n(\Delta t)]^2 = 2 \int_0^\infty \int_0^\tau \langle {}^kW_n(t, t-\tau)\, {}^kW_n(t, t-\nu)\rangle\, \Phi_{nn}(\tau-\nu)\, d\tau\, d\nu, \quad (4.4\text{-}1)$$

because the integrand of (2-33) is symmetric around the straight line $\tau = \nu$ in the τ, ν-plane. After having specified the autocorrelation function of the noise input Φ_{nn}, the additive noise output $[\sigma_n(\Delta t)]^2$ can be obtained from (4.4-1) using the expressions (4.1-12) defining the weighting function average $\langle {}^kW_n(t, t-\tau)\, {}^kW_n(t, t-\nu)\rangle$. There then remains to evaluate the time-average value $\overline{\sigma_n^2}$ of $[\sigma_n(\Delta t)]^2$ according to (2-34).

As before we specialize the correlation function Φ_{nn} to the form

$$\Phi_{nn}(\tau) = \exp\{-K_n|\tau|\}, \quad (4.4\text{-}2)$$

where K_n is the cut-off angular frequency of the input noise process. From (4.4-2), (4.1-12), (4.4-1), and the corresponding relations (4.3-2),

(4.1-11), (4.1-12), and (4.3-1) used in the preceding section when computing the dynamic error $[\sigma_d(\Delta t)]^2$, we immediately infer that $[\sigma_n(\Delta t)]^2$ becomes

$$[\sigma_n(\Delta t)]^2 = \frac{2}{\varkappa^2} N_2, \tag{4.4-3}$$

where the quantity N_2 is the same as M_2 in relation (4.3-6) when we let the function $\Lambda \to 1$ and replace x_s by $x_n = K_n t_0$, i. e.

$$N_2 = \int_0^{\Delta} d\xi \int_0^{\xi} \exp\left\{-\left[\chi(\xi+\eta)(\xi+\eta) + \frac{x_n}{x_0}(\xi-\eta)\right]\right\} d\xi +$$

$$+ \frac{1}{1-\exp\left\{-\left[\chi(x_0) + \frac{x_n}{x_0}\right]x_0\right\}} \int_0^{x_0} \exp\left\{-\left[\chi(\xi) + \frac{x_n}{x_0}\right]\xi\right\} d\xi \cdot$$

$$\cdot \int_0^{\Delta} \exp\left\{-\left[\chi(\Delta+\eta)(\Delta+\eta) + \frac{x_n}{x_0}(\Delta-\eta)\right]\right\} d\eta +$$

$$+ \frac{1}{1-\exp\left\{-\left[\chi(x_0) + \frac{x_n}{x_0}\right]x_0\right\}} \frac{\exp\{-2\chi(2\Delta)\Delta\}}{1-\exp\{-2\chi(2x_0)x_0\}} \cdot$$

$$\cdot \int_0^{x_0} \exp\left\{-\left[\chi(\xi) + \frac{x_n}{x_0}\right]\xi\right\} d\xi \int_0^{x_0} \exp\left\{-\left[\chi(x_0+\eta)(x_0+\eta) +\right.\right.$$

$$\left.\left. + \frac{x_n}{x_0}(x_0-\eta)\right]\right\} d\eta + \frac{\exp\{-2\chi(2\Delta)\Delta\}}{1-\exp\{-2\chi(2x_0)x_0\}} \cdot$$

$$\cdot \int_0^{x_0} d\xi \int_0^{\xi} \exp\left\{-\left[\chi(\xi+\eta)(\xi+\eta) + \frac{x_n}{x_0}(\xi-\eta)\right]\right\} d\eta \tag{4.4-4}$$

with

$$\left.\begin{aligned} x_0 &= K_0 t_0, \\ x_n &= K_n t_0, \\ \Delta &= K_0 \Delta t. \end{aligned}\right\} \tag{4.4-5}$$

The form above for $[\sigma_n(\Delta t)]^2$ assumes a stable system, i. e. that $\chi(x_0)$ and $\chi(2x_0) > 0$.

The expression (4.4-4) for the output noise can be further reduced. In the same way as when dealing with the dynamic error we obtain [compare relation (4.3-9)]:

$$\left.\begin{aligned} &\varkappa^2 [\sigma_n(\Delta)]^2 = \frac{\exp\{-2\chi(2\Delta)\Delta\}}{1-\exp\{-2\chi(2x_0)x_0\}} h_n(x_0) + h_n(\Delta), \\ &\text{where} \\ &h_n(\Delta) = \int_0^{\Delta} \xi \frac{1-\exp\left\{-\frac{x_n}{x_0}\xi\right\}}{\frac{x_n}{x_0}\xi} \exp\{-\chi(\xi)\xi\}\, d\xi + \\ &+ \int_0^{\Delta} (\Delta-\xi) \frac{1-\exp\left\{-\frac{x_n}{x_0}(\Delta-\xi)\right\}}{\frac{x_n}{x_0}(\Delta-\xi)} \exp\{-\chi(\Delta+\xi)(\Delta+\xi)\}\, d\xi + \\ &+ \frac{2}{1-\exp\left\{-\left[\chi(x_0)+\frac{x_n}{x_0}\right]x_0\right\}} \int_0^{x_0} \exp\left\{-\left[\chi(\xi)+\frac{x_n}{x_0}\right]\xi\right\} d\xi \cdot \\ &\cdot \int_0^{\Delta} \exp\left\{-\left[\chi(\Delta+\xi)(\Delta+\xi)+\frac{x_n}{x_0}(\Delta-\xi)\right]\right\} d\xi. \end{aligned}\right\} \tag{4.4-6}$$

The desired time-average $\overline{\sigma_n^2} = \frac{1}{t_0}\int_0^{t_0} [\sigma_n(\Delta t)]^2\, d(\Delta t)$ can then be computed from (4.4-6). After simplifying the double integrals appearing in this computation by means of (4.3-8) of the preceding section, we arrive at the following final expression for $\varkappa^2 \overline{\sigma_n^2}$:

$$\varkappa^2 \overline{\sigma_n^2} = \frac{1}{x_0} \int_0^{x_0} (x_0 - \xi)\, \xi \frac{1 - \exp\left\{-\frac{x_n}{x_0}\,\xi\right\}}{\frac{x_n}{x_0}\,\xi} \exp\{-\chi(\xi)\,\xi\}\, d\xi +$$

$$+ \frac{1}{4 x_0} \left[\int_0^{x_0} \xi^2 \frac{\exp\left\{-\frac{x_n}{x_0}\,\xi\right\} + \frac{x_n}{x_0}\,\xi - 1}{\frac{1}{2}\left(\frac{x_n}{x_0}\,\xi\right)^2} \exp\{-\chi(\xi)\,\xi\}\, d\xi + \int_0^{x_0} (x_0 - \xi)^2 \cdot \right.$$

$$\left. \cdot \frac{\exp\left\{-\frac{x_n}{x_0}(x_0 - \xi)\right\} + \frac{x_n}{x_0}(x_0 - \xi) - 1}{\frac{1}{2}\left\{\frac{x_n}{x_0}(x_0 - \xi)\right\}^2} \exp\{-\chi(x_0 + \xi)(x_0 + \xi)\}\, d\xi \right] +$$

$$+ \frac{1}{2 x_0} \frac{\int_0^{2x_0} \exp\{-\chi(\xi)\,\xi\}\, d\xi}{1 - \exp\{-2\chi(2x_0)\, x_0\}} \left[\left(1 + 2 \frac{1 - \exp\{-2\chi(2x_0)\, x_0\}}{1 - \exp\left\{-\left[\chi(x_0) + \frac{x_n}{x_0}\right] x_0\right\}} \cdot \right.\right.$$

$$\left. \cdot \frac{\int_0^{x_0} \exp\left\{-\left[\chi(\xi) + \frac{x_n}{x_0}\right]\xi\right\} d\xi}{\int_0^{2x_0} \exp\{-\chi(\xi)\,\xi\}\, d\xi} \right) \left(\int_0^{x_0} \xi \frac{1 - \exp\left\{-\frac{x_n}{x_0}\,\xi\right\}}{\frac{x_n}{x_0}\,\xi} \exp\{-\chi(\xi)\,\xi\}\, d\xi + \right.$$

$$\left. + \int_0^{x_0} (x_0 - \xi) \frac{1 - \exp\left\{-\frac{x_n}{x_0}(x_0 - \xi)\right\}}{\frac{x_n}{x_0}(x_0 - \xi)} \exp\{-\chi(x_0 + \xi)(x_0 + \xi)\}\, d\xi \right) +$$

$$+ \frac{2}{1 - \exp\left\{-\left[\chi(x_0) + \frac{x_n}{x_0}\right] x_0\right\}} \int_0^{x_0} \exp\left\{-\left[\chi(\xi) + \frac{x_n}{x_0}\right]\xi\right\} d\xi \cdot$$

$$\left. \cdot \int_0^{x_0} \exp\left\{-\left[\chi(x_0 + \xi)(x_0 + \xi) + \frac{x_n}{x_0}(x_0 - \xi)\right]\right\} d\xi \right]. \qquad (4.4\text{-}7)$$

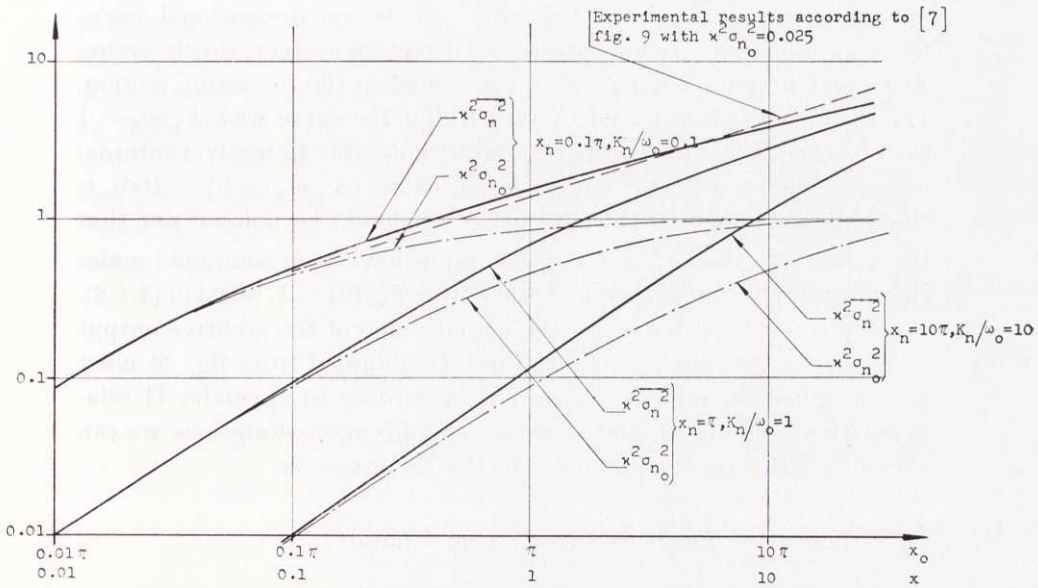

Fig. 24. The contribution of additive noise to the output of the tracking servo as a function of x_0 or x for various values of x_n or K_n/ω_0 for constant $(\sigma_{n_0}{}^2)$ and quasi-stationary random Rayleigh-distributed amplification $(\overline{\sigma_n{}^2})$.

If in the above expression for the additive noise output contribution we let the function $\chi(\xi)$ approach the value 1 we obtain the output noise in the case of a time-invariant tracking servo with $F(t) = \varkappa$ as

$$\left(\overline{\sigma_n^2}\right)_{\chi(\xi)\to 1} = \frac{1}{\varkappa^2}\,\frac{x_0}{x_0 + x_n} = \frac{1}{\varkappa^2}\,\frac{y_n}{1 + y_n} = \sigma_{n_0}^2. \qquad (4.4\text{-}8)$$

Fig. 24 shows the result of numerical calculations of the output noise $\overline{\sigma_n^2}$ according to (4.4-7) performed by SARA and applying to the case that the amplification of the tracking servo is Rayleigh-distributed, i. e. the function $\chi(\xi)$ given by (4.2-5). In the figure are shown $\varkappa^2\overline{\sigma_n^2}$ and $\varkappa^2\sigma_{n_0}^2$ as functions of the variable x_0 or $x = x_0/\pi$ when x_n or $K_n/\omega_0 = x_n/\pi$ has certain given values (compare fig. 16 valid for a case of Gaussian-distributed stationary random amplification).

The results presented in fig. 24 can also be used for providing an idea on the contribution of additive noise caused by target glint

or receiver internal noise to the output of the one-dimensional angle-tracking monopulse radar with linear detection system, slowly acting AGC, and simple tracking servo, considered in the preceding section. For the output noise caused by target glint the curve with $K_n/\omega_0 = 1$ is to be used, while in the case of output noise due to receiver internal noise, a curve with a larger K_n/ω_0-value ($K_n/\omega_0 = 10 - 100$) is the applicable one. In this connection it should be pointed out that the values of $\overline{\sigma_n^2}$ and $\sigma_{n_0}^2$ given in the graphs have been computed under the assumption that the input noise power $\Phi_{nn}(0) = 1$, relation (4.4-2). Consequently, in order to get the actual value of the additive output noise in the two applications the results obtained from fig. 24 must be multiplied by suitable constants. According to appendix II relations (II-8) and (II-9), under certain simplifying assumptions we can therefore write the output noise in the two cases as:

a) output noise due to receiver internal noise:

$$\overline{\sigma_{n_r}^2} = \frac{1}{2}\frac{1}{G^2}\frac{1}{(P/N)_{\text{in}}}\frac{[E_a^2]_{\text{Av}}}{\varkappa^2}\cdot\varkappa^2\overline{\sigma_n^2} = \frac{1}{2}\frac{1}{G^2}\frac{1}{(P/N)_{\text{in}}}(1+\eta)\cdot\varkappa^2\overline{\sigma_n^2}; \quad (4.4\text{-}9)$$

b) output noise due to target glint (in case of ordinary targets such as airplanes and ships):

$$\overline{\sigma_{n_g}^2} = \frac{1}{24}\left(\frac{L'}{R}\right)^2\frac{[E_a^2]_{\text{Av}}}{\varkappa^2}\cdot\varkappa^2\overline{\sigma_n^2} = \frac{1}{24}\left(\frac{L'}{R}\right)^2(1+\eta)\cdot\varkappa^2\overline{\sigma_n^2}. \quad (4.4\text{-}10)$$

In the relations above G is the so called angular gain of the radar antenna, $(P/N)_{\text{in}}$ is a suitably defined signal-to-noise power ratio, R is the distance between radar and target, L' is the extent of the target, and $[E_a^2]_{\text{Av}}$ is the average square value of the echo envelope, i. e. $[E_a^2]_{\text{Av}} = \langle F^2\rangle = \varkappa^2 + \sigma_0^2 = \varkappa^2(1+\eta)$.

Results of experimental investigations of the accuracy of a practical angle-measuring or tracking monopulse radar carried out with simulated echo signals from actual targets for different bandwidths of the automatic gain control have recently been published by DUNN and HOWARD [7]. For comparison there has also been drawn in fig. 24 a curve corresponding to the experimentally obtained output noise due to target glint ($K_n/\omega_0 \cong 1$) for a slowly acting AGC according to fig. 9 in [7]. We see from fig. 24 that the agreement is not quite

perfect between our theoretical curve with $K_n/\omega_0 = 1$ and the experimental curve but, on the other hand, the theoretical curve with $K_n/\omega_0 = 0.1$ agrees very well with the experimental curve. As far as the additive noise output is concerned the qualitative agreement must be regarded as satisfactory between what our theoretical investigation gives for a strongly simplified abstract system and what Dunn and Howard have obtained experimentally with a practical radar.

5. Fundamental relations in the case of a linear, randomly time-varying AGC-servo

In this and the following chapters we shall investigate in some detail the linear, randomly time-varying AGC-servo shown in fig. 2, the purpose of which is to give an output signal $e_u(t)$ deviating as little as possible from the wanted output or reference e_{u_0} in spite of random variations with time of the input signal $F(t)$. From the block-diagram of fig. 2 we see that the function of the simple AGC-servo is given by the following linear differential equation of the first order

$$\frac{d}{dt}\left[\frac{e_u(t)}{F(t)}\right] + [\alpha + K\alpha F(t)]\frac{e_u(t)}{F(t)} = K\left[\alpha e_{u_0}(t) + \frac{de_{u_0}(t)}{dt}\right] + \\ + \alpha g_0(t) + \frac{dg_0(t)}{dt}, \tag{5-1}$$

where g_0 is the so called initial amplification, see fig. 2, K is a constant, and α the cut-off angular frequency of the low-pass filter in the feed-back branch of the servo. If the system starts from rest at time $t = 0$ the solution of equation (5-1) is readily obtained as

$$e_u(t) = \int_0^t W(t,\tau)\left[K\left\{\alpha e_{u_0}(\tau) + \frac{de_{u_0}(\tau)}{d\tau}\right\} + \left\{\alpha g_0(\tau) + \frac{dg_0(\tau)}{d\tau}\right\}\right]d\tau, \tag{5-2}$$

where the weighting function $W(t,\tau)$ is given by

$$W(t,\tau) = F(t)\exp\left\{-[\alpha(t-\tau) + K\alpha\int_\tau^t F(\varrho)\,d\varrho]\right\} = \\ = \frac{\exp\{-\alpha(t-\tau)\}}{K\alpha}\frac{\partial}{\partial t}\left[\exp\left\{-K\alpha\int_\tau^t F(\varrho)\,d\varrho\right\}\right]. \tag{5-3}$$

For simplicity we shall suppose that the wanted output signal or reference $e_{u_0} = 1$, and that the initial amplification of the system is so chosen, $g_0 = 1/\varkappa$, that in the absence of stochastic variations of the input $F(t)$, $F(t) = \varkappa =$ a positive constant, the stationary value of the output becomes $e_u = e_{u_0} = 1$ (see appendix I). With the assumptions

$$e_{u_0}(t) = \begin{cases} 1, & t > 0, \\ 0, & t \leqq 0, \end{cases} \tag{5-4}$$

and

$$g_0(t) = \begin{cases} 1/\varkappa, & t > 0, \\ 0 \quad , & t \leqq 0, \end{cases} \tag{5-5}$$

the solution (5-2) takes the form

$$e_u(t) = \frac{\alpha + K\varkappa\alpha}{\varkappa} \int_0^t W(t, \tau)\, d\tau + \frac{1 + K\varkappa}{\varkappa} W(t, 0), \tag{5-6}$$

where the first term gives the stationary value of the output valid for large t and the second term represents a transient that rapidly disappears in a stable system. If the AGC-servo is time-invariant with $F(t) = \varkappa$, the weighting function $W(t, \tau)$ is

$$W(t, \tau) = \exp\{-(\alpha + K\varkappa\alpha)(t - \tau)\} \tag{5-7}$$

and according to (5-6) the output becomes

$$e_u(t) = 1 + K\varkappa \exp\{-(\alpha + K\varkappa\alpha)\, t\}, \tag{5-8}$$

which has the stationary value 1 in agreement with the choice of initial amplification g_0.

As for the stochastically time-varying input signal $F(t)$ we shall treat the two cases that $F(t)$ is generated either by a stationary Gaussian process with arbitrary spectrum or by the quasi-stationary random process with arbitrary distribution and a spectrum of low-pass character defined in (2-8), (2-9), and (2-17). The particular stochastic output signal and the weighting function corresponding to a certain member ${}^kF(t)$ of the ensemble $\{{}^kF(t)\}$ of random input signals are

denoted by ${}^k e_u(t)$ and ${}^k W(t, \tau)$. For these we consequently have, according to (5-6) and (5-3),

$$ {}^k e_u(t) = \frac{\alpha + K\varkappa\alpha}{\varkappa} \int_0^t {}^k W(t, \tau)\, d\tau + \frac{1 + K\varkappa}{\varkappa} {}^k W(t, 0) \qquad (5\text{-}9) $$

and

$$ {}^k W(t, \tau) = {}^k F(t) \exp\{-[\alpha(t - \tau) + K\alpha \int_\tau^t {}^k F(\varrho)\, d\varrho]\} = $$

$$ = -\frac{1}{K\alpha} \exp\{-\alpha(t-\tau)\} \frac{\partial}{\partial t} [\exp\{-K\alpha \int_\tau^t {}^k F(\varrho)\, d\varrho\}]. \qquad (5\text{-}10) $$

We are also interested in a study of the "resultant signal amplification" ${}^k g(t) = {}^k e_u(t)/{}^k F(t)$ of the system (see fig. 2), which according to the above, can be written as

$$ {}^k g(t) = \frac{\alpha + K\varkappa\alpha}{\varkappa} \int_0^t {}^k W_g(t, \tau)\, d\tau + \frac{1 + K\varkappa}{\varkappa} {}^k W_g(t, 0), \qquad (5\text{-}11) $$

where the weighting function ${}^k W_g(t, \tau)$ is

$$ {}^k W_g(t, \tau) = \exp\{-[\alpha(t - \tau) + K\alpha \int_\tau^t {}^k F(\varrho)\, d\varrho]\}. \qquad (5\text{-}12) $$

The ensemble average value $m_1(t)$ for time t of the output signal of the AGC-servo is easily obtained from equation (5-9), assuming that the averaging process can be carried out under the integral sign, as

$$ m_1(t) = \langle {}^k e_u(t) \rangle = $$

$$ = (1 + K\varkappa) \left[\alpha \int_0^t \frac{1}{\varkappa} \langle {}^k W(t, \tau) \rangle\, d\tau + \frac{1}{\varkappa} \langle {}^k W(t, 0) \rangle \right]. \qquad (5\text{-}13) $$

In a similar way we also get the average square value of the output $m_2(t)$ and the resultant signal amplification $m_3(t)$:

$$ m_2(t) = \langle [{}^k e_u(t)]^2 \rangle = (1 + K\varkappa)^2 \left[\alpha^2 \int_0^t \int_0^t \frac{1}{\varkappa^2} \langle {}^k W(t, \tau)\, {}^k W(t, \nu) \rangle\, d\tau\, d\nu + \right. $$

$$ \left. + 2\alpha \int_0^t \frac{1}{\varkappa^2} \langle {}^k W(t, \tau)\, {}^k W(t, 0) \rangle\, d\tau + \frac{1}{\varkappa^2} \langle {}^k W(t, 0)\, {}^k W(t, 0) \rangle \right] \qquad (5\text{-}14) $$

and

$$m_3(t) = \langle [{}^k g(t)]^2 \rangle = (1 + K\varkappa)^2 \left[\alpha^2 \int_0^t \int_0^t \frac{1}{\varkappa^2} \langle {}^k W_g(t,\tau)\, {}^k W_g(t,\nu) \rangle \, d\tau \, d\nu + \right.$$

$$\left. + 2\alpha \int_0^t \frac{1}{\varkappa^2} \langle {}^k W_g(t,\tau)\, {}^k W_g(t,0) \rangle \, d\tau + \frac{1}{\varkappa^2} \langle {}^k W_g(t,0)\, {}^k W_g(t,0) \rangle \right]. \quad (5\text{-}15)$$

In the following we shall only be interested in those values of the averages m_1, m_2, and m_3 which are valid for large t. If, as we assume, the AGC-servo is stable, all the transient terms in (5-9) and (5-11) and the corresponding transient terms in the expressions of m_1, m_2, and m_3 can be neglected for large values of t. For large t we can therefore put

$$\left.\begin{aligned} m_1(t) &\cong (\alpha + K_0') \int_0^\infty \frac{1}{\varkappa} \langle {}^k W(t, t-\tau) \rangle \, d\tau, \\ m_2(t) &\cong (\alpha + K_0')^2 \int_0^\infty \int_0^\infty \frac{1}{\varkappa^2} \langle {}^k W(t, t-\tau)\, {}^k W(t, t-\nu) \rangle \, d\tau \, d\nu, \\ m_3(t) &\cong (\alpha + K_0')^2 \int_0^\infty \int_0^\infty \frac{1}{\varkappa^2} \langle {}^k W_g(t, t-\tau)\, {}^k W_g(t, t-\nu) \rangle \, d\tau \, d\nu, \end{aligned}\right\} \quad (5\text{-}16)$$

where

$$K_0' = \alpha K \varkappa.$$

By means of the average values $m_1(t)$ and $m_2(t)$ defined above one can also express the ensemble average square $[\varepsilon(t)]^2$ of the deviation of the output from the wanted signal $e_{u_0} = 1$:

$$[\varepsilon(t)]^2 = \langle [{}^k e_u(t) - 1]^2 \rangle = 1 - 2\, m_1(t) + m_2(t) \quad (5\text{-}17)$$

and the ensemble average square $[\sigma(t)]^2$ of the difference between the output signal and the average value $m_1(t)$:

$$[\sigma(t)]^2 = \langle [{}^k e_u(t) - \langle {}^k e_u(t) \rangle]^2 \rangle = m_2(t) - [m_1(t)]^2. \quad (5\text{-}18)$$

We shall study these quantities in the following.

As one easily sees, the average values m_1, m_2, m_3, ε^2, and σ^2 according to (5-16) — (5-18) become independent of time of observation t in the case of stationary stochastic Gaussian input signal $F(t)$, but in

the other case of a quasi-stationary random input they will vary periodically with time with the period t_0. In this latter case we therefore form the time-averages $\overline{m_1}$, $\overline{m_2}$, and $\overline{m_3}$ of the corresponding quantities:

$$\left.\begin{aligned} \overline{m_1} &= \frac{1}{t_0}\int_0^{t_0} m_1(\Delta t)\, d(\Delta t), \\ \overline{m_2} &= \frac{1}{t_0}\int_0^{t_0} m_2(\Delta t)\, d(\Delta t), \\ &\text{and} \\ \overline{m_3} &= \frac{1}{t_0}\int_0^{t_0} m_3(\Delta t)\, d(\Delta t). \end{aligned}\right\} \tag{5-19}$$

According to (5-17) we get

$$\overline{\varepsilon^2} = \frac{1}{t_0}\int_0^{t_0} [\varepsilon(\Delta t)]^2\, d(\Delta t) = \overline{m_2} - 2\,\overline{m_1} + 1. \tag{5-20}$$

If the random input signal $F(t)$ is quasi-stationary the time-average of $[\sigma(t)]^2$ according to (5-18) is not of any great interest. On the other hand, in this case it may be valuable to have a measure of the time-average $\overline{\sigma_1^2}$ of the square deviation $[\sigma_1(t)]^2$ of the output of the AGC-servo from its average value $\overline{m_1}$ given by

$$[\sigma_1(t)]^2 = \left\langle \left[{}^k e_u(t) - \overline{m_1}\right]^2 \right\rangle = m_2(t) - 2\, m_1(t)\,\overline{m_1} + (\overline{m_1})^2. \tag{5-21}$$

The time-average value $\overline{\sigma_1^2}$ can therefore be written as

$$\overline{\sigma_1^2} = \frac{1}{t_0}\int_0^{t_0} [\sigma_1(\Delta t)]^2\, d(\Delta t) = \overline{m_2} - (\overline{m_1})^2. \tag{5-22}$$

6. The characteristics of the AGC-servo for a Gaussian-distributed, stationary random input signal with arbitrary spectrum

6.1 Deduction of the expressions for certain ensemble average values

The expressions for the ensemble average values $\langle {}^kW(t, t-\tau)\rangle$, $\langle {}^kW(t, t-\tau)\,{}^kW(t, t-\nu)\rangle$, and $\langle {}^kW_g(t, t-\tau)\,{}^kW_g(t, t-\nu)\rangle$ needed in the further analysis of the characteristics of the AGC-servo output are derived in the same way as those for $\langle {}^kW_{e_i}(t, t-\tau)\rangle$ etc. in section 3.1.

We introduce the following function notations:

$$R(t, \tau) = \langle \exp\{-K\alpha \int_{\tau}^{t} {}^kF(\varrho)\, d\varrho\}\rangle \tag{6.1-1}$$

and

$$S(t, T, \tau, \nu) = \langle \exp\{-K\alpha \int_{\tau}^{t} {}^kF(\varrho)\, d\varrho - K\alpha \int_{\nu}^{T} {}^kF(\varrho)\, d\varrho\}\rangle. \tag{6.1-2}$$

By means of the functions R and S above and the relations (5-10) and (5-12), the desired weighting function averages can be expressed as

$$\langle {}^kW(t, \tau)\rangle = \frac{1}{K\alpha} \exp\{-\alpha(t-\tau)\} \frac{\partial}{\partial t} R(t, \tau), \tag{6.1-3}$$

$$\langle {}^kW(t, \tau)\,{}^kW(t, \nu)\rangle = \frac{1}{(K\alpha)^2} \exp\{-\alpha(t-\tau+t-\nu)\} \cdot$$

$$\cdot \left[\frac{\partial^2}{\partial t\, \partial T} S(t, T, \tau, \nu)\right]_{T=t}, \tag{6.1-4}$$

and

$$\langle {}^kW_g(t, \tau)\,{}^kW_g(t, \nu)\rangle = \exp\{-\alpha(t-\tau+t-\nu)\} S(t, t, \tau, \nu). \tag{6.1-5}$$

$R(t, \tau)$ and the auxiliary function $P(t, \tau)$ used in section 3.1, relation (3.1-1), are identical except for a coefficient before the integral in the exponent. Therefore, we immediately get the function $R(t, \tau)$ from (3.1-18) by a simple change of the coefficient $K_0 = \varkappa K$ for $K_0' = \varkappa K\alpha$, i. e.

$$R(t, \tau) = \exp\left\{ - K_0'(t - \tau) + \frac{1}{2} \frac{(K_0')^2}{\varkappa^2} \sum_{n=1}^{N} \frac{4 \sin^2 \frac{n\Delta\omega\,(t - \tau)}{2}}{(n\Delta\omega)^2} \cdot \right.$$

$$\left. \cdot\, G(n\Delta\omega)\, \Delta\omega \right\}, \tag{6.1-6}$$

where $G(n\Delta\omega)$ is the power density of the Gaussian-distributed random process $\{{}^kF(t)\}$ for the angular frequency $n\Delta\omega$. For a deduction of the expression of the function $S(t, T, \tau, \nu)$ we first write, taking ${}^kF(t)$ according to the assumption (2-6), the integrals

$$K\alpha \int_{\tau}^{t} {}^kF(\varrho)\, d\varrho + K\alpha \int_{\nu}^{T} {}^kF(\varrho)\, d\varrho = K_0' [t - \tau + T -$$

$$- \nu + \sum_{n=1}^{N} \alpha_n\, {}^ka_n - \beta_n\, {}^kb_n], \tag{6.1-7}$$

where

$$\left.\begin{aligned} \alpha_n &= \frac{1}{\varkappa} \frac{\sin n\Delta\omega t - \sin n\Delta\omega\tau + \sin n\Delta\omega T - \sin n\Delta\omega\nu}{n\Delta\omega}, \\ \beta_n &= \frac{1}{\varkappa} \frac{\cos n\Delta\omega t - \cos n\Delta\omega\tau + \cos n\Delta\omega T - \cos n\Delta\omega\nu}{n\Delta\omega}. \end{aligned}\right\} \tag{6.1-8}$$

The function $S(t, T, \tau, \nu)$ can then be expressed as

$$S(t, T, \tau, \nu) = \exp\{- K_0'(t - \tau + T - \nu)\} \langle \exp\{-$$

$$- K_0' \sum_{n=1}^{N} \alpha_n\, {}^ka_n - \beta_n\, {}^kb_n\}\rangle. \tag{6.1-9}$$

The type of ensemble average value appearing in (6.1-9) was computed in section 3.1, relation (3.1-17), and therefore we immediately get

$$S(t, T, \tau, \nu) = \exp\{- K_0'(t - \tau + T - \nu) + \tfrac{1}{2} (K_0')^2 \cdot$$

$$\cdot \sum_{n=1}^{N} (\alpha_n^2 + \beta_n^2)\, G(n\Delta\omega)\, \Delta\omega\},$$

which by using the expressions for α_n and β_n in (6.1-8) results in

$$S(t, T, \tau, \nu) = \exp\left\{-K_0'(t-\tau+T-\nu) + \frac{1}{2}\frac{(K_0')^2}{\varkappa^2}\sum_{n=1}^{N}\left[4\sin^2\frac{n\Delta\omega\,(t-\tau)}{2} + \right.\right.$$

$$+ 4\sin^2\frac{n\Delta\omega\,(T-\tau)}{2} + 4\sin^2\frac{n\Delta\omega\,(t-\nu)}{2} + 4\sin^2\frac{n\Delta\omega\,(T-\nu)}{2} -$$

$$\left.\left. - 4\sin^2\frac{n\Delta\omega\,(t-T)}{2} - 4\sin^2\frac{n\Delta\omega\,(\tau-\nu)}{2}\right]\frac{G(n\Delta\omega)\,\Delta\omega}{(n\Delta\omega)^2}\right\}. \qquad (6.1\text{-}10)$$

There now remains to compute the wanted weighting function average values $\langle {}^kW(t,\tau)\rangle$, $\langle {}^kW(t,\tau)\,{}^kW(t,\nu)\rangle$, and $\langle {}^kW_g(t,\tau)\,{}^kW_g(t,\nu)\rangle$ according to (6.1-3) — (6.1-5) by means of the relations (6.1-6) and (6.1-10) and then to let the discrete spectrum of the random input $F(t)$ change into a continuous spectrum, i. e. to let $N \to \infty$ and $n\Delta\omega \to \omega$. Because these computations are somewhat time-consuming but elementary in principle we here give only the results, which can be formulated as

$$\left.\begin{aligned}
&\frac{1}{\varkappa}\langle {}^kW(t, t-\tau)\rangle = \left[1 - \frac{K_0'}{\varkappa^2}\tau g_2(\tau)\right]\exp\left\{-(\alpha + K_0')\,\tau + \right.\\
&\qquad \left. + \frac{1}{2}\frac{(K_0')^2}{\varkappa^2}\,\tau^2\, g_1(\tau)\right\},\\
&\frac{1}{\varkappa^2}\langle {}^kW(t, t-\tau)\,{}^kW(t, t-\nu)\rangle = \left[\left\{1 - \frac{K_0'}{\varkappa^2}[\tau g_2(\tau) + \right.\right.\\
&\qquad \left.\left. + \nu g_2(\nu)]\right\}^2 + \frac{1}{\varkappa^2}\varrho_{FF}(0)\right]\exp\left\{-(\alpha + K_0')(\tau+\nu) + \right.\\
&\qquad \left. + \frac{(K_0')^2}{\varkappa^2}\left[\tau^2 g_1(\tau) + \nu^2 g_1(\nu) - \frac{1}{2}(\tau-\nu)^2 g_1(\tau-\nu)\right]\right\},
\end{aligned}\right\} \qquad (6.1\text{-}11)$$

and

$$\left.\begin{aligned}
&\langle {}^kW_g(t, t-\tau)\,{}^kW_g(t, t-\nu)\rangle = \exp\left\{-(\alpha + K_0')(\tau+\nu) + \right.\\
&\qquad \left. + \frac{(K_0')^2}{\varkappa^2}\left[\tau^2 g_1(\tau) + \nu^2 g_1(\nu) - \frac{1}{2}(\tau-\nu)^2 g_1(\tau-\nu)\right]\right\},
\end{aligned}\right\}$$

where the functions g_1, g_2, and ϱ_{FF} are defined by (3.1-23) and (3.1-22).

6.2 The characteristics of the output signal of the AGC-servo

By means of the expressions deduced in section 6.1 for the weighting function average values we are now able to analyze in more detail the average $m_1(t)$ of the output of the AGC-servo, the average square $[\varepsilon(t)]^2$ of the deviation of the output from the wanted value $e_{u_0} = 1$, and the average square $[\sigma(t)]^2$ of the deviation of the output from its average value, holding for large values of the time of observation t (stationary average values). A condition for m_1, ε^2, and σ^2 to take on stationary values for large t is that the transient terms $\langle {}^kW(t, 0)\rangle$ and $\langle {}^kW(t, 0)\, {}^kW(t, 0)\rangle$ in the expressions (5-13) and (5-14) for $m_1(t)$ and $m_2(t)$ can be neglected. As is evident from (6.1-11) of the preceding section this condition is satisfied if for large t

$$\alpha + K_0' - \frac{(K_0')^2}{\varkappa^2}\, t\, g_1(t) > 0$$

or, after using relation (3.1-24) of chapter 3, if

$$\alpha + K_0' - \frac{(K_0')^2}{\varkappa^2}\, \pi\, G(0) > 0. \tag{6.2-1}$$

One easily ascertains that if the condition (6.2-1) is fullfilled then the remaining transient term $2\,\alpha \int_0^t \langle {}^kW(t, \tau)\, {}^kW(t, 0)\rangle\, d\tau$ in the expression for $m_2(t)$, relation (5-14) is also negligible for large t and the stationary values of $m_1(t)$, $m_2(t)$, $[\varepsilon(t)]^2$, and $[\sigma(t)]^2$ become bounded. The same argumentation also holds for the average square $m_3(t)$ of the resultant signal amplification of the AGC-servo. The relation (6.2-1) can therefore be said to represent the condition for the treated AGC-servo to be stable [compare the corresponding condition given in (3.2-4) and applicable to the tracking servo].

If we introduce the weighting function averages given in (6.1-11) into (5-16) we can express the stationary output signal average values of interest in the following way:

$$
\left.
\begin{aligned}
m_1 &= (\varkappa + K_0') \int_0^\infty \left[1 - \frac{K_0'}{\varkappa^2}\, \tau\, g_2(\tau)\right] \exp\left\{-(\varkappa + K_0')\,\tau + \right. \\
&\quad \left. + \frac{1}{2}\, \frac{(K_0')^2}{\varkappa^2}\, \tau^2\, g_1(\tau)\right\} d\tau, \\
m_2 &= (\varkappa + K_0')^2 \int_0^\infty \int_0^\infty \left[\left\{1 - \frac{K_0'}{\varkappa^2}\,[\tau\, g_2(\tau) + \nu\, g_2(\nu)]\right\}^2 + \right. \\
&\quad \left. + \frac{1}{\varkappa^2}\, \varrho_{FF}(0)\right] \exp\left\{-(\varkappa + K_0')\,(\tau + \nu) + \frac{(K_0')^2}{\varkappa^2}\,[\tau^2 g_1(\tau) + \right. \\
&\quad \left. + \nu^2\, g_1(\nu) - \tfrac{1}{2}\,(\tau - \nu)^2\, g_1(\tau - \nu)]\right\} d\tau\, d\nu, \\
\varepsilon^2 &= 1 - 2\, m_1 + m_2, \text{ and} \\
\sigma^2 &= m_2 - m_1^2.
\end{aligned}
\right\} \qquad (6.2\text{-}2)
$$

By means of (6.2-2) and the definition of g_1 and g_2 in (3.1-23), the output averages m_1, m_2, ε^2, and σ^2 can be computed for arbitrary power density $G(\omega)$ of the randomly time-varying input $F(t)$ of the AGC-servo. As in the case of the tracking servo, we shall here study numerically only the case that the power spectrum $G(\omega)$ is rectangular, i. e. we shall put

$$
\left.
\begin{aligned}
G(\omega) &= \begin{cases} \sigma_0^2/\omega_0, & 0 \leqq \omega \leqq \omega_0, \\ 0, & \omega > \omega_0, \end{cases} \\
&\text{where the total power } \sigma_0^2 \text{ is given by} \\
\sigma_0^2 &= \varrho_{FF}(0) = \int_0^\infty G(\omega)\, d\omega.
\end{aligned}
\right\} \qquad (6.2\text{-}3)
$$

Under these assumptions the functions g_1 and g_2 are defined by relation (3.2-7) of chapter 3 and (6.2-2) can be written as

$$
\left.
\begin{aligned}
m_1 &= \int_0^\infty \left[1 - \frac{\pi}{2}\,\frac{K_0'}{\alpha+K_0'}\,\eta x\, I_2\left(\frac{\tau}{x}\right)\right] \exp\left\{-\tau + \frac{\pi}{2}\left(\frac{K_0'}{\alpha+K_0'}\right)^2 \eta x \cdot \right. \\
&\quad \left. \cdot\, \tau\, I_1\left(\frac{\tau}{2\,x}\right)\right\} d\tau, \\
m_2 &= \int_0^\infty \int_0^\infty \left[\left\{1 - \frac{\pi}{2}\,\frac{K_0'}{\alpha+K_0'}\,\eta x \left[I_2\left(\frac{\tau}{x}\right) + I_2\left(\frac{\nu}{x}\right)\right]\right\}^2 + \eta\right] \exp\left\{-(\tau+\nu) + \right. \\
&\quad \left. + \pi \left(\frac{K_0'}{\alpha+K_0'}\right)^2 \eta x \left[\tau\, I_1\left(\frac{\tau}{2\,x}\right) + \nu\, I_1\left(\frac{\nu}{2\,x}\right) - \frac{1}{2}(\tau-\nu)\, I_1\left(\frac{\tau-\nu}{2\,x}\right)\right]\right\} d\tau\, d\nu, \\
\varepsilon^2 &= 1 - 2\,m_1 + m_2, \\
\sigma^2 &= m_2 - m_1^2,
\end{aligned}
\right\} \qquad (6.2\text{-}4)
$$

where

$$
\left.
\begin{aligned}
x &= (\alpha + K_0')/\omega_0, \\
\eta &= \sigma_0^2/\varkappa^2, \\
K_0' &= K\varkappa\alpha,
\end{aligned}
\right\} \qquad (6.2\text{-}5)
$$

and as previously the functions I_1 and I_2 are given by

$$
\left.
\begin{aligned}
I_1(\xi) &= \frac{2}{\pi} \int_0^\xi \frac{\sin^2 y}{y^2}\, dy, \\
I_2(\xi) &= \frac{2}{\pi} \int_0^\xi \frac{\sin y}{y}\, dy.
\end{aligned}
\right\} \qquad (6.2\text{-}6)
$$

The results of numerical calculations carried out on SARA of the output signal average m_1, ε^2, and σ^2 according to (6.2-4) above are shown graphically in figs 25—27 as functions of the variable x with η as a parameter, in the two cases that the ratio $K_0'/(\alpha + K_0')$ or $\varkappa K/(1 + \varkappa K)$ is 1/2 and 1. The quantity $\varkappa K$ is identical with the so called open-loop zero frequency gain used in the small signal theory of automatic gain controls [appendix I, relation (I-21) with $e_{i_0} = \varkappa$]. Consequently, the value 1/2 of the ratio $K_0'/(\alpha + K_0')$ means a very low open-loop zero frequency gain of the AGC-servo ($\varkappa K = 1$), whereas the limiting case $K_0'/(\alpha + K_0') = 1$ ($\varkappa K \to \infty$) best corresponds

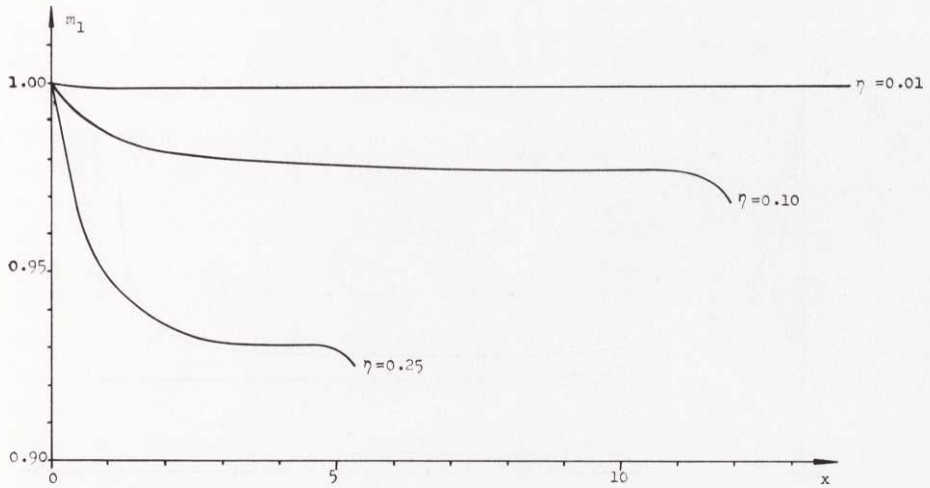

Fig. 25. The average value m_1 of the output of the AGC-servo as a function of x with η as a parameter and $K_0'/(\alpha+K_0') = 1/2$ in the case of stationary random Gaussian input signal.

to the usual practical case that the open-loop gain is considerably larger than one. The variable x is a measure of the ratio between the bandwidths of the AGC-servo and the random input signal variations. For instance, by means of the bandwidth ω_{AGC} of the AGC-servo defined in appendix I, relation (I-24) with $e_{i_0} = \varkappa$, the variable x can be written as

$$x = \frac{1 + \varkappa K}{\sqrt{(1 + \varkappa K)^2 - 2}} \frac{\omega_{AGC}}{\omega_0} . \tag{6.2-7}$$

This means that $x = \sqrt{2} \frac{\omega_{AGC}}{\omega_0}$ when $\varkappa K = 1$ and $x \cong \frac{\omega_{AGC}}{\omega_0}$ when $\varkappa K \gg 1$.

As is evident from figs 25—27, the average values increase beyond limit when the variable x approaches $1 \Big/ \left\{ \pi\eta \left(\frac{K_0'}{\alpha+K_0'} \right)^2 \right\}$ in accordance with the stability condition (6.2-1). Fig. 25 shows the average value m_1 as a function of x for various values of the input "noise-to-signal power ratio" η in the case that $K_0'/(\alpha + K_0') = 1/2$, i. e. for an extremely low open-loop gain of the AGC-servo. The quantity m_1 deviates relatively little from the desirable value 1 and the deviation decreases with η, as is evident from the figure. In the limiting case

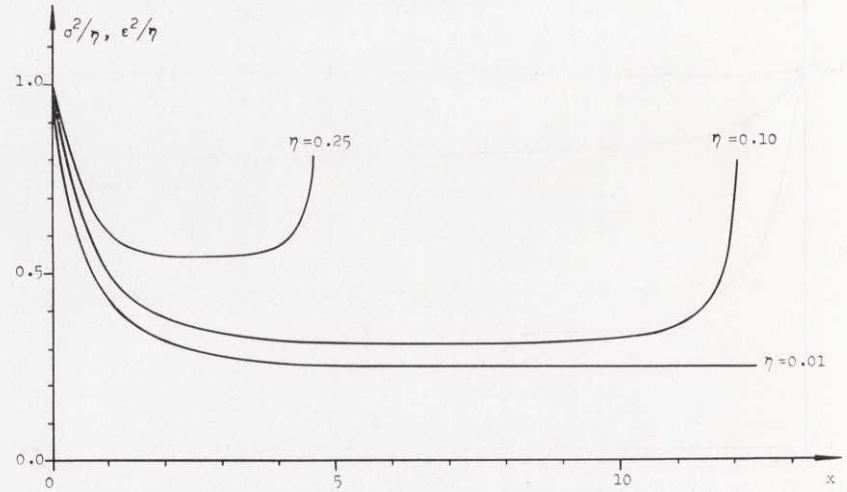

Fig. 26. The output signal deviation σ^2 or ε^2 of the AGC-servo as a function of x with η as a parameter and $K_0'/(\alpha+K_0') = 1/2$ in the case of stationary random Gaussian input signal.

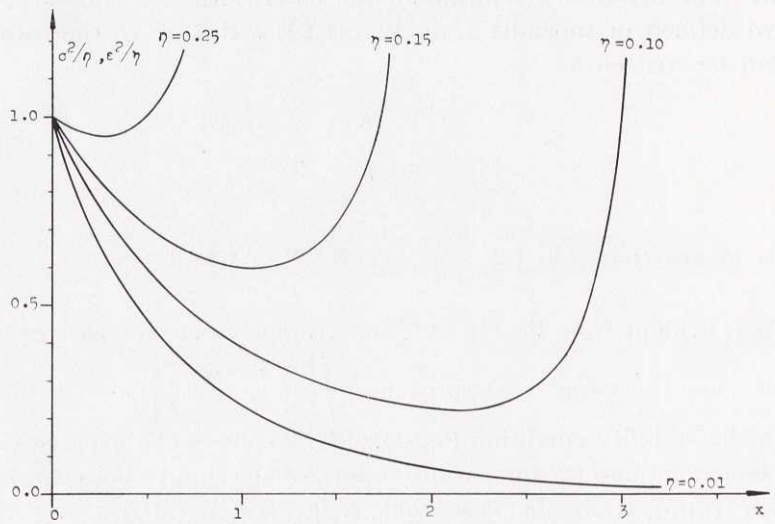

Fig. 27. The output signal deviation σ^2 or ε^2 of the AGC-servo as a function of x with η as a parameter and $K_0'/(\alpha+K_0') \cong 1$ in the case of stationary random Gaussian input signal.

$K_0'/(\varkappa + K_0') = 1$, i. e. for an extremely large open-loop gain, $m_1 = 1$ independently of η in the stable region of x.

The average values ε^2 and σ^2 differ slightly from each other as long as m_1 is close to 1 and they are consequently identical in the limiting case $K_0'/(\varkappa + K_0') = 1$, fig. 27. In the other case investigated, with $K_0'/(\varkappa + K_0') = 1/2$, the difference between ε^2 and σ^2 falls within the computational error (several per cent). From the figures we see that the decrease of the noise-to-signal power ratio ε^2 at the output of the AGC-servo compared to the ratio η of the random input that can be obtained by a suitable choice of the variable x decreases as η increases. This is in agreement with general experience: a good signal-to-noise ratio can easily be improved, but a poor signal-to-noise ratio can be improved only with great difficulty.

Starting from relations (6.2-4) above one can show that for small η and not too large x-values the following approximately holds:

$$\left.\begin{aligned} & m_1 \cong 1, \\ & \varepsilon^2/\eta \cong \sigma^2/\eta \cong 1 - x \tan^{-1}(1/x) + \frac{x}{(1 + \varkappa K)^2} \tan^{-1}(1/x), \end{aligned}\right\} \qquad (6.2\text{-}8)$$

which is a result given by the small signal theory of an AGC as well. The curves for $\eta = 0.01$ presented in figs 26 and 27 agree very well with the results of (6.2-8). For $\eta = 0.1$ the agreement is, however, not quite so good. Further, from (6.2-4) one can show that for $x \ll 1$ and $K_0'/(\varkappa + K_0') \cong 1$,

$$\varepsilon^2/\eta \cong \sigma^2/\eta \cong 1 - \frac{\pi}{2}(1 - 3\,\eta)\,x. \qquad (6.2\text{-}9)$$

This also agrees with the results in fig. 27.

6.3 The resultant signal amplification of the AGC-servo

The stationary ensemble average square value m_3 of the resultant signal amplification of the AGC-servo that exists if the stability condition (6.2-1) is satisfied is given by relations (5-16) and (6.1-11) as

$$m_3 = \frac{1}{\varkappa^2}(\varkappa + K_0')^2 \int_0^\infty \int_0^\infty \exp\left\{-(\varkappa + K_0')(\tau + \nu) + \frac{(K_0')^2}{\varkappa^2}\left[\tau^2 g_1(\tau) + \right.\right.$$

$$\left.\left. + \nu^2 g_1(\nu) - \tfrac{1}{2}(\tau - \nu)^2 g_1(\tau - \nu)\right]\right\} d\tau\, d\nu. \qquad (6.3\text{-}1)$$

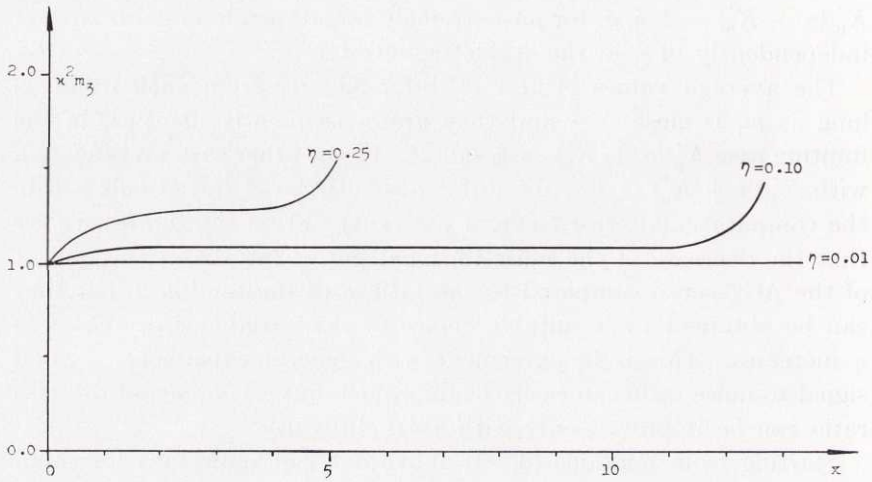

Fig. 28. The average square value m_3 of the resultant signal amplification of the AGC-servo as a function of x with η as a parameter and $K_0'/(\alpha+K_0') = 1/2$ in the case of stationary random Gaussian input signal.

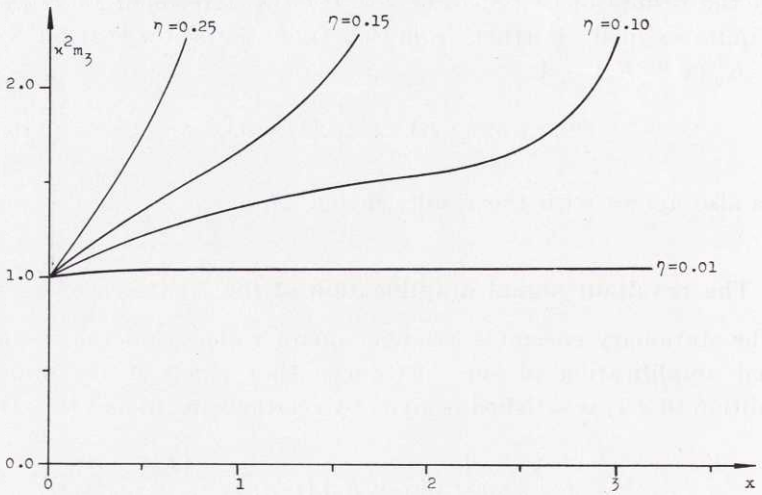

Fig. 29. The average square value m_3 of the resultant signal amplification of the AGC-servo as a function of x with η as a parameter and $K_0'/(\alpha+K_0') \cong 1$ in the case of stationary random Gaussian input signal.

In the numerically analyzed case that the Gaussian-distributed random input $F(t)$ of the AGC-servo has a rectangular power density $G(\omega)$ according to (6.2-3) the expression for m_3 takes the form

$$m_3 = \frac{1}{\varkappa^2} \int_0^\infty \int_0^\infty \exp\left\{ -(\tau+\nu) + \pi \left(\frac{K_0'}{\alpha + K_0'}\right)^2 \eta x \left[\tau I_1\left(\frac{\tau}{2x}\right) + \right.\right.$$

$$\left.\left. + \nu I_1\left(\frac{\nu}{2x}\right) - \frac{1}{2}(\tau-\nu) I_1\left(\frac{\tau-\nu}{2x}\right) \right] \right\} d\tau\, d\nu, \qquad (6.3\text{-}2)$$

where as before x, η, K_0', and the functions I_1 and I_2 are defined by (6.2-5) and (6.2-6).

The figures 28 and 29 show the average value m_3 as a function of the variable x for some different values of η in the two cases that $K_0'/(\alpha + K_0') = 1/2$ and $K_0'/(\alpha + K_0') = 1$. The quantity m_3 increases monotonically from the value $1/\varkappa^2$ with increasing x, and the rate of growth increases with the ratio $K_0'/(\alpha + K_0')$. An approximate evaluation of the double integral (6.3-2) for the case that x is small and the ratio $K_0'/(\alpha + K_0') \cong 1$ gives the result

$$\varkappa^2 m_3 \cong 1 + \tfrac{3}{2} \pi \eta x, \qquad (6.3\text{-}3)$$

which results from the SARA calculations upon which fig. 29 is based.

7. The characteristics of the AGC-servo for arbitrarily distributed quasi-stationary random input signal with a power spectrum of low-pass character

7.1 Deduction of the expressions for certain ensemble average values

The analytical expressions for the weighting function average values $\langle {}^{k}W(t, t-\tau)\rangle$, $\langle {}^{k}W(t, t-\tau)\,{}^{k}W(t, t-\nu)\rangle$, and $\langle {}^{k}W_g(t, t-\tau)\,{}^{k}W_g(t, t-\nu)\rangle$ needed for a study of the characteristics of the AGC-servo in the case of an arbitrarily distributed random input signal $F(t)$ according to (2-8) and (2-9) will now be deduced. The procedure will be the same as the one used in section 4.1 for the deduction of certain analogous average values of the tracking servo.

Let us make the same assumptions as under (4.1-1) above regarding the fixed time of observation t and the time variables τ and ν. We consequently restrict ourselves for τ and ν to the part of the τ, ν-plane for which $\nu \leqq \tau$. This is possible because the averages $\langle {}^{k}W(t, t-\tau)\,{}^{k}W(t, t-\nu)\rangle$ and $\langle {}^{k}W_g(t, t-\tau)\,{}^{k}W_g(t, t-\nu)\rangle$ are symmetric functions in τ and ν around the straight line $\nu = \tau$ in the τ, ν-plane, as one easily understands. Starting from relations (5-10) and (5-12) we write the ensemble average values in the following way:

$$
\left.
\begin{aligned}
&\frac{1}{\varkappa}\,\langle {}^{k}W(t, t-\tau)\rangle = \exp\{-\alpha\tau\}\left\langle \frac{{}^{k}F(t)}{\varkappa}\,\exp\{-I_1'(t,\tau)\}\right\rangle,\\
&\frac{1}{\varkappa^2}\,\langle {}^{k}W(t, t-\tau)\,{}^{k}W(t, t-\nu)\rangle = \exp\{-\alpha(\tau+\nu)\}\cdot\\
&\cdot\left\langle \left(\frac{{}^{k}F(t)}{\varkappa}\right)^2 \exp\{-I_2'(t,\tau,\nu)\}\right\rangle, \text{ and}\\
&\langle {}^{k}W_g(t, t-\tau)\,{}^{k}W_g(t, t-\nu)\rangle = \exp\{-\alpha(\tau+\nu)\}\cdot\\
&\cdot\langle \exp\{-I_2'(t,\tau,\nu)\}\rangle,
\end{aligned}
\right\} \qquad (7.1\text{-}1)
$$

where the integrals I_1' and I_2' are the same as those given in (4.1-3) and (4.1-4), except for the fact that the quantity $K_0 = \varkappa K$ is replaced by $K_0' = \varkappa K \alpha$, i. e.

$$\left.\begin{aligned} I_1'(t,\tau) &= [I_1(t,\tau)]_{K_0 = K_0'}, \\ I_2'(t,\tau,\nu) &= [I_2(t,\tau,\nu)]_{K_0 = K_0'}. \end{aligned}\right\} \tag{7.1-2}$$

By using the average value formulas (4.1-7) and (4.1-9) valid for the independent random variables F_μ, we compute in a similar way, as previously under section 4.1, the weighting function averages in (7.1-1). The results of this computation can be written as

$$\left.\begin{aligned} &1)\ 0 \leqq \tau < \Delta t, \\ &\frac{1}{\varkappa}\langle {}^kW(t, t-\tau)\rangle = \Lambda(K_0'\tau)\exp\{-\alpha\tau - K_0'\chi(K_0'\tau)\tau\}, \\ &2)\ \Delta t + m t_0 \leqq \tau < \Delta t + (m+1)t_0, \quad m = 0, 1, 2, \ldots (n-1), \\ &\frac{1}{\varkappa}\langle {}^kW(t, t-\tau)\rangle = \Lambda(K_0'\Delta t)\exp\{-\alpha\tau - K_0'\chi(K_0'\Delta t)\Delta t - \\ &- K_0'\chi(K_0' t_0)\, m t_0 - K_0'\chi(K_0'[\tau - m t_0 - \Delta t])(\tau - m t_0 - \Delta t)\}, \end{aligned}\right\} \tag{7.1-3}$$

$$\left.\begin{aligned} &1)\ 0 \leqq \tau < \Delta t, \\ &0 \leqq \nu \leqq \tau, \\ &\frac{1}{\varkappa^2}\langle {}^kW(t, t-\tau)\, {}^kW(t, t-\nu)\rangle = \big[\{\Lambda(K_0'[\tau+\nu])\}^2 - \\ &- \Lambda'(K_0'[\tau+\nu])\big]\,\Theta(\tau,\nu), \\ &\langle {}^kW_g(t, t-\tau)\, {}^kW_g(t, t-\nu)\rangle = \Theta(\tau,\nu), \\ &\Theta(\tau,\nu) = \exp\{-\alpha(\tau+\nu) - K_0'\chi(K_0'[\tau+\nu])(\tau+\nu)\}, \\ &2)\ \Delta t + m t_0 \leqq \tau < \Delta t + (m+1)t_0, \quad m = 0, 1, 2, \ldots (n-1), \\ &0 \leqq \nu < \Delta t, \\ &\frac{1}{\varkappa^2}\langle {}^kW(t, t-\tau)\, {}^kW(t, t-\nu)\rangle = \big[\{\Lambda(K_0'[\Delta t+\nu])\}^2 - \end{aligned}\right\}$$

$$
\begin{aligned}
&- \Lambda'(K_0'[\Delta t + \nu])]\ \Theta(\tau, \nu),\\
&\langle {}^k W_g(t, t-\tau)\, {}^k W_g(t, t-\nu)\rangle = \Theta(\tau, \nu),\\
&\Theta(\tau, \nu) = \exp\{-\alpha(\tau+\nu) - K_0'\chi(K_0' t_0)\, m t_0 - K_0' \cdot\\
&\cdot \chi(K_0'[\tau - m t_0 - \Delta t])(\tau - m t_0 - \Delta t) - K_0'\chi(K_0'[\Delta t +\\
&+ \nu])(\Delta t + \nu)\},\\
3)\ &\Delta t + m t_0 \leqq \tau < \Delta t + (m+1)\, t_0, \quad m = 1, 2, \ldots (n-1),\\
&\Delta t + l t_0 \leqq \nu < \Delta t + (l+1)\, t_0, \quad l = 0, 1, \ldots (m-1),\\
&\frac{1}{\varkappa^2}\langle {}^k W(t, t-\tau)\, {}^k W(t, t-\nu)\rangle =\\
&= [\{\Lambda(2 K_0' \Delta t)\}^2 - \Lambda'(2 K_0' \Delta t)]\ \Theta(\tau, \nu),\\
&\langle {}^k W_g(t, t-\tau)\, {}^k W_g(t, t-\nu)\rangle = \Theta(\tau, \nu),\\
&\Theta(\tau, \nu) = \exp\{-\alpha(\tau+\nu) - 2 K_0'\chi(2 K_0' t_0)\, l t_0 - K_0'\chi(K_0' t_0)\cdot\\
&\cdot (m-l-1)\, t_0 - 2 K_0'\chi(2 K_0'\Delta t)\,\Delta t - K_0'\chi(K_0'[\tau - m t_0 - \Delta t])\cdot\\
&\cdot (\tau - m t_0 - \Delta t) - K_0'\chi(K_0'[t_0 + \nu - l t_0 - \Delta t])(t_0 + \nu - l t_0 - \Delta t)\},\\
4)\ &\Delta t + m t_0 \leqq \tau < \Delta t + (m+1)\, t_0, \quad m = 0, 1, 2, \ldots (n-1),\\
&\Delta t + m t_0 \leqq \nu \leqq \tau,\\
&\frac{1}{\varkappa^2}\langle {}^k W(t, t-\tau)\, {}^k W(t, t-\nu)\rangle =\\
&= [\{\Lambda(2 K_0' \Delta t)\}^2 - \Lambda'(2 K_0' \Delta t)]\ \Theta(\tau, \nu),\\
&\langle {}^k W_g(t, t-\tau)\, {}^k W_g(t, t-\nu)\rangle = \Theta(\tau, \nu),\\
&\Theta(\tau, \nu) = \exp\{-\alpha(\tau+\nu) - 2 K_0'\chi(2 K_0' t_0)\, m t_0 -\\
&- 2 K_0'\chi(2 K_0'\Delta t)\,\Delta t - K_0'\chi(K_0'[\tau - m t_0 - \Delta t + \nu -\\
&- m t_0 - \Delta t])(\tau - m t_0 - \Delta t + \nu - m t_0 - \Delta t)\}.
\end{aligned}
\qquad (7.1\text{-}4)
$$

Fig. 18 shows the different regions of definition in the τ, ν-plane for the average values $\langle {}^k W(t, t-\tau)\, {}^k W(t, t-\nu)\rangle$ and $\langle {}^k W_g(t, t-\tau) \cdot {}^k W_g(t, t-\nu)\rangle$.

7.2 The characteristics of the output signal of the AGC-servo

Starting from the weighting function average values $\langle {}^{k}W(t, t-\tau)\rangle$ and $\langle {}^{k}W(t, t-\tau)\,{}^{k}W(t, t-\nu)\rangle$ deduced in the previous section, we first compute the output signal ensemble averages $m_1(t)$ and $m_2(t)$ according to (5-16) and after that their time-average values $\overline{m_1}$ and $\overline{m_2}$ from (5-19). These we need in order to be able to investigate the stationary output signal deviation $\overline{\varepsilon^2}$ and $\overline{\sigma_1^2}$ of the AGC-servo holding for large values of time t, relations (5-20) and (5-22), in the case of the quasi-stationary random input $F(t)$ with a low-pass spectrum. We here suppose that the average values $\overline{\varepsilon^2}$ and $\overline{\sigma_1^2}$ exist, as is the case if the AGC-servo is stable (see below).

After elementary but somewhat lengthy calculations we obtain the ensemble average values $m_1(t)$ and $m_2(t)$ for $t = nt_0 + \Delta t$ from (5-16), (7.1-3), and (7.1-4) as

$$m_1(\Delta t) = \left(1 + \frac{x_\alpha}{x_0}\right)\left[\int_0^{\Delta} \Lambda(\xi)\exp\left\{-\left[\chi(\xi) + \frac{x_\alpha}{x_0}\right]\xi\right\} d\xi + \right.$$

$$\left. + \frac{\Lambda(\Delta)\exp\left\{-\left[\chi(\Delta) + \frac{x_\alpha}{x_0}\right]\Delta\right\}}{1 - \exp\left\{-\left[\chi(x_0) + \frac{x_\alpha}{x_0}\right]x_0\right\}} \int_0^{x_0} \exp\left\{-\left[\chi(\xi) + \frac{x_\alpha}{x_0}\right]\xi\right\} d\xi\right] \quad (7.2\text{-}1)$$

and

$$m_2(\Delta t) = 2\left(1 + \frac{x_\alpha}{x_0}\right)^2\left[\int_0^{\Delta} d\xi \int_0^{\xi} [\{\Lambda(\xi+\eta)\}^2 - \Lambda'(\xi+\eta)]\exp\left\{-\left[\chi(\xi+\eta) + \right.\right.\right.$$

$$\left.\left.\left. + \frac{x_\alpha}{x_0}\right](\xi+\eta)\right\} d\eta + \frac{1}{1 - \exp\left\{-\left[\chi(x_0) + \frac{x_\alpha}{x_0}\right]x_0\right\}} \int_0^{x_0} \exp\left\{-\left[\chi(\xi) + \right.\right.\right.$$

$$\left.\left.\left. + \frac{x_\alpha}{x_0}\right]\xi\right\} d\xi \int_0^{\Delta} [\{\Lambda(\Delta+\xi)\}^2 - \Lambda'(\Delta+\xi)]\exp\left\{-\left[\chi(\Delta+\xi) + \right.\right.\right.$$

$$+\frac{x_\alpha}{x_0}\Big](\Delta+\xi)\Big\}\,d\xi+\frac{[\{\Lambda(2\Delta)\}^2-\Lambda'(2\Delta)]\exp\left\{-2\left[\chi(2\Delta)+\frac{x_\alpha}{x_0}\right]\Delta\right\}}{\left[1-\exp\left\{-\left[\chi(x_0)+\frac{x_\alpha}{x_0}\right]x_0\right\}\right]\left[1-\exp\left\{-2\left[\chi(2x_0)+\frac{x_\alpha}{x_0}\right]x_0\right\}\right]}$$

$$\cdot\int_0^{x_0}\exp\left\{-\left[\chi(\xi)+\frac{x_\alpha}{x_0}\right]\xi\right\}d\xi\int_0^{x_0}\exp\left\{-\left[\chi(x_0+\xi)+\frac{x_\alpha}{x_0}\right](x_0+\xi)\right\}d\xi+$$

$$+\frac{[\{\Lambda(2\Delta)\}^2-\Lambda'(2\Delta)]\exp\left\{-2\left[\chi(2\Delta)+\frac{x_\alpha}{x_0}\right]\Delta\right\}}{1-\exp\left\{-2\left[\chi(2x_0)+\frac{x_\alpha}{x_0}\right]x_0\right\}}\cdot$$

$$\cdot\int_0^{x_0}d\xi\int_0^{\xi}\exp\left\{-\left[\chi(\xi+\eta)+\frac{x_\alpha}{x_0}\right](\xi+\eta)\right\}d\eta\Bigg], \tag{7.2-2}$$

where

$$\left.\begin{aligned} x_0 &= K_0' t_0, \\ x_\alpha &= \alpha t_0, \\ \Delta &= K_0' \Delta t. \end{aligned}\right\} \tag{7.2-3}$$

The expressions above for m_1 and m_2 are limited and the transient phenomena can be neglected for large t (stable system) if

$$\chi(x_0)+\frac{x_\alpha}{x_0}\text{ and }\chi(2x_0)+\frac{x_\alpha}{x_0}>0. \tag{7.2-4}$$

In case of a Gaussian-distributed input $F(t)$, the function $\chi(\xi)=$ $=1-\frac{1}{2}\frac{\sigma_0^2}{\varkappa^2}$ according to relation (4.2-3) in chapter 4, and with (7.2-3) and (2-18) taken into consideration the condition (7.2-4) turns into

$$\alpha+K_0'-\frac{(K_0')^2}{\varkappa^2}\pi G(0)>0, \tag{7.2-5}$$

which agrees with the stability condition (6.2-1), as it ought to. For a Rayleigh-distributed input signal $F(t)$, which we shall study numerically, there is no risk of instability because χ is always positive (absolutely stable system).

For AGC-servos of interest in practice the open-loop zero frequency gain $\varkappa K$ is always considerably greater than 1, which means that the ratio $x_\alpha/x_0 \ll 1$. In order not to complicate the treatment unnecessarily in the following we therefore suppose that $x_\alpha/x_0 = 0$. By means of relation (4.3-8) the double integrals in (7.2-2) can simply be transformed into single integrals, all such single integrals in (7.2-2), as well as the integral in (7.2-1) with the variable Δ as the upper limit, can then be evaluated by taking into consideration the fact that $\Lambda(\xi) = \dfrac{d}{d\xi}[\chi(\xi)\,\xi]$. As a result of such simplifications in the case $x_\alpha/x_0 = 0$ we get

$$m_1(\Delta t) = 1 - \exp\{-\chi(\Delta)\,\Delta\} + \\ + \frac{\Lambda(\Delta)\exp\{-\chi(\Delta)\,\Delta\}}{1-\exp\{-\chi(x_0)\,x_0\}} \int_0^{x_0} \exp\{-\chi(\xi)\,\xi\}\,d\xi \qquad (7.2\text{-}6)$$

and

$$m_2(\Delta t) = 1 - 2\exp\{-\chi(\Delta)\,\Delta\} + \exp\{-2\,\chi(2\,\Delta)\,\Delta\} + \\ + 2\frac{\Lambda(\Delta)\exp\{-\chi(\Delta)\Delta\} - \Lambda(2\Delta)\exp\{-2\chi(2\Delta)\Delta\}}{1-\exp\{-\chi(x_0)\,x_0\}} \int_0^{x_0} \exp\{-\chi(\xi)\,\xi\}\,d\xi + \\ + \frac{[\{\Lambda(2\Delta)\}^2 - \Lambda'(2\Delta)]\exp\{-2\chi(2\Delta)\Delta\}}{1-\exp\{-2\,\chi(2\,x_0)\,x_0\}} \left[\int_0^{x_0} \xi\exp\{-\chi(\xi)\,\xi\}\,d\xi + \right. \\ + \int_0^{x_0} (x_0-\xi)\exp\{-\chi(x_0+\xi)\,(x_0+\xi)\}\,d\xi + \frac{2}{1-\exp\{-\chi(x_0)\,x_0\}} \cdot \\ \left. \cdot \int_0^{x_0} \exp\{-\chi(\xi)\,\xi\}\,d\xi \int_0^{x_0} \exp\{-\chi(x_0+\xi)\,(x_0+\xi)\}\,d\xi \right]. \qquad (7.2\text{-}7)$$

There remains only to compute the average of $m_1(\Delta t)$ and $m_2(\Delta t)$ over the time period t_0 according to (5-19). From (7.2-6) we readily get that

$$\overline{m_1} = \frac{1}{x_0}\int_0^{x_0} m_1(\Delta)\,d\Delta = 1 \qquad (7.2\text{-}8)$$

and, therefore, the wanted average values $\overline{\varepsilon^2}$ and $\overline{\sigma_1^2}$ according to (5-20) and (5-22) become equal, or

$$\overline{\varepsilon^2} = \overline{\sigma_1^2} = \overline{m_2} - 1 \tag{7.2-9}$$

[compare the previously treated case with Gaussian-distributed input $F(t)$ and $K_0'/(\alpha + K_0') = 1$ in 6.2]. From (7.2-7) we finally obtain

$$\overline{\varepsilon^2} = \overline{\sigma_1^2} = \frac{1}{x_0} \int_0^{x_0} m_2(\Delta)\, d\Delta - 1 = \frac{1}{2\,x_0} \int_0^{2x_0} \exp\{-\chi(\xi)\,\xi\}\, d\xi -$$

$$- \frac{1}{x_0} \frac{1 - \exp\{-2\,\chi(2\,x_0)\,x_0\}}{1 - \exp\{-\chi(x_0)\,x_0\}} \int_0^{x_0} \exp\{-\chi(\xi)\,\xi\}\, d\xi +$$

$$+ \frac{1}{2\,x_0} \frac{1 - \Lambda(2\,x_0) \exp\{-2\,\chi(2\,x_0)\,x_0\}}{1 - \exp\{-2\,\chi(2\,x_0)\,x_0\}} \left[\int_0^{x_0} \xi \exp\{-\chi(\xi)\,\xi\}\, d\xi + \right.$$

$$+ \int_0^{x_0} (x_0 - \xi) \exp\{-\chi(x_0 + \xi)(x_0 + \xi)\}\, d\xi + \frac{2}{1 - \exp\{-\chi(x_0)\,x_0\}} \cdot$$

$$\left. \cdot \int_0^{x_0} \exp\{-\chi(\xi)\,\xi\}\, d\xi \int_0^{x_0} \exp\{-\chi(x_0 + \xi)(x_0 + \xi)\}\, d\xi \right]. \tag{7.2-10}$$

If we specialize the result (7.2-10) above to the case of Gaussian-distributed quasi-stationary input $F(t)$ when the function $\chi(\xi) = 1 - \frac{1}{2} \frac{\sigma_0^2}{\varkappa^2} \xi$, it is easily shown that for $x_0 \ll 1$ we have approximately

$$\overline{\varepsilon^2}/\eta = \overline{\sigma_1^2}/\eta \cong 1 - \tfrac{1}{2}(1 - 3\,\eta)\,x_0, \tag{7.2-11}$$

where as usual $\eta = \sigma_0^2/\varkappa^2$. With $x_0 = K_0'\,t_0 = K_0'/\omega_0 = \pi x$ the result (7.2-11) agrees with that given in (6.2-9) and valid for a Gaussian-distributed stationary stochastic input signal with a rectangular low-pass spectrum, as it should.

In fig. 30 is shown as a function of x_0 the output average square deviation $\overline{\varepsilon^2}$ or $\overline{\sigma_1^2}$ of the AGC-servo according to (7.2-10) in the practically interesting case of a Rayleigh-distributed input signal $F(t)$, i. e. with the function $\chi(\xi)$ given by relation (4.2-5). Fig. 30 is to be

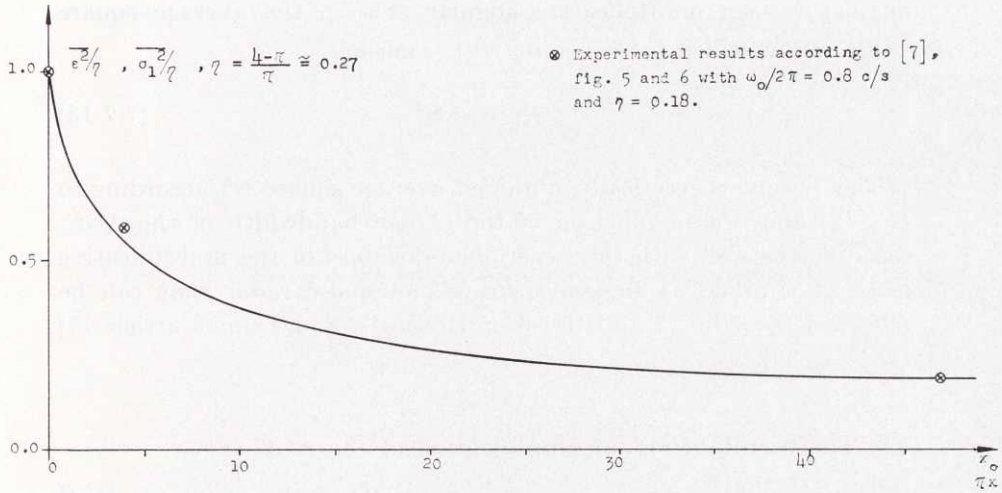

Fig. 30. The output signal deviation $\overline{\varepsilon^2}$ or $\overline{\sigma_1^2}$ of the AGC-servo as a function of x_0 with $\alpha/K_0' \cong 0$ for quasi-stationary random Rayleigh-distributed input signal.

compared in the first place with fig. 27 ($\eta \cong 0.27$ and $x = x_0/\pi$) valid for a Gaussian-distributed stationary random input. From this it is evident that for the same power spectrum the distribution of the stochastic input signal $F(t)$ generally has extremely great effect upon the magnitude of the output signal variations of the AGC-servo. The result presented in fig. 30 is interesting in showing how slowly $\overline{\varepsilon^2}$ and $\overline{\sigma_1^2}$ decrease with increasing x_0, i. e. with increasing bandwidth of the AGC-servo. This is connected with the fact that for Rayleigh-distributed inputs η, and therefore the initial value of the output signal noise for small x_0, is comparatively large.

The results given in fig. 30 can for instance be applied to the case of an angle-measuring monopulse radar with a linear detection system (open-loop system) according to appendix II in order to compute the effect of an arbitrarily fast AGC upon the angle-measuring accuracy in the absence of additive noise [see fig. 37, appendix II with $n(t) = 0$]. As is seen from fig. 37 of appendix II, the indicated angular position Θ_{ind} of a target of actual position Θ_i can be written as

$$\Theta_{\text{ind}} = e_{\text{AGC}}(t)\,\Theta_i = \Theta_i + [e_{\text{AGC}}(t) - 1]\,\Theta_i, \qquad (7.2\text{-}12)$$

where e_{AGC} is the output of the AGC, or with our notations $e_{\text{AGC}}(t) = e_u(t)$. The term $\Theta_m = [e_{\text{AGC}}(t) - 1]\,\Theta_i$ in (7.2-12) represents an

angular error ("multiplicative angular noise"), the average square value $\overline{\Theta_m^2}$ of which for constant Θ_i becomes

$$\overline{\Theta_m^2} = \overline{\varepsilon^2}\,\Theta_i^2. \tag{7.2-13}$$

The purely theoretically obtained average square $\overline{\Theta_m^2}$ according to (7.2-13) above as a function of the chosen bandwidth of the AGC-servo agrees well with the experimental values of the multiplicative noise of a practical angle-measuring monopulse radar that can be obtained from fig. 5 and fig. 6 of Howard's and Dunn's article [7] (see fig. 30).

7.3 The resultant signal amplification of the AGC-servo

The ensemble average square value $m_3(t)$ of the resultant signal amplification of the AGC-servo that exists if the servo is stable, condition (7.2-4), is obtained from (5-16) and (7.1-4) with $t = n t_0 + \Delta t$ as

$$m_3(\Delta t) = \frac{2}{\varkappa^2}\left(1 + \frac{x_\alpha}{x_0}\right)^2 \left[\int_0^{\Delta} d\xi \int_0^{\xi} \exp\left\{-\left[\chi(\xi+\eta) + \frac{x_\alpha}{x_0}\right](\xi+\eta)\right\} \mathrm{d}\xi + \right.$$

$$+ \frac{1}{1 - \exp\left\{-\left[\chi(x_0) + \frac{x_\alpha}{x_0}\right] x_0\right\}} \int_0^{x_0} \exp\left\{-\left[\chi(\xi) + \frac{x_\alpha}{x_0}\right]\xi\right\} d\xi \cdot$$

$$\cdot \int_0^{\Delta} \exp\left\{-\left[\chi(\Delta + \xi) + \frac{x_\alpha}{x_0}\right](\Delta + \xi)\right\} d\xi +$$

$$\left. + \frac{\exp\left\{-2\left[\chi(2\Delta) + \frac{x_\alpha}{x_0}\right]\Delta\right\}}{\left[1 - \exp\left\{-\left[\chi(x_0) + \frac{x_\alpha}{x_0}\right] x_0\right\}\right]\left[1 - \exp\left\{-2\left[\chi(2x_0) + \frac{x_\alpha}{x_0}\right] x_0\right\}\right]} \cdot \right.$$

$$\cdot \int_0^{x_0} \exp\left\{-\left[\chi(\xi) + \frac{x_\alpha}{x_0}\right]\xi\right\} d\xi \int_0^{x_0} \exp\left\{-\left[\chi(x_0 + \xi) + \frac{x_\alpha}{x_0}\right] \cdot\right.$$

$$\cdot (x_0 + \xi)\Big\} d\xi + \frac{\exp\left\{-2\left[\chi(2\Delta) + \frac{x_\alpha}{x_0}\right]\Delta\right\}}{1 - \exp\left\{-2\left[\chi(2x_0) + \frac{x_\alpha}{x_0}\right]x_0\right\}} \cdot$$

$$\cdot \int_0^{x_0} d\xi \int_0^{\xi} \exp\left\{-\left[\chi(\xi+\eta) + \frac{x_\alpha}{x_0}\right](\xi+\eta)\right\} d\eta \Bigg], \tag{7.3-1}$$

where as before

$$\left.\begin{aligned} x_0 &= K_0' t_0, \\ x_\alpha &= \alpha t_0, \\ \Delta &= K_0' \Delta t. \end{aligned}\right\} \tag{7.3-2}$$

We now specialize our further study of $m_3(\Delta t)$ to the interesting case that $x_\alpha/x_0 = 0$, i. e. we assume that the open-loop zero frequency gain of the AGC-servo is considerably greater than one. After simplification of the double integrals in (7.3-1) we obtain

$$\left.\begin{aligned} &\varkappa^2 m_3(\Delta) = \frac{\exp\{-2\chi(2\Delta)\Delta\}}{1 - \exp\{-2\chi(2x_0)x_0\}} h(x_0) + h(\Delta), \\ &\text{where} \\ &h(\Delta) = \int_0^{\Delta} \xi \exp\{-\chi(\xi)\xi\} d\xi + \int_0^{\Delta} (\Delta - \xi) \exp\{-\chi(\Delta+\xi)(\Delta+\xi)\} d\xi + \\ &\quad + \frac{2}{1 - \exp\{-\chi(x_0)x_0\}} \int_0^{x_0} \exp\{-\chi(\xi)\xi\} d\xi \cdot \\ &\quad \cdot \int_0^{\Delta} \exp\{-\chi(\Delta+\xi)(\Delta+\xi)\} d\xi \end{aligned}\right\} \tag{7.3-3}$$

[compare relation (4.4-6), valid for the additive output noise σ_n^2 of the tracking servo]. The time-average value $\overline{m_3} = \frac{1}{x_0} \int_0^{x_0} m_3(\Delta)\, d\Delta$

can then be computed easily starting from (7.3-3). The result is [compare (4.4-7) for $\overline{\sigma_n^2}$ with $x_n/x_0 = 0$]:

$$\varkappa^2 \overline{m_3} = \frac{1}{x_0} \int_0^{x_0} (x_0 - \xi)\, \xi \exp\{-\chi(\xi)\,\xi\}\, d\xi + \frac{1}{4\,x_0} \cdot$$

$$\cdot \left[\int_0^{x_0} \xi^2 \exp\{-\chi(\xi)\,\xi\}\, d\xi + \int_0^{x_0} (x_0 - \xi)^2 \exp\{-\chi(x_0+\xi)\,(x_0+\xi)\}\, d\xi \right] +$$

$$+ \frac{1}{2\,x_0} \frac{\int_0^{2x_0} \exp\{-\chi(\xi)\,\xi\}\, d\xi}{1 - \exp\{-2\,\chi(2\,x_0)\,x_0\}} \cdot$$

$$\cdot \left[\left(1 + 2 \frac{1 - \exp\{-2\,\chi(2\,x_0)\,x_0\}}{1 - \exp\{-\chi(x_0)\,x_0\}} \frac{\int_0^{x_0} \exp\{-\chi(\xi)\,\xi\}\, d\xi}{\int_0^{2x_0} \exp\{-\chi(\xi)\,\xi\}\, d\xi} \right) \cdot \right.$$

$$\cdot \left(\int_0^{x_0} \xi \exp\{-\chi(\xi)\,\xi\}\, d\xi + \int_0^{x_0} (x_0 - \xi) \exp\{-\chi(x_0+\xi)\,(x_0+\xi)\}\, d\xi \right) +$$

$$+ \frac{2}{1 - \exp\{-\chi(x_0)\,x_0\}} \int_0^{x_0} \exp\{-\chi(\xi)\,\xi\}\, d\xi \int_0^{x_0} \exp\{-\chi(x_0+\xi) \cdot$$

$$\left. \cdot (x_0 + \xi)\}\, d\xi \right]. \qquad (7.3\text{-}4)$$

If the input $F(t)$ is Gaussian-distributed, i. e. $\chi(\xi) = 1 - \frac{1}{2} \frac{\sigma_0^2}{\varkappa^2} \xi$ according to (4.2-3), and if $x_0 \ll 1$, the integrals in (7.3-4) can be computed approximately and one gets

$$\varkappa^2 \overline{m_3} \cong 1 + \tfrac{3}{2}\, \eta\, x_0, \qquad (7.3\text{-}5)$$

where $\eta = \sigma_0^2/\varkappa^2$. With $x_0 = \pi x$ this result agrees with the one previously deduced in section 6.3, relation (6.3-3), and holding for the case of stationary random Gaussian input $F(t)$.

The quantity $\varkappa^2 \overline{m_3}$ has been computed numerically on SARA for the case that the input $F(t)$ is Rayleigh-distributed [$\chi(\xi)$ according to (4.2-5)], which is the most interesting case in radar applications. The results of these calculations are presented in fig. 31, giving $\varkappa^2 \overline{m_3}$

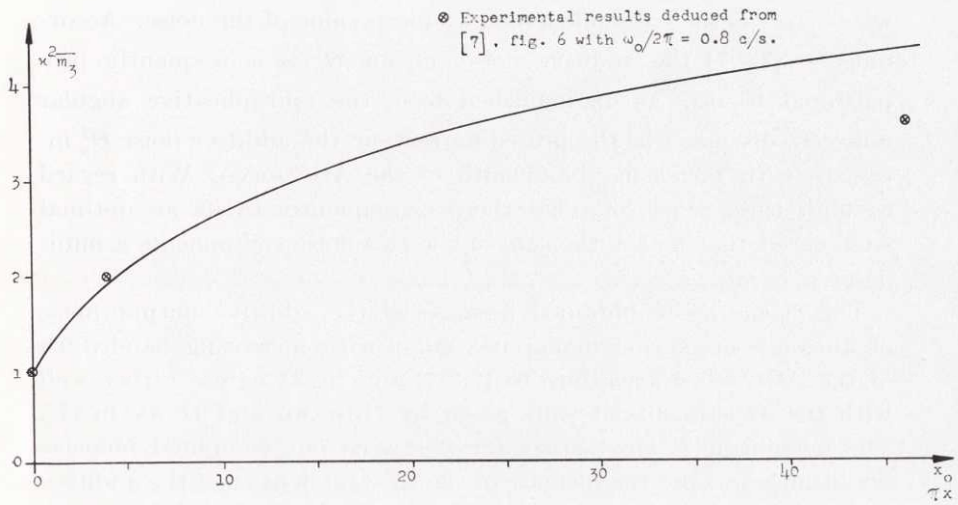

Fig. 31. The average square value $\overline{m_3}$ of the resultant signal amplification of the AGC-servo as a function of x_0 with $\alpha/K_0' \cong 0$ for quasi-stationary random Rayleigh-distributed input signal.

as a function of x_0. The figure shows that the average square value $\overline{m_3}$ of the resultant signal amplification is a bounded monotonically increasing function of x_0 with the initial value $1/\varkappa^2$ for $x_0 = 0$ [compare fig. 29 givning m_3 for a stationary Gaussian input $F(t)$].

The results in fig. 31 can be used for an angle-measuring monopulse radar with a linear detection system (open-loop system) according to fig. 37 in appendix II in order to predict the effect of the speed of the AGC-servo upon the magnitude of the contribution of additive stationary random noise $n(t)$ to the angular error for ordinary types of targets [Rayleigh-distributed echo envelope $E_a(t)$, or with our notation Rayleigh-distributed input $F(t)$]. As is seen from appendix II, fig. 37, this angular error Θ_n can be written as

$$\Theta_n(t) = K_s(t)\, n(t) = g(t)\, n(t), \tag{7.3-6}$$

because $K_s(t)$ is just what we call the resultant signal amplification $g(t)$ of the AGC-servo. If, as we assume, the noise and the input signal processes are independent the time-average $\overline{\Theta_n^2}$ of the ensemble average square value of the angular error becomes

$$\overline{\Theta_n^2} = \overline{m_3}\, \langle n^2 \rangle, \tag{7.3-7}$$

where $\langle n^2 \rangle$ is the ensemble average square value of the noise. According to (7.3-7) the additive noise output $\overline{\Theta_n^2}$ is consequently proportional to $\overline{m_3}$. As distinguished from the multiplicative angular noise $\overline{\Theta_m^2}$ discussed in the preceding section, the additive noise $\overline{\Theta_n^2}$ increases with increasing bandwidth of the AGC-servo. With regard to both these types of noise there consequently exists an optimal AGC-speed that makes the sum of the two noise components a minimum.

The theoretically obtained increase of the additive output noise of an angle-measuring monopulse radar with increasing bandwidth of the AGC-servo according to (7.3-7) and fig.31 agrees rather well with the experimental results given by HOWARD and DUNN in [7]. The agreement is also satisfactory between our computed increase of output noise and the increase of the spectral density of the additive radar angular noise output at low frequencies that has been established experimentally by DELANO and PFEFFER by realistic simulation of actual conditions in an angle-measuring radar, [9], fig. 4.

8. Concluding remarks

The theoretical study in this paper of the two randomly time-varying control systems, the tracking servo and the AGC-servo, only concerns the characteristics of average values and average square values of certain important system quantities, above all the output signals. It is possible to generalize the study to include also the autocorrelation and crosscorrelation functions of these quantities and thereby provide a better understanding of their statistical characteristics. The analytical difficulties, however, become very great.

Finally, it can be mentioned that it is possible to extend our study of the two first order linear but randomly time-varying control systems to the corresponding higher order systems with one arbitrarily distributed stochastically varying parameter, if this has the quasi-stationary form assumed in this article.

9. Appendix I

Equivalent circuit of an amplifier with a linearized automatic gain control

The block-diagram of a linear bandpass amplifier with automatic gain control ("linear AGC system") is shown in fig. 32. The bandpass amplifier is assumed to be tuned to the carrier angular frequency ω_c and to have a bandwidth considerably greater than the bandwidth of the AGC loop. We also suppose that the gain of the amplifier g can be controlled without time-lag by the AGC voltage $e_A(t)$ in fig. 32. The AGC detector is assumed to be ideal, giving an output signal that is the envelope $e_u(t)$ of the output $e_u(t)\ e^{j\omega_c t}$ of the amplifier. The detector output is fed through a linear constant low-pass filter. The control signal $e_A(t)$, developed by a wideband d. c. amplifier in the feedback branch of the AGC system, is proportional to the amount by which the output of the filter exceeds a certain constant threshold or "delay" voltage E. The purpose of the system is to give a constant output signal envelope $e_u(t)$ for a wide range of low frequency amplitude variations of the input signal envelope $e_i(t)$ without in some applications suppressing higher frequency modulations in $e_i(t)$ which contain useful information [14].

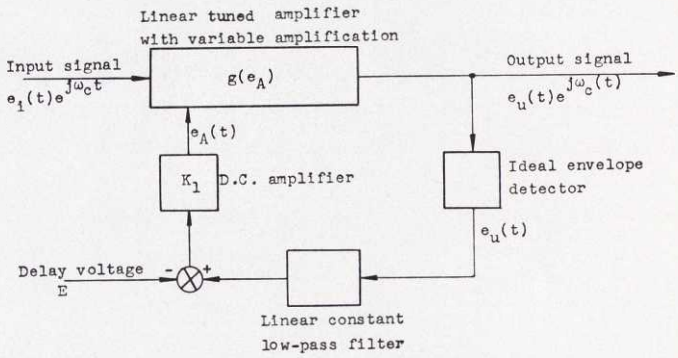

Fig. 32. Block-diagram of a linear bandpass amplifier with automatic gain control (linear AGC system).

For the amplifier with AGC according to the above, the following relations hold:

$$e_u(t) = g(e_A(t))\, e_i(t), \tag{I-1}$$

$$e_A(t) = K_1 \left[\int_{-\infty}^{t} W_F(t-\tau)\, e_u(\tau)\, d\tau - E \right], \tag{I-2}$$

where W_F is the weighting function of the linear constant low-pass filter and K_1 is the gain of the d. c. amplifier of the feedback branch of the system. We start by considering the simple case that the input signal envelope $e_i(t)$ is constant or varies very slowly with time, $e_i(t) = \bar{e}_i$. In the steady state condition the amplifier output signal envelope also becomes constant, $e_u(t) = \bar{e}_u$, as well as the control voltage $e_A(t)$, $e_A(t) = \bar{e}_A$, and according to (I-1) and (I-2) these relations become

$$\bar{e}_u = g(\bar{e}_A)\, \bar{e}_i, \tag{I-3}$$

$$\bar{e}_A = K_1 (\bar{e}_u - E). \tag{I-4}$$

For simplicity, in obtaining (I-4) from (I-2) we have supposed that the passive low-pass filter does not attenuate a d. c. signal, i. e. $\int_{-\infty}^{t} W_F(t-\tau)\, d\tau \to 1$ as $t \to \infty$. In many practical applications (see for instance [15]) the gain function g has the simple exponential form

$$g(e_A) = G_0 \exp\{-C\, e_A\}, \tag{I-5}$$

where G_0 and C are given constants, and the expressions (I-3) and (I-4) give

$$\bar{e}_u = G_0 \exp\{-K_1 C (\bar{e}_u - E)\}\, \bar{e}_i. \tag{I-6}$$

Fig. 33 shows graphically the relation between $\bar{e}_u$ and $\bar{e}_i$ in an example of an "undelayed" AGC system ($E = 0$) with $G_0 = 10^5$ and $K_1 C = 4$.

In order to be able to treat analytically the problem of an amplifier with an AGC in the case of an arbitrarily varying input signal $e_i(t)$ with time, it is necessary to simplify considerably the relation (I-1). Let us linearize this relation and put

$$e_u(t) \cong \left\{ g(e_{A_0}) + \left(\frac{dg}{de_A} \right)_{e_A = e_{A_0}} [e_A(t) - e_{A_0}] \right\} e_i(t), \tag{I-7}$$

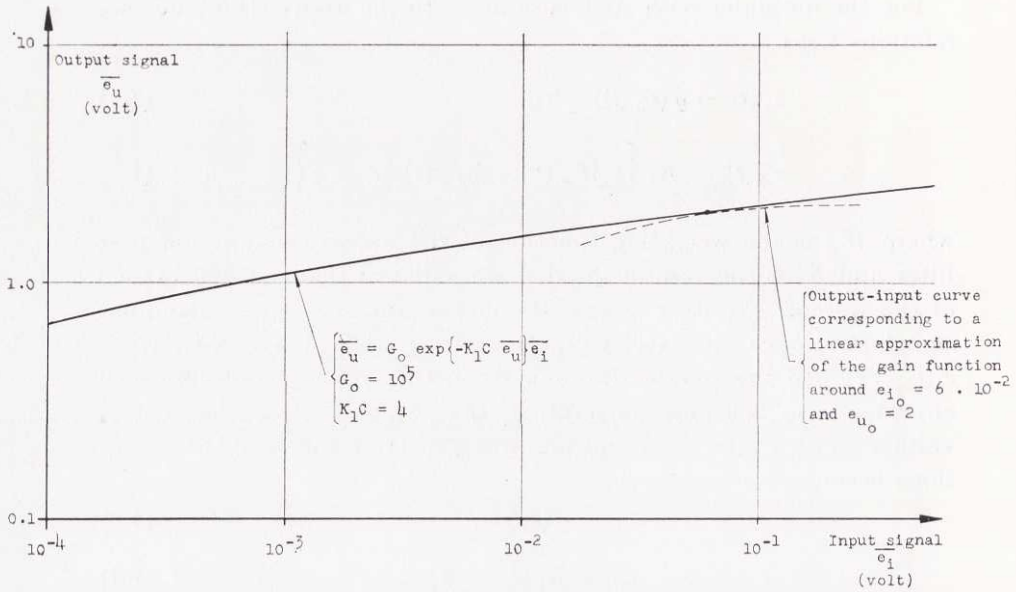

Fig. 33. An example of the relation between the output and input signal envelopes of a linear amplifier with AGC and an exponential gain function in the case of a slowly varying input signal envelope.

valid at least for small variations of the AGC voltage $e_A(t)$ around a constant or slowly varying value with time $e_A = e_{A_0}$.

To get an idea about the permissible range of control voltages $e_A(t)$ for which the Taylor series approximation of the gain function used in (I-7) is suitable, let us consider the stationary case that $e_A(t) = \bar{e}_A$, $e_u(t) = \bar{e}_u$, and $e_i(t) = \bar{e}_i$ and put

$$\left.\begin{aligned} \Delta e_A &= \bar{e}_A - e_{A_0}, \\ \Delta e_u &= e_u - e_{u_0}, \\ \Delta e_i &= e_i - e_{i_0}, \end{aligned}\right\} \tag{I-8}$$

where e_{A_0}, e_{u_0}, and e_{i_0} are the chosen related reference values of the AGC-voltage, the output and the input signal envelopes satisfying the equations

$$e_{u_0} = g(e_{A_0})\, e_{i_0}, \tag{I-9}$$

$$e_{A_0} = K_1 (e_{u_0} - E). \tag{I-10}$$

Using the Lagrange form for the remainder in a Taylor series [16], we can say that the gain function approximation is acceptable if

$$\left|\frac{1}{2!}(\Delta e_A)^2\left(\frac{d^2 g}{de_A^2}\right)_{e_A=e_{A_0}+\Theta\Delta e_A}\right| < \left|\Delta e_A\left(\frac{dg}{de_A}\right)_{e_A=e_{A_0}}\right|,$$

where $0 \leqq \Theta \leqq 1$, or if

$$\left|\Delta e_A\right| < 2\left|\frac{dg}{de_A}\Big/\frac{d^2 g}{de_A^2}\right|. \tag{I-11}$$

But according to (I-3), (I-4), (I-8), (I-9), and (I-10) we have approximately

$$\left.\begin{aligned} \Delta e_u &\cong \frac{1}{K_1}\Delta e_A, \\ \Delta e_i &\cong \left[1 - K_1 e_{u_0}\left(\frac{1}{g}\frac{dg}{de_A}\right)_{e_A=e_{A_0}}\right]\frac{\Delta e_u}{g(e_{A_0})} \end{aligned}\right\} \tag{I-12}$$

and, therefore, the condition (I-11) is approximately equivalent to

$$\left|\frac{\Delta e_i}{e_{i_0}}\right| < \left|\frac{2}{K_1 e_{u_0}}\left[1 - K_1 e_{u_0}\frac{1}{g}\frac{dg}{de_A}\right]\left(\frac{dg}{de_A}\Big/\frac{d^2 g}{de_A^2}\right)\right|. \tag{I-13}$$

For the usual case of an exponential gain function of the form (I-5), (I-13) becomes (Θ is put equal to zero):

$$\left|\frac{\Delta e_i}{e_{i_0}}\right| < 2\,\frac{1 + K_1 C e_{u_0}}{K_1 C e_{u_0}}. \tag{I-14}$$

In (I-14) the quantity $K_1 C e_{u_0}$ is the open-loop zero frequency gain of the AGC system (see further below), which is generally much larger than 1, and therefore

$$\left|\frac{\Delta e_i}{e_{i_0}}\right| < 2. \tag{I-15}$$

Consequently, the linearized relation (I-7) holds over a comparatively wide range of input signal variations, which is also evident from the chosen example in fig. 33.

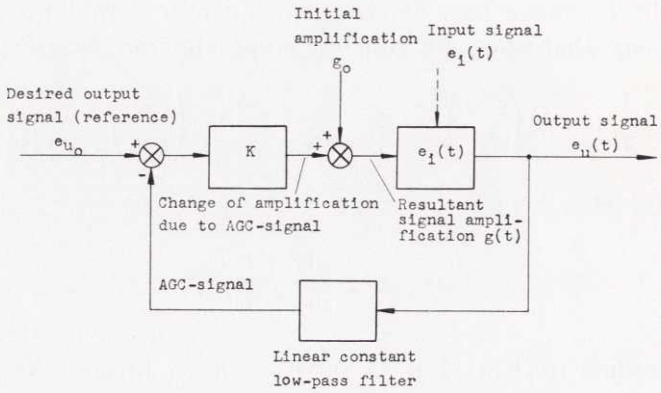

Fig. 34. Equivalent circuit of an amplifier with linearized AGC.

By means of the relations (I-7), (I-10), and (I-12) the simplified linearized function of an amplifier with automatic gain control can be described by

$$\left.\begin{aligned} e_u(t) &= \{g_0 + K\,[e_{u_0} - e'_A(t)]\}\, e_i(t), \\ e'_A(t) &= \int^{t} W_F(t-\tau)\, e_u(\tau)\, d\tau, \end{aligned}\right\} \qquad \text{(I-16)}$$

where

and

$$\left.\begin{aligned} g_0 &= g(e_{A_0}) \\ K &= -K_1 \left(\frac{dg}{de_A}\right)_{e_A = e_{A_0}}. \end{aligned}\right\} \qquad \text{(I-17)}$$

The equivalent circuit of an amplifier with a linearized AGC is therefore immediately given by fig. 34.

We have demonstrated above that the linearized relations (I-16) can describe the function of the AGC system even for relatively large variations of the input signal envelope $e_i(t)$ around the chosen reference value e_{i_0}. If we further specialize these relations to the case of small input envelope deviations we get the expressions for the small signal behaviour of an AGC system already discussed in [14].

Putting

$$\left.\begin{aligned} e_i(t) &= e_{i_0} + \Delta e_i(t), \\ e_u(t) &= e_{u_0} + \Delta e_u(t), \\ &\text{and} \\ e'_A(t) &= e_{A_0}' + \Delta e'_A(t), \end{aligned}\right\} \tag{I-18}$$

into (I-16) and neglecting second order terms we obtain

$$\left.\begin{aligned} \Delta e_u(t) &= g_0 \Delta e_i(t) - K e_{i_0} \Delta e'_A(t), \\ \Delta e'_A(t) &= \int_0^t W_F(t-\tau) \Delta e_u(\tau)\, d\tau. \end{aligned}\right\} \tag{I-19}$$

Alternatively, supposing the system to start from rest at $t = 0$ the relations (I-19) can be written in the following operator form

$$\frac{\Delta e_u(s)}{\Delta e_i(s)} = \frac{g_0}{1 + K e_{i_0} Y_F(s)}, \tag{I-20}$$

where $\Delta e_u(s)$, $\Delta e_i(s)$, and $Y_F(s)$ are the Laplace transforms corresponding to $\Delta e_u(t)$, $\Delta e_i(t)$, and $W_F(t)$. From (I-20) it is evident that the quantity $K' = K e_{i_0}$ represents the open-loop zero frequency gain of the AGC system $\left[Y(0) = 1 \text{ because we assumed } \int_0^\infty W_F(\tau)\, d\tau = 1 \right]$. By means of equations (I-17) and (I-9) the open-loop gain K' becomes

$$K' = K e_{i_0} = - K_1 e_{u_0} \left(\frac{1}{g} \frac{dg}{de_A} \right)_{e_A = e_{A_0}}, \tag{I-21}$$

which expression is the same as the one given in equation (11) in [14]. If the gain function g is of the exponential form (I-5), K' is $K' = K_1 C e_{u_0}$.

If the low-pass filter of the AGC system is of the simplest RC-type with a 3 dB cut-off angular frequency α, i. e.

$$Y_F(s) = \frac{\alpha}{s + \alpha}, \tag{I-22}$$

relation (I-20) becomes

$$\frac{\Delta e_u(s)}{\Delta e_i(s)} = g_0 \frac{s + \alpha}{s + \alpha(1 + K')}, \tag{I-23}$$

from which we see that the AGC acts as a high-pass filter introduced between the input and output envelope signals. The attenuation of this filter at low frequencies, $(1 + K')/g_0$, is large so long as the loop gain K' is high. The same is true with the filter cut-off angular frequency or the bandwidth of the AGC system ω_{AGC} given by:

$$\left.\begin{aligned} \omega_{\text{AGC}} &= \alpha \sqrt{(1 + K')^2 - 2} \cong \\ &\cong \alpha (1 + K') = \alpha (1 + K\, e_{i_0}) \end{aligned}\right\} \qquad \text{(I-24)}$$

for

$$K' \gg 1.$$

10. Appendix II

The equivalent circuits of one-dimensional angle-measuring and tracking monopulse radars

In the present appendix we shall summarize in block-diagram form the function of an angle-measuring or tracking monopulse radar on the basis of reference [17]. Analogous block-diagrams or equivalent circuits can be constructed for other types of angle- or range-measuring and tracking radars.

Under certain conditions according to relations (5-5), (5-6), (5-33), and (5-34) in [17], the envelopes of the output signal pulses from the phase sensitive and the AGC-detector of a one-dimensional angle-measuring monopulse radar, S^a_{det} and S^a_{AGC}, can be written as

$$\left.\begin{aligned} S^a_{\text{det}} &= 2\,[F(\Theta_0)]^2\,[K_s(t)]^2\,[E_a(t)]^2\,G\left[\Theta + \frac{n(t)}{E_a(t)}\right] \\ \text{and} \\ S^a_{\text{AGC}} &= 4\,[F(\Theta_0)]^2\,[K_s(t)]^2\,[E_a(t)]^2. \end{aligned}\right\} \qquad \text{(II-1)}$$

In (II-1) Θ denotes the difference in angle between the direction of the target, which we can call Θ_i, and a direction defined by the antenna system, Θ_u, i. e. $\Theta = \Theta_i - \Theta_u$. The quantity G is a constant, the so called angular gain, determined principally by the configuration of the radar antenna, and $F(\Theta_0)$ is another antenna constant. $K_s(t)$ stands for the amplification of the intermediate frequency (if) amplifier of the sum-signal channel, which is here assumed to be the same as the corresponding amplification $K_D(t)$ of the difference-signal channel. The quantity $E_a(t)$ represents the envelope or amplitude of the target echo pulses. For ordinary targets such as airplanes and ships, $E_a(t)$ varies stochastically with time, and if the distance to the target does not change too rapidly it can be supposed to be generated by a stationary random process. The ratio $n(t)/E_a(t)$ is a stochastic angular error caused by internal noise in the radar receiver and target glint. It can also be assumed to be generated by more or less stationary

stochastic processes with zero average value. The relations (II-1) hold only for a monopulse radar with a square-law detection system, i. e. a radar having a phase sensitive detector of the product type and a square-law AGC-detector. It is further understood that the angular deviation Θ should be small compared with the beamwidth of the antenna system.

The stochastic angular error function $n(t)$ appearing in (II-1) can be written as the sum

$$n(t) = n_1(t) + n_2(t), \tag{II-2}$$

where $n_1(t)$ and $n_2(t)$ represent the two independent contributions from receiver internal noise and target angular glint, or from [17]:

$$n_1(t) = \frac{N_D(t) \cos \Phi_{nD}(t)}{2\, G\, F(\Theta_0)}, \tag{II-3}$$

$$n_2(t) = V(t). \tag{II-4}$$

The so called angular glint function $V(t)$ in (II-4) is given by equation (5-32) in [17]. In relation (II-3), $N_D(t)$ is the envelope and $\Phi_{nD}(t)$ the phase angle of the receiver internal noise signal referred to the input of the if-amplifier of the difference-channel. For the relations (II-3) and (II-4) above to hold strictly, two conditions must be satisfied. The signal-to-noise power ratio shall be considerably larger than 1 so that the effect of the internal noise of the sum-channel can be neglected, and the whole of the glinting target shall be inside the linear angle-measuring region of the radar.

As pointed out earlier, the relations (II-1) are valid for a monopulse radar with a square-law detection system. If, on the other hand, the detection system is linear, which is the case when the phase sensitive detector is of a linear type and the AGC-detector an ideal envelope detector, but the conditions otherwise the same, one readily finds that the envelopes S^a_{det} and S^a_{AGC} become

$$\left.\begin{aligned} S^a_{\text{det}} &= C \cdot 2\, F(\Theta_0)\, K_s(t)\, E_a(t)\, G\left[\Theta + \frac{n(t)}{E_a(t)}\right] \\ \text{and} \\ S^a_{\text{AGC}} &= 2\, F(\Theta_0)\, K_s(t)\, E_a(t), \end{aligned}\right\} \tag{II-5}$$

where C is a constant dependent upon the phase sensitive detector.

If we neglect irrelevant constants in the expressions (II-1) and (II-5) for the envelopes of the output signals from the phase sensitive and the AGC-detector in the two cases, these envelopes, now denoted by e_{det} and e_{AGC}, can be written as:

square-law detection system:

$$\left.\begin{aligned} e_{\text{det}} &= [K_s(t)]^2\,[E_a(t)]^2\left[\Theta + \frac{n(t)}{E_a(t)}\right], \\ e_{\text{AGC}} &= [K_s(t)]^2\,[E_a(t)]^2, \end{aligned}\right\} \tag{II-6}$$

linear detection system:

$$\left.\begin{aligned} e_{\text{det}} &= K_s(t)\,E_a(t)\left[\Theta + \frac{n(t)}{E_a(t)}\right], \\ e_{\text{AGC}} &= K_s(t)\,E_a(t). \end{aligned}\right\} \tag{II-7}$$

The actual output signals received immediately after the phase sensitive and the AGC-detector can be supposed to be the signal pulses obtained from the continuous envelopes e_{det} and e_{AGC} by sampling with the constant period T, where $T = 1/f_r$ and f_r is the pulse repetition frequency used. There normally follows after each detector some sort of a hold circuit or a smoothing filter, which cuts off all signal frequencies larger than and including f_r. The pulse repetition frequency f_r is generally much higher than the cut-off frequencies of the echo envelope $E_a(t)$ and the glint component $n_2(t)$, but very low compared with the cut-off frequency of the internal noise component $n_1(t)$, which is approximately half the if-bandwidth. We can therefore suppose in the following that relations (II-6) and (II-7) approximately give the continuous outputs from the phase sensitive and the AGC-detector after holding or filtering, provided that the internal noise component $n_1(t)$ in $n(t)$ is replaced by $n_1'(t)$, which can be assumed to have the character of band-limited Gaussian noise with the cut-off frequency f_r and the same average square value as $n_1(t)$.

According to (II-3) and equation (5-16) in [17], the time average square value of the noise component $n_1(t)$, and consequently that of $n_1'(t)$, is

$$[n_1^2]_{\text{Av}} = [(n_1')^2]_{\text{Av}} = \frac{1}{2}\,\frac{1}{G^2}\,\frac{1}{(P/N)_{\text{in}}}\,[E_a^2]_{\text{Av}}, \tag{II-8}$$

where $(P/N)_{in}$ is a suitably defined signal-to-noise power ratio of the radar receiver (see [17]), and $[E_a^2]_{Av}$ is the time average square of the echo amplitude. (Between the time averages used in [17] and in this appendix and the ensemble averages used in the rest of this article there is no difference in the case of stationary random processes if, as we assume for simplicity, the processes are ergodic; see for example [2], pp 1-8).

The random echo amplitude $E_a(t)$ and the glint function $V(t)$ of ordinary targets such as airplanes and ships can be supposed to be independent, $E_a(t)$ more or less Rayleigh-distributed, and $V(t)$ more or less Gaussian-distributed with zero mean. Under certain simplifying assumptions (see [17], p. 28) the following relation holds between their time average square values:

$$[V^2]_{Av} = \frac{1}{24}\left(\frac{L'}{R}\right)^2 [E_a^2]_{Av} = [n_2^2]_{Av}, \qquad \text{(II-9)}$$

where R is the distance between radar and target and L' is the extent of the target in a direction perpendicular to the line radar-target. The cut-off frequencies of the power spectrum of $E_a(t)$ and $V(t)$, which do not differ significantly from each other, are often less than 10 c/s.

Summing up we can consequently say that the continuous signals of interest immediately after the phase sensitive and the AGC-detector of a one-dimensional angle-measuring monopulse radar are given by the relations (II-6) and (II-7) above, with $n(t) = n_1'(t) + n_2(t)$ in the two cases of a square-law and a linear detection system. The echo amplitude $E_a(t)$ and the error functions $n_1'(t)$ and $n_2(t)$ can be supposed to be generated by independent stationary stochastic processes. Usually, the amplitude $E_a(t)$ is more or less Rayleigh-distributed while both the internal receiver noise component $n_1'(t)$ and the target glint component $n_2(t)$ are approximately Gaussian- or normally distributed with the average value zero and the average square values (under the reasonable assumptions given in [17]) given by the relations (II-8) and (II-9) above. The cut-off frequencies of the power spectrum (power density function) of $E_a(t)$ and $n_2(t)$ can amount to several cycles per second while the corresponding cut-off frequencies for $n_1'(t)$ is about the pulse repetition frequency.

On the basis of relations (II-6) and (II-7) one easily constructs

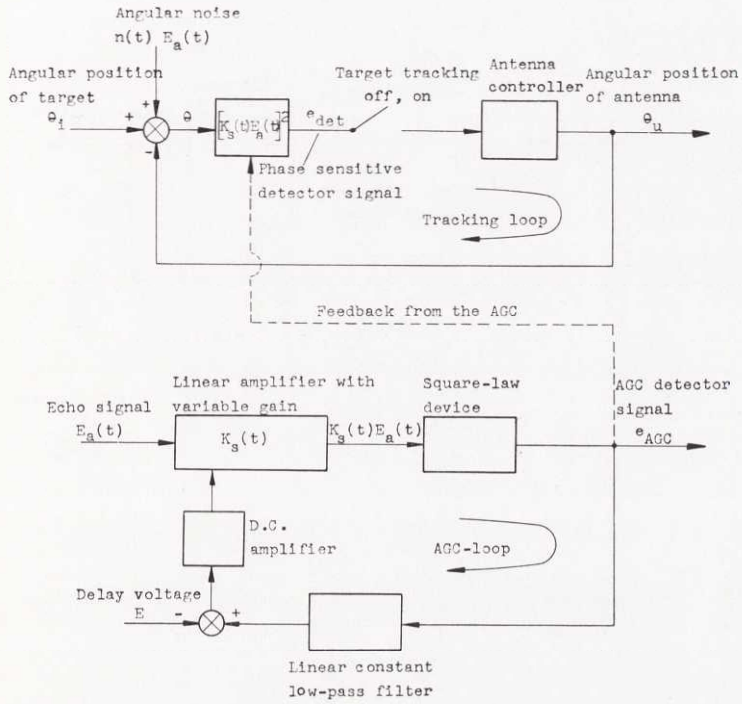

Fig. 35. The equivalent circuit of a one-dimensional angle-measuring or tracking monopulse radar with a square-law detection system.

the equivalent circuits shown in figs 35 and 36 for the two types of monopulse radars. In the non-tracking mode of operation, when only the target angular deviation Θ is measured the indicated switch is in the "off" position. When tracking the target, switch in "on" position, the angular "error" Θ controls the orientation of the antenna via the antenna controller shown. In the AGC-loops, linear constant low-pass filters are introduced between the detectors and the variable amplifiers, which determine the bandwidth or speed of the AGC systems.

By a slow AGC we mean an AGC that does not respond to the rapid variations of the echo envelope $E_a(t)$ but controls the amplification $K_s(t)$ so that the time average of the detector output e_{AGC} is a constant, which for simplicity we assume to be 1. In this limiting case (II-6) and (II-7) become:

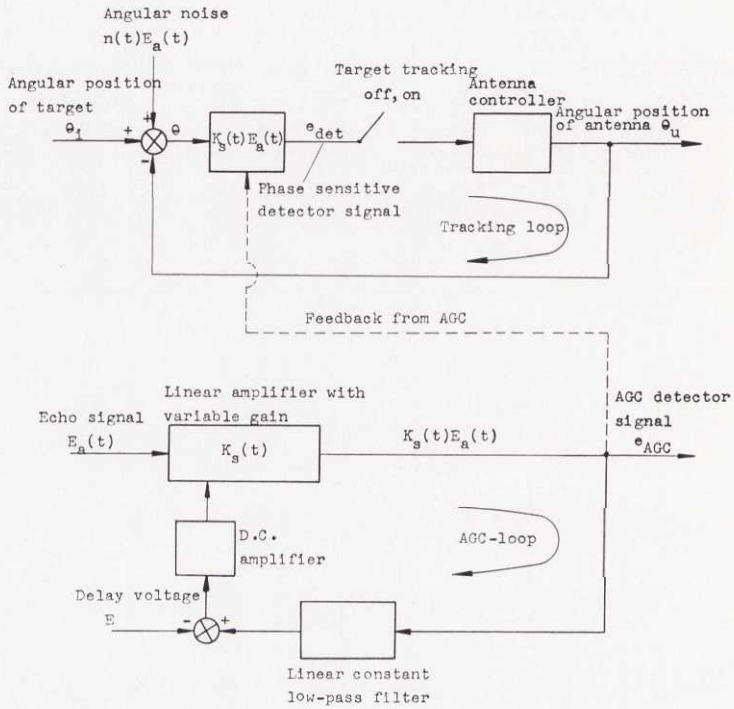

Fig. 36. The equivalent circuit of a one-dimensional angle-measuring or tracking monopulse radar with a linear detection system.

square-law detection system:

$$\left.\begin{aligned} e_{\mathrm{det}} &= \frac{[E_a(t)]^2}{[E_a^2]_{\mathrm{Av}}}\left[\Theta + \frac{n(t)}{E_a(t)}\right], \\ [e_{\mathrm{AGC}}]_{\mathrm{Av}} &= [K_s(t)]^2\,[E_a^2]_{\mathrm{Av}} = 1, \end{aligned}\right\} \tag{II-10}$$

linear detection system:

$$\left.\begin{aligned} e_{\mathrm{det}} &= \frac{E_a(t)}{[E_a]_{\mathrm{Av}}}\left[\Theta + \frac{n(t)}{E_a(t)}\right], \\ [e_{\mathrm{AGC}}]_{\mathrm{Av}} &= K_s(t)\,[E_a]_{\mathrm{Av}} = 1. \end{aligned}\right\} \tag{II-11}$$

If, on the other hand, the AGC is fast, i. e. the AGC responds to all variations of $E_a(t)$, the corresponding expressions become:

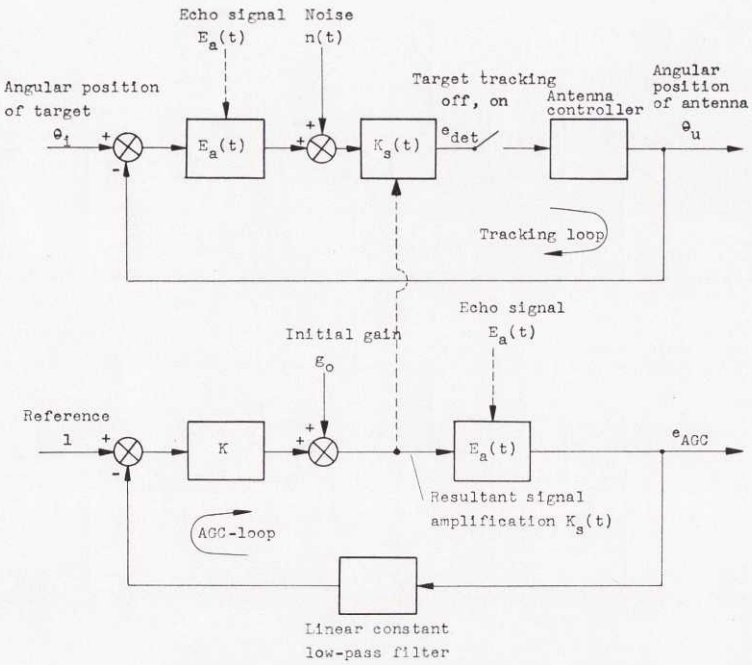

Fig. 37. The equivalent circuit of a one-dimensional angle-measuring or tracking monopulse radar with a linear detection system and a linearized AGC.

square-law detection system:

$$\left.\begin{aligned} e_{\text{det}} &= \Theta + \frac{n(t)}{E_a(t)}, \\ e_{\text{AGC}} &= [K_s(t)]^2\,[E_a(t)]^2 = 1, \end{aligned}\right\} \qquad \text{(II-12)}$$

linear detection system:

$$\left.\begin{aligned} e_{\text{det}} &= \Theta + \frac{n(t)}{E_a(t)}, \\ e_{\text{AGC}} &= K_s(t)\,E_a(t) = 1. \end{aligned}\right\} \qquad \text{(II-13)}$$

Neither of the cases slow and fast AGC is quite ideal; a slow AGC gives large variations of the legitimate output signal due to a certain angular deviation Θ and a fast AGC causes a large additive angular

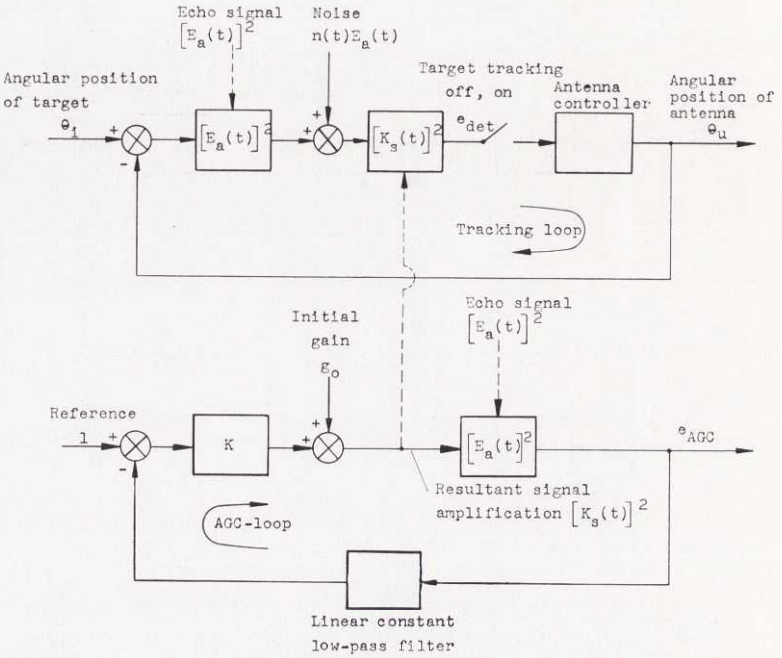

Fig. 38. The equivalent circuit of a one-dimensional angle-measuring or tracking monopulse radar with a square-law detection system and a linearized AGC.

error. From the relations above, there would appear to be no significant difference between the two different types of detection systems, both for the limiting cases of slow or fast AGC and for any other type of AGC.

If the function of the AGC of a monopulse radar with linear detection system in fig. 36 is linearized according to appendix I one obtaines the equivalent, completely linear circuit in fig. 37. In fig. 37 the initial gain g_0 is to be chosen as $g_0 = 1/[E_a]_{Av}$ and the quantity K, an AGC-constant determined by the operating point of interest, is given by equation (I-17) in appendix I. By means of the equivalent circuit in fig. 37 and the general results obtained in this paper for the two linear stochastically time-varying control systems investigated some interesting aspects of certain simple special cases of this type of radar can be discussed. Fig. 38, finally, shows the equivalent circuit of a one-dimensional angle-measuring or tracking monopulse radar with a square-law detection system when the AGC-function has been linearized. The quantity g_0 is to be chosen here as $g_0 = 1/[E_a^2]_{Av}$.

11. Acknowledgement

The author is very much indepted to Professor HENRY WALLMAN of the Chalmers University of Technology, Gothenburg, Sweden, for invaluable aid and encouragement in the accomplishment of this work.

12. References

1. LANING, J. H., JR. and BATTIN, R. H. Random processes in automatic control. McGraw-Hill, New-York, 1956.
2. BENDAT, J. S. Principles and applications of random noise theory. John Wiley & Sons, Inc., New-York, 1958.
3. ROSENBLOOM, A., HEILFRON, J., and TRAUTMAN, D. L. Analysis of linear systems with randomly varying inputs and parameters. IRE Convention Record, Part 4, 1955, pp 106—113.
4. TIKHONOV, V. J. Fluctuation action in the simplest parametric systems. Automation and remote control. The Soviet Journal Avtomatika i Telemekhanika in English translation, Vol. XIX, No. 8, August 1958, pp 705—711.
5. SAMUELS, J. CLIFTON and ERINGEN, A. CEMAL. On stochastic linear systems. Journal of Mathematics and Physics, Vol. 38, No. 7, July 1959, pp 83—103.
6. BUCHAN, J. F. and RAVEN, R. S. Gain modulation of servomechanisms. IRE Wescon Convention Record, Part 4, August 1957, pp 201—204.
7. DUNN, J. H. and HOWARD, D. D. The effects of automatic gain control performance on the tracking accuracy of monopulse radar systems. Proc. IRE, Vol. 47, No. 3, March 1959, pp 430—435.
8. DUNN, J. H. and HOWARD, D. D. Phenomena of scintillation noise in radar-tracking systems. Proc. IRE, Vol. 47, No. 5, May 1959, pp 855—863.
9. DELANO, R. H. and PFEFFER, IRWIN. The effect of AGC on radar tracking noise. Proc. IRE, Vol. 47, No. 6, June 1956, pp 801—810.
10. RICE, S. O. Mathematical analysis of random noise. Section 1.7, Bell System Tech. J., Vol. 23, July 1944, pp 282—332, Vol. 24, January 1945, pp 46—156.
11. SAMUELS, J. CLIFTON. On the mean square stability of random linear systems. IRE Transactions, Vol. CT-6, May 1959, pp 248—259.
12. BERTRAM, J. E. and SARACHIK, P. E. Stability of circuits with randomly time-varying parameters. IRE Transactions, Vol. CT-6, May 1959, pp 260—270.
13. JAHNKE, EUGENE and EMDE, FRITZ. Tables of functions with formulae and curves.
14. OLIVER, B. M. Automatic volume control as a feedback problem. Proc. IRE, Vol. 36, No. 4, April 1948, pp 466—473.
15. FIELD, J. C. G. The design of automatic-gain-control systems for auto-tracking radar receivers. Proc. IEE, Part C, No. 7, March 1958, pp 93—108.
16. WHITTAKER, E. T. and WATSON, G. N. A course of modern analysis.
17. HELLGREN, GÖSTA. On the principles and angular accuracy of monopulse radar. SAAB Technical Notes, TN 42, March 1959.

GÖTEBORG
ELANDERS BOKTRYCKERI AKTIEBOLAG
1960